Drug resistance, and the role of p53, in lung cancer cell lines

A thesis submitted for the degree of Ph.D.

by

Laura Breen, B.Sc. Hons

The experimental work described in this thesis was carried out under the supervision of Professor Martin Clynes Ph.D.

at the

National Institute for Cellular Biotechnology,
Dublin City University,
Glasnevin,
Dublin 9,
Republic of Ireland.

December 2005

I hereby certify that this material, which I now submit for assessment on the programme of study leading to the award of Ph.D. is entirely my own work and has not been taken from the work of others save and to the extent that such work has been cited and acknowledged within the text of my work.

Signed: Laura Bree **ID No.:** 97362816

Date: 1/12/05

This thesis is dedicated to my parents and Brian

Abbreviations

Ab	-	Antibody
ABC	-	ATP Binding Cassette
ATP	-	Adenosine-triphosphate
ATCC	-	American Tissue Culture Collection
BAC	-	Bronchioloalveolar carcinoma
BSA	-	Bovine Serum Albumin
cDNA	-	Complementary DNA
CKI	-	Cyclin-dependent kinase inhibitor
CPT	-	Carboplatin
Da	-	Daltons
DEPC	-	Diethyl Pyrocarbonate
DMEM	-	Dulbecco's Minimum Essential Medium
DMSO	-	Dimethyl sulfoxide
DNase	-	Deoxyribonuclease
DNA	-	Deoxyribonucleic Acid
dNTP	-	Deoxynucleotide triphosphate (N= A, C, T, G or U)
DTT	-	Dithiothreitol
ECM	-	Extracellular matrix
EDTA	-	Ethylene diamine tetracetic acid
ETS	-	Environmental tobacco smoke
FCS	-	Fetal Calf Serum
FU	-	Fluorouracil
GCOS	-	GeneChip Operating Software
IC_{50}	-	Inhibitory Concentration 50%
Ig	-	Immunoglobulin
IMS	-	Industrial Methylated Spirits
kDa	-	Kilo Daltons
LRP	-	Lung Resistance-related Protein
MAb	-	Monoclonal Antibody
MAP	-	Microtubule-associated protein
MDR	-	Multiple Drug Resistance
MRP	-	Multidrug Resistance-associated Protein
MEM	-	Minimum Essential Medium
MMLV-RT	-	Moloney Murine Leukemia Virus-Reverse Transcriptase
mRNA	-	Messenger RNA
NRK	-	Normal Rat Kidney
NSAID	-	Nonsteroidal anti-inflammatory drug
NSCLC	-	Non-Small Cell Lung Carcinoma
OD	-	Optical Density
Oligos	-	Oligonucleotides

PAH	-	Polycyclic aromatic hydrocarbon
PCR	-	Polymerase Chain Reaction
P-gp	-	P-glycoprotein
PTGS	-	Post Translational Gene Silencing
RISC	-	RNA-induced silencing complex
RNA	-	Ribonucleic Acid
RNase	-	Ribonuclease
RPA	-	RNase protection assay
RNasin	-	Ribonuclease Inhibitor
rpm	-	Revolution(s) Per Minute
RT-PCR	-	Reverse Transcriptase-PCR
SCLC	-	Small Cell Lung Carcinoma
SDS	-	Sodium Doedecyl Sulphate
sec(s)	-	Second(s)
siRNA	-	Small interfering RNA
SF	-	Serum-Free
SFM	-	Serum-Free Medium
TAX	-	Taxol
TBE	-	Tris-boric acid-EDTA buffer
TBP	-	TATA binding protein
TBS	-	Tris Buffered Saline
TE	-	Tris-EDTA
Topo II	-	Topoisomerase II
Td	-	Thymidine
TEMED	-	N, N, N', N'-Tetramethyl-Ethylenediamine
Tris	-	Tris(hydroxymethyl)aminomethane
UHP	-	Ultra high pure water
v/v	-	volume/volume
w/v	-	weight per volume

Table of Contents

Section 1.0 Introduction

Drug resistance, and the role of p53, in lung cancer cell lines

Abstract

This thesis sets out to increase our knowledge of mechanisms by which lung cancer cells develop resistance to chemotherapeutic agents. The involvement of the tumour suppressor p53 in the development of drug resistance in lung cancer cell lines was investigated. p53 is a tumour suppressor gene, which is mutated in more than half of all tumours. Most chemotherapeutic drugs cause DNA damage that is sensed by p53, which either arrests the cell cycle to allow DNA repair or induces apoptosis. Wild-type p53 was transfected into several cell lines; A549, which expresses wild-type p53, DLKP-SQ, which expresses mutant p53 and H1299 which is p53 null. Clones were isolated from these cell lines and tested for changes in sensitivity to the chemotherapeutic agents adriamycin, taxol and carboplatin. A549 transfected clones showed an increase in p53 protein after transfection, however, these cells did not display substantial changes in sensitivity to the chemotherapeutic agents tested. The cell line H1299, which is p53 null, expressed p53 protein after stable transfection, and was chosen for further analysis. This p53-expressing cell line displayed only small changes in sensitivity to chemotherapeutic agents compared to control-transfected cells. No correlation was observed between the p53 status of the cell lines and the ease of developing resistant variants. To further investigate the molecular basis of drug resistance in lung cancer, a panel of four cell lines were chosen for pulse-selection with chemotherapeutic agents. The cell lines include two adenocarcinoma (AC) and two large cell carcinoma (LCC) cell lines. They were pulse-selected with taxol and carboplatin, both of which are clinically relevant drugs for treatment of this type of cancer. The eight novel cell lines obtained were tested for sensitivity to a cross-section of chemotherapeutic agents and for expression of the multidrug resistance (MDR) efflux pump proteins, Pgp and MRP-1. The taxol-selected variants were chosen for further analysis because the resistance profile was stable and the concentration of drug used for selection was at a clinically achievable level. Microarray analysis was used to identify genes associated with the development of taxol resistance. Ten differentially expressed genes with a possible role in taxol resistance were chosen from this analysis. These genes were further investigated by siRNA transfection, in order to determine the functional relevance of these genes in drug resistance. The taxol-selected variants analysed by microarray analysis provide a unique opportunity to study less well characterised mechanisms of taxol resistance, since these variants do not display classical MDR.

Section 1.0: Introduction

1.1 Lung Cancer

Cancer has become the most feared disease of the last century in the western world. In fact, the term "cancer" includes over a hundred different forms of the disease. Cancer can develop from nearly every tissue in the body. It develops when a mutation occurs in a gene in a normal cell resulting in its transformation. The cell might then undergo uncontrolled proliferation and gain the ability to migrate away from its tissue of origin (Weinberg, 1996). Among all types of cancer, lung cancer is the most common form. The national cancer registry (All-Ireland cancer statistics 1994-1996) reported that there is an average of 2300 lung cancer deaths per year in Ireland. It is approximated that 87% of lung cancer cases are caused by cigarette smoking (Hecht, 2002), but this figure may be as high as 95%. Smoking has also been associated with many cancers other than lung cancer such as oral and oesophageal cancers. The most powerful carcinogens in tobacco are polycyclic aromatic hydrocarbons (PAHs), *N*-nitrosamines and aromatic amines. Since only approximately 20% of smokers develop lung cancer (Hecht, 2002), it is believed that some people are more susceptible to the carcinogens in tobacco than others. Other causes of lung cancer include exposure to chemicals such as asbestos and arsenic, as well as the naturally occurring radioactive gas radon. Passive smoking of environmental tobacco smoke (ETS) has been linked with the development of lung cancer in non-smokers. Lung cancer, therefore is one of the easiest cancers to prevent, but remains one of the most difficult to cure.

1.1.1 Lung cancer classification

Symptoms associated with lung cancer are cough, dyspnoea, haemoptysis and post obstructive pneumonia, (Hoffman *et al.*, 2000), although lung cancer can present initially with no symptoms. Diagnosis is achieved by either invasive or non-invasive methods. Non-invasive methods for diagnosing lung cancer include sputum cytology and chest radiography. From here, invasive techniques such as bronchoscopy and lung biopsy are usually necessary. While the location and size of the lung tumour can be estimated from a chest x-ray or CT scan, accurate diagnosis and staging requires a biopsy, to histologically type the cells and determine if local nodes are involved.

Lung cancer is divided into 2 main groups, small cell lung cancer (SCLC) and non-small cell lung cancer (NSCLC). The cellular classification of lung cancer types can be seen in Table 1.1.

Table 1.1 Lung cancer – cellular classification

NSCLC	**Squamous cell carcinoma**
	(a) Spindle cell variant
	Adenocarcinoma
	(a) Acinar
	(b) Papillary
	(c) Bronchioalveolar
	(d) Solid carcinoma with mucin formation
	Large cell carcinoma
	(a) Giant cell carcinoma
	(b) Clear cell carcinoma
SCLC	**Small cell carcinoma**
	(a) Oat cell carcinoma
	(b) Intermediate cell type
	(c) Combined oat cell carcinoma

This histologic classification was compiled by the World Health Organisation (WHO). SCLC and the subtypes of NSCLC – adenocarcinoma, squamous cell carcinoma and large cell carcinoma, account for 95% of lung cancers. SCLC accounts for approximately 20% of all lung cancers. These tumours are very aggressive and generally present with distant metastases at diagnosis. SCLC usually originates from a central location in the lung. These tumours have a rapid growth rate, and have the poorest prognosis of all lung cancer subtypes.

NSCLC is further divided into three categories, squamous cell carcinoma (30% of all lung cancers), adenocarcinoma (40%) and large cell carcinoma (10%). Squamous cell carcinoma usually develops from within a central bronchus in the lung and commonly displays central cavitation from necrosis. They are characterised by keratin formation. Squamous cell carcinomas are slow growing and develop metastases at a late stage. Adenocarcinomas usually develop centrally from surface epithelial cells in larger bronchi. They are characterised by gland formation or the presence of mucus production. These tumours tend to metastasise early and have a rapid growth rate. A common subtype of adenocarcinoma is bronchioloalveolar carcinoma (BAC). This is one of the rarer classes of lung cancer that is not associated with tobacco. Large cell carcinoma is characterised by large cells with large nuclei and prominent nucleoli. These tumours are usually poorly differentiated and tend towards large peripheral masses.

Staging of lung cancer is very important, since it will determine the type of treatment received. The international staging system for lung cancer can be seen in Table 1.2. This staging system classifies the cancer based on the Tumour, Node, Metastasis (TNM) designation.

The designation T1-4 refers to the size and location of the primary tumour: T1 refers to a tumour that is less than 3cm in size; T2 refer to a tumour that is greater than 3cm dimension, involves the main bronchus and invades visceral bronchus; T3 refers to a tumour of any size involving chest wall, diaphragm, mediastinal pleura or parietal pericardium and T4 refers to a tumour of any size that invades major structures e.g. heart, oesophagus, mediastinum, or has a malignant pleural effusion.

The involvement of regional lymph nodes is assessed next in the staging process: N0 – no metastasis to nodes; N1 – metastasis to ipsilateral peribronchial and intrapulmonary nodes; N2 – metastasis to isilateral mediastinal or subcarinal lymph nodes and N3 – metastasis to contralateral mediastinal, hilar scalene or supraclavicular lymph nodes.

In cases where distant metastases are present (M1), the tumour is diagnosed as stage IV lung cancer. Early stage lung cancers are the most treatable, with later stage cancers such as stage IIIB and IV being virtually incurable.

Table 1.2 International staging system for lung cancer

Stage	Tumour (T)	Nodes (N)	Metastasis (M)
Occult	TX	N0	M0
0	Tis	N0	M0
IA	T1	N0	M0
IB	T2	N0	M0
IIA	T1	N1	M0
IIB	T2	N1	M0
	T3	N0	M0
IIIA	T1	N2	M0
	T2	N2	M0
	T3	N1	M0
	T3	N2	M0
IIIB	Any T	N3	M0
	T4	N2	M0
IV	Any T	Any N	M1

(TX – primary tumour cannot be assessed; Tis – carcinoma *in situ*)

1.1.2 Treatment of lung cancer

The choice of treatment for patients with lung cancer depends strongly on the stage. Other details taken into account include clinical stage, pulmonary function and cell type. Surgery is the major therapeutic option for lung cancer patients, however; approximately 75% of lung cancers are inoperable at time of diagnosis. The type of surgery available for treatment of lung cancer are segmental resection, lobectomy, sleeve resection and pnemonectomy. Surgery is only curative in patients with early stage lung cancer. Radiation therapy can also be curative for a small percentage of patients. Currently, chemotherapy can offer improvement in median survival, but overall survival from lung cancer is poor. Chemotherapy is the use of pharmaceutical agents for the treatment of a disease and overall has been very successful in the

treatment of certain types of cancer. The main aim of chemotherapy is to kill the tumour cells with the least possible effect on normal cells. Chemotherapy is mainly based on empirical data and clinical experience (Debatin, 2000). Chemotherapy is often used in combination with surgery or other therapies such as radiotherapy, known as adjuvant chemotherapy. It is especially important for increased survival in cancer patients were these other treatments have failed.

For patients with early stage (I or II) NSCLC, surgery is the treatment of choice. After resection of these tumours, adjuvant chemotherapy is generally given to the patients. Locally advanced NSCLC is treated with a combination of radiotherapy and chemotherapy. In advanced NSCLC, surgery is not usually attempted. Chemotherapy is the treatment of choice for these tumours. This generally consists of a platinum agent in combination with another anticancer agent. In these situations, chemotherapy is used to increase survival time, rather than to cure the patient. Chemotherapeutic drugs used to treat NSCLC patients are traditionally cisplatin, carboplatin, VP-16, vinblastine, vindesine and more recently taxol, taxotere, irinotecan, vinorelbine and gemcitabine. Regimens using a combination of two or more chemotherapy drugs have shown higher response rates and increased survival for lung cancer patients. In particular, the combination of gemcitabine and cisplatin has been shown to be a very effective combination against NSCLC (Manegold, 2002).

SCLC is such an aggressive cancer that at diagnosis, median survival time is 3 months without treatment (Chrystal *et al.*, 2004). In the treatment of SCLC primarily cisplatin, carboplatin VP-16, cyclophosphamide, adriamycin, vincristine, lomustine and ifosfamide are used. Although combination therapy has shown good response rates, median survival time of SCLC patients remains low. The most commonly used combination in the treatment of SCLC is etoposide and cisplatin.

Chemotherapy has a role in increasing median survival time in advanced lung cancer, and preventing recurrence in resected early stage lung cancer. However, the promise of better treatments for lung cancer lies in a better understanding of the disease. New agents such as tyrosine kinase inhibitors and angiogenesis inhibitors show potential both on their own and particularly in combination with the standard treatments (Hirsch *et al.*, 2002).

1.2 Chemotherapeutic agents

The most commonly used chemotherapy drugs are classified in different chemical groups, e.g. taxanes, vinca alkaloids, platinum compounds, antracyclines, epipodophyllotoxins and antimetabolites, to name only a few. The agents used in this study are discussed below.

1.2.1 Taxol and Taxotere

Taxol (paclitaxel) and taxotere (docetaxel) are members of the taxane family. The taxanes are complex esters. Taxol was originally isolated from the pacific yew tree (*Taxus brevifolia)* in 1971. Taxotere is a semisynthetic derivative from the european yew tree (*Taxus baccata*). Both drugs share a tricyclic taxane skeleton (Figures 1.1 and 1.2). Taxanes interfere with microtubules by reversible high affinity binding of the drugs to polymerised microtubules (Francis *et al.*, 1995). The drugs promote assembly of microtubules by shifting the equilibrium between soluble tubulin and microtubules towards assembly. This results in a stabilisation of microtubules even under conditions that usually promote disassembly. This stabilisation damages the cells by disturbing microtubule-dependent cytoplasmic structures that are required for mitosis and maintenance of cellular morphology. Inhibition of depolymerisation of microtubles leads to cell cycle arrest between the prophase and anaphase stages and to eventual apoptosis (Miller & Ojima, 2001). Resistance to taxol is usually associated either with altered expression of α- and β- tubulins or with overexpression of P-gp.

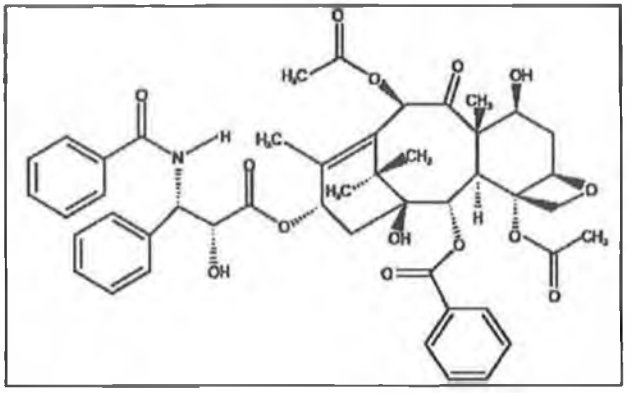

Figure 1.1 Structure of taxol

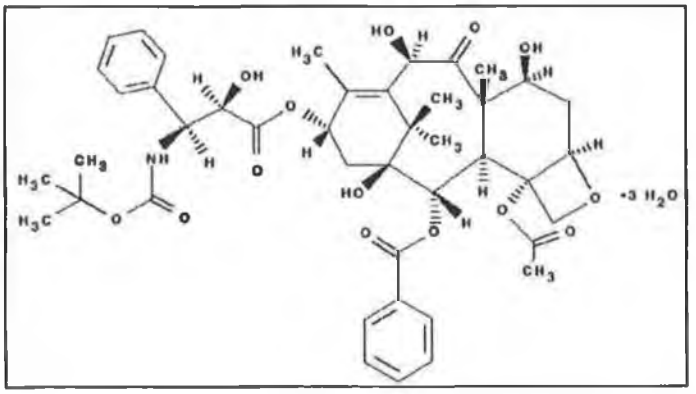

Figure 1.2 Structure of taxotere

1.2.2 Vincristine

Vincristine is a naturally occurring vinca alkaloid derived from the periwinkle plant *Catharanthus roseus*. The structure of vincristine is shown in Figure 1.3. Vincristine is used in the treatment of many cancers including leukaemia, breast cancer and lung cancer. This agent may have a variety of mechanisms of action, but it is mainly believed to exert its antitumour effect by interfering with the function of microtubules. Vincristine inhibits polymerisation of mitotic spindle microtubules by binding to tubulin, resulting in the inhibition of mitosis (Gidding *et al*, 1999). Resistance to vincristine is usually associated with an overexpression of P-gp and MRPs. Other possible mechanisms of resistance to vincristine include changes in tubulin and apoptosis.

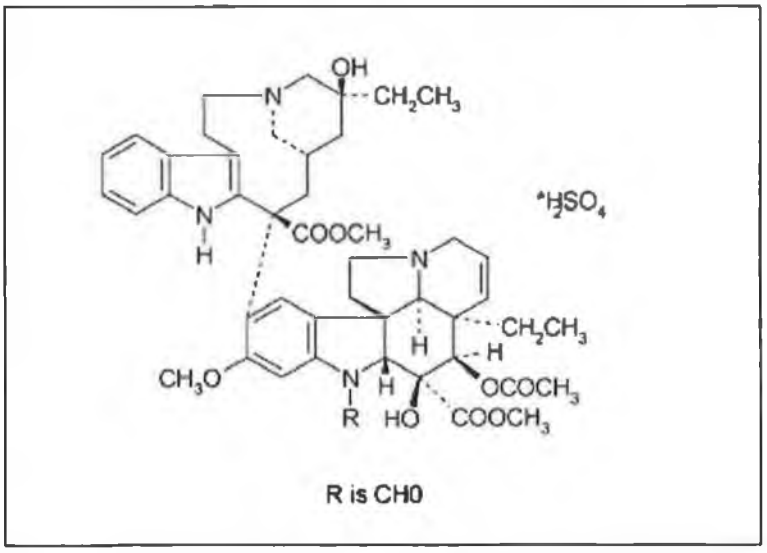

Figure 1.3 Structure of vincristine

1.2.3 Carboplatin and Cisplatin

Two platinum agents were used in this work, cisplatin (cis-diamminedichloro-platinum (II)) and carboplatin (cis-diammine-1,1-cyclobutandicarboxylateplatinum (II)). Their structures can be seen in Figure 1.4. Platinum-containing chemotherapeutic agents most likely exert their cytotoxic effect by reacting with DNA and interfering with DNA replication and cell division, however the mechanism of action is not very well understood. Resistance to cisplatin and carboplatin is associated with decreased uptake of the drug into the cells; inactivation of the drug by cellular thiol compounds and enhanced repair of platinum-related DNA damage and absence of mismatch repair. The formation of conjugates between the thiol glutathione (GSH) and platinum drugs results in a complex, which is a substrate for ABC transporter proteins. This is considered a key step in the mechanism of resistance for these drugs (Longley & Johnston, 2005).

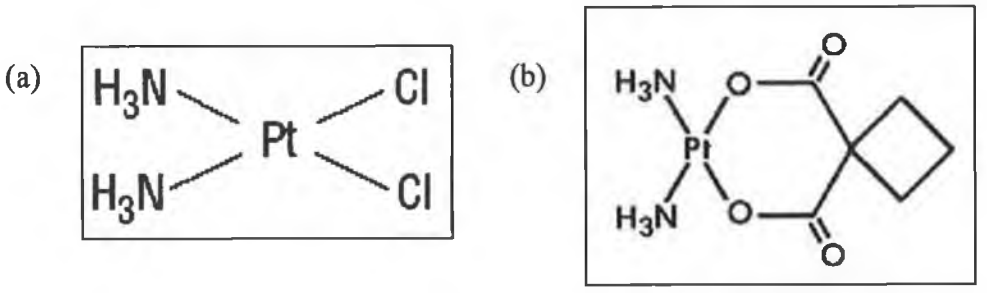

Figure 1.4 Structure of (a) cisplatin and (b) carboplatin

1.2.4 Adriamycin

Adriamycin, also known as doxorubicin, is a member of the anthracyclines. The structure of adriamycin can be seen in Figure 1.5. Antracyclines are widely used in the treatment of cancer. Adriamycin has a number of known mechanisms of action. It can bind tightly to DNA by intercalation, interfering with RNA and DNA synthesis. Adriamycin also induces protein-linked double stranded DNA breaks and interferes with the repair mechanism of topoisomerase II. The drug somehow interferes with the DNA strand breakage reunion of topoisomerase II. Resistance to adriamycin is usually caused by decreased drug accumulation due to actions of members of the ATP-binding cassette family. Resistance may also be caused by downregulation or mutation of Topoisomerase II.

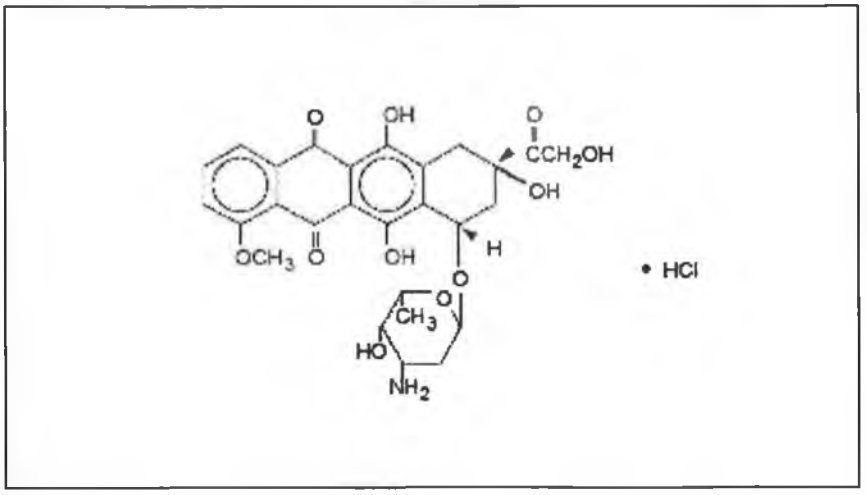

Figure 1.5 Structure of adriamycin

1.2.5 VP-16

VP-16 (etoposide) is a semi-synthetic derivative of podophyllotoxin, a microtubule inhibitor found in extracts of the mandrake plant (Figure 1.6). The enzyme topoisomerase II is the major target of this drug in eukaryotic cells. VP-16 poisons Topoisomerase II converting the enzymes into physiological toxins and generally leading to cell death by apoptosis (Hande, 1998). Resistance to VP-16 may involve altered expression of Topoisomerase II or overexpression of P-gp and MRP-1 leading to decreased intracellular accumulation of the drug.

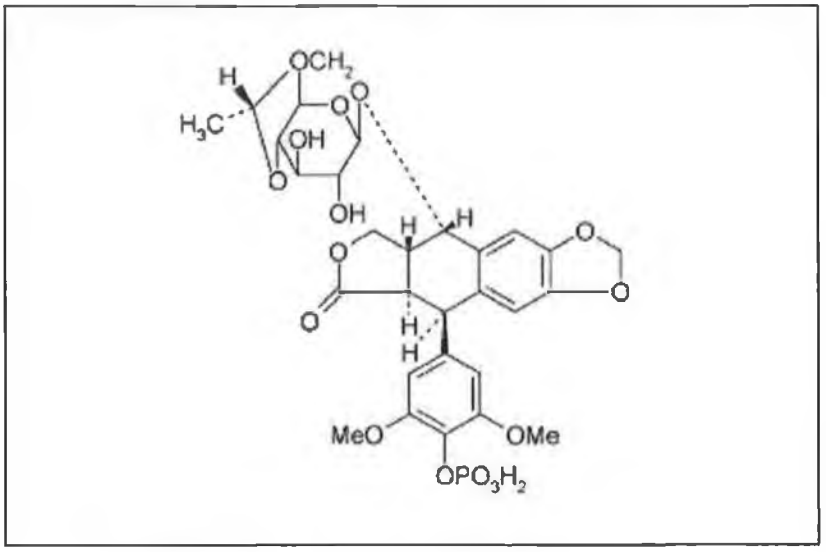

Figure 1.6 Structure of VP-16

1.2.6 5-Fluorouracil

The most commonly used member of the antimetabolite group of agents is 5-Fluorouracil (5-FU). Its structure is shown in Figure 1.7. 5-FU has several major mechanisms of action. It can be metabolised to 5-Fluorodeoxyuridine monophosphate (5dUMP), which inhibits thymidylate synthetase and consequently DNA synthesis. Secondly, it can be converted to 5-fluorouridine triphosphate (FUTP) which is incorporated into RNA leading to impairment in the function and processing of RNA. 5-FU residues can also be incorporated into DNA. These residues are excised leading to DNA damage. Resistance to 5-FU may be due to increased expression of thymidylate synthetase and alterations in the metabolism of the drug.

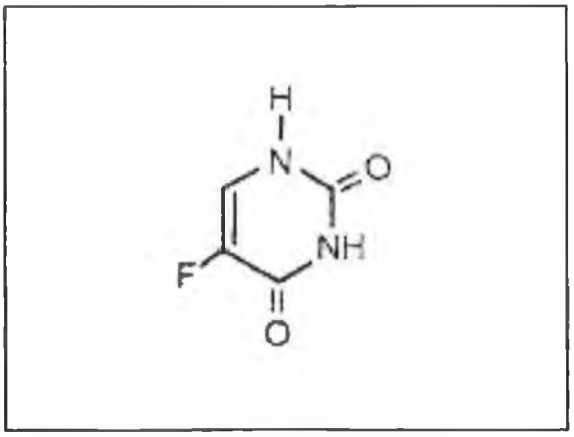

Figure 1.7 Structure of 5-Fluorouracil

1.3 Chemotherapy resistance

A major obstacle in the use of chemotherapy for cancer treatment is the development of resistance. Consequently, a better understanding of the mechanisms of drug resistance would help to overcome this obstacle. Intrinsic and acquired drug resistance are believed to cause treatment failure in over 90% of patients with metastatic cancer (Longley & Johnston, 2005). Some tumours are initially sensitive to an anticancer agent and, over time, develop a resistance to it and this is referred to as acquired resistance. Whereas, other tumours are resistant before treatment and this is known as intrinsic resistance. One of the major factors leading to drug resistance is decreased drug accumulation. This is caused by decreased drug influx or enhanced drug efflux, both of which result in the chemotherapeutic agent not exerting its effect on the tumour. Drug resistance can also be caused by modified drug activation, drug inactivation, alterations in DNA repair mechanisms and altered response to apoptosis. Treatment with one agent can often lead to associated resistance to a number of unrelated agents. The development of resistance to a variety of unrelated chemotherapeutic drugs is called multiple drug resistance (MDR). MDR is caused by a variety of changes in the cancer cells and is almost always multifactorial.

1.3.1 P-gp

Classical multidrug resistance is mediated by P-glycoprotein (P-gp) and is the best-characterised mechanism of resistance. P-gp is a member of the ATP-binding cassette (ABC) family of transporter molecules. It is a 170kDa membrane-bound glycoprotein, encoded by the MDR1 gene present on chromosome 7q21. P-gp is made up of two homologous halves which contain six transmembrane domains and an ATP-binding domain, separated by a linker protein. P-gp is an energy dependent pump, capable of transporting hydrophobic compounds out of the cell (Ambudkar *et al.*, 1999). P-gp is frequently overexpressed in post-chemotherapy tumours where it hinders the cytotoxic response to drugs, thus somewhat desensitising the cells. Overexpression of P-gp is associated with decreased cellular uptake of a drug, which allows cells to survive in the presence of higher drug concentrations. This drug transport can happen against a concentration gradient. Drug enters the cells via a non-energy dependent mechanism and leaves via this active ATP pump (Germann, 1993). P-gp can transport a wide

range of compounds, which share little significant structural similarity. These compounds can vary in size from 250Da to 1.9kDa and are usually organic (Schinkel, 1997). Chemotherapeutic agents known to be pumped by P-gp include vincristine, taxol and adriamycin (Figure 1.8).

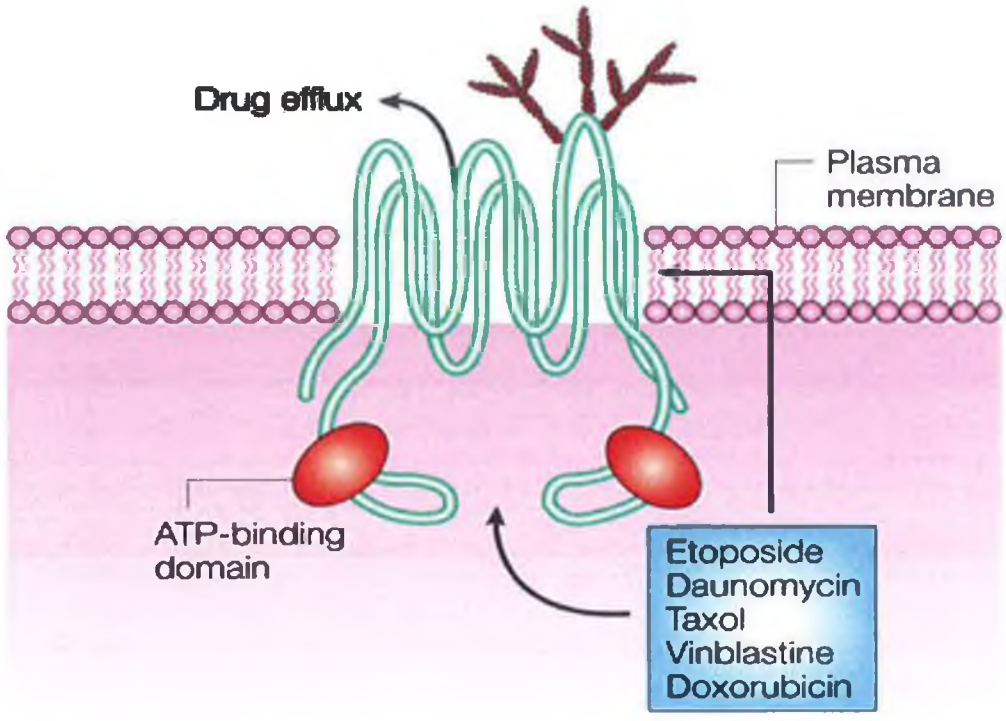

Figure 1.8 P-glycoprotein (P-gp) as a transmembrane drug efflux pump. (Sorrentino, 2002).

1.3.2 MRP family

Multidrug resistance-associated proteins (MRPs) are ATP-binding cassette transmembrane transporter proteins. MRP1 is the most characterised member of the group. The MRP1 gene encodes a 190kDa transmembrane protein whose structure is somewhat homologous to P-gp/MDR1. It is located in the plasma membrane and endoplasmic reticulum of drug-resistant cells. MRP1 is thought to transport both hydrophobic compounds and anionic drug conjugates (Klein *et al.*, 1999). In general, MRP1 relies on intracellur levels of glutathione (GSH) for drug transport. Chemotherapeutic agents known to be pumped by MRP1 include etoposide and adriamycin. Increased expression of MRP1 is associated with drug resistance, which can be reversed by a decrease in its expression. MRPs are often overexpressed in NSCLC.

Both P-gp and MRP are members of the ABC-protein family. These proteins function as transport ATPases hydrolysing ATP in conjunction with transporting their substrate molecules through cellular or intracellular membranes. Although P-gp and MRP-1 have only 15% sequence homology, both function in an energy-dependent drug efflux system which reduces intracellular accumulation of drug. Other members of the ABC family of transporters include MRP2, MRP3, MRP4, MRP5 and BCRP. These family members are also involved in drug efflux, however, they are not as extensively studied as P-gp and MRP1.

1.3.3 LRP

Lung resistance-related protein (LRP) is a 110kDa vesicular protein which is overexpressed in a variety of tumour cells that display intrinsic or acquired chemoresistance. LRP is identical to the human major vault protein. Vaults are the largest known ribonucleoprotein complexes and are highly conserved among eukaryotes. The function of vaults is not fully understood; they might play a role in the transport of drugs into cytoplasmic vesicles or directly out of a cell (Borst *et al.*, 1997). Upregulation of LRP has been shown to be associated with an increase in drug resistance, however, a study by Siva *et al.* (2001), showed that upregulation of this protein alone is not sufficient to confer drug resistance to a cell line *in vitro*.

1.3.4 Reversal of MDR

A large number of studies have focussed on blocking the function of multidrug resistance pumps, thus attempting to reverse MDR. Some non-toxic compounds can inhibit drug transport by acting as competitive or non-competitive inhibitors or inhibiting ATP binding. Non-steroidal anti-inflammatory drugs (NSAIDS) such as sulindac and indomethacin have been shown to increase the cytotoxic effects of commonly used chemotherapy drugs in cells which have become resistant. Early studies in this area observed that P-gp inhibitors such as verapamil were efficient *in vitro* but were poor inhibitors *in vivo*. This led to the development of second- and third-generation P-gp inhibitors such as GF120918, also known as elacridar. This inhibitor is highly effective and was developed specifically for P-gp (Schinkel and Jonker, 2003). It has proven more difficult to obtain a specific MRP1 inhibitor. Studies in our laboratories show that sulindac is a potent inhibitor of MRP1, enhancing the effect of doxorubicin in human tumour xenografts (O'Connor *et al.*, 2004).

1.3.5 MDR and invasion and metastasis

The ability of tumour cells to move from the primary tumour, travel through the circulatory system and establish a secondary tumour at a distant site is known as metastasis and is a leading cause of death among cancer patients. Many processes are necessary to allow a tumour cell to metastasise. These include angiogenesis, changes in cellular attachment, degradation of the extracellular matrix and the ability of the tumour cells to grow in the secondary site (Woodhouse *et al*, 1997).

Invasion is a critical step in the process of metastasis. Invasion is the active translocation of neoplastic cells across tissue boundaries and through host cellular and extracellular barriers (Liang *et al.*, 2002). In order for a cancer cell to invade, three steps must occur: proteolysis of the extracellular matrix (ECM); pseudopodial extension and cell migration (Woodhouse *et al.*, 1997). Proteolysis of the ECM can be caused by matrix metalloproteinases, a family of zinc-binding enzymes.

The correlation between drug resistance and invasion in cancer cells remains unclear. There is reason to suspect a link considering that tumour cells selected for resistance to chemotherapeutic drugs often become more invasive relative to sensitive parental cells (Liang *et al.*, 2004) and that it has been observed that secondary metastatic tumours are in some cases more resistant to chemotherapy than primary tumours (Furukawa *et al.*, 2000). Studies in our laboratories on the human nasal carcinoma cell line, RPMI-2650, indicate that pulse-selection with taxol while leading to an increase in drug resistance, did not promote *in vitro* invasiveness in the human nasal carcinoma cell line. However, selection with the anticancer agent melphalan increased *in vitro* invasiveness (Liang *et al.*, 2001). Furthermore, mitoxantrone, 5-FU, methotrexate, BCNU, cisplatin and chlorambucil induced an invasive phenotype in the human lung carcinoma cell line, DLKP, whereas VP-16, vincristine, taxotere and CCNU did not (Liang *et al.*, 2004.).

1.4 Taxol resistance

As mentioned earlier, taxol is a drug from the taxane family used in the treatment of many cancers. Resistance to taxol is a significant problem associated with the use of this drug. Studies have shown that development of resistance to taxol is associated with cellular transport of the drug and the binding of taxol to microtubules. It has also been shown recently that certain oncogenes may be involved in taxol resistance.

Taxol-resistant cell lines have been shown to overexpress the efflux pump P-gp, but not MRP1 (Van Ark-Otte *et al.*, 1998; Dumontet *et al.*, 1996). Huang *et al.* (1997) demonstrated that in a taxol resistant subline of HL60, P-gp overexpression led to decreased taxol accumulation in the cells and impaired taxol-induced apoptosis. This group also demonstrated that MRP1 overexpression did not confer resistance against taxol in HL60 cells. In an earlier study by this group various taxol-resistant sublines of HL60 were found to overexpress P-gp and the resistance to taxol observed in these sublines was partially circumvented by treatment with cyclosporine or verapamil. This study demonstrated that the taxol resistance observed was not solely due to P-gp overexpression, since treatment with P-gp inhibitors only partially reversed taxol resistance (Bhalla *et al.*, 1994).

Other groups have demonstrated that resistance to taxol can be due to a P-gp-unrelated mechanism. The main target of taxol in cells is the microtubules. Microtubules are involved in a wide range of cellular functions, for example, mitosis and maintenance of cell shape. Microtubules are hollow cylindrical tubes consisting of highly dynamic polymers made up of α and β tubulin heterodimers (Jordan, 2002). These heterodimers are associated to form protofilaments and these arrange laterally to form the hollow microtubules (Orr *et al.*, 2003). Microtubules exhibit dynamic instability. This non-equilibrium behaviour occurs due to the association and dissociation of tubulin dimers from the microtubule ends, which leads to rapid growth and shrinkage of the microtubules. Microtubule-associated proteins (MAPs) and proteins such as stathmin can stabilise microtubules through interaction with tubulin dimers and play a role in regulation of microtubule stability.

Alterations in assembly and disassembly dynamics of microtubules play a key role in the antimitotic effects of stabilising agents such as taxol. *In vitro*, taxol can bind to the microtubule polymer, enhancing the polymerisation of taxol. Taxol binds to the β-tubulin subunit in microtubules in a specific and reversible manner (Orr *et al.*, 2003). The effect of taxol is to alter the kinetics of microtubules assembly. Taxol treatment leads to a decrease in the critical concentration of microtubule protein needed for microtubule assembly but also increases polymer mass and induces microtubule bundle formation. Since the microtubules of a cell are the target for the action of taxol, changes associated with microtubules have been implicated in resistance to the agent.

A study by Goncalves *et al.* (2001) on taxol resistant variants of the lung cancer cell line A549, which are also dependent on taxol for normal growth, determined that dynamic instability of microtubules was significantly increased in these resistant/dependent cells. They hypothesise that this instability might explain the dependence of these resistant cell lines on taxol for growth.

Parekh *et al.* (1997) established a series of taxol-resistant human ovarian carcinoma clones with increasing degrees of resistance. These were used to study the mechanisms by which cancer cells develop resistance to taxol. The cell lines displayed resistance to taxol in the range of 250 to >1500–fold. They found that taxol resistance could develop via P-gp-mediated and non-P-gp-mediated mechanisms. Non-P-gp-mediated resistance to taxol may be due to alterations in the taxol-binding affinity of the microtubules and alterations in tubulins.

There are six β-tubulin isotypes termed class I, II, III, IVa, IVb and VI (Kavallaris *et al.*, 1997). Numerous studies have demonstrated that mutations in β-tubulin, and differential expression of these β-tubulin isotypes have a role in determining sensitivity to taxol. Kavallaris *et al.* (1997) demonstrated the involvement of altered expression of β-tubulin in taxol resistance *in vivo*. This group studied tubulin expression in untreated primary and taxol-resistant ovarian tumours. They found that the taxol-resistant samples displayed increased expression of β-tubulin isotypes class I, III and IVa and proposed that it was these alterations that led to the taxol-resistant phenotype. In agreement with this study, Derry *et al.* (1997) found that microtubules composed of $\alpha\beta_{III}$- and $\alpha\beta_{IV}$-tubulin were less sensitive to the suppressive effects of taxol than other forms of tubulin.

A study by Monzo *et al.* (1999) identified a correlation between taxol resistance and mutations in β-tubulin. Missense mutations of β-tubulin were discovered in NSCLC patients, without prior chemotherapy treatment. The group postulate that these mutations might provide a survival advantage to the cells when treated with a microtubules-stabilising agent such as taxol. Similarly, Giannakakou *et al.* (1997) identified specific point mutations in β-tubulin which lead to decreased taxol activity *in vitro* and confer resistance to taxol. This group suggests that the mutated β-tubulin may alter the taxol binding site on β-tubulin, so that taxol binding is inhibited by the mutations.

More recently alterations in α-tubulin have been implicated in taxol resistance. This was the focus of a study by Han *et al.* (2000). The group developed a taxol-resistant NCI-H460 cell line (H460/T800), which is 1000 fold more resistant to taxol than the parent cells and showed cross-resistance to colchicine, vinblastine and doxorubicin. Besides an increased expression of P-gp, the resistant cells had an overexpression of α- and β-tubulin. They found that down-regulation of the α-tubulin expression by antisense resulted in an increased drug sensitivity of the cell line, suggesting a role for α-tubulin in determining sensitivity to taxol. Martello *et al.* (2003) demonstrated that two taxol-resistant variants of the lung cancer cell line A549, although they display normal binding of taxol to the microtubules, have a mutation in the major α-tubulin isotype Kα1. The location of this mutation suggests that it may lead to altered binding of the regulatory proteins stathmin or MAP4 to α-tubulin.

Other studies on the development of taxol resistance have focussed on individual proteins involved in cell processes such as apoptosis. Survivin is a member of the family of inhibitors of apoptosis proteins (IAPs). IAPs are evolutionarily conserved proteins that interfere with the process of cell death by inhibiting caspases. Survivin has been linked to taxol resistance in several studies. Zafforoni *et al.* (2002) reported a correlation *in vitro* and *in vivo* between expression of survivin and resistance to taxol and taxotere in ovarian cancer. Similarly, Ling *et al.* (2004) demonstrated that survivin expression is induced by taxol treatment and that survivin is involved in the evasion of taxol-induced apoptosis in resistant cells. Other proteins involved in apoptosis such as the Bcl family of proteins have also been implicated in taxol resistance (Huang *et al.*, 1997; Tang *et al.*, 1994; Liu *et al.*, 1998).

The tumour suppressor gene p53 has also been associated with taxol resistance. Rakovitch *et al.* (1999) demonstrated that colorectal carcinoma cells lacking functional p53 were more sensitive to taxol than cells expressing functional wild-type p53. There is conflicting literature on the importance of p53 status in determining sensitivity to chemotherapeutic agents. A recent study by Reinecke *et al.* (2005) showed p53 status of renal cell carcinomas did not correlate with sensitivity of these cells to taxol. The role of p53 in drug resistance is further discussed in section 1.6.

Recent studies have identified novel genes and proteins believed to be involved in taxol resistance in cancer. Duan *et al.* (1999) discovered a novel gene that was overexpressed in a taxol resistant cell line called taxol resistance associated gene-3 (TRAG-3). This gene was also found to be overexpressed in other cell lines displaying resistance to taxol. TRAG-3 is not expressed in normal tissue but is expressed in 43% of cancer cell lines. More recently, the same group have identified a novel intracellular mitochondrial protein MM-TRAG believed to be involved in both taxol resistance *in vitro* (Duan *et al.*, 2004). Early studies on this novel gene indicate that it may have an association with Mdr1 expression.

A study by Parekh *et al.* (2002) detected overexpression of a calcium-binding protein, sorcin, in a taxol-resistant ovarian carcinoma cell line. Introduction of sorcin into a number of cell lines led to a low-level taxol resistance developing. The group concluded that sorcin has a role in determining taxol sensitivity; however since no changes in calcium were detected, the mechanism was unclear. Interestingly, another study by Padar *et al.* (2004) indicated that altered intracellular calcium homeostasis might be involved in the development of taxol resistance in NSCLC.

Wang *et al.* (2004) identified a role for the helix-loop-helix protein TWIST in taxol acquired resistance. Upregulation of TWIST was observed in a number of different cancer types in association with treatment of microtubule-disrupting agents. Recent studies have implicated the expression of other proteins in taxol resistance such as E-cadherin (Ferreira *et al.*, 2005), the mitotic kinesin Eg5 (Marcus *et al.*, 2005) and caveolin-1 (Yang *et al.*, 1998; Roussel *et al.*, 2004).

The various studies that have focussed on mechanisms of taxol resistance reveal the complexity of this problem in the treatment of cancer patients with taxol.

1.5 Drug resistance in lung cancer

Most lung cancers exhibit an intrinsic resistance to chemotherapy already at the time of diagnosis. Most SCLCs are chemotherapy sensitive at diagnosis, but any recurrence of the disease usually displays acquired drug resistance. NSCLC, on the other hand, are predominantly intrinsically resistant to chemotherapy. It is likely that both acquired and intrinsic resistance share common factors, such as expression of drug transporters.

Many groups have studied the expression of the genes involved in this type of resistance. Canitrot and his co-workers examined MRP-1 and MDR-1 gene expression in a panel of seventeen SCLC xenografts established from tumours of chemotherapy-treated and -untreated patients (Canitrot *et al.*, 1998). The previously treated SCLC expressed MRP-1 but not MDR-1, whereas within the untreated tumour samples, six expressed only MRP-1, three expressed only MDR-1, five expressed both and two expressed none. The expression of the drug resistance markers MRP-1, LRP and topoisomerase II (α and β) was studied in advanced NSCLC (Dingemans *et al.*, 2001). This study found that expression of these markers did not correlate with the response of patients with NSCLC to standard chemotherapy. The chemotherapy regimens used in the study were in three combinations: cisplatin and paclitaxel; cisplatin and VP16/VM26; cisplatin and VP16 and ifosfamide.

Many groups have compared *in vitro* and *in vivo* lung cancer samples in order to determine similarities in the development of resistance. For example, Young *et al.* (1999) examined a panel of 23 unselected cell lines (SCLC and NSCLC) as well as 15 patient samples to determine possible correlations between the expression of MRPs and the resistance to four chemotherapeutic agents. They showed that the cell lines exhibited a wide range of sensitivities. They found a higher level of resistance to all tested drugs in the NSCLC compared to the SCLC, a strong correlation between MRP3 mRNA levels and the resistance to doxorubicin and a moderate correlation with resistance to vincristine, VP-16 and cisplatin.

Another study linked chemoresistance of the lung cell line A549 to the expression of LRP (Meschini *et al.*, 2002). The group studied two cell lines established from untreated tumours, A549 and the breast cell line MCF-7. A549 was much more resistant to doxorubicin, whereas MCF-7 cells treated with doxorubicin had significantly higher intracellular levels of the drug. Both cell lines express P-gp and MRP-1 at similar levels, but the study revealed much higher levels of lung resistance protein LRP in A549 cells, which could account for the difference.

1.6 The tumour suppressor p53

Termed "Guardian of the genome" p53 is a tumour suppressor gene, whose 53kDa phosphoprotein product is involved primarily in cell cycle arrest and apoptosis. Li Fraumeni syndrome (LFS) is a genetic disease where there is a germline mutation in p53, (Cadwell & Zambetti, 2001). People who have this disease usually develop malignant tumours early in life. A mutation in the p53 gene occurs in over half of all tumours. Mice that lack p53 can develop normally but usually die from a malignancy within six months, (Cadwell & Zambetti, 2001).

1.6.1 Structure and function of p53

Discovered in 1979, the p53 gene is located on human chromosome 17 and is approximately 20kb in length. The p53 gene is mutated in more than half of all tumours, giving rise to a mutated protein with a single amino acid substitution in most cases. Initially p53 was believed to be an oncogene because of its involvement in so many cancers. It was later discovered that it is the mutant form of p53 that is capable of immortalising and transforming cells (Cadwell & Zambetti, 2001). The gene contains five domains that are highly conserved through evolution, (Figure 1.9A).

The structure of p53 can be seen in Figure 1.9B. The N-terminal sequence from amino acids 1-42 contains an acidic domain that is involved in activation of transcription of target genes. From amino acids 64-92 there is a proline rich domain consisting of five PXXP repeats (where P is proline and X is any amino acid). This domain is required for apoptosis and may be involved in the negative regulation of p53, (Figure 1.9B). The central core domain from amino acids 102-292 is involved in sequence specific DNA binding. From amino acids 324-355 the oligomerisation domain of p53 is responsible for the formation of p53 tetramers which is important for DNA-binding in a sequence specific manner. The C-terminus of p53 holds a nuclear localisation region capable of non-specific DNA and RNA binding, (Cadwell & Zambetti, 2001).

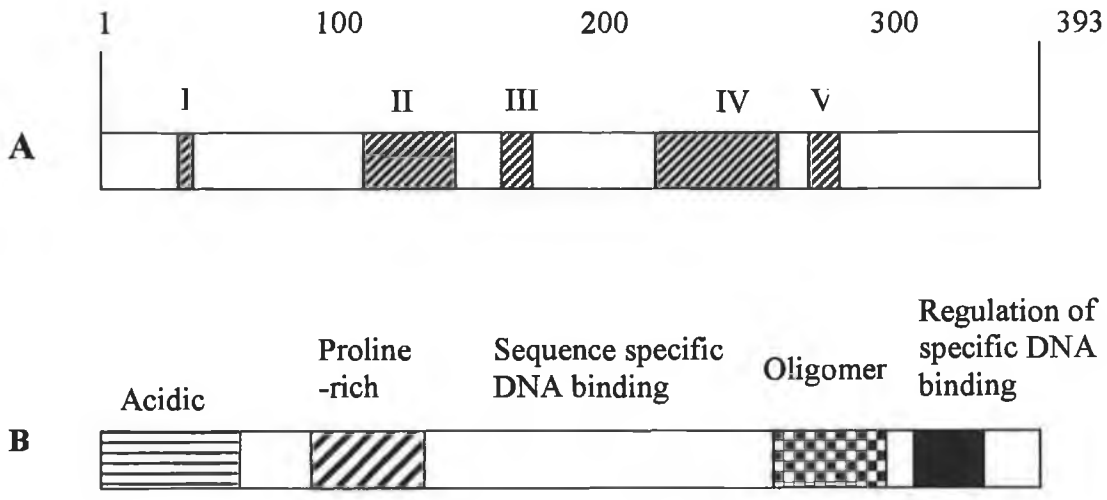

Figure 1.9 Structural and functional domains of p53 protein, (Cadwell & Zambetti, 2001). A - The five evolutionary conserved domains of p53. B – The functional domains of p53

p53 is a sequence specific transcription factor and usually executes its function by activation or repression of target genes, predominantly involved in cell cycle arrest and apoptosis, (Colman *et al.*, 2000). It has a hydrophobic interface in the N-terminal for interaction with transcriptional machinery of the cell, and with its negative regulators, (Levine, 1997). p53 carries out its functions by interacting with specific protein partners (Gallagher & Brown, 1999).

1.6.2 Activation and stabilisation of p53

In normal cells, p53 is inactive and is found at low levels, due to its relatively short half-life. When a genotoxic stress causes DNA damage, p53 becomes phosphorylated and p53 protein levels rapidly accumulate in the cell. DNA strand breaks induce rapid and specific activation of p53 (Pluquet & Hainaut, 2001). P53 accumulates due to enhanced translation of mRNA and is stabilised by post-translational modifications, (Cadwell & Zambetti, 2001). These post-translational modifications have been shown to improve the sequence specific DNA binding and transcriptional activities of p53, (Ryan *et al.*, 2001). P53 translocates to the nucleus where p53 tetramers target p53-responsive genes to activate transcription of proteins necessary to carry out the p53 function required, for example apoptosis or cell cycle arrest, (Colman *et al.*, 2000). Since p53 senses DNA damage, it is important in determining drug sensitivity. Non-genotoxic stress, such as oncogene activation, hypoxia and ribonucleotide depletion, can also induce activation of p53, (Pluquet & Hainaut, 2001).

Activation of p53 can occur by three separate pathways. Ionising radiation causes DNA damage that is sensed by 'checkpoints' that suspend progress through the cell cycle until the damage has been repaired. These checkpoint proteins include DNA-dependent protein kinase, ATM, Chk1 and Chk2. These kinases activated by DNA damage, phosphorylate p53 at amino-terminal sites close to the Mdm2-binding region of the protein, blocking its interaction with Mdm2 and leading to stabilisation of the protein (Vogelstein *et al.*, 2000). Aberrant growth signals, caused by oncogenes such as *ras* and *myc*, leads to activation of p53 by $p14^{ARF}$. These oncogenes stimulate the transcription of the $p14^{ARF}$ protein, which then binds to Mdm2 and inhibits its activity. Activation of p53 by cytotoxic drugs, UV and protein kinase inhibitors is mediated by ATR kinase and casein kinase II (Figure 1.10).

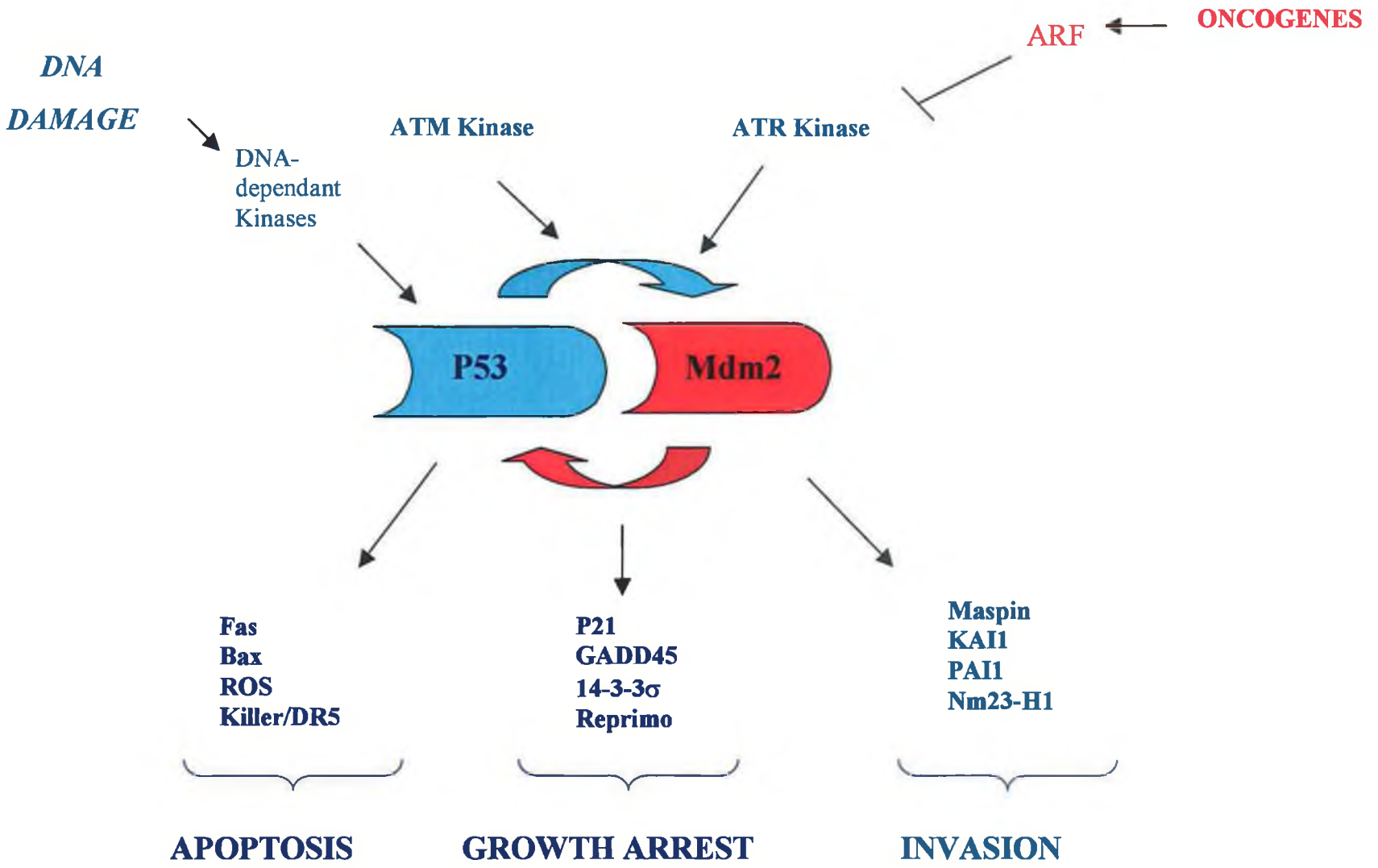

Figure 1.10 p53 activation and downstream functions

1.6.3 Regulation of p53

Accumulation of p53 is regulated by an autoregulatory negative feedback loop involving Mdm2. Mdm-2 gene expression is controlled by p53 and is overexpressed in many tumours (Gallagher and Brown, 1999). When p53 levels are high in the cell, Mdm-2 is transcribed and translated. Mdm-2 binds to the amino-terminal transactivation domain of p53 in the nucleus, preventing its interaction with TATA binding protein (TBP)-associated factors necessary for the regulation of transcription of p53 genes. A leucine-rich area in the Mdm-2 protein, which is a nuclear export signal, causes transport of the Mdm-2:p53 complex into the cytoplasm. Mdm-2 can then induce p53 degradation through ubiquitin-mediated proteolysis, (Colman *et al*, 2000). This can be seen in Figure 1.11. When p53 is inactive, the protein is unstable and in a conformation whereby the C-terminal domain blocks function of the DNA-binding domain (Pluquet and Hainaut, 2001). The disruption of the Mdm2 pathway is the most important mechanism for stabilisation and accumulation of p53 (Zeimet *et al.*, 2000).

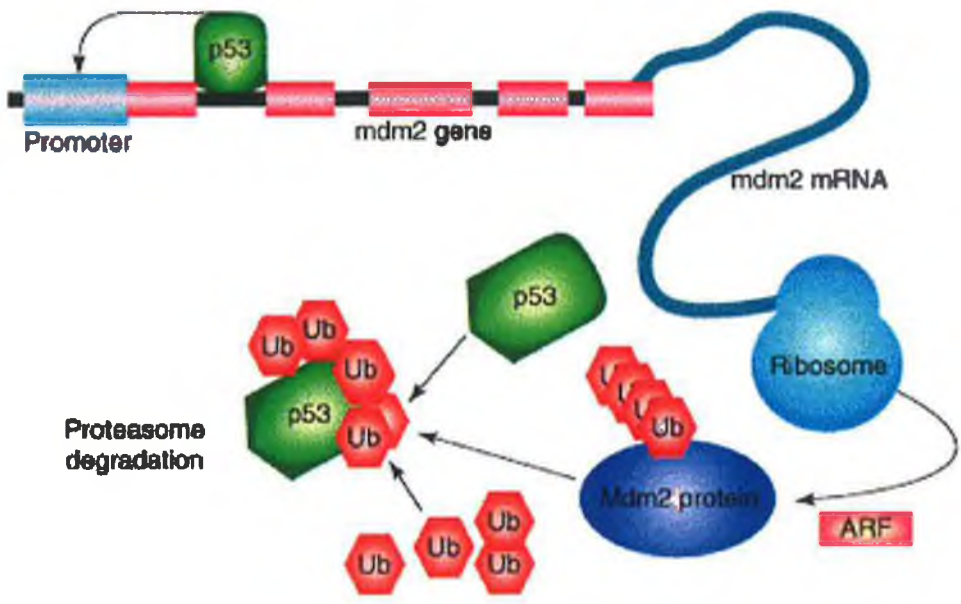

Figure 1.11 The p53 autoregulatory feedback-loop mechanism (Lane & Lain, 2002)

1.6.4 Cell cycle arrest and p53

When DNA is damaged, the activation of p53 occurs which stops the cell cycle to allow for DNA repair. The protein product of the Waf1/Cip1 gene is p21. This gene is a transcriptional target of p53, with two p53-binding sites. $p21^{WAF1/CIP1}$ has a major role to play in p53-mediated cell cycle arrest (Gallagher and Brown, 1999). G1 arrest in response to DNA damage is caused by inhibition of CDKs by cyclin-dependent kinase inhibitors (CKIs). P21 is a CKI induced by p53, p63 and p73. Without CDKs the retinoblastoma protein (Rb) cannot become phosphorylated. Phosphorylation of Rb allows E2F to be released, leading to continuation of the cell cycle. Gadd45α (growth arrest and DNA damage) is also induced with Cdc2 and PCNA, which are associated with the cell cycle, and involved in DNA repair and G2/M cell cycle arrest (Cadwell and Zambetti, 2001).

1.6.5 Apoptosis

The p53 gene family are involved in all pathways of apoptosis. When DNA damage cannot be repaired, p53 can induce programmed cell death or apoptosis. Apoptosis can be triggered intrinsically or extrinsically. Within the cell, a death signal can cause release of cytochrome C from the mitochondria, which can interact with apaf-1 to activate caspases, the executioners of apoptosis. From outside the cell, certain ligands can bind death receptors on the cell surface, and this interaction can also lead to the activation of caspases. Whether apoptosis or cell cycle arrest is the p53 function carried out depends on the stimulus that activated p53, on the cell type (Bunz, 2001) and also on the environment surrounding the cell (Gallagher and Brown, 1999). Apoptosis can also occur by p53-independent pathways. Some of the main proteins involved in apoptosis are under the transcriptional control of wild-type p53. Members of the Bcl family of proteins can regulate apoptosis in the cell. Pro-apoptotic members heterodimerise with anti-apoptotic members, and relative levels of these proteins decide the fate of the cell. The BAX gene, whose protein is pro-apoptotic, is transcribed by p53, since its promoter contains a p53 recognition motif. In addition, the expression of the Bcl-2 protein, which is anti-apoptotic, is repressed by wild-type p53 (Gallagher and Brown, 1999), as is the expression of c-myc, a proto-oncogene (Cadwell and Zambetti, 2001). Overexpression of Bcl-2 can block p53-mediated apoptosis (Levine, 1997). Wild-type p53 also upregulates other pro-apoptotic proteins

like the insulin-like growth factor binding protein IGF-BP3, killer/DR5 and fas/apo1 which are membrane receptors in the tumour necrosis factor receptor (TNFR) family (Cadwell and Zambetti, 2001). When p53 is mutated, less pro-apoptotic proteins are produced and proteins such as Bcl-2 and c-myc are expressed, leading to improper signalling and cell growth (Cadwell and Zambetti, 2001).

1.6.6 Invasion and metastasis and p53

Inhibition of metastasis may be partly controlled by p53 inducing expression of genes that block ECM degradation. The expression of two serpins (inhibitors of serine proteases), Maspin and PAI1 are regulated by p53 (Harms *et al.*, 2004). PAI1 inhibits urokinase-type plasminogen activator (u-PA). U-PA usually leads to the activation of plasmin, which degrades ECM proteins. However, maspin is not thought to inhibit migration or metastasis *in vivo*. KAI1 is a target of p53 and has been shown to inhibit metastasis. The metastasis suppressor gene *Nm23-H1*, a nucleoside diphosphate kinase, is also induced by p53 (Harms *et al.*, 2004).

1.6.7 Mutations in p53

Mutant p53 is also capable of acting as a transcriptional activator, and can upregulate proteins such as MDR-1 (multiple drug resistance), PCNA, Bag1 and c-myc (Cadwell and Zambetti, 2001). Along with these proteins involved in intrinsic apoptosis, p53 can sometimes induce CD95 expression on the cell surface of tumours, which can lead to extrinsic apoptosis (Ferreira *et al.*, 1999). The most common mutation of p53 is missense mutation, which leads to a protein with a single amino acid substitution. These mutations are usually found within the sequence-specific DNA-binding domain (Pfeifer and Holmquist, 1997). In a study carried out by Jassem *et al.*, (2001), on 332 non-small cell lung cancer patients, 96 were found to have a p53 mutation. Of these mutations, more than half were located on either exon 5 or exon 8.

There are three mechanisms by which p53 mutations affect its ability to suppress tumourigenesis (Cadwell & Zambetti, 2001):

(1) Loss of wild-type p53 tumour suppressor function
(2) Dominant-negative inhibition of wild-type p53 function
(3) Gain of function giving selective growth advantage to cells expressing mutant p53.

These can be seen schematically in Figure 1.12. Most p53 mutants are highly stable and accumulate in the cell, in contrast to wild-type p53. In dominant negative inhibition, both wild-type and mutant p53 are present, but wild-type p53 becomes overwhelmed by the formation of dysfunctional tetramers between wild-type and mutant p53 (Gallagher and Brown, 1999). Mutant p53 proteins may also gain oncogenic properties which are not dependent on inhibition of wild-type p53, such as the ability to transcribe different genes as mentioned earlier. Wild-type p53 function can be inactivated not only by mutations, but by cellular or viral proteins which can sequester or degrade the protein (Gallagher & Brown, 1999). Mdm2, the main regulator of p53 is an example of this since it can sequester p53.

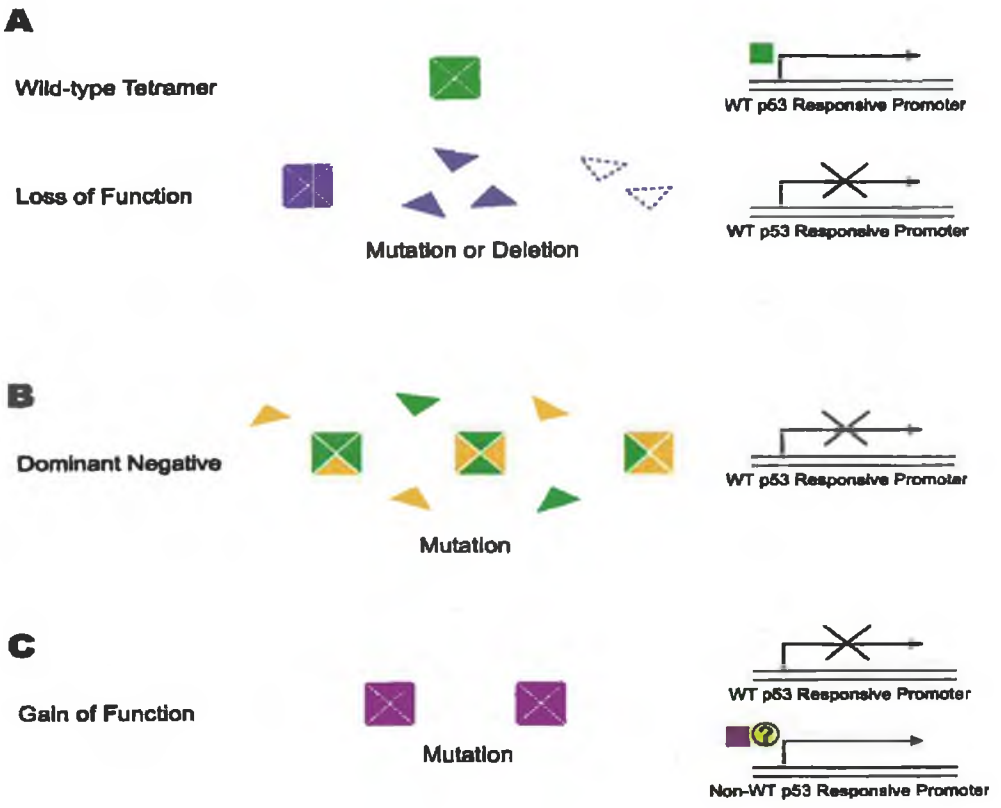

Figure 1.12 The role of p53 mutations in tumorigenesis (Cadwell & Zambetti, 2001)

1.6.8 Family members

The proteins p63 and p73 are homologues of p53. They both transactivate p53 target gene expression and induce apoptosis when overexpressed. These family members, unlike p53, are rarely mutated in human cancer. While p53 has predominantly a single isoform, there are three isoforms of p63 and seven isoforms of p73. All of the family members contain at least one proline-rich domain. All p53 family members are activated and stabilised after DNA damage (Harms *et al.*, 2004). The proteins are activated and stabilised in response to common and distinct signals, allowing them to function independently.

1.6.9 Role of p53 in Multiple Drug Resistance (MDR)

Mutation of p53 is thought to play a major role in conferring multiple drug resistance to cells. Since p53 can control apoptosis and the cell cycle, if the action of p53 is blocked, then apoptosis or cell cycle arrest may fail to occur in response to DNA damage caused by drug administration. If a cell fails to die after treatment with the drug, it has become resistant. In other words, resistance will develop with loss of the genes necessary for death (Krishna and Mayer, 2000). A study carried out by Sampath *et al.* (2001), found that mutant p53 strongly upregulates human MDR1, but does not activate MRP1 (multidrug resistance protein). MDR1 and MRP1 are two of the most commonly expressed drug resistance genes.

Taking into account the functions of p53, a contradictory two-possibility scenario emerges. On one hand, p53 can mediate apoptosis in response to DNA damage caused by chemotherapy, thereby helping the cell to die. On the other hand, by inducing cell cycle arrest and favouring DNA repair p53 has the potential to increase resistance by allowing cells to live after DNA has been damaged by chemotherapeutic agents (Ferreira *et al.*, 1999). This can be seen visually in Figure 1.13.

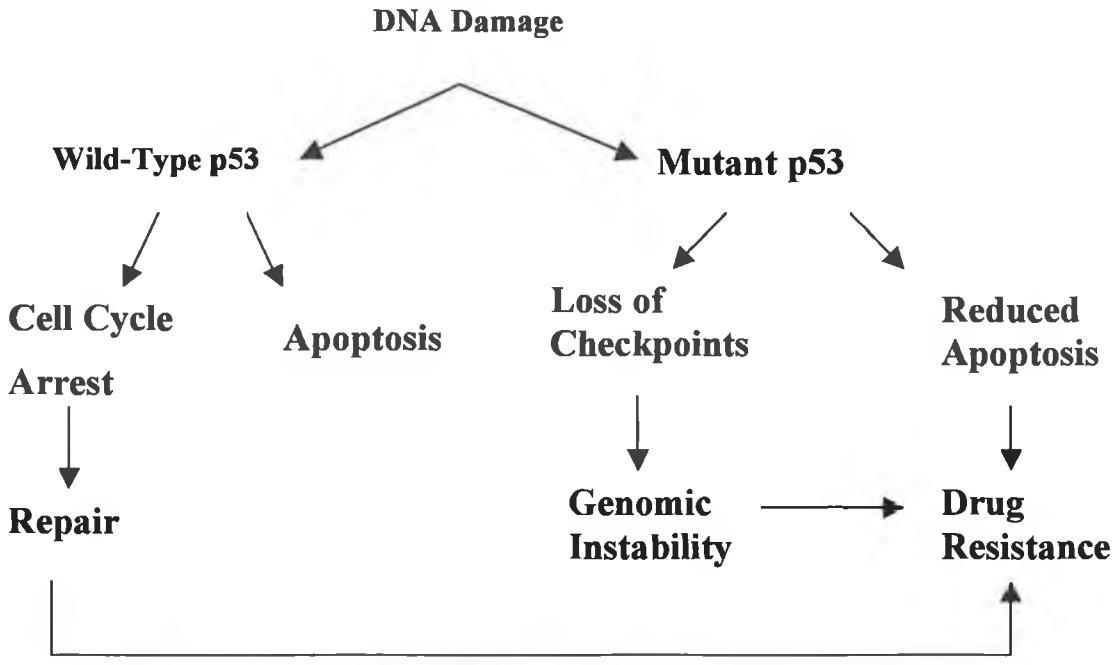

Figure 1.13 Outlined of the proposed influence of p53 on cellular processes relevant to cytotoxic therapy, (Zunino *et al.*, 1997).

Lowe *et al.*, (1993) carried out a study exploring the effects of p53 expression on normal and oncogene expressing cells following irradiation and treatment with various chemotherapeutic agents, and found that p53 was required for the efficient activation of apoptosis after treatment. Cells not expressing p53 were found to be much more resistant to the agents. They also noted that p53-independent cytotoxicity was more prevalent at high doses of irradiation or chemotherapy. The role of p53 in cell cycle arrest and apoptosis was investigated following treatment of lymphoma cell lines with γ-rays, etoposide, nitrogen mustard and cisplatin (Fan *et al.*, 1994). γ-rays and etoposide were found to induce strong G1 arrest in wild-type p53 cells but not in mutant p53 cells, and caused rapid accumulation of p53 and $p21^{WAF1/CIP1}$. Nitrogen mustard and cisplatin induced relatively little G1 arrest and a slower accumulation of p53. The conclusion drawn from the results was that p53 mutations are often

associated with increased resistance to DNA damage and that this is related to evasion of p53-mediated apoptosis.

Zhu *et al.* (1999), compared two gastric cancer cell lines HKN28, (expresses mutant p53), and AGS (expresses wild-type p53), for their response to treatment with the nonsteroidal anti-inflammatory drug (NSAID) indomethacin. It was found that the wild-type p53 cell line was more sensitive to growth inhibition and that in this cell line, indomethacin-induced apoptosis occurred more readily than in the mutant p53 cell line. Interestingly, neither cell line showed cell cycle phase alteration in response to drug treatment.

The involvement of the Fas/FasL system in drug-induced apoptosis in lung cancer cells was investigated (Ferreira *et al.*, 2000). It was found that although a functional Fas pathway existed in the cells, an independent apoptosis pathway occured after cisplatin, gemcitabine, topotecan and paclitaxel exposure. The study also showed that by comparing fas expression in wild-type and mutant p53 cell lines, Fas is probably under transcriptional control of wild-type p53.

Galmarini *et al.* (2001) studied the role of p53 in the cytotoxicity of tubulin binding agents on cancer cells. Tubulin-binding agents, i.e. vinca alkaloids and taxanes, are used regularly in treatment of cancer. This study was carried out on the breast cancer cell line MCF-7 and used drugs such as vinblastine and paclitaxel. The results obtained show that inactivation of p53 with a dominant negative mutant p53 is associated with resistance to the chemotherapeutic agents used.

Whether p53 status influences the level of induction of MRP family members in response to prooxidants was investigated in a study on the MRP family by Lin-Lee *et al.*, (2001). MRP1, as mentioned earlier, is a protein associated with drug resistance, and is overexpressed in many cancers. The study observed that mutations in p53 were associated with increased expression of MRP1 in some of the colorectal cancer cells examined. The mechanisms by which p53 regulated the expression of MRP1 have not been discovered. It was shown that wild-type p53 can suppress MRP1, since null-p53 cell lines express more MRP1 that wild-type p53 cell lines (Lin-Lee *et al.*, 2001).

A study by Qin and Ng (2002) investigated cisplatin-induced apoptosis and its effect on the cell cycle. The study involved two hepatoma cell lines, HepG2 (wild-type p53) and Hep3B (deleted p53). It was found that in wild-type p53 cells, a low dose of cisplatin induced transient G1 arrest, S phase block and upregulation of p53 and $p21^{WAF1/CIP1}$ proteins. However a high dose of cisplatin led to cell growth inhibition and apoptosis in both cell lines. In p53 null cells there was no evidence of G1 arrest or accumulation of p53 or $p21^{WAF1/CIP1}$ (Qin and Ng, 2002). This study importantly shows that cisplatin is capable of inducing apoptosis by p53 dependent and independent pathways. Most studies carried out have found that a mutation in p53 is connected with increased resistance to chemotherapy.

Interestingly, a few studies have found that p53 mutations can have the opposite effect. For example, Hawkins *et al.* (1996), investigated the role of p53 mutations on efficacy of chemotherapeutic drugs and found that a lack of p53 conferred sensitivity to the cells. Das *et al.*, (2001) compared the effect of taxol on two lung cancer cell lines: A549 which expresses wild-type p53, and H1299 which does not express p53. Taxol was found to induce apoptosis in both cell lines efficiently at low doses, but the process was more regulated and maximum apoptosis reached at a lower drug concentration in the presence of p53. G2/M arrest was induced in both cell lines, independent of p53.

1.6.10 The role of p53 in treatment of cancer

Mutations of p53 in tumours are associated with bad prognosis. The tumours tend to be aggressive, with early metastasis, and lead to low survival rates. Since p53 plays a major role in response to chemotherapy, restoration of wild-type p53 function in tumour cells could increase the cells sensitivity to chemotherapy. Gene therapy is one of the most promising areas of cancer treatment. It involves the delivery of the wild-type p53 gene into tumour cells *in vivo*. The aim is that wild-type p53 function could be restored to the tumour cells so that they will become more sensitive to drug-induced DNA damage. The requirements for this kind of gene therapy are that there must be an efficient delivery system to get the genes to the tumour cells. After this there must be sufficient expression of the wild-type protein to mediate cell cycle arrest or cell death or increase sensitivity to anti-cancer agents (Gallagher and Brown, 1999).

Many groups have transfected a wild-type p53 gene into cancer cell lines to try to restore its function. While there is an apparent problem with isolating clones that express exogenous wild-type p53, some groups have been successful in this.
For example, Wang and Beck (1998), transfected H1299 with wild-type p53 to investigate the relationship between p53 and MRP. They checked for p53 protein expression by western blot. More recently, Liu *et al.*, (2004) transfected H1299 with wild-type p53. The transfection used a GFP-tagged p53 plasmid, and p53 expression was observed under a fluorescent microscope.

The first group to report growth suppression induced by high level expression of exogenous wild-type p53 in lung cancer cells, which express normal endogenous p53 was Cajot *et al.* (1992). Both wild-type and mutant p53 were transfected into the cell line Hut292DM using the polybrene-dimethyl sulphoxide technique. Expression of exogenous wild-type p53 inhibited growth of the cell line, so that low transfection efficiency resulted, whereas expression of exogenous mutant p53 had no apparent effect on the transfection efficiency. They were unable to isolate any wild-type p53-transfected clones that stably expressed normal exogenous p53, whereas exogenous mutant p53 was stably expressed in all mutant-transfected clones. They did isolate stable transfection clones expressing various truncated forms of p53, detected by PCR and northern blotting, but these clones did not affect *in vitro* growth properties.

Baker *et al.* (1990) found similar results working with two colorectal carcinoma lines-SW837 and SW480 which express mutant p53. They transfected wild-type cDNA and mutant cDNA-containing vectors into these cell lines. Of the mutant p53-transfected cells, 38% were found to express exogenous mutant p53 mRNA, while no expression of wild-type p53 mRNA was seen in any transfected clones. Clones isolated from wild-type p53-transfected cells were found to contain deleted or rearranged exogenous p53 sequences. The group concluded that the wild-type p53 gene was incompatible with proliferation of these cell lines.

Examination of wild-type p53 for suppression of growth of lung cancer cells, and how mutations of single amino acids changes the biological effects of the wild-type p53 gene was carried out (Takahashi *et al.*, 1992). They worked with two cell lines, NCI-H358, which is p53 null and NCI-H23, which expresses mutant p53, and transfected each with a wild-type p53 expression vector, and a mutant p53 expression vector. They found that expression of exogenous wild-type p53 was incompatible with cell growth in the p53 null cell line, while stable expression of the mutant protein was found in the mutant p53-transfected clones. Again, this group isolated no wild-type p53-transfected clones that contained an intact p53 gene. Introduction of wild-type p53 into the mutant p53-expressing cell line had no significant effect, suggesting the mutant protein was sufficient to inactivate the growth suppressive effect of wild-type p53. In the mutant-p53 cell line, exogenous wild-type p53 was stably expressed after transfection, but at a lower level than the endogenous mutant p53.

Matsumoto *et al.* (1997), looked at the relationship between p53 functions and cellular thermosensitivity using murine fibroblasts transfected with either wild-type p53 or mutant p53 or cells with no p53 expression. Cells transfected with wild-type p53 were approximately two-fold more sensitive to heat than cells transfected with mutant p53. Also G1 arrest was observed in all cell lines in response to heat but it was more prominent in wild-type p53-transfected cells.

In a similar study, Ota *et al.* (2000) confirmed that cancer cells show p53-dependent heat sensitivity through an apoptosis-related mechanism in cells with different p53 status. The cell line SAS was used which have a point mutation at codon 336 of exon 10 of the p53 gene, but expresses a wild-type p53 phenotype. A stable transfection of a mutant p53 gene, which produces a dominant negative mutant p53 protein, was carried out by electroporation. The parent cells were found to be more sensitive to heat than clones expressing the mutant p53 gene. It was also found that the rate of apoptosis was approximately seven-fold higher in the parent cell line than in the mutant clonal cell line.

Shaw *et al.* (1992) investigated the function of wild-type p53 by studying effects of wild-type p53 re-expression in the human colon tumour cell line EB, which is deficient in endogenous p53. Expression of the p53 gene was induced by induction of the

metallothionein promoter. They found that induction of wild-type p53 expression prevented tumour formation in nude mice, and also that two months of wild-type p53 expression resulted in elimination of established tumours in mice.

More commonly, p53 function has been restored using adenovirus-mediated gene transfer. For example, Inoue *et al.* (2000) constructed a recombinant adenoviral vector expressing wild-type p53 and applied this vector with anti-cancer drugs to three human NSCLC cell lines – one with wild-type p53, one with mutated p53 and one with deleted p53. The major finding was that Ad-p53 infection combined with anticancer drugs can induce G1 arrest, cell growth inhibition and possibly apoptosis, especially in the deleted p53 cell line. In a similar study, the efficiency of adenovirus-mediated transfer of p53 gene with anti-cancer agents *in vitro* and *in vivo* was investigated (Osaki *et al.*, 2000). It was found that expression of p53 influenced chemosensitivity. Several drugs were tested for their suitability in combination with gene transfer, and it was decided that CPT-11 and 5-FU would be successful in NSCLC, (Osaki *et al.*, 2000). They also noted that the presence of mutant p53, rather than the loss of wild-type p53 protein, confers a selective growth advantage and promotes clonal expansion of tumour cells.

Liu *et al.* (1995) examined the mechanism of growth suppression by wild-type p53 overexpression induced via adenovirus-mediated gene transfer. A wild-type p53-containing adenovirus Ad5CMV-p53 was used to infect two cell lines Tu-138, which expresses mutant p53, and MDA 686LN, which expresses wild-type p53. They found that growth suppression occurred in cells after p53 gene transfer and that this suppression was independent of the endogenous p53 status. However, growth suppression occurred earlier and was more profound in the Tu-138 cell line, which expresses endogenous mutant p53. The wild-type p53 gene was introduced into H358 cells, which are p53 null, using an adenoviral vector (Fujiwara *et al.*, 1994). They determined that this increases the cells sensitivity to a chemotherapy drug, *in vitro* and *in vivo*.

The efficacy of adenovirus-mediated p53 gene therapy in combination with paclitaxel against a number of tumour cell lines was examined by infecting cell lines expressing mutant p53, or with no p53 expression with an adenovirus containing the wild-type

p53 gene (Ad-p53) (Nielsen *et al.*, 1998). They found that paclitaxel had a synergistic or additive effect in combination with Ad-p53 independent of whether cells expressed mutant p53 or no p53 protein.

Huang *et al.* (2000) examined levels of p53, p21, BAX, Bcl2, MDM-2 and pRb after transfection of Ad5-p53 into three cervical cancer cell lines in order to discover how the cell decides between p53 dependent apoptosis versus cell cycle arrest. In the cell line expressing mutant p53, the levels of exogenous wild-type p53 were much higher than levels of endogenous mutant protein after transfection. Overall, the transfection resulted in restoration of wild-type p53 function, causing G1 arrest and also apoptosis in these cell lines.

1.7 Microarrays

Each cell in the body contains a full set of chromosomes containing identical genes. At any given time only a fraction of these genes are expressed. It is this group of expressed genes that makes each cell type unique. Aberrant gene expression profiles are responsible for many diseases. The completion of the Human Genome project (HGP) in 2003 has led to a huge amount of information becoming available about almost every gene in the genome, and is necessary to understand more about the functions of these gene products. New advances in technology, for example, the development of full genome expression microarrays, have allowed researchers to study the expression of almost every gene simultaneously. It is important to note, however, that we may not yet have identified all genes correctly, from the sequence data, and certainly our knowledge of the range of splice variants is incomplete.

1.7.1 Introduction to microarray technology

Microarrays are artificially constructed grids of DNA such that each element of the grid contains a specific oligodeoxynucleotide probe. This enables researchers to simultaneously measure the expression of thousands of genes in a given sample. Microarray experiments rely on the ability of RNA to bind specifically to a corresponding sequence-complementary probe. DNA microarrays are classified based on the DNA molecule that is immobilised on the slide. There are two basic types: either "oligodeoxynucleotide" or "cDNA" arrays. Oligodeoxynucleotide arrays are typically made up of 25-80 mer oligodeoxynucleotides while cDNA arrays are printed with 500-5000 base pair PCR products.

Microarray technology can be used to detect specific gene changes in, for example diseased tissue compared to normal healthy tissue, or the changing gene expression profiles of developing tissues at incremental time points. These types of experiments have the potential to explain not only why a disease occurs, but also how best to overcome it by enhancing our understanding of the mechanisms behind diseases, their development and progression.

The steps of a microarray experiment are shown in Figure 1.14. This is an example of an affymetrix genechip experimental workflow:

1. Total RNA is isolated from the cells being studied
2. The RNA is enzymatically converted into a double stranded DNA copy known as a complementary DNA (cDNA). This is done through reverse transcription (RT).
3. The cDNA is allowed to go through *in vitro* transcription (IVT) to RNA (now known as cRNA). This RNA is labelled with Biotin by incorporating a biotin-labelled ribonucleotide during the IVT reaction.
4. This labelled cRNA is then fragmented in to pieces anywhere from 30 to 200 base pairs in length by metal-induced hydrolysis.
5. The fragmented, Biotin-labelled cRNA is then hybridized to the array for 16 hours.
6. The array is then washed to remove any unhybridized cRNA and then stained with a fluorescent molecule streptavidin phycoerythrin (SAPE), which sticks to Biotin.
7. Lastly, the entire array is scanned with a laser and the information is automatically transferred to a computer for analysis of what genes were expressed and at what approximate level.

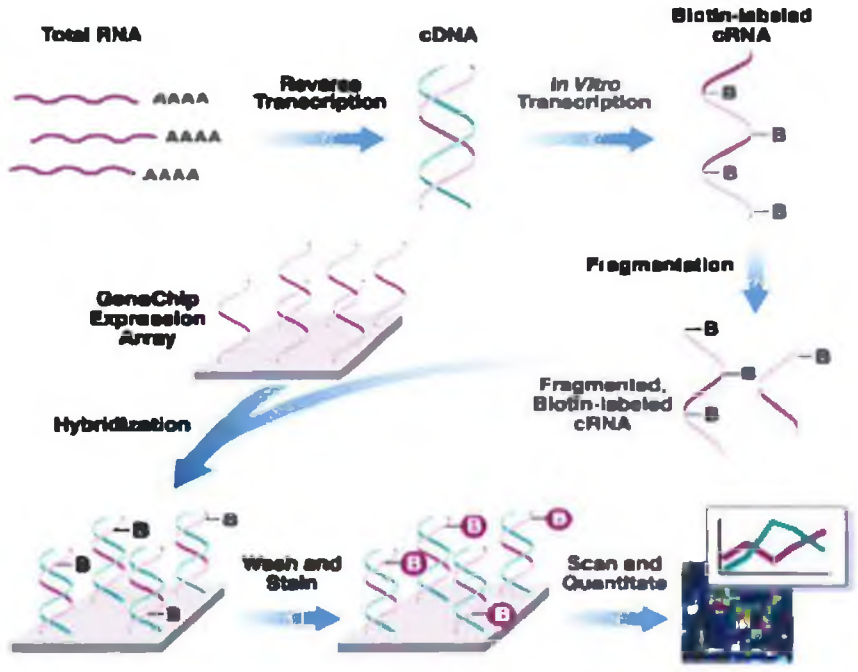

Figure 1.14 Steps in a microarray experiment (www.affymetrix.com)

1.7.2 Microarray analysis

Microarray experiments generate vast amounts of data in a short period of time. For the results of a microarray experiment to be acceptable, the raw data from the experiment must be validated. Good experimental design is the first step. It is important that the proper controls and replicates are included in each experiment. Replicates are particularly important since the methods used to identify differentially expressed genes are predominantly statistical. Microarray data is normalised to measure real biological changes by minimising processing variation. This process standardises the data so that the gene expression levels are comparable.

Quality control checks must also be included at all stages of the experiment. These checks would usually include quality checks on the initially isolated RNA and processed sample at regular intervals, e.g. Agilent Bioanalyzer. The Agilent Bioanalyzer analyses sample RNA in order to determine quality. Detailed information about the condition of RNA samples is displayed in the form of highly sensitive electropherograms. Post-experimental quality control checks include the chip controls shown in Table 1.3.

Table 1.3 Array quality control measures

QC measure	Result
Background	Measure of non-specific binding
3'/5' Ratio	Indicates how well IVT reaction has proceeded
Hybridisation controls	Checks spike controls added to each sample
Percentage present	All samples should have comparable % genes present
Noise	The electrical noise from scanner
Scale factor	Measures the brightness of array- All chips in an experiment should have scale factors within 3-fold of each other

The ideal format for reporting microarray data was reported by Brazma *et al.* (2001), and is called the "minimum information about a microarray experiment" (MIAME). MIAME has two general principles. The first is that there should be sufficient information recorded about each experiment to allow interpretation of the experiment, comparison to similar experiments and replication of the experiment. The second principle is that the data should be structured to allow automated data analysis and mining.

1.7.3 Affymetrix GeneChips

The microarray experiments carried out in these studies employed the Affymetrix Genechip system, which are oligodeoxynucleotide microarrays. Affymetrix probes are designed using publicly available information (NCBI database). The probes are manufactured on the chip using photolithography, which is adapted from the computer chip industry. Each genechip contains approximately 1,000,000 features. Each probe is spotted as a pair, one being a perfect match (PM), the other with a mismatch at the centre (MM). Each gene or transcript is represented on the genechip by 11 probe pairs (PM+MM). This can be seen in Figure 1.15. As well as helping estimate and eliminate background, with 22 different probes in total, researchers can be sure that the microarray is detecting the correct piece of RNA. The amount of light emitted at 570nm from stained chip is proportional to the amount of labelled RNA bound to each probe. Therefore, after scanning, the initial computer file generated (.DAT) contains a numerical value for every probe on the array.

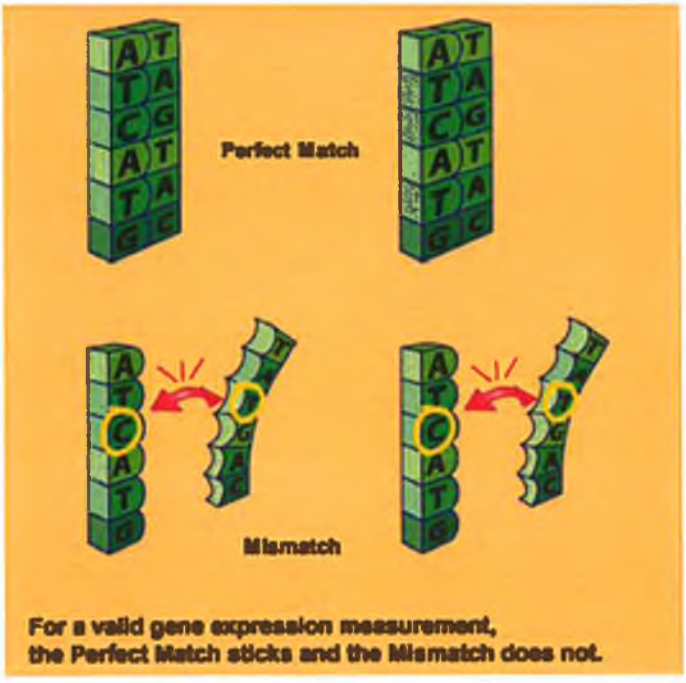

Figure 1.15 Perfect match and mismatch probe pairs on Affymetrix GeneChips (www.affymetrix.com)

1.7.4 Bioinformatics

Bioinformatics is the collection, organization and analysis of large amounts of biological data, using networks of computers and databases. Software packages are available to analyse microarray data e.g. Genespring and Spotfire. The data analysis software used for the analysis of these microarray experiments was dChip, (Lin *et al.*, 2004). This software is capable of probe-level and high-level analysis of Affymetrix gene expression arrays. High-level analysis in dChip includes comparing samples and hierarchical clustering in order to identify differentially expressed genes. Hierarchical clustering displays the relationships among genes or samples. These are represented by a tree where the length of the branches reflect the degree of similarity between the objects (Eisen *et al.*, 1998). An example of a cluster can be seen in Figure 1.16.

Other bioinformatics software available facilitates pathway analysis of genes differentially regulated in the systems studied.

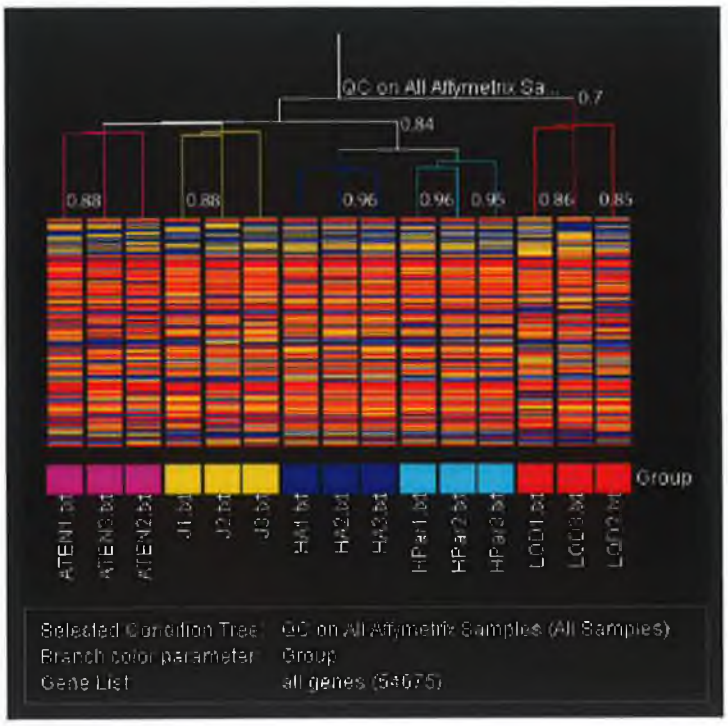

Figure 1.16 Example of a hierarchical cluster of microarray samples

1.7.5 Microarrays and cancer

Microarray technology is and has been used intensively to better understand the development of resistance to chemotherapeutic agents, both *in vivo* and *in vitro*. Whiteside *et al.* (2004) reported a novel method using time-course cDNA microarray analysis designed to evaluate which differentially expressed genes are directly involved in the development of drug resistance. The study used two lung cancer cell lines; one which readily developed resistance to cisplatin and another which after treatment with cisplatin did not display stable resistance. They identified seven genes that are likely to be involved in cisplatin resistance; three of them are newly identified in terms of cisplatin resistance.

Microarray analysis was used to identify differentially expressed genes associated with the development of resistance against adriamycin, cisplatin or 5-fluorouracil in gastric cancers (Kang *et al.*, 2004). Analysing the resistant cell lines, they identified eight genes that were differentially expressed in more than one of three drug subsets.

Using cDNA microarrays the expression of 9216 genes in 39 human cancer cell lines treated with various anticancer drugs were investigated (Dan *et al.*, 2002). They observed that susceptibility of cancer cells to a particular drug is determined by many factors. Fifty-five agents were tested and these were grouped together on the basis of mode of action. They noted that fifty genes were associated with greater than ten of the drugs and that genes associated with drugs of similar action clustered together. The study concluded that expression levels of up and down regulated genes could be used as a predictive marker of drug efficacy and could be used to predict mode of action of a novel compound.

Chen and his co-workers identified genes which are related to invasion and metastasis (Chen *et al.*, 2001). They used cDNA microarrays on human lung adenocarcinoma cell lines with varying invasive abilities and metastatic potentials to identify metastasis-associated genes. They also confirmed that the cell lines had equivalent *in vivo* invasiveness. They identified hundreds of genes that were differentially expressed in their model cell lines. Many of these genes had already been found to play a role in metastasis, for example keratin-18 and Mts-1.

Another study focused on differences in gene expression profiles between tumour cell lines and normal lung tissue using high-density oligonucleotide arrays (Sugita *et al.*, 2002). They found that fourteen genes were overexpressed only in SCLC, four genes were overexpressed only in NSCLC and two genes were overexpressed in both. They discovered that a large proportion of the genes overexpressed were cancer/testis antigens, and that these could possibly be used as biomarkers.

A 7685-element microarray was employed to create expression profiles for lung tumours and cell lines (Virtanen *et al.*, 2002). Hierarchical clustering resulted in tumour samples and cell lines forming two distinct groups. Within the tumour group, SCLC and NSCLC grouped separately. Most SCLC cell lines grouped with the SCLC tumour samples. Smilarly, most of the squamous cell carcinomas clustered together. None of the adenocarcinoma cell lines tested grouped with adenocarcinoma tumour tissue.

Comparison of expression profiles of twenty-one SCLC cell lines and eight xenografted tumours from these cell lines to expression profiles of seventeen normal adult tissues using microarray technology was carried out in order to find tumour-specific genes (Pedersen *et al.*, 2003). The results indicate that the cell lines expressed a set of genes not expressed in tumours, and that tumour samples are contaminated with normal tissue. The study yielded a set of genes expressed specifically in SCLC. This set of genes includes neuroendocrine markers, oncogenes and genes involved in proliferation and division.

Amundson *et al.* (2000) compared basal levels of ten transcripts of the sixty cell lines used in the National Cancer Institute *in vitro* anticancer drug screen (NCI-ACDS). The transcripts were chosen according to their known role in the response to cellular damage or cancer biology and as potential modifiers of toxicity. They included *BAX*, *BCL-X_L*, *MDM2* and *cMYC*. The most significant finding of this study was that *BCL-X_L* protected all cancer types against p53-mediated apoptosis.

cDNA microarrays were also used to monitor mRNA expression in breast cancer cells selected for resistance to doxorubicin (Kudoh *et al.*, 2000). They studied two breast

cell lines, MCF-7 and MCF-7/D40, a doxorubicin resistant variant. These cell lines were compared after transient treatment with the drug. The results show that the resistant cell line showed far fewer changes in gene expression after treatment than the parent cell line. The group found that a subset of genes that are transiently induced by doxorubicin intersects with a distinct set of genes that are overexpressed in the stably resistant cell line. These genes may represent a signature profile of doxorubicin resistance.

1.8 RNA Interference

RNA interference is the biological mechanism by which double-stranded RNA (dsRNA) induces gene silencing at the level of translation by targeting complementary mRNA for degradation. RNAi has the potential to help elucidate the complex issues involved in eukaryotic development, to aid in dissecting cellular pathways, and to identify targets for chemotherapeutic intervention that otherwise would remain unidentified

1.8.1 Introduction to siRNA technology

The phenomenon of post translational gene silencing (PTGS) was first discovered in plant studies. A major study into the silencing of specific genes in *C. elegans* by the introduction of dsRNA by Fire and Mello in 1998 showed that the presence of just a few molecules of dsRNA was sufficient to almost completely abolish the expression of a gene that was homologous to the dsRNA (McManus and Sharp, 2002).

A four-step mechanism of the RNAi pathway has been suggested by experiments conducted in *Drosophila*. The first step is that long dsRNA is cleaved in a ATP-dependent manner into 21-25nt double stranded fragments, termed small interfering RNAs (siRNAs). These siRNAs are incorporated into a protein complex. ATP-dependent unwinding of the siRNA duplex leads to activation of the complex to an RNA-induced silencing complex (RISC). The RISC can recognise and cleave a target RNA complementary to the guide strand of the siRNA (Hutvagner and Zamore, 2002). A schematic diagram of the mechanism of RNAi can be seen in Figure 1.17. Dicer, a member of the RNase III family of endonucleases is responsible for the production of siRNAs. Certain structural features are important for entry of siRNAs into the RNAi pathway, such as a 5' phosphate and 3' hydroxyl termini and two single-stranded nucleotides on the 3' ends.

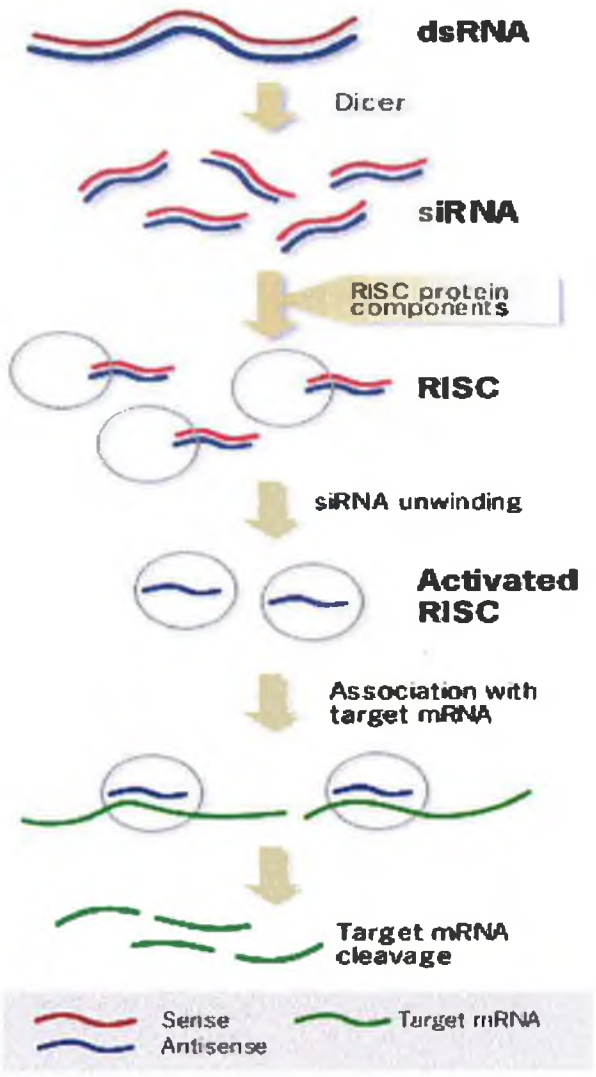

Figure 1.17 The mechanism of RNAi (www.ambion.com)

The enzymatic machinery for generating siRNA also appears to be used for the production of a second class of endogenously encoded small RNA molecules termed microRNAs. These miRNAs are a newly identified and large family of RNAs with highly conserved expression patterns. Hundreds of miRNAs have been found in *C. elegans*, plants and mammals. A common feature throughout miRNAs, but not seen in siRNAs is that the sequences of miRNAs are found in the stem of a stem-loop structure (Kim, 2003). Many of the miRNA targets identified so far are transcription factors or proteins involved in cell growth and development (Ke *et al.*, 2003). The specificity of miRNA (through Watson & Crick base pairing) and the rapidity at which miRNAs can be generated (when compared to the time taken to synthesise regulatory proteins), result in regulatory molecules that are ideally suited for the precise temporal control required during development. miRNAs might even explain the diversity of phenotypes among higher organisms despite a limited number of protein coding genes.

The PTGS mechanisms of siRNA and miRNA are largely identical, as demonstrated by the fact that endogenously encoded human miRNAs can cleave exogenously added RNA substrates with fully complimentary target sites while siRNAs can repress translation without RNA cleavage when there are slight central mismatches (Zeng *et al.*, 2003).

1.8.2 Applications of RNAi

With the advent of the Human Genome Project (HGP) completion and the development of microarray technology, there are thousands of genes whose sequences are fully known, but whose function is unknown. Gene silencing using siRNA is quickly becoming the most common method to study the function of these genes. Other methods of knocking down expression of a gene (e.g. antisense and ribozymes) are laborious and time-consuming. Libraries of siRNAs and automatic screening systems are now available which make it possible to screen large sections of the human genome simultaneously.

It is clear that siRNA may have multiple applications in disease therapy. Diseases that could benefit from RNAi technology include viral infections, cancer and genetic disorders (Kim, 2003). The dosage of the siRNA applied is a crucial point for therapeutic applications considering the fact that siRNAs applied at a concentration of 100 nM were found to nonspecifically induce the expression of a number of genes involved in apoptosis and cellular stress responses, reduction of the dosage to 20 nM eliminated this effect however (Semizarov *et al.*, 2003). In the case of cancer, siRNA could theoretically be used to target oncogenes such as mutant p53 for example (Martinez *et al.*, 2002) or a host of other targets, but it is more likely that it will be used in conjunction with chemotherapy, in fact siRNA could be used to sensitise tumours to chemotherapy through repression of drug resistance proteins e.g. MDR1 (Wu *et al.*, 2003). In order for siRNA to become a potential therapy, problems with delivery must be overcome.

1.8.3 Problems associated with RNAi

Long dsRNA has been found to induce an immune response when introduced into mammals (Bridge *et al.*, 2003; Sledz *et al.*, 2003), leading to induction of the IFN response, which triggers the PKR pathway to inhibit protein translation and activates RNase L. In mammalian systems this can be overcome by introduction of synthetic siRNAs.

In early studies using RNAi, there was questions regarding siRNA specificity. In a study by Jackson and colleagues (2003), using gene expression profiling, it was revealed that there was direct silencing of non-targeted genes (some containing as little as 11 contiguous nucleotides homology to the siRNA). This is similar to the finding that siRNAs can suppress expression of off-target proteins even with 3-4 base mismatches and additional G-U mismatches (Saxena *et al.*, 2003). Scacheri *et al.*, (2004) also described changes in the levels of p53 and p21 protein in cells that were transfected with siRNA against the MEN1 gene. These genes are considered sensitive markers of cell state and the effects do not appear to be part of an IFN mediated response. This effect may be due to a partial complimentary sequence matches that result in miRNA-like inhibition of translation. Interestingly, this group discovered that

the levels of actin were not affected by this non-specific silencing indicating perhaps that unaffected actin levels are not an ideal control in siRNA experiments.

These results are disputed however in a study by Chi *et al* (2003), where DNA microarray analysis demonstrated the precise sequence specificity of siRNA constructs. In general, it is recognized that good siRNA design will result in no "off-target" effects, and that many failures in RNAi experiments may have been caused by lack of experiment optimisation.

1.8.4 Delivery of siRNA

The most widely used technique for RNAi is siRNA transfection. Design of siRNAs is crucial for an experiment to work. Choice of target site, transfection method and turnover rate of the protein must be taken into consideration. There are certain guidelines available for siRNA design. Secondary structures and mRNA binding proteins may influence the ability of an siRNA to bind its target. Companies such as Ambion create siRNAs using algorithms that overcome these issues. The choice of transfection reagent and conditions, such as cell density, also play a major role in the success of an siRNA transfection. Transfection of synthetic siRNA duplexes at low concentration can help to avoid the IFN response of cells (Kim *et al.*, 2004). This method of siRNA delivery is relatively transient and inhibition is lost after a number of days. To allow the expression of short hairpin RNAs (shRNAs, these undergo post-transcriptional processing into 21nt duplex siRNAs by Dicer), plasmids have been designed using promoters based on RNA polymerase II or III e.g. Sui *et al.*, 2002. The plasmids can contain a selectable marker so that clonal populations of cells with permanently silenced target genes can be isolated. Viruses are excellent vehicles for siRNA delivery, especially retroviruses (Devroe & Silver, 2004). Other viral delivery vehicles include HIV based, lentivirus based vectors (Stewart *et al.*, 2003) or adenoviruses (Shen *et al.*, 2003). A lentiviral vector capable of expressing a siRNA against GFP was used to silence GFP in a transgenic mouse that had stable expression of GFP (Tiscornia *et al.*, 2003).

1.9 Aims of Thesis

1. The first aim of this work was to study p53 in order to determine its role in the development of resistance. Most chemotherapeutic drugs cause DNA damage that is sensed by p53, which either arrests the cell cycle to allow DNA repair or induces apoptosis. The role of p53 in drug resistance is unclear in the literature. Pulse-selection of cell lines with differing p53 status was carried out to discover if p53 status is a factor in the development of resistance *in vitro*. Wild-type p53 was also transfected into a number of lung cancer cell lines in order to investigate changes in resistance to chemotherapeutic agents and invasion in the p53 expressing cell lines.

2. The second aim was to identify mechanisms of the development of resistance to the chemotherapeutic agents, taxol and carboplatin in lung cancer cell lines. This was achieved by pulse-selecting lung cancer cell lines with pharmacologically relevant levels of taxol and establishing variants which display resistance to a clinically relevant degree. These cell lines were used as models for the study of taxol resistance by microarrays. Functional studies on a number of target genes identified by microarray analysis to be associated with taxol treatment were performed using siRNA technology.

Section 2.0: Materials and Methods

2.1 Preparation of cell culture media

Ultrapure water (UHP) was purified to a standard of 12-18 MΩ/cm resistance by a reverse osmosis system (Millipore MilII-RO 10 Plus, Elgastat UHP). Glassware required for cell culture related applications were soaked in a 2% RBS-25 (AGB Scientific) for 1 hour, washed in an industrial dishwasher, using Neodisher detergent and rinsed twice with UHP. All thermostable solutions, water and glassware were sterilised by autoclaving at 121°C for 20 minutes at 15 bar (Thermolabile solutions were filtered through 0.22 μm sterile filters (Millipore, Millex-GV SLGV025BS)).

All 1X basal media were prepared in-house as follows: 10X media was added to sterile UHP water, buffered with HEPES (N-(2-Hydroxyethyl) piperazine-N-(2-ethanesulfonic acid) and $NaHCO_3$ as required and adjusted to pH 7.5 using sterile 1.5 N NaOH or 1.5 N HCl. The media was then filtered through sterile 0.22μm bell filters (Gelman, 12158) and stored in sterile 500ml bottles at 4°C. Sterility checks on all media bottles for bacterial, yeast and fungal contamination were made using Colombia blood agar (Oxoid, CM217), Sabauraud dextrose (Oxoid, CM217) and Thioglycolate broths (Oxoid, CM 173) respectively. All sterility checks were then incubated at both 25°C and 37°C. Basal media were stored at 4°C for up to three months in the dark. Complete media was then prepared as follows: supplements of 2mM L-glutamine (Gibco, 11140-0350) for all basal media and 1ml 100X non-essential amino acids (Gibco, 11140-035) and 100mM sodium pyruvate (Gibco, 11360-035) were added to MEM. Other components were added as described in Table 2.1. Complete media was stored at 4°C for a maximum of one month in the dark.Preparation for cell culture

Table 2.1 Additional components in media.

Cell Line	Basal Media	FCS (%)	Additions
A549	ATCC	5	N/A
NCI-H1299	RPMI 1640	5	Sodium pyruvate
NCI-H460	RPMI 1640	5	Sodium pyruvate
SKLU-1	MEM	5	Sodium pyruvate, non-essential amino acids
DLKP-SQ	ATCC	5	N/A

2.2 Cells and Cell Culture

All cell culture work was carried out in a class II laminar airflow cabinet (Holten LaminAir). All experiments involving cytotoxic compounds were conducted in a cytogard laminar airflow cabinet (Holten LaminAir Maxisafe). Before and after use the laminar airflow cabinet was cleaned with 70% industrial methylated spirits (IMS). All items brought into the cabinet were also swabbed with IMS. Only one cell line was used in the laminar air-flow cabinet at a time and upon completion of work with any given cell line the laminar air-flow cabinet was allowed to clear for at least 15 minutes before use to eliminate any possibilities of cross-contamination between the various cell lines. The cabinets were cleaned weekly with the industrial disinfectant Virkon (Antech International, P0550). Details pertaining to the cell lines used for the experiments detailed in this thesis are provided in Table 2.2. All cells were incubated at 37°C and where required, in an atmosphere of 5% CO_2. Cells were fed with fresh media or subcultured (see Section 2.5.1) every 2-3 days in order to maintain active cell growth. All of the cell lines listed in Table 2.5.1 are anchorage-dependent cell lines.

Table 2.2 Cell lines used in this thesis

Cell Line	Details	Source
A549	Lung adenocarcinoma	ATCC
A549-tax	Taxol-selected variant of A549	NCTCC
A549-cpt	Carboplatin-selected variant of A549	NCTCC
NCI-H1299	Lung large cell carcinoma	ATCC
H1299-tax	Taxol-selected variant of H1299	NCTCC
H1299-cpt	Carboplatin-selected variant of H1299	NCTCC
NCI-H460	Lung large cell carcinoma	ATCC
H460-tax	Taxol-selected variant of H460	NCTCC
H460-cpt	Carboplatin-selected variant of H460	NCTCC
SKLU-1	Lung adenocarcinoma	ATCC
SKLU-1-tax	Taxol-selected variant of SKLU-1	NCTCC
SKLU-1-cpt	Carboplatin-selected variant of SKLU-1	NCTCC

2.2.1 Subculturing of cell lines

The cell culture medium was removed from the tissue culture flask and discarded into a sterile bottle. The flask was then rinsed out with 1ml of trypsin/EDTA solution (0.25% trypsin (Gibco, 043-05090), 0.01% EDTA (Sigma, E9884) solution in PBS (Oxoid, BRI4a)) to ensure the removal of any residual media. Trypsin was added to the flask, which was then incubated at 37°C, for approximately 5 minutes, until all of the cells detached from the inside surface of the flask. The amount of trypsin used varies with flask size, i.e., 1ml for T25, 2ml for T75 and 5ml for T175. The trypsin was deactivated by adding an equal volume of complete media to the flask. The cell suspension was removed from the flask and placed in a sterile universal container (Sterilin, 128a) and centrifuged at 1000rpm for 5 minutes. The supernatant was then discarded from the universal and the pellet was suspended in complete medium. A cell count was performed and an aliquot of cells was used to re-seed a flask at the required density.

2.2.2 Assessment of cell number and viability

Cells were trypsinised, pelleted and resuspended in media. An aliquot of the cell suspension was then added to trypan blue (Gibco, 525) at a ratio of 5:1. The mixture was incubated for 3 minutes at room temperature. A 10µl aliquot of the mixture was then applied to the chamber of a glass coverslip enclosed haemocytometer. Cells in the 16 squares of the four grids of the chamber were counted. The average cell numbers per 16 squares were multiplied by a factor of 10^4 and the relevant dilution factor to determine the number of cells per ml in the original cell suspension. Non-viable cells stained blue, while viable cells excluded the trypan blue dye as their membrane remained intact, and remained unstained. On this basis, percentage viability was calculated.

2.2.3 Cryopreservation of cells

Cells for cryopreservation were harvested in the log phase of growth and counted as described in Section 2.5.2. Cell pellets were resuspended in a suitable volume of foetal calf serum (FCS). An equal volume of a 10 – 20% Dimethylsulphoxide (DMSO)/FCS

solution was added dropwise to the cell suspension. Volumes of 1ml of this suspension was then aliquoted into cryovials (Greiner, 122278), and immediately placed in the vapour phase of a liquid nitrogen container, which was equivalent to a temperature of –80°C. After a period of four hours, vials were removed from the vapour phase and transferred to the liquid phase for long-term storage (- 196°C).

2.2.4 Thawing of cryopreserved cells

A volume of 5ml of fresh warmed growth medium was added to a sterile universal. The cryopreserved cells were removed from the liquid nitrogen and thawed at 37°C quickly. The cells were removed from the vials and transferred to the aliquoted media. The resulting cell suspension was centrifuged at 1,000 rpm for 5 minutes. The supernatant was removed and the pellet resuspended in fresh culture medium. An assessment of cell viability on thawing was then carried out (Section 2.2.2). Thawed cells were then added to an appropriately sized tissue culture flask with a suitable volume of growth medium and allowed to attach overnight. The following day, flasks were fed with fresh media to remove any non-viable cells.

2.2.5 Monitoring of sterility of cell culture solutions

Sterility testing was performed in the case of all cell culture media and cell culture related solutions. Samples of prepared basal media were incubated at 37°C for a period of seven days. This ensured that no bacterial or fungal contamination was present in the media.

2.2.6 Serum Batch Testing

Batch to batch variation is a major problem associated with the use of FCS in cell culture. In extreme cases this variation may result in a lack of cell growth, whereas in more moderate cases growth may be retarded. To avoid the effects of the above variation, a range of FCS batches were screened for growth of each cell line. Screening involved seeding cells in 96 well plates and determining growth as a percentage of a serum with known acceptable growth rate.

2.2.7 Isolation of Clonal Populations by Clonal Dilution

Clonal populations were isolated by plating cells in 96-well plates at a concentration of 1 cell per 3 wells. After 2 days, the 96-well plates were monitored for single cells in wells. Single cell wells were marked and then allowed to grow until they reached levels that would allow them to be scaled up initially into 24-well plates.

2.3 *Mycoplasma* analysis of cell lines

Cell lines were tested for possible *mycoplasma* contamination by Ms. Aine Adams and Mr. Michael Henry at the National Cell and Tissue Culture Centre. The protocol used is detailed in the following Sections 2.6.1 and 2.6.2. All cell lines described in this thesis were free from mycoplasma contamination.

2.3.1 Indirect staining procedure for *Mycoplasma* analysis

Mycoplasma negative NRK (Normal rat kidney fibroblast) cells were used as an indicator cells for this analysis. The cells were incubated with a sample volume of supernatant from the cell lines in question and then examined for *Mycoplasma* contamination. A fluorescent Hoechst stain was used in this analysis. The stain binds specifically to DNA and so stains the nucleus of the cell in addition to any *Mycoplasma* present. *Mycoplasma* infection was indicated by fluorescent bodies in the cytoplasm of the NRK cells.

2.3.2 Direct staining procedure for *Mycoplasma* analysis

Direct staining for *Mycoplasma* analysis involved inoculating samples on to a *Mycoplasma* culture broth (Oxoid, CM403). This was supplemented with 16% serum, 0.002% DNA (BDH, 42026), 2μg/ml fungizone (Gibco, 042 05920), $2x10^3$ units penicillin (Sigma, Pen-3) and 10ml of a 25% yeast extract solution. Incubation was carried out at 37°C for a period of 48 hours. Samples of this broth were then streaked onto plates of *Mycoplasma* agar base (Oxoid, CM401) which had been supplemented as described above. The plates were incubated for three weeks at 37°C while exposed

to $C0_2$. The plates were examined microscopically every 7 days. The appearance of small oval shaped colonies indicated the presence of *Mycoplasma* infection.

2.4 *In vitro* toxicity assays

Cells in the exponential phase of growth were harvested by trypsinisation as described in Section 2.5.1. Cell suspensions containing $1x10^4$ cells/ml were prepared in cell culture medium. Volumes of 100µl/well of these cell suspensions were added to 96-well plates (Costar, 3599) using a multichannel pipette. Plates were agitated gently in order to ensure even dispersion of cells over the surface of the given well. Cells were then incubated overnight at 37°C in an atmosphere containing 5% CO_2. Cytotoxic drug dilutions were prepared at 2X their final concentration in cell culture medium. Volumes of the drug dilutions (100µl) were then added to each well using a multichannel pipette. Plates were then mixed gently as above. Cells were incubated for a further 6-7 days at 37°C and 5% CO_2 until the control wells had reached approximately 80-90% confluency. Assessment of cell survival in the presence of drug was determined by the acid phosphatase assay (Section 2.4.2). The concentration of drug which caused 50% cell kill (IC_{50} of the drug) was determined from a plot of the % survival (relative to the control cells) versus cytotoxic drug concentration.

2.4.1 Combination toxicity assays

Cells for combination assays were set up as for *in vitro* toxicity assays (Section 2.4). Following overnight incubation of cells, cytotoxic drug dilutions and non-steroidal anti-inflammatory drug (NSAID) dilutions were prepared at 4X their final concentration in media. Volumes of 50µl of the drug dilution and 50µl of the NSAID dilution were then added to each relevant well so that a total final volume of 200µl was present in each well. All potential toxicity-enhancing agents were dissolved in DMSO, ethanol or media. Stock solutions were prepared at approximately 15mg/10ml media, filter sterilised with a 0.22µm filter (Millex-GV, SLGV025BS) and then used to prepare all subsequent dilutions. Cells were incubated for a further 6 days at 37°C in an atmosphere containing 5% CO_2. At this point the control wells would have reached

approximately 80-90% confluency. Cell number was assessed using the acid phosphatase assay (Section 2.4.2).

2.4.2 Assessment of cell number - Acid Phosphatase assay

Following the incubation period of 6-7 days, media was removed from the plates. Each well on the plate was washed twice with 100µl PBS. This was then removed and 100µl of freshly prepared phosphatase substrate (10mM *p*-nitrophenol phosphate (Sigma 104-0) in 0.1M sodium acetate (Sigma, S8625), 0.1% triton X-100 (BDH, 30632), pH 5.5) was added to each well. The plates were then incubated in the dark at 37°C for 2 hours. Colour development was monitored during this time. The enzymatic reaction was stopped by the addition of 50µl of 1N NaOH. The plate was read in a dual beam plate reader at 405nm with a reference wavelength of 620nm.

2.4.3 Statistical Analysis

Analysis of the significance of the difference in the mean IC_{50} value calculated from toxicity assays were performed using a student t-test (two-tailed with unequal variance), which was run on Microsoft Excel.

A p value > 0.05 was deemed not significant
A p value < 0.05 was deemed significant
A p value < 0.005 was deemed highly significant

2.5 Safe handling of cytotoxic drugs

Cytotoxic drugs were handled with extreme caution at all times in the laboratory, due to the potential risks in handling these drugs. Disposable nitrile gloves (Medical Supply Company Ltd) were worn at all times and all work was carried out in cytotoxic cabinets (Holten LaminAir Maxisafe). All drugs were stored in a safety cabinet at room temperature or in designated areas at 4°C. The storage and means of disposal of the cytotoxic drugs used in this work are outlined in Table 2.3.

Table 2.3 Storage and disposal details for chemotherapeutic agents

Cytotoxic Agent	Storage	Disposal
Adriamycin	4°C in dark	Incineration
Taxol	Room temperature in dark	Incineration
Taxotere	Room temperature in dark	Incineration
Vincristine	4°C in dark	Incineration
VP-16	Room temperature in dark	Incineration
Carboplatin	Room temperature in dark	Incineration
Cisplatin	Room temperature in dark	Incineration
5-Fluorouracil	Room temperature in dark	Incineration

2.6 Pulse selection of parent cell lines

A number of drug resistant variants were established from the cell lines A549, H1299, SKLU-1 and H460 by pulse-selection with taxol or carboplatin.

2.6.1 Determination of drug concentration for pulse selection

Cells were seeded into twelve 25cm^2 flasks at 1.5 × 10^5 cells per flask and allowed to attach overnight at 37°C. The following day media was removed from the flask and a range of concentrations of appropriate drug was added to the flasks in duplicate (concentrations based on miniaturised assays). Complete media was added to two flasks as a 100% survival control. Flasks were returned to the 37°C incubator for a 4 hour incubation, after which the drug was removed, the flasks were rinsed and fed with fresh complete media. The flasks were then incubated for 5-7 days until the cells in the control flasks had reached approximately 80% confluency. At this point, medium was removed from the flasks and cells were trypsinised and counted in duplicate as described in Section 2.2.2. The concentration of drug that caused appropriate cell kill was determined from a plot of the percentage survival relative to the control cells versus cytotoxic drug concentration.

Concentrations chosen for pulse selection of A549, H1299 and H460 gave an 80-90% kill, i.e. IC80 - IC90. SKLU-1 was pulsed at a concentration that gave a much lower kill, since these cells found it more difficult to recover from each pulse (Table 2.4).

Table 2.4 Concentrations for pulse-selection

Cell Line	Taxol (ng/ml)	Carboplatin (μg/ml)
A549	150	100
H1299	150	50
SKLU-1	10	10
H460	50	50

2.6.2 Pulse selection

Cells at low confluency in 75cm^2 flasks were exposed to the chosen concentration of taxol or carboplatin for 4 hours. After this period, the drug was removed and the flasks were rinsed and fed with fresh complete media. The cells were then grown in drug-free media for 6 days, refeeding every 2-3 days. This was repeated once a week for ten weeks. If the cells had not recovered sufficiently from the previous pulse, a week was skipped, but all cell lines received ten pulses.

2.7 *In vitro* invasion assays

Invasion assays were performed using the method of Albini (1998). Matrigel (Sigma E-1270) (11mg/ml) was diluted to 1mg/ml in serum free culture media. Matrigel was kept ice cold at all times. Into each insert (Falcon 3097) (8.0μm pore size, 24 well format) 100μl of 1mg/ml Matrigel was placed. The insert and the plate were incubated for one hour at 37°C to allow the gel to polymerise. Cells were harvested and resuspended in culture media containing 5% FCS at the concentration of 1×10^6 cells/ml. Excess media was removed from the inserts, and they were rinsed in culture media. Volumes of 100μl of the suspension cells were added to each insert. A further 100μl of culture media was added to each insert and 500μl of culture media containing

5% FCS was added to the well underneath the insert. Cells were incubated at 37°C for 24 hours. After this time period, the inner side of the insert was wiped with a cotton swab dampened with PBS, while the outer side of the insert was stained with 0.25% crystal violet for 10 minutes and then rinsed in UHP and allowed to dry. The inserts were then viewed and photographed under the microscope. The invasion assays were quantified by counting cells within a graticule at 40X magnification.

2.8 Western blotting

2.8.1 Whole cell extract preparation

Cells were grown to 80-90% confluency in 75cm^2 flasks. Media was removed and cells were trypsinised as described in Section 2.2.1. Cells were washed twice with ice cold PBS. All procedures from this point forward were performed on ice. Cells were resuspended in 100-200µl of NP-40 lysis buffer and incubated on ice for 30 minutes. Table 2.5 below provides the details of the lysis buffer. Immediately before use, 10µl of the 100X stocks listed in Table 2.6 were added to 1ml of lysis buffer.

Table 2.5 NP-40 lysis buffer

Addition required per 500ml stock	Final concentration
425ml UHP water	-
25ml 1M Tris-HCl (pH 7.5)	50mM Tris-HCl (pH 7.5)
15ml 5M NaCl	150 mM NaCl
2.5ml NP-40	0.5% NP-40

Table 2.6 NP-40 lysis buffer 100X stocks

100X stock	Preparation instructions
100mM DTT	154mg in 10ml UHP
100mM PMSF	174mg in 10ml 100% ethanol
100X Protease inhibitors	2.5 mg/ml leupeptin, 2.5 mg/ml aprotinin, 15 mg/ml benzamidine and 1mg/ml trypsin inhibitor in UHP water

After incubation on ice, lysates were centrifuged on a bench centrifuge at 14000rpm for 15 minutes at 4°C. Supernatant containing extracted protein was transferred to a fresh chilled eppendorf tube. Protein concentration was quantified using the Biorad assay as detailed in Section 2.8.2. Samples were then stored in aliquots at -80°C.

2.8.2 Protein Quantification

Protein levels were determined using the Bio-Rad protein assay kit (Bio-Rad, 500-0006) as follows. A 2mg/ml bovine serum albumin (BSA) solution (Sigma, A9543) was prepared freshly in lysis buffer. A protein standard curve (0, 0.2, 0.4, 0.6, 0.8 and 1.0mg/ml) was prepared from the BSA stock with dilutions made in lysis buffer. The Bio-Rad reagent was diluted 1:5 in UHP water. A 20µl volume of protein standard dilution or sample (diluted 1:10) was added to 980µl of diluted dye reagent and the mixture vortexed. After 5 minutes incubation, absorbance was assessed at 570nm. The concentration of the protein samples was determined from the plot of the absorbance at 570nm versus concentration of the protein standard.

2.8.3 Gel electrophoresis

Proteins for analysis by Western blotting were resolved using SDS-polyacrylamide gel electrophoresis (SDS-PAGE). The Atto dual mini slab kit was used (AE 6450). The stacking and resolving gels were prepared as illustrated in Table 2.7. The gels were set in clean 9cm x 8cm gel cassettes, which consisted of 2 glass plates separated by a rubber gasket to a width of 1mm. The resolving gel was added to the gel cassette and allowed to set. Once the resolving gel had set, stacking gel was poured on top. A comb was placed into the stacking gel after pouring, in order to create wells for sample loading (maximum sample loading volume of 15-20µl).

Table 2.7 Preparation protocol for SDS-PAGE gels (2 x 0.75mm gels)

Components	10% Resolving Gel	5% Stacking Gel
Acrylamide stock	4.6 ml	670µl
UHP water	5.6ml	2.7ml
1.875 M Tris-HCl pH 8.8	3.5ml	-
1.25 M Tris-HCl pH 6.8	-	500µl
10% SDS	140µL	40µL
10% NH_4- persulfate	140µL	40µL
TEMED	5.6µL	4µL

The acrylamide stock in Table 2.7 consists of a 30% (29:1) ratio of acrylamide:bis-acrylamide (Sigma, A2792). In advance of samples being loaded in to the relevant sample wells, 20µg of protein was diluted in 10X loading buffer. Molecular weight markers (Sigma, C4105) were loaded alongside samples. The gels were run at 250V and 45mA until the bromophenol blue dye front was found to have reached the end of the gel, at which time sufficient resolution of the molecular weight markers was achieved.

2.8.4 Western blotting

Western Blotting was performed by the method of Towbin *et al.* (1979). Once electrophoresis had been completed, the SDS-PAGE gel was equilibrated in transfer buffer (25mM Tris (Sigma, T8404), 192mM glycine (Sigma, G7126), pH 8.3-8.5) for approximately 30 minutes. Five sheets of Whatman 3mm filter paper were soaked in freshly prepared transfer buffer. These were then placed on the cathode plate of a semi-dry blotting apparatus (Bio-rad). Air pockets were then removed from between the filter paper. PVDF membrane (Boehringer Mannheim 1722026) or nitrocellulose membrane (Amersham Pharmacia Biotech, RPN 303D), which had been equilibrated in the same transfer buffer, was placed over the filter paper on the cathode plate. Air pockets were once again removed. The gels were then aligned on to the membrane. Five additional sheets of transfer buffer soaked filter paper were placed on top of the gel and all air pockets removed. The proteins were transferred from the gel to the

membrane at a current of 34mA at 15V for 30-40 minutes, until all colour markers had transferred. Following protein transfer, membranes were stained using Ponceau (Sigma, P7170) to ensure efficient protein transfer. The membranes were then blocked overnight using 5% milk powder (Cadburys; Marvel skimmed milk) in PBS at 4°C. The membranes were washed with PBS prior to addition of the primary antibody.

Membranes were treated with primary antibody for 2-3 hours at room temperature (or overnight at 4°C) and a negative control where the membrane was exposed to antibody diluent was also performed. Antibodies were prepared in 1% Marvel in PBS. Primary antibody was removed after this period and the membranes rinsed 3 times with PBS containing 0.5% Tween 20 (Sigma P1379) for a total of 15-30 minutes. Secondary antibody (1 in 1,000 dilution of anti-mouse IgG peroxidase conjugate (Sigma, A4914) in PBS, was added for 1.5 hour at room temperature. The membranes were washed thoroughly in PBS containing 0.5% Tween for 15 minutes.

Table 2.8 List of Primary antibodies and dilutions

Primary Antibody	Dilution
p53 (Calbiochem, OP43)	1:1000
P73 (Calbiochem, OP109)	1:200
MDM2 (Calbiochem, OP144)	1:200
β-actin (Sigma, A5441)	1:10,000
Pgp (Santa Cruz, SC-13131)	1:200
MRP1 (Santa Cruz, SC-18835)	1:200
ID3 (Santa Cruz, SC-490	1:200
CRIP1 (BD Biosciences, 610976)	1:200

2.8.5 Enhanced chemiluminescence (ECL) detection

Immunoblots were developed using an Enhanced Chemiluminescence kit (Amersham, RPN2109), which facilitated the detection of bound peroxidase-conjugated secondary antibody. Following the final washing membranes were subjected to ECL. A layer of parafilm was flattened over a glass plate and the membrane placed gently upon the

plate. A volume of 3ml of a 50:50 mixture of ECL reagents was used to cover the membrane. The ECL reagent mixture was completely removed after a period of one minute and the membrane wrapped in clingfilm. All excess air bubbles were removed. The membrane was then exposed to autoradiographic film (Kodak, X-OMATS) for various times (from 10 seconds to 30 minutes depending on the signal). The exposed autoradiographic film was developed for 3 minutes in developer (Kodak, LX-24). The film was then washed in water for 15 seconds and transferred to a fixative (Kodak, FX-40) for 5 minutes. The film was then washed with water for 5-10 minutes and left to dry at room temperature.

2.9 RT-PCR analysis

2.9.1 Preparation of materials for RNA analysis

Due to the labile nature of RNA and the high abundance of RNase enzymes in the environment a number of precautionary steps were followed when analysing RNA throughout the course of these studies.

- General laboratory glassware and plasticware are often contaminated by RNases. To reduce this risk, glassware used in these studies were baked at 180°C (autoclaving at 121°C does not destroy RNase enzymes) for at least 8hours. Sterile, disposable plasticware is essentially free of RNases and was therefore used for the preparation and storage of RNA without pre-treatment. Polyallomer ultracentrifuge tubes, eppendorf tubes, pipette tips etc., were all autoclaved before use. All spatulas which came in to contact with any of the solution components were baked, chemicals were weighed out onto baked aluminium-foil and a stock of chemicals for "RNA analysis only" was kept separate from all other laboratory agents. All solutions (which could be autoclaved) that came in to contact with RNA were all prepared from sterile ultra-pure water and treated with 0.1% diethyl pyrocarbonate (DEPC) (Sigma, D5758) before autoclaving (autoclaving inactivates DEPC).
- Disposable gloves were worn at all times to protect both the operator and the experiment (hands are an abundant source of RNase enzymes). This prevents the introduction of RNases and foreign RNA/DNA in to the reactions. Gloves were changed frequently.

2.9.2 Total RNA extraction from cultured cell lines

Adherent cells were grown in 75cm^2 flasks until approximately 80% confluent. Media was then removed and 1ml per 75cm^2 flasks of TRI reagent (Sigma, T-9424) was added to the flask for 5 minutes ensuring that all cells were covered with the solution. TRI reagent is a mixture of guanidine thiocyanate and phenol in a mono-phase solution. It effectively dissolves DNA, RNA, and protein on lysis of cell culture samples. After addition of the reagent, the cell lysate should be passed several times through a pipette to form a homogenous lysate. To ensure complete dissociation of nucleoprotein complexes, the sample was allowed to stand for 5 minutes at room temperature. A volume of 200µl of chloroform (not containing isoamyl alcohol or any other additive) per ml of TRI reagent was added to the cell lysate. The sample was covered tightly, shaken vigorously for 15 seconds and allowed to stand for 2-15 minutes at room temperature. The resulting mixture was centrifuged at 13,000rpm for 15 minutes at 4°C. Centrifugation separated the mixture into 3 phases: an organic phase (containing protein), an interphase (containing DNA) and a colourless upper aqueous phase (containing RNA). The aqueous phase was then transferred to a fresh tube and 0.5ml of isopropanol per ml of TRI reagent used in sample preparation and mixed. The sample was then allowed to stand for 5-10 minutes at room temperature. The sample was then centrifuged at 13,000rpm for 10 minutes at 4°C. The RNA precipitate formed a pellet on the side and the bottom of the tube. The supernatant was removed and the RNA pellet was washed by adding 1ml (minimum) of 75% ethanol per 1ml of TRI reagent. The sample was vortexed and centrifuged at 8000rpm for 5 minutes at 4°C. Samples can be stored in ethanol at 4°C for at least 1 week and up to one year at -20°C. The RNA pellet was air-dried briefly. Approximately 30µl DEPC treated H_2O was added to the pellet. The RNA was then stored at -80°C until required for PCR analysis.

2.9.3 RNA quantification using Nanodrop

RNA was quantified spectrophotometrically at 260nm and 280nm using the Nanodrop. A 1µl aliquot of suitably diluted RNA was placed on the nanodrop. The software calculated the amount of RNA present using the fact that an optical density of 1 at

260nm is equivalent to 40mg/ml RNA. The ratio of A_{260}/A_{280} was used to indicate the purity of the RNA.

2.9.4 Reverse transcription of RNA isolated from cell lines

The following components were used in the reverse transcriptase (RT) reaction for RNA isolated from cell lines: 1µl oligo $(dT)_{12-18}$ primers (1µg/ml) (Promega, C1101); 2µl of total RNA (0.5µg/ml) and 2µl of DEPC-H_2O were mixed together and heated at 70°C for 10 min and then chilled on ice to remove any RNA secondary structure formation and allow oligo (dT) primers to bind to the poly $(A)^+$ tail on the mRNA. To this, 4µl of a 5X buffer (consisting of 250mM Tris-HCL, pH 8.3, 375mM KCl and 15mM $MgCl_2$), 2µl of DTT (100mM), 1µl of dNTPs (10mM each of dATP, dCTP, dGTP and dTTP), 7µl of water and 1µl of Moloney murine leukaemia virus-reverse transcriptase (MMLV-RT) (Sigma, M1302) was then added to the heat-denatured RNA complex and the mixture was incubated at 37°C for 1 hour to allow the MMLV-RT enzyme catalyse the formation of cDNA on the mRNA template. The enzyme was then inactivated and the RNA and cDNA strands separated by heating to 95°C for 2 minutes. The cDNA was used immediately in the PCR reaction or stored at -20°C until required for analysis.

2.9.5 Polymerase Chain Reaction (PCR) analysis of cDNA formed from mRNA isolated from cell lines

PCR reactions were set up as 50µl volumes using 5 µl of cDNA formed during the RT reaction (see Section 2.9.4). Complemetary DNA (cDNA) was amplified for varying cycle numbers but where possible amplification was carried out in the exponential phase of amplification. The sequences of all primers used for PCR in this thesis are shown in Table 2.9. Each PCR reaction tube contained: 5µl 10X buffer (100mM Tris-HCl, pH 9.0, 50mM KCl, 1% Triton X-100); 2µl 25mM $MgCl_2$; 1µl of first strand target primer* (250ng/µl); 1µl of second strand target primer* (250ng/µl); 0.5µl of first strand endogenous β-actin control primer* (250ng/µl); 0.5µl of second strand endogenous β-actin control primer* (250ng/µl) and 35.5µl UHP. A volume of 5µl of

cDNA (pre-heated to 95°C for 3minutes to separate strands and remove any secondary structure if the sample had been stored at -20°C) was added. The mixture was heated to 94°C for 5minutes (reduces non-specific binding of primers to template). A volume of 1µl of 10mM dNTP (Sigma, DNTP-100), and 0.5µl of Taq DNA Polymerase enzyme (Sigma; D4545) and water to a total volume of 8.5µl was then added. The cDNA was then amplified by PCR (Techne; PHC-3) using the following program:

- 94°C for 3min (denature double stranded DNA)
- 25-35 cycles 94°C for 30sec (denature double stranded DNA);
  X°C for 30sec (anneal primers to cDNA);
  72°C for 30sec (extension);
- 72°C for 7min (extension).
- Storage at 4°C

Table 2.9 Sequences of primers used for PCR

Gene	Length (bp)	Tm (°C)	Size (bp)	Sequence
β-actin (large)	29 22	55	383	GAA ATC GTG CGT GAC ATT AAG -GAG AAG CT TCA GGA GGA GCA ATG ATC TTG A
β-actin (small)	23 22	55	142	TGG ACA TCC GCA AAG ACC TGT AC TCA GGA GGA GCA ATG ATC TTG A
p53	26 26	55	293	CAG CCA AGTCTG TGA CTT GCA CGT AC CTA TGT CGA AAA GTG TTT CTG TCA TC

A 10µl aliquot of tracking buffer, consisting of 0.25% bromophenol blue (Sigma, B5525) and 30% glycerol in water, was added to each tube of amplified cDNA products. A volume of 20µl of cDNA products from each tube were then separated by electrophoresis at 100mV through a 2% agarose (Sigma, A9539) gel containing ethidium bromide (Sigma, E8751), using TBE (22.5mM Tris-HCl, 22.5mM boric acid (Sigma, B7901) and 0.5mM EDTA) as running buffer. Molecular weight markers "ϕ-X174" Hae III digest (Sigma, P0672) were run, simultaneously, as size reference. The

resulting product bands were visualised as pink bands (due to the intercalation of the cDNA with the ethidium bromide) when the gels were placed on a transilluminator (UVP Transilluminator). The gels were photographed.

2.10 Transfection of Mammalian Cells with Exogenous DNA

In order to understand the role of p53 more clearly, it was found necessary to introduce foreign DNA into host cells to increase the level of expression of the p53 gene by transfecting with an expression plasmid. Sufficient plasmid was produced by transforming JM109 with the plasmid required, growing up a large stock of these cells and isolating the plasmid from them. This isolated plasmid was then transfected into the chosen cell line.

2.10.1 Plasmid details

A 2kb *Bam* H1 fragment was digested and purified from a p53 clone (ATCC) and subcloned into the *Bam* H1 site of pcDNA3.1 Zeo^{+}. This was carried out by Invitrogen.

2.10.2 $MgCl_2$ / $CaCl_2$ Transformation of JM109 Cells

A bacterial cell suspension (100µl) of competent JM109 (Promega, L2001) was mixed with 20ng DNA and placed on ice for 40min after which the mixture was heat-shocked at 42°C for 90 seconds and then placed on ice for 3 minutes. LB broth (1ml) ((10g Tryptone (Oxoid, L42), 5g Yeast Extract (Oxoid, L21) 5g NaCl (Merck, K1880814))/litre LB, autoclaved before use) was added to the competent cell suspension and incubated at 37°C for 40min. A volume of 400µl of this suspension was spread on a selecting agar plate (LB agar containing appropriate antibiotic conc.) and incubated overnight at 37°C. Single colonies, which grew on these selecting plates, were further streaked onto another selecting plate and allowed to grow overnight at 37°C.

2.10.3 DNA miniprep of plasmid DNA

To determine and select the colonies containing the inserted DNA sequence, a miniprep of the plasmid DNA was carried out. Plasmid DNA was isolated using the QIAprep spin miniprep kit (Qiagen, 27104). Single colonies were selected off the plates (Section 2.10.2) and incubated in universals containing 5mls LB/Amp shaking at 180rpm at 37^0C overnight. After incubation, the cells were centrifuged at 8,500rpm for 3 minutes. Pelleted cells were resuspended in 250µl of buffer P1 and the cell suspension was transferred to an microcentrifuge tube. To this solution, 250µl buffer P2 was added and mixed gently. A volume of 350µl buffer N3 was added to the solution and the tube was mixed immediately. This mixture was centrifuged for 10 minutes at 13,000 rpm. The supernatant was applied to a QIAprep spin column and centrifuged for 60 seconds. The flow-through was discarded. The column was washed by adding 500µl buffer PB and centrifuging for 60 seconds. The flow through was discarded. This step was repeated with 750µl buffer PB. The column was centrifuged for a further 60 seconds to remove all of the wash buffer. The column was then placed in a clean microcentrifuge tube. To elute the DNA, 50µl of buffer EB was added to the column. The column was let stand for 60 seconds and tehn centrifuged for 60 seconds.

2.10.4 Restriction digest of plasmid

After miniprep of the plasmid in *E. Coli* JM109 cells, a restriction digest of the pcDNA + p53 and the empty vector pcDNA plasmids was carried out to ensure that the plasmid was intact. Three digests were set up for each plasmid:

- No enzyme
- EcoR1
- BamH1

For each digestion the follwing was added to 2µl DNA: 2µl enzyme buffer; 1µl enzyme and 15µl water. The samples were run out on a 1% agarose gel, together with 3 µls loading dye. From this information, samples were selected for large-scale plasmid preparation. The p53 plasmid was inserted in to the pcDNA vector at a BamH1 cutting site. Subsequently, when the plasmid is cut with BamH1 enzyme, two bands should result, one the size of the vector, and the other corresponding to the p53

inserted fragment. Ligation with another enzyme like EcoR1 only results in one band since it doesn't separate the p53 fragment.

2.10.5 Preparation/Purification of plasmid DNA

Plasmid DNA was purified using an endofree plasmid maxi kit (Qiagen, 12362). A single colony from selecting plates (Section 2.10.2) was used to inoculate 5 ml LB/Amp broth. This was incubated for 8 hours at 300rpm and 37^{0}C. This culture was diluted 1/500 (400µl into 200mls) into selective media and incubated overnight at 300rpm and 37^{0}C. The bacterial cells were harvested by centrifugation at 6,000rpm for 15 minutes at 4^{0}C. The pellet was resuspended in 10ml buffer P1. To this, 10 ml buffer P2 was added, mixed gently and incubated at room temperature for 5 minutes. A volume of 10ml chilled buffer P3 was added to the lysate and mixed immediately and gently. The lysate was poured into the barrel of the QIAfilter cartridge and incubated at room temperature for 10 minutes. The cap from the QIA filter outlet nozzle was removed and the plunger was gently inserted in to the cartridge, The cell lysate was filtered into a 50ml tube. To the lysate, 2.5ml buffer ER was added and mixed by inverting repeatedly. This was incubated on ice for 30 minutes. A qiagen-tip 500 was equilibrated by applying 10ml buffer QBT and the column was allowed to empty by gravity flow. The filtered lysate was tehn applied to the qiagen-tip and allowed to enter the resin by gravity flow. The qiagen-tip was washed twice with 30ml buffer QC. The DNA was eluted by addition of 15ml buffer QN and the eluate was collected in a 30ml tube. The DNA was precipitated by adding 10.5ml isopropanol to the eluated DNA. This was mixed and centrifuged at ~10,000rpm for 30 minutes at 4^{0}C. The DNA pellet was washed with 5ml of 70% ethanol and this was centrifuged at ~10,000rpm for 10 minutes. The pellet was air-dried and dissolved in 500µl buffer TE. The DNA concentration was determined by measuring the OD_{260nm}.

2.10.6 Lipofectin transfection

Cells were seeded into a 25cm^2 flask at a density of 1 x 10^5 cells per flask in 4 mls culture medium. The cells were then incubated overnight at 37°C overnight. For each transfection, 2µg DNA was diluted into 100µl of serum free media (SFM). For each

transfection, 20µl lipofectin reagent (Invitrogen, 18292-011) was diluted into 100µl SFM and left at room temperature for 30-45 minutes. The two solutions were then combined and incubated at room temperature for 10-15 minutes. The cells were washed with 2 ml SFM. To the DNA-lipofectin mixture, 1.8ml SFM was added. This solution was mixed gently and overlaid onto the cells. The cells were then incubated for a further 24 hours. After this time, the DNA containing media was replaced with serum-containing growth media and incubated for a further 48 hours. The cells were subcultured 1:5 into zeocin-containing media.

2.10.7 Selection and Isolation of Clones

In order to study the true effect of transfection studies, single clones of stably transfected cells were selected and isolated. The selection process was carried out by feeding the "transfected" cells with media containing zeocin (Invitrogen R250-01), the plasmids used had a zeocin-resistant gene, therefore, only those cells containing the plasmid will survive treatment with zeocin. Two days after transfection the cells were fed with media containing zeocin. The concentration of the drug was increased until a concentration known to kill untransfected cells was reached. At this stage the cells were plated at clonal density and clonal populations were propagated as described in Section 2.2.7. Transfected cells were periodically challenged with zeocin to establish stability of transfectants.

2.11 Microarrays

Figure 2.1 shows a schematic of the gene expression workflow.

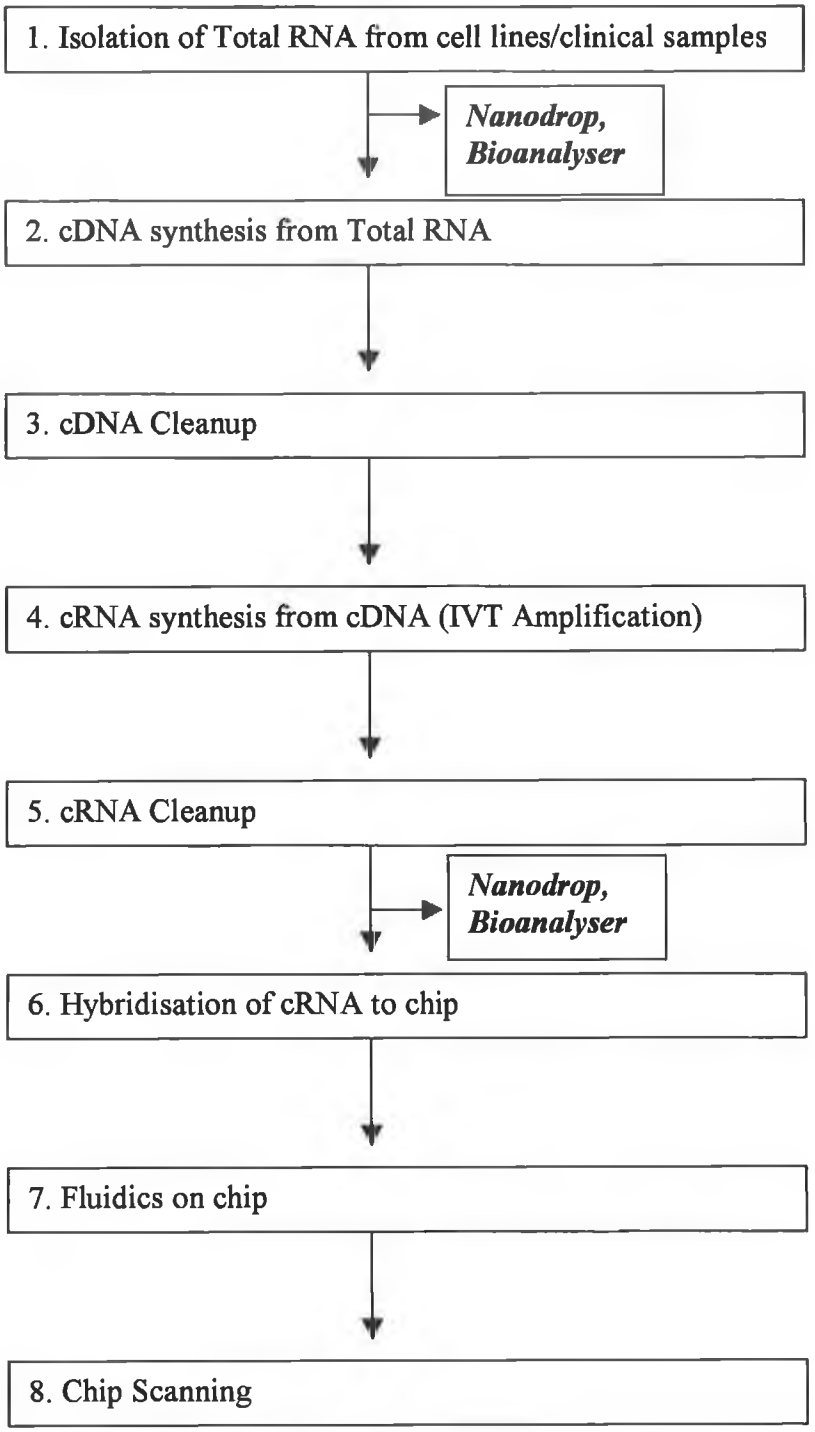

Figure 2.1 Gene expression workflow

2.11.1 Isolation of total RNA from cell lines

Total RNA was extracted from cells using the RNeasy Mini prep kit (Qiagen, 74104). Cells were lysed in 600µl buffer RLT (2-β-mercaptoethanol was added prior to use - 10µl/ml). Cells were homogenised by passing samples five times through a 20-gauge needle fitted to an RNase-free syringe. One volume (600µl) 70% ethanol was added and the lysate was applied to an RNeasy column. Samples were centrifuged for 15 seconds at 10,000rpm and flow through was discarded. A volume of 700µl Buffer RW1 was added. Samples were centrifuged for 15 seconds at 10,000rpm and flow through and collection tube were discarded. A volume of 500µl Buffer RPE was pipetted onto the column, and samples were centrifuged for 15 seconds at 10,000rpm and flow through was discarded. A further 500µl Buffer RPE was added. The columns were centrifuged for 2 min at 10,000rpm. The column was transferred to a new 1.5ml tube and the RNA was eluted with 20 µl RNase free water. A 1:4 dilution of the eluted RNA was applied to the nanodrop to quantify the RNA (Section 2.9.3).

2.11.2 Determination of RNA purity using Bioanalyser

The RNA 6000 Nano assay™ was used to ensure RNA samples subjected to microarray analysis were of good quality. A 550µl aliquot of RNA 6000 Nano gel matrix was placed into a spin filter tube and centrifuged at 1500g for 10 minutes. The filtered gel was aliquoted into 65µl amounts. During the 10 minute spin, 2µl aliquots of suitably diluted RNA samples (see Section 2.11.1) and RNA ladder were prepared in 0.5µl RNase free tubes and heated to 70 °C for at least 2 minutes followed by cooling on ice for 1 minute. The dye concentrate was allowed to equilibrate to room temperature for 30 minutes, then vortexed for 10 seconds and 1µl of the dye was added to 65µl of filtered gel matrix. The solution was vortexed well and centrifuged for 10 minutes at 13,200rpm. A new chip was placed on the chip priming station and 9µl of the gel dye mix was pipetted into the well marked with the bold **G**. The Chip priming station was closed gently and the plunger pressed and held in place by the clip. After exactly 30 seconds, the plunger was released by pressing the clip. After a further 30 seconds, 9µl of gel dye mix was pipetted into the remaining wells marked G. RNA 6000 Nano Marker (5µl) was loaded into the well marked with the ladder and into all the 12 sample wells. If any well remained unused, 6µl Nano Marker was added to

those wells. 1µl of each sample prepared earlier (Section 2.11.1) was added into each of the sample wells. The chip was placed in the special vortex adapter and vortexed at 2400 rpm for 1 minute. The chip was then run on the Agilent Bioanalyzer within 5 minutes.

2.11.3 cDNA synthesis from total RNA

Synthesis of cDNA was carried out using the One-cycle cDNA synthesis kit (Affymetrix, 900431). Total RNA (10µg) was placed in a 0.5ml tube. To each tube, 2µl of diluted poly-A RNA controls were added along with 2µl of 50µM T7-Oligo(dT) Primer. RNase-free water was added to a final volume of 11µl. The tubes were flicked to mix and then centrifuged briefly. This reaction was incubated for 10 minutes at 70°C. The sample was then cooled to 4 °C for at least 2 minutes. The first strand mastermix was assembled, allowing for an extra half a sample. For a single reaction the master mix contained, 4µl 5X 1st strand reaction mix, DTT (0.1M), dNTP (10mM). A volume of 7µl of mastermix was added to each reaction tube to a final volume of 18µl. The tubes were mixed by flicking, and then centrifuged briefly and placed immediately at 42°C for 2 minutes. To each RNA sample, 2µl of SuperScript II was added. The tubes were mixed well and centrifuged briefly. The tubes were incubated at 42°C for 1 hour and then cooled at 4°C for 2 minutes. The second strand mastermix was assembled containing: 91µl RNase-free water; 30µl 5X 2nd strand reaction mix; 3µl dNTP(10mM); 1µl *E.coli* DNA ligase; 4µl *E.coli* DNA polymerase I and 1µl RNase H. To each first strand synthesis sample, 130µl of second-strand mastermix was added. The tubes were mixed and centrifuged briefly and incubated for 2 hours at 16°C. After incubation, 2µl of T4 DNA Polymerase was added to each sample, and incubated for 5 minutes at 16°C. To stop any further reaction, 10µl of EDTA (0.5M) was then added to each tube.

2.11.4 cDNA cleanup

Synthesized cDNA was cleaned-up using a sample clean-up module (Affymetrix, 900371). cDNA binding buffer (600µl) was added to each double-stranded cDNA

synthesis preparation and mixed by vortexing for 3 seconds. A volume of 500µl of the sample was then applied to a cDNA cleanup spin column sitting in a 2ml collection tube. The columns were centrifuged for 1 minute at 10,000rpm and the flow through was discarded. The column was loaded with the remaining sample and centrifuged as above. The collection tube and flow through were discarded. The spin column was placed in a clean 2ml collection tube. To the column, 750µl of cDNA wash buffer was added and centrifuged for 1 minute at 10,000rpm. The columns were then centrifuged with the caps open for 5 minutes at 13,000rpm to allow the membrane to dry. The spin columns were placed in a 1.5ml tube and 14µl of cDNA elution buffer was pipetted directly onto column membrane. The tubes were centrifuged for 1 minute at 13,000rpm. Eluted cDNA was stored at -80°C.

2.11.5 cRNA synthesis from cDNA

Genechip IVT labelling kit (Affymetrix, 900449) was used to prepare cRNA. To each 0.5ml tube, 6µl of cDNA was added. For the IVT reaction the following reagents were added to the cDNA: 14µl RNase-free water; 4µl 10X IVT labelling buffer; 12µl labelling NTP mix and 4µl IVT labelling enzyme mix. These reagents were mixed carefully and centrifuged briefly. The reaction tubes were then incubated for 16 hours at 37°C.

2.11.6 cRNA cleanup

Synthesized cRNA was cleaned-up using a sample clean-up module (Affymetrix, 900371). To the labelled cRNA, 60µl of RNase-free water was added and mixed by vortexing for 3 seconds. After mixing, 350µl of IVT cRNA binding buffer was added and again mixed by vortexing for 3 seconds. A volume of 250µl of ethanol (96-100%) was added and pipetted up and down to mix. This sample was applied to an IVT cRNA cleanup spin column sitting in a 2ml collection tube. This was centrifuged for 15 seconds at 10,000rpm and the flow through discarded. To the column, 500µl of 80% (v/v) ethanol was added and centrifuged for 15 seconds at 10,000rpm. The flow through was discarded and the column was centrifuged for 5 minutes at 13,000rpm with the cap open to allow the membrane to dry. The column was transferred to a

1.5ml tube and 11µl of RNase-free water was applied directly to the membrane. The column was centrifuged for 1 minute at 13,000rpm. A further 10µl of RNase-free water was applied to the membrane and centrifuges again for 1 minute at 13,000rpm. The eluted cRNA was diluted 1:100 for quantification using the Nanodrop (Section 2.9.3). A 1:2 dilution of the cRNA was also analysed on the Bioanalyser (Section 2.11.2).

2.11.7 Hybridisation of cRNA to genechips

Fragmentation of the labelled cRNA was carried out prior to hybridisation onto the array using the sample clean up module (Affymetrix, 900371). This was achieved by incubating 15µg of cRNA with 5X fragmentation buffer at 94°C for 35 minutes. To each tube of fragmented RNA, 270µl of hybridisation cocktail was added which contained per reaction: 5µl control oligonucleotide B2 3nM (Hybridization control kit, Affymetrix, 900454); 15µl 20X eukaryotic hybridisation controls (Hybridization control kit, Affymetrix, 900454); 3µl Herring sperm DNA 10mg/ml (Promega, D1811); 3µl BSA 50mg/ml (Invitrogen, 15561-020); 150µl 2X Hybridisation buffer (Hybridization control kit, Affymetrix, 900454); 30µl DMSO (Sigma, D5879) and 34µl water. The genechips were placed at room temperature 30 minutes before use to allow the rubber septa to equilibrate to room temperature. This prevents leakage of the sample. The genechips used were Affymetrix U133 Plus 2.0 chips. The arrays were wetted by filling with 200µl of 1X hybridisation buffer and incubated at 45°C for 15 minutes at a rotation speed of 60rpm. The hybridisation cocktail was heated to 99°C for five minutes and then cooled to 45°C for 5 minutes and then centrifuged at 13,000rpm for 5 minutes. The buffer solution was removed from the genechips and replaced with 300µl of hybridisation cocktail and sample. The genechips were then placed into the hybridisation oven at 45°C at a rotation of 60rpm for 16 hours.

2.11.8 Array washing and staining

After hybridisation, the hybridisation buffer was removed from the chips and replaced with non-stringent wash buffer. Streptavidin phycoerythrin (SAPE) stain solution was freshly prepared: 600µl 2X stain buffer (100mM MES stock buffer, 1M Na^+, 0.05%

Tween-20); 48µl 50mg/ml BSA (Invitrogen, 15561-020); 12µl 1mg/ml SAPE (Molecular probes, S-866) and 540µl deionised (DI) water. This was divided into two aliquots per array. Antibody was prepared as follows: 300µl 2X stain buffer; 24µl 50mg/ml BSA; 6µl 10mg/ml goat IgG stock (Sigma, I5256); 3.6µl 0.5mg/ml biotinylated antibody (Vector Laboratories BA-0500) and 266.4µl DI water. The Affymetrix Genechip Operating Software™ (GCOS™) manages the fluidics protocol. The fluidics station was prepared by running a priming protocol. This step checks that the buffers are properly connected and fills the tubes with the appropriate fluid. When primed, each module was set up with one genechip, two vials of SAPE solution and one vial of antibody solution. The antibody amplification for eukaryotic targets protocol was initiated. The details of the protocol EukGE-WS2v4_450 can be seen in Table 2.10. This process takes approximately 75 minutes to complete.

Table 2.10 Details of fluidics protocol for staining probe array

Fluidics protocol – EukGE-WS2v4_450	
Post-hyb wash #1	10 cycles of 2 mixes/cycle with wash buffer A at 25°C
Post-hyb wash #2	4 cycles of 15 mixes/cycle with wash buffer B at 50°C
Stain	Probe array stained for 10mins in SAPE solution at 25°C
Post-stain wash	10 cycles of 4 mixes/cycle with wash buffer A at 25°C
2nd Stain	Probe array stained for 10mins in SAPE solution at 25°C
3rd Stain	Probe array stained for 10mins in SAPE solution at 25°C
Final wash	15 cycles of 4 mixes/cycle with wash buffer A at 30°C
Hold	Hold temperature of 25°C

2.11.9 Array scanning

After staining and washing, the chips were scanned using an affymetrix genechip scanner. Similarly to the fluidics station, GCOS manages the scanning protocol. The chips were placed in the scanner and scanned. The scan generated an initial image file (*.DAT), which contains the values for each gene probe. As there are 11 probes for each gene (one probe set), these values were averaged out into another file that is

generated automatically by GCOS (*.CEL). GCOS can then generate another file from the .CEL file that will contain numerical values for each probe set (*.CHP).
Finally, a quality control report file (*.RPT) is generated which is used to check the reliability/QC of each sample.

2.11.10 Chip Quality Control

After carrying out the array experiments, some quality control must be carried out on the chips before continuing for analysis. GCOS generates a report for each chip that is scanned and a chip information form was filled out for each chip from this report with the following information:

- Background – level of non-specific binding
- 3'/5' Ratio – how well labelling reaction has proceeded
- Hybridisation controls - comparable sample levels added
- Percentage present
- Noise – electrical noise from scanner
- Scale factor – brightness of array

Once a chip report was deemed satisfactory, the data from the chip was transferred into the analysis software, dChip.

2.12 Bioinformatics

2.12.1 Raw data transfer into dChip

DNA-Chip Analyzer (dChip) is a software package for analysis of microarray data. The CEL files generated by GCOS (Section 2.11.9) were imported into dChip. These CEL files contain all of the intensity values from the genechips scanned. In order to make sense of these files, a Chip Description File (CDF) file was also imported into D-Chip which specifies which arrays were used and what each probe on the array represents. A sample information file was also brought into dChip that contained more detailed information on each sample on the arrays. This facilitated interpretaion of the data in dChip.

2.12.2 Normalisation in dChip

Dchip is a software package implementing model-based expression analysis of oligonucleotide arrays (Li and Wong, 2001) and several high-level analysis procedures. This model-based approach allowed probe-level analysis on multiple arrays. By pooling information across multiple arrays, it was possible to assess standard errors for the expression indexes. In this normalisation procedure an array with median overall intensity was chosen as the baseline array against which other arrays were normalised at probe level intensity. Subsequently a subset of PM probes, with small within-subset rank difference in the two arrays, served as the basis for fitting a normalisation curve. This approach also allowed automatic probe selection in the analysis stage to reduce errors due to cross-hybridizing probes and image contamination. High-level analysis in dChip included comparative analysis and hierarchical clustering. Normalisation of the data was performed to adjust the brightness of the arrays to a comparable level. The array with the median overall intensity was taken as the baseline and the other arrays were normalised at probe intensity level. All low-intensity values were truncated to 1. The chips were also viewed in dChip to ensure that the overall appearance of the chip was of even intensity.

2.12.3 Hierarchical clustering

Hierarchical clustering is a quality control step that was carried out in dChip. It allowed comparison of the list of gene expression values for each sample and shows which are most similar to each other. At this point, before further analysis it was ensured that the triplicate samples had clustered correctly. Hierarchical clustering was used to represent the relationship between replicate samples and different sets of replicate samples. The tree represents relationships amongst genes in which, branch lengths represent degrees of similarities. This method was useful in its ability to represent varying degrees of similarity and distant relationships among groups of closely related genes. The computed tree was used to organize genes in the original data table, so that genes with similar expression patterns were adjacent.

2.12.4 Data analysis

In dChip samples were compared in triplicate e.g. baseline vs experiment. This created genelists in Microsoft Excel of differentially expressed genes in the two groups. These genelists contained information on baseline and experiment intensity, fold change and p value. Each parent cell line was compared, in triplicate, to its taxol-resistant variant. Genelists created contained genes that were differentially expressed in the triplicates of the two cell lines using certain filtering parameters. The filtering parameters used were a fold change of >1.2, a difference of intensity of >100 and a p value <0.05. These comparison criteria require the fold change between the group means to exceed 1.2; the absolute difference between the two group means to exceed 100 and that the difference of the means is statistically significant using an unpaired two-tailed t-test so that p-value <0.05.

2.12.5 Comparison of genelists

The genelists created in dChip were compared using Microsoft Access. A database was created to compare genes that were differentially expressed in two or more genelists from dChip. Firstly a list of genes that were differentially regulated in all four taxol-resistant variants, compared to parent cell lines was created. Secondly, a genelist that contained genes differentially regulated in three of the four taxol-resistant variants was created. This genelist was shortened to only include only genes that were

upregulated in three of the four taxol-resistant variants, or downregulated in three –f the four taxol-resistant variants

2.12.6 Pathway analysis

Pathway analysis was carried out using Pathway Assist software. Genelists to be studied in Pathway Assist were imported in the form of *txt files. PathwayAssist is a product aimed at the visualisation and analysis of biological pathways, gene regulation networks and protein interaction maps. It comes with a comprehensive database that gives a snapshot of all information available in PubMed, with the focus on pathways and cell signalling networks. This product was useful in assisting in the interpretation of Microarray results. It allowed visualisation of results in the context of pathways, gene regulation networks and protein interaction maps. This was done using curated and automatically created pathways. Graph drawing, layout optimisation, data filtering, pathway expansion and classification and prioritization of proteins were all possible. PathwayAssist worked by identifying relationships among genes, small molecules, cell objects and processes and built pathways based on these relationships.

2.13 RNA interference (RNAi)

RNAi using small interfering RNAs (siRNAs) was carried out to silence specific genes. The siRNAs used were chemically synthesized and purchased from Ambion Inc. These siRNAs were 21-23 bps in length and were introduced to the cells via reverse transfection with the transfection agent siPORT™ *Neo*FX™ (Ambion inc., 4511).

2.13.1 Transfection optimisation

In order to determine the optimal conditions for siRNA transfection, an optimisation with a siRNA for kinesin (Ambion Inc., 16704) was carried out for each cell line. Cell suspensions were prepared at $1x10^4$, $2.5x10^4$ and $5x10^4$ cells per ml. Solutions of negative control and kinesin siRNAs at a final concentration of 30nM were prepared in optiMEM (Gibco™, 31985). NeoFX solutions at a range of concentrations were prepared in optiMEM in duplicate and incubated at room temperature for 10 minutes.

After incubation, either negative control or kinesin siRNA solution was added to each neoFX concentration. These solutions were mixed well and incubated for a further 10 minutes at room temperature. Replicates of 10µl of the siRNA/neoFX solutions were added to a 96-well plate. The cell suspensions were added to each plate at a final cell concentration of $1x10^3$, $2.5x10^3$ and $5x10^3$ cells per well. The plates were mixed gently and incubated at 37°C for 24 hours. After 24 hours, the transfection mixture was removed from the cells and the plates were fed with fresh medium. The plates were assayed for changes in proliferation at 72 hours using the acid phosphatase assay (Section 2.4.2). Optimal conditions for transfection were determined as the combination of conditions which gave the greatest reduction in cell number after kinesin siRNA transfection and also the least cell kill in the presence of transfection reagent. The optimised conditions for the cell lines are shown in Table 2.11.

Table 2.11 Optimised conditions for siRNA transfection

Cell line	Seeding density per well	Volume NeoFX per well (µl)
A549 and variants	2.5×10^3	0.2
H1299 and variants	5×10^3	0.3
H460 and variants	1×10^3	0.1

2.13.2 Proliferation effects of siRNA transfection

Using the optimised conditions in Table 2.11, each of the siRNAs was tested to see changes in proliferation of the cells after transfection. Two separate siRNAs were used for each target gene (Table 2.12), with the exception of ABCB1 since a validated siRNA was available for this target. All siRNAs were purchased from Ambion Inc.

Solutions of siRNA at a final concentration of 30nM were prepared in optiMEM (Gibco™, 31985). NeoFX solution was prepared in optiMEM and incubated at room temperature for 10 minutes. After incubation, an equal volume of neoFX solution was added to each siRNA solution. These solutions were mixed well and incubated for a further 10 minutes at room temperature. Replicates of 10µl of the siRNA/neoFX solutions were added to a 96-well plate. The cell suspensions were added to each plate at the appropriate final cell concentration (Table 2.11). The plates were mixed gently

and incubated at 37°C for 24 hours. After 24 hours, the transfection mixture was removed from the cells and the plates were fed with fresh medium. The plates were assayed for changes in proliferation at 72 hours using the acid phosphatase assay (Section 2.4.2).

Table 2.12 List of siRNAs used

Target name	Ambion IDs
Scrambled	Negative control #2
ABCB1	4123 (Validated)
CTGF	146149, 146150
ID3	122173, 122294
CRIP1	145761, 215088
IGFBP6	44812, 44907
EMP1	145889, 145890
CRYZ	112817, 146128
GULP1	121783, 121784
SCP	27500, 27593
FSTL1	136252, 146149

2.13.3 Toxicity assays on siRNA transfected cells

To assay for changes in sensitivity to chemotherapeutic agents, siRNA experiments in 96-well plates were set up as in Section 2.13.2. Transfection medium was removed after 24 hours and replaced with fresh growth medium. Concentrations of the chemotherapeutic agent (2X) were added to the plates in replicates of four 48 hours after transfection. The plates were assayed for changes in proliferation at 96 hours using the acid phosphatase assay (Section 2.4.2).

Section 3.0: Results

3.1 p53

3.1.1 Transfection with wild-type p53

In order to better understand the role of p53 in drug resistance, a wild-type p53 plasmid was introduced to the cell lines in table 3.1.1.

Table 3.1.1 p53 status of parent cell lines

Cell line	p53 status
A549	Wild-type
H1299	Null
DLKP-SQ	Mutant

3.1.2 Restriction digest of plasmid

Restriction digest of the pcDNA + p53 and the empty vector pcDNA plasmids was carried out to ensure that the plasmid was intact. Three digests were set up for each plasmid:

- No enzyme
- EcoR1
- BamH1

The p53 plasmid was inserted in to the pcDNA vector at a BamH1 cutting site. Subsequently, when the plasmid is cut with BamH1 enzyme, two bands should result, one the size of the vector, and the other corresponding to the p53 inserted fragment. Ligation with another enzyme like EcoR1 only results in one band since it doesn't separate the p53 fragment. The results seen in Figure 3.1.1 show that the plasmid obtained from the large scale preparation is intact, so the transfection can be carried out.

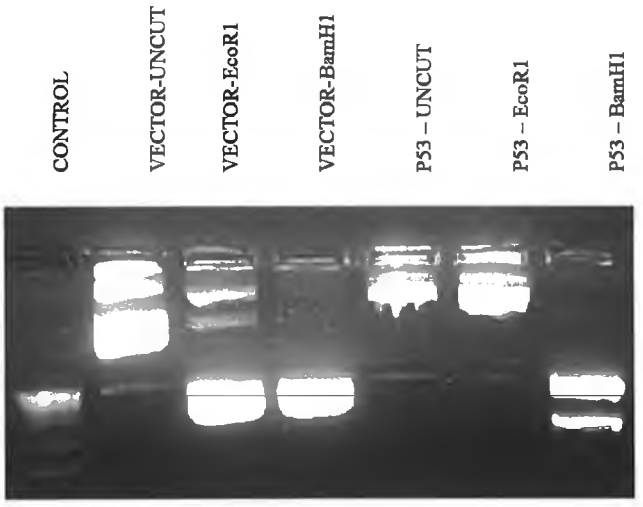

Figure 3.1.2 Restriction digest of plasmid preparation

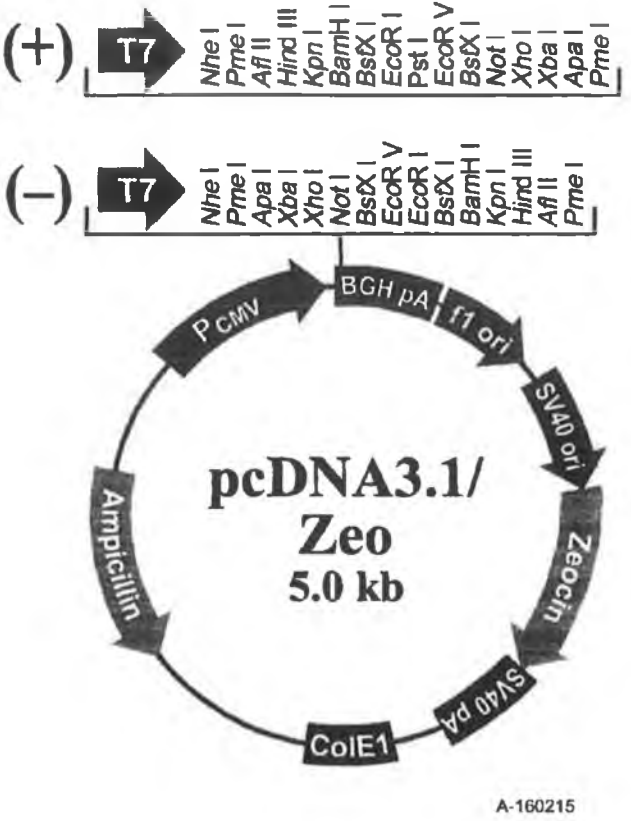

Figure 3.1.1 Map of plasmid

3.1.3 Lipofectin transfection

The wild-type p53 plasmid was transfected into four cell lines using lipofectin reagent. Three transfections were carried out per cell line

- No plasmid
- pcDNA empty vector
- pcDNA + p53

These controls ensure that any changes observed in the cell lines after transfection are due to the p53 expression and not caused by the transfection procedure itself.

3.1.4 Changes in sensitivity to chemotherapeutic drugs in mixed populations

Initially the mixed populations of the transfected cell lines were tested for any changes in sensitivity. The empty vector (EV) control transfected cell lines were also included in this analysis. Some changes in sensitivity were observed in both EV-transfected and p53-transfected cells as seen in Table 3.1.2.

Table 3.1.2 IC50s of mixed population transfection

	Adr (ng/ml)	Taxol (ng/ml)	Carbo (μg/ml)
A549-parent	15.4 ± 4.2	1.1 ± 0.2	6.7 ± 0.4
A549-ev mp	13.6 ± 3.1	1.7 ± 0.5	12.4 ± 3.8
A549-p53 mp	25.5 ± 1.4	2 ± 0.2	15.5 ± 0.7
H1299-parent	31 ± 0.8	4.3 ± 0.1	5.4 ± 0.2
H1299-ev mp	13.2 ± 1.1	4.2 ± 0.6	4.1 ± 0.2
H1299-p53 mp	14.6 ± 2.6	2.8 ± 0.4	3.1 ± 0.3
SQ parent	10.9 ± 0.8	2.2 ± 0.2	2.3 ± 0.2
SQ – ev mp	15.7 ± 1.4	2.2 ± 0.1	3.3 ± 0.2
SQ – p53 mp	10.3 ± 0.7	1.6 ± 0.2	2.2 ± 0.3

(Results are expressed as IC50 ± SD, n=3)

ev – empty vector control transfection
p53- p53 transfection
mp – mixed population

3.1.5 Analysis of p53 function

In non-drug treated cells (control) wild-type p53 protein should be present in small amounts because it is degraded rapidly by the cell. However, when cells are subjected to stress, such as DNA damage induced by drug treatment, wild-type p53 protein should accumulate, if the gene is functional. To test the function of the introduced gene transfected cells were treated with a range of different adriamycin concentrations with subsequent analysis of p53 protein content.

3.1.5.1 A549

A549 cells express endogenous wild-type p53, therefore accumulation of p53 is present in untransfected cells. Figure 3.1.3 shows the presence of p53 in A549 and the mixed population of p53-transfected A549 (A549-p53 mp) before and after treatment with adriamycin at 15, 30, 45 and 60ng/ml. There is an increased amount of wild-type p53 protein in the mixed population, demonstrating that the p53 gene is functional. An increase in p53 accumulation after DNA damage would demonstrate that exogenous p53 is functional. The mixed population was subsequently cloned out and ten individual clones isolated. Some of these clones show variances in the amount of p53 protein expressed as shown in Figure 3.1.4.

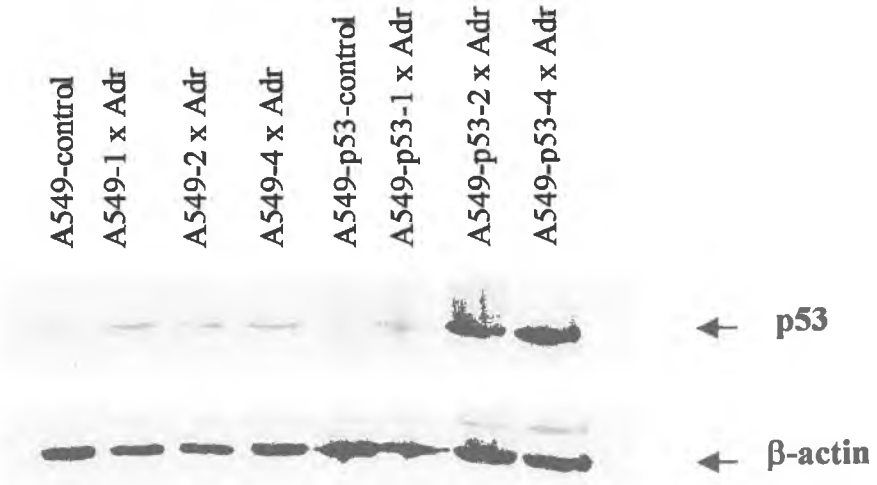

Figure 3.1.3 Western blot analysis of p53 expression in A549 parent and p53-transfected mixed population before and after adriamycin treatment

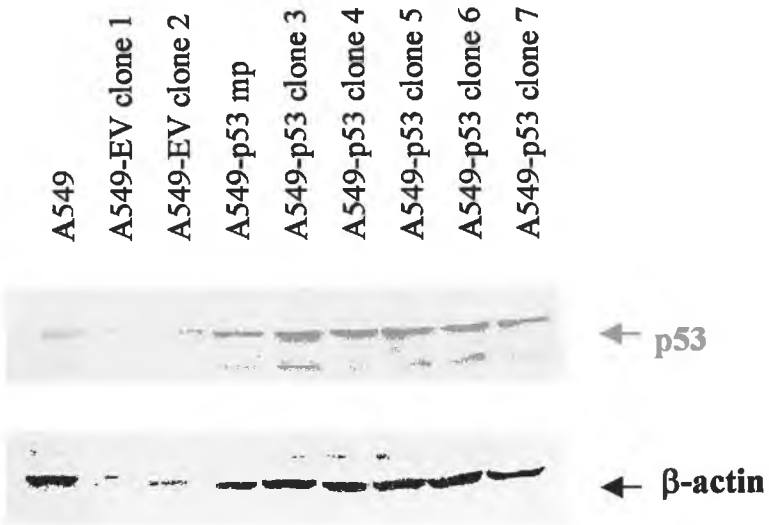

Figure 3.1.4 Western blot of A549 parent and transfected clones

3.1.5.2 H1299

H1299 parent cells have a p53 deletion which results in no endogenous p53 mRNA or protein expression. Western blot analysis revealed no p53 protein expression before or after drug treatment in the H1299-p53 mixed population. However, the cells were resistant to zeocin proving that the transfection was successful. After cloning out the mixed population and screening them for p53 protein expression clone 8 demonstrated the presence of p53 protein (Figure 3.1.6). p53 mRNA was present in two of the p53-transfected clones, 6 and 8 (Figure 3.1.5)

Figure 3.1.7 shows this cell line H1299-p53 clone 8 before (-) and after (+) adriamycin treatment. The p53 protein expressed in H1299-p53 clone 8 does not accumulate after DNA damage caused by the chemotherapeutic agent adriamycin.

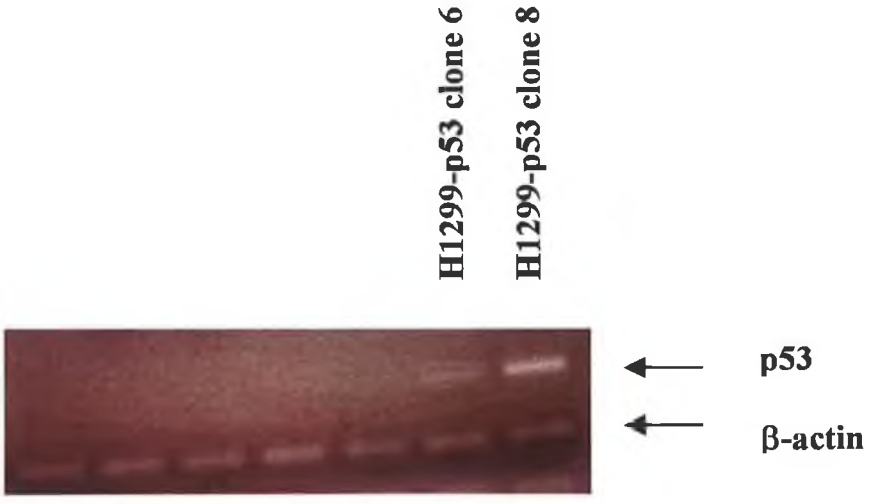

Figure 3.1.5 RT-PCR mRNA expression of p53 in H1299-p53 transfected clones

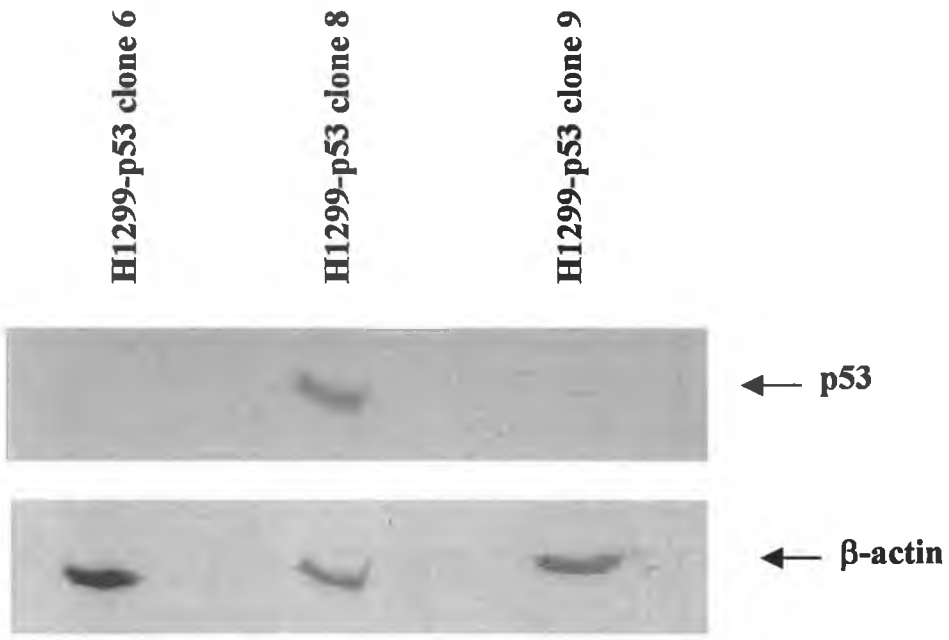

Figure 3.1.6 Detection of p53 protein in clone 8 of H1299-p53

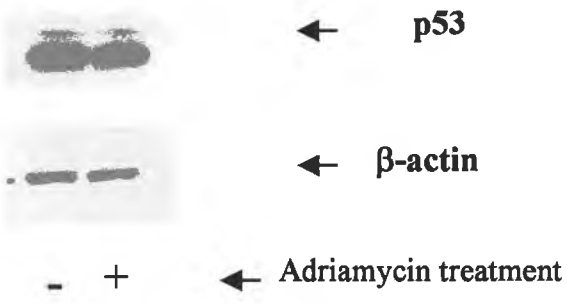

Figure 3.1.7 p53 expression in H1299-p53 clone 8 after drug treatment

3.1.6 Changes in sensitivity of p53 clones to chemotherapeutic drugs

In order to determine the role of p53 in resistance to chemotherapeutic agents, the p53 transfected clones were tested for differences in sensitivity to the agents adriamycin, taxol and carboplatin.

3.1.6.1 A549

It was expected that p53 would sensitise cells to chemotherapeutic drugs, however the general trend in the A549-p53 transfected cells was an increase in resistance with the introduction of p53 as shown in table 3.1.3. Some clones (e.g. clone 3) showed increased sensitivity to adriamycin with no significant change in resistance to taxol or carboplatin graphically shown in Figure 3.1.8.

Table 3.1.3 IC50s for some chemotherapeutic drugs in A549 transfected clones

Cell Line	Adriamycin (ng/ml)	Taxol (ng/ml)	Carboplatin (μg/ml)
A549 parent	15.43 ± 4.2	1.1 ± 0.1	6.7 ± 0.4
A549 EV mp	13.6 ± 3.1	1.7 ± 0.5	12.4 ± 3.8
A549 EV clone 1	9.9 ± 0.4	2.2 ± 0.1	8.3
A549 EV clone 2	11 ± 0.9	1.7 ± 0.4	6.1 ± 0.9
A549 EV clone 3	8.8 ± 0.9	2.1 ± 0.1	9.6 ± 0.2
A549 p53 mp	25.5 ± 1.4	2.1 ± 0.2	15.5 ± 0.7
A549 p53 clone 1	14.2 ± 1.5	2.6 ± 0.6	8.5 ± 0.5
A549 p53 clone 2	14.9 ± 1.9	1.4 ± 0.4	9.6 ± 1.2
A549 p53 clone 3	11.1 ± 0.3	1.5 ± 0.6	8.9 ± 1.4
A549 p53 clone 4	17.8 ± 2.1	1.9 ± 0.1	13.5 ± 2.3
A549 p53 clone 5	20.5 ± 1.4	2.1 ± 0.1	12.5 ± 1.7
A549 p53 clone 6	15.8 ± 1.7	2 ± 0.2	18.6 ± 2.2
A549 p53 clone 7	19.4 ± 0.6	2 ± 0.2	15.4 ± 1.1
A549 p53 clone 8	24.2 ± 1.3	1.9 ± 0.6	11.7 ± 2.6
A549 p53 clone 9	13.9 ± 1.5	1.1 ± 0.5	8.9 ± 1.2

(a)

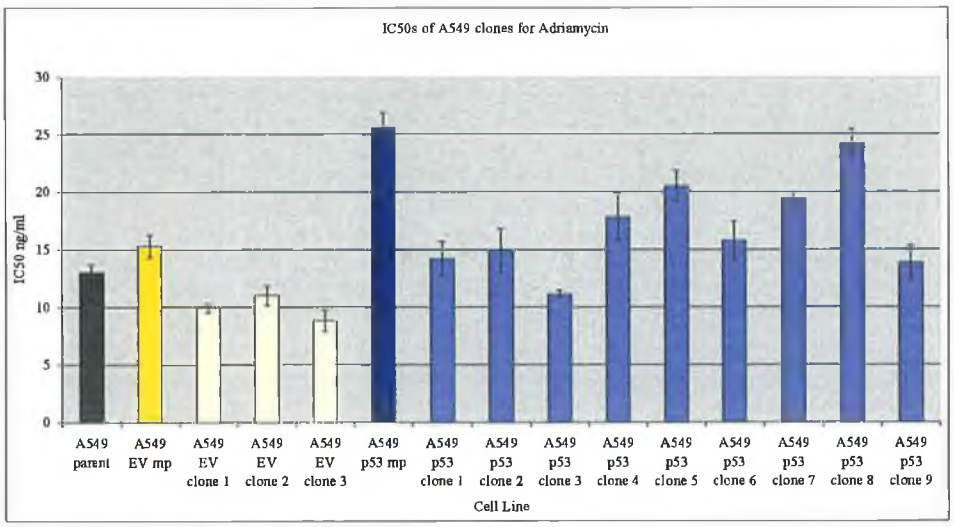

(b)

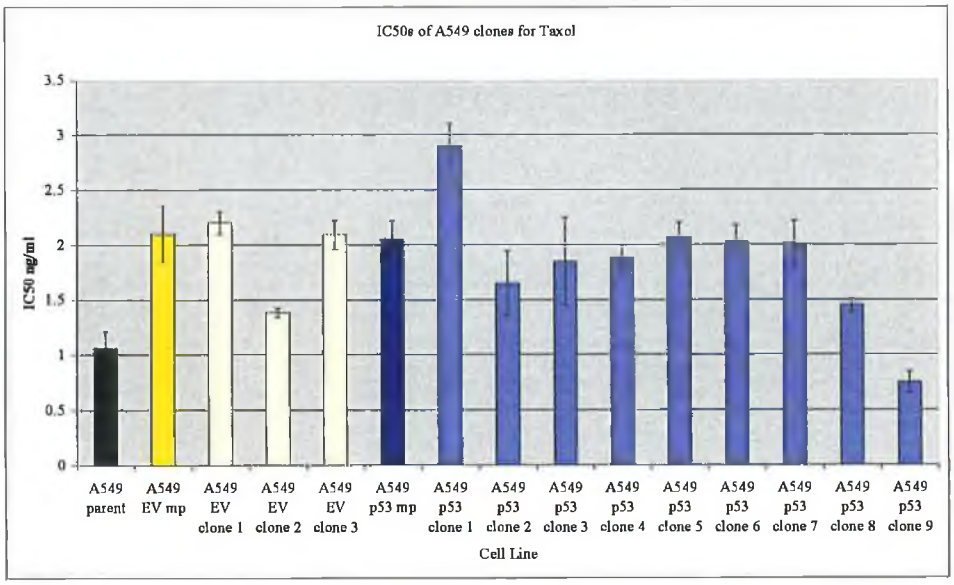

(c)

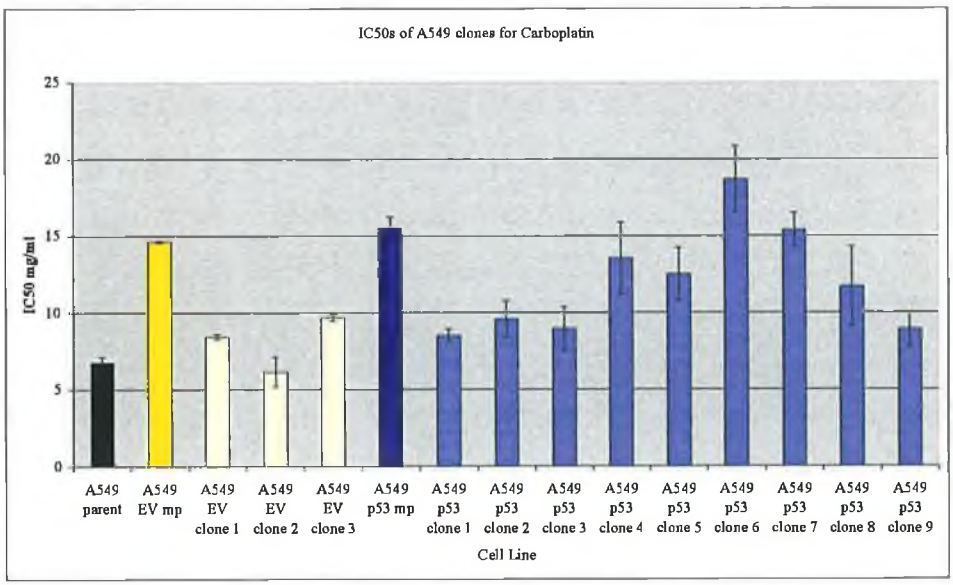

Figure 3.1.8 IC50s for (a) Adriamycin, (b) Taxol and (c) Carboplatin in A549 transfected clones

3.1.6.2 H1299

In contrast to the A549 transfected cells the introduction of wild-type p53 sensitised most clones of the H1299 transfected cell line. An increase in sensitivity to adriamycin, taxol and carboplatin was seen in all clones but H1299-p53 clone 3, which was more resistant to the drugs tested. However, the empty vector mixed population showed enhanced sensitivity, equivalent to the p53-transfected mixed population, so a role for p53 in the enhanced sensitivity is uncertain. No p53 protein was detected in the mixed population of H1299-p53 by western blot analysis. These results are shown in Table 3.1.4 and Figure 3.1.9.

Table 3.1.4 IC50s of H1299 clones to the chemotherapeutic agents adriamycin, taxol and carboplatin.

Cell Line	Adriamycin (ng/ml)	Taxol (ng/ml)	Carboplatin (μg/ml)
H1299 parent	31 ± 0.8	4.3 ± 0.1	5.4 ± 0.2
H1299 EV mp	13.2 ± 1.1	4.2 ± 0.6	4.1 ± 0.2
H1299 EV clone 2	30.7 ± 3.5	6 ± 0.7	2.9 ± 0.4
H1299 p53 mp	14.6 ± 2.6	2.8 ± 0.4	3.1 ± 0.3
H1299 p53 clone 1	31.8 ± 1	2.4 ± 0.3	1.3 ± 0.2
H1299 p53 clone 2	24.5 ± 2.2	2.1 ± 0.8	4 ± 0.2
H1299 p53 clone 3	43.7 ± 9.2	8.1 ± 0.7	7.1 ± 4.4
H1299 p53 clone 4	23.3 ± 2.4	4.1 ±1.1	3.1 ± 0.5
H1299 p53 clone 5	18.2 ± 1.5	3.6 ± 1.6	1.7 ± 0.1
H1299 p53 clone 6	18 ± 2.3	2.9 ± 1.1	1.9 ± 0.1
H1299 p53 clone 8	31.4 ± 1.1	2 ± 0.6	4.1 ± 0.3
H1299 p53 clone 9	21.5 ± 3.4	3.8 ± 1.5	4.8 ± 0.7

(a)

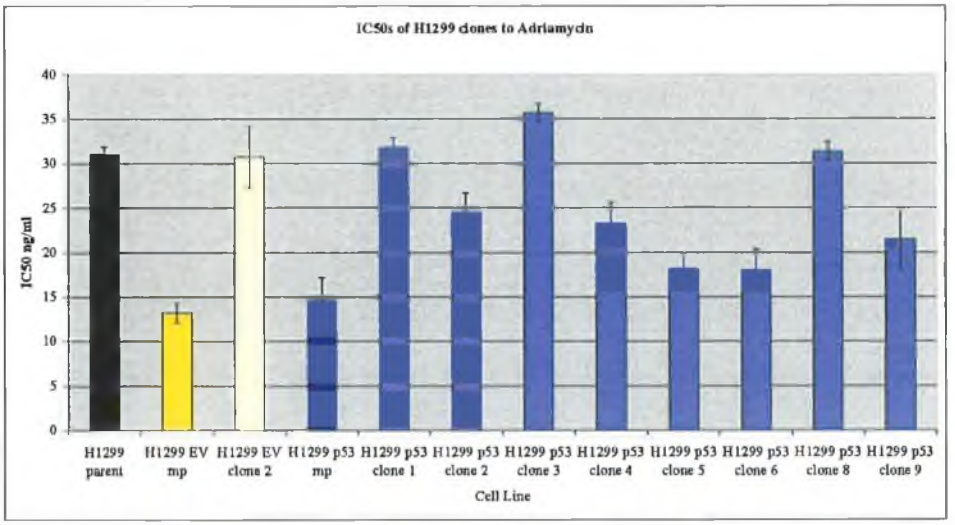

(b)

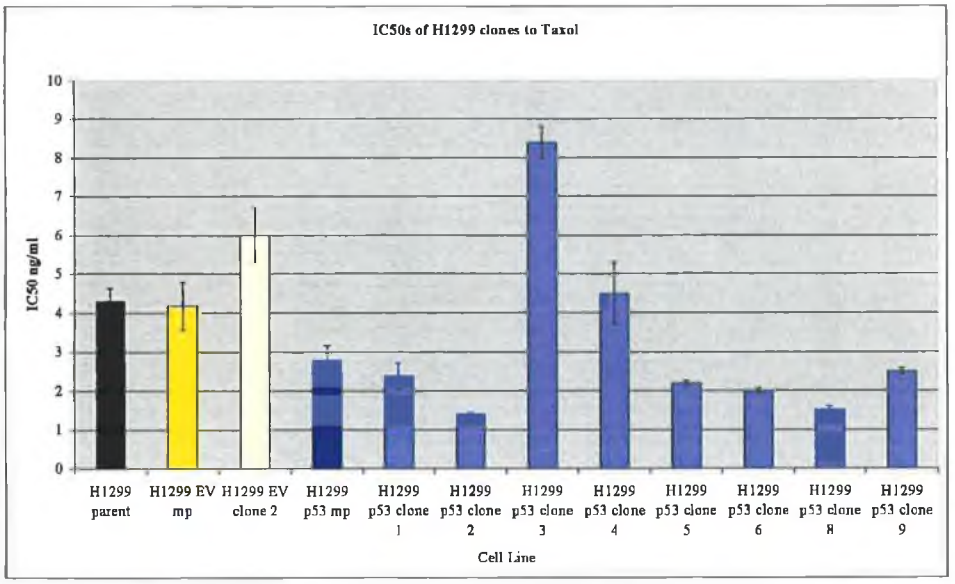

(c)

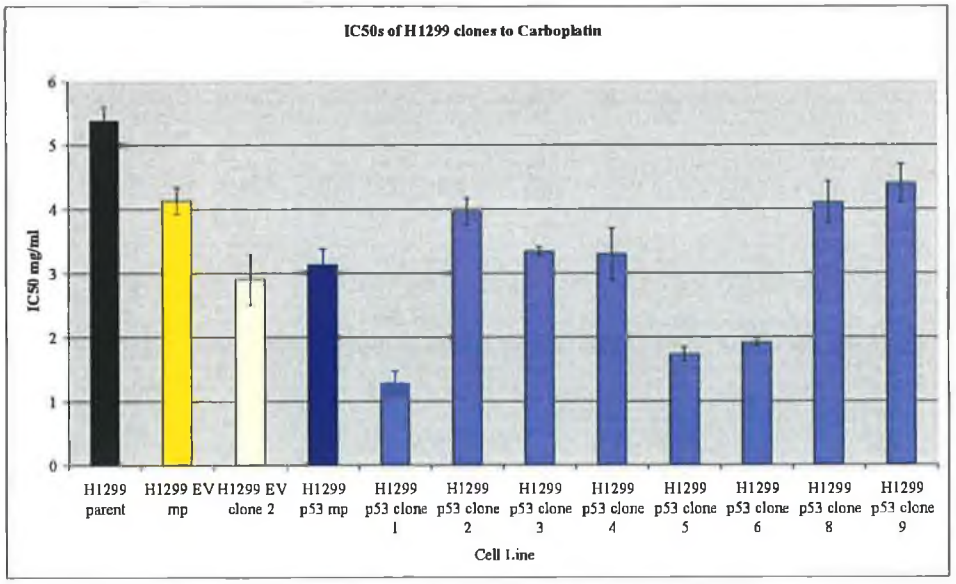

Figure 3.1.9 IC50s for (a) Adriamycin, (b) Taxol and (c) Carboplatin in H1299 transfected clones

3.1.6.3 DLKP-SQ

DLKP-SQ cells endogenously express mutant p53. It was expected that the introduction of wild-type p53 should increase the sensitivity of the cells to chemotherapeutic drugs The IC50s of the DLKP-SQ clones to some chemotherapeutic agents are shown in table 3.1.5. Some of the p53-transfected clones show slight sensitisation to adriamycin and taxol, but not to carboplatin (Figure 3.1.10). However, an effect on sensitivity was again observed in the empty vector-transfected cells, so there is no clear evidence for the impact of wild-type p53 on drug sensitivity.

Table 3.1.5 IC50s of SQ clones to the chemotherapeutic agents adriamycin, taxol and carboplatin

Cell Line	Adriamycin (ng/ml)	Taxol (ng/ml)	Carboplatin (μg/ml)
SQ parent	10.8 ± 0.8	2.2 ± 0.2	2.2 ± 0.2
SQ EV mp	14.7 ± 1.4	2.2 ± 0.1	3.2 ± 0.2
SQ EV clone 1	11.6 ± 0.5	1.6 ± 0.2	3.8 ± 0.1
SQ EV clone 3	14.4 ± 0.1	1.3 ± 0.3	4.6 ± 0.3
SQ p53 mp	10.3 ± 0.7	1.6 ± 0.4	2.2 ± 0.3
SQ p53 clone 1	12.2 ± 1	1.2 ± 0.1	2.3 ± 0.5
SQ p53 clone 2	7.1 ± 0.2	2.1 ± 0.1	3.4 ± 0.5
SQ p53 clone 3	10.3 ± 1.5	1.2 ± 0.1	2.5 ± 0.3
SQ p53 clone 5	9.2 ± 0.4	1.1 ± 0.1	2.7 ± 0.1
SQ p53 clone 6	8.9 ± 0.4	1.8 ± 0.1	2.9

(c)

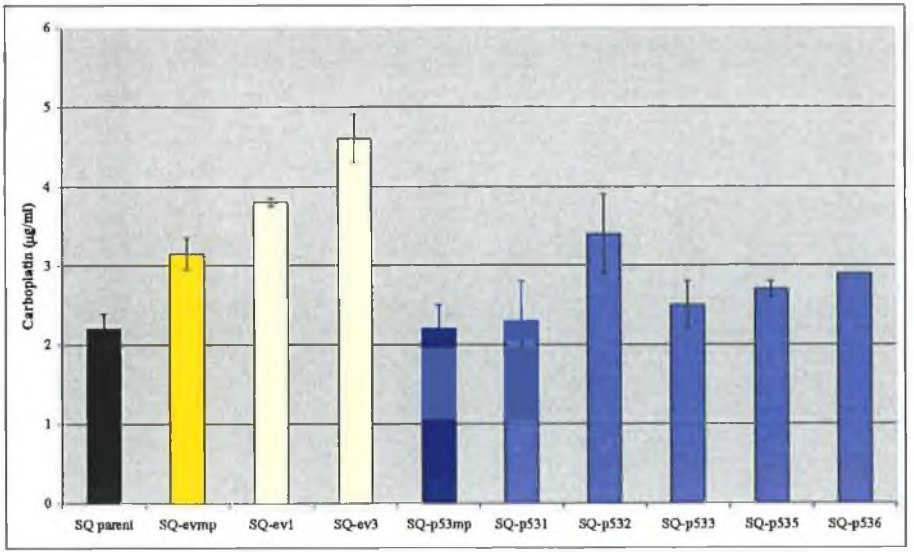

Figure 3.1.10 IC50s for (a) Adriamycin, (b) Taxol and (c) Carboplatin in DLKP-SQ transfected clones

(a)

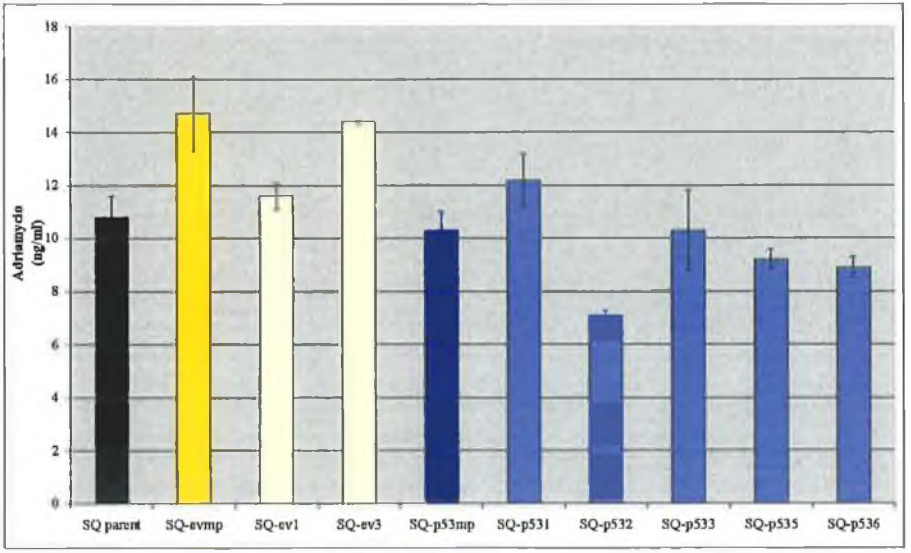
Adriamycin (ng/ml)
18
16
14
12
10
8
6
4
2
0
SQ parent
SQ-evmp
SQ-ev1
SQ-ev3
SQ-p53mp
SQ-p531
SQ-p532
SQ-p533
SQ-p535
SQ-p536

(b)

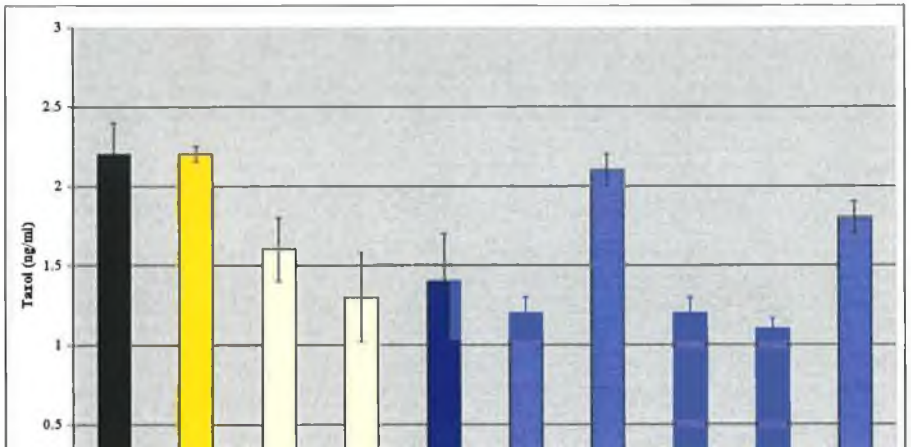
Taxol (ng/ml)
3
2.5
2
1.5
1
0.5

3.1.7 Changes in sensitivity of H1299-p53 clone 8

The only p53-expressing clone 8 showed an increase in sensitivity to taxol. Other p53-transfected clones, which did not express detectable p53 protein, show some changes in sensitivity to these drugs. H1299-p53 clone 6 expresses p53 mRNA but does not express any protein and showed increased sensitivity to taxol and carboplatin and increased resistance to adriamycin (Figure 3.1.11).

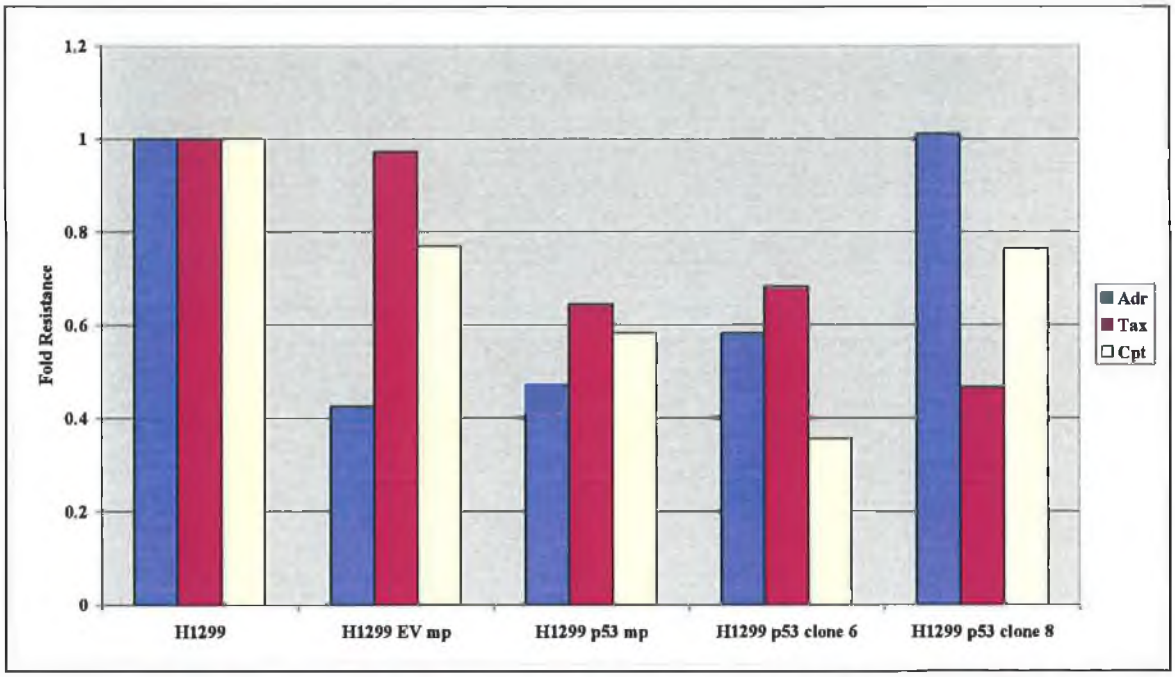

Figure 3.1.11 Fold resistance of H1299-p53 clones to the chemotherapeutic agents adriamycin, taxol and carboplatin.

3.1.8 Expression of p53 family members

The expression of p53 family members, p63 and p73 were determined by western blotting. Since the p53 expressed by H1299-p53 clone 8 does not accumulate after DNA damage (Figure 3.1.5), this cell must have alternate mechanisms in place for dealing with stress. It is possible that this is regulated in the H1299 cells by p63 or p73. The expression of p73 in H1299 cell lines is shown in Figure 3.1.12. This blot shows H1299 parent, control-transfected clones and H1299-p53 8 before (-) and after (+) treatment with adriamycin at 25ng/ml. All of the cell lines express the protein, although there is more expressed after DNA damage in H1299, but not in the transfected cell lines. The other family member p63 was not detected in any of the cell lines.

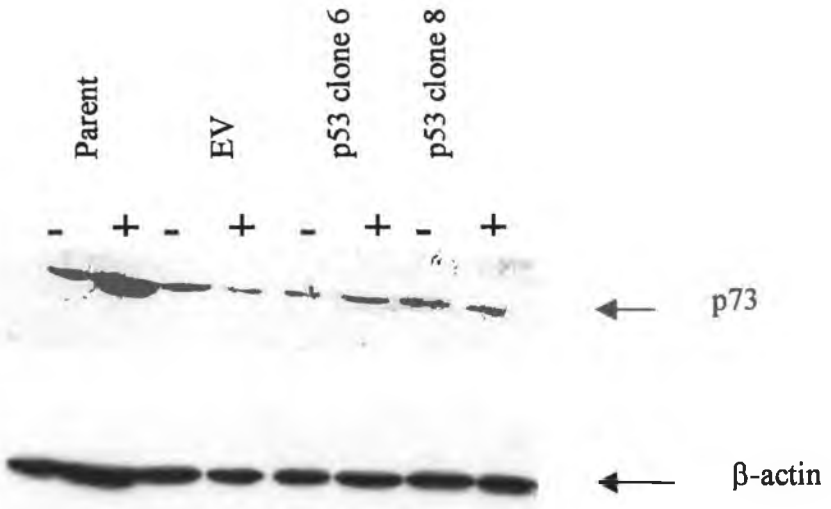

Figure 3.1.12 Western blot of H1299 cell lines for p73 and β-actin

3.1.9 Expression of Mdm2

Mdm2 is the major regulator of p53. Figure 3.1.13 shows the expression of Mdm2 in H1299 parent, control-transfected clones and H1299-p53 8 before (-) and after (+) treatment with adriamycin at 25ng/ml. Low levels of Mdm2 protein were detected in all of the H1299 cell lines (parental and clones) tested.

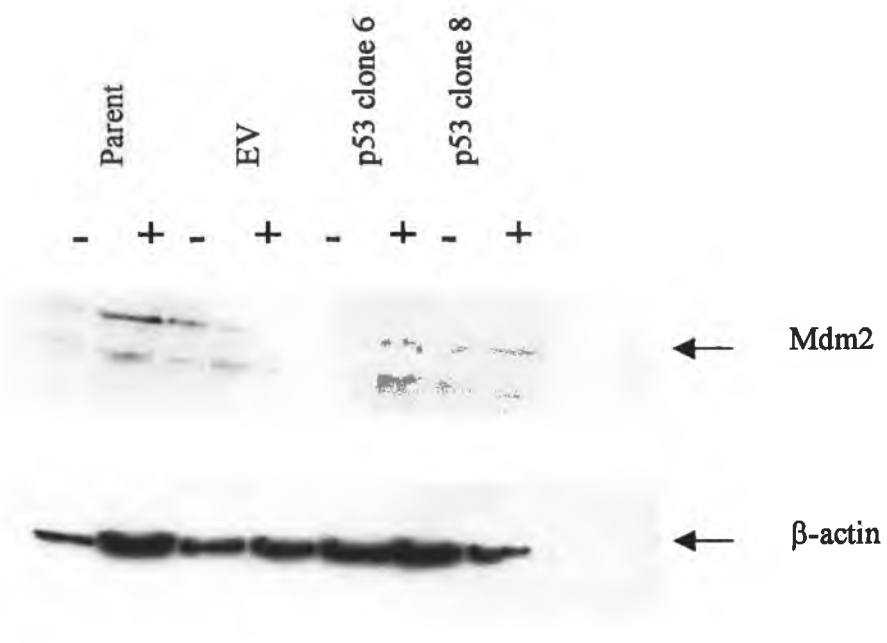

Figure 3.1.13 Western blot of H1299 cell lines for Mdm2 and β-actin

3.1.10 Changes in invasion of H1299-p53 clone 8

In order to see if p53 plays any role in invasion, H1299-p53 clone 8, the only clone expressing detectable p53 protein, was tested along with the parent cell line in the invasion assay. Invasive ability of these cell lines is shown in Figure 3.1.14 and Figure 3.1.15. The p53-expressing clone appears considerably less invasive than the parental cells. However, these effects may be due to transfection since control transfected cells appear to have differing invasive potentials. Nevertheless, the decrease in invasion observed in H1299-p53 clone 8 is substantial and offers an opportunity to study genes and proteins involved in invasion.

(a)

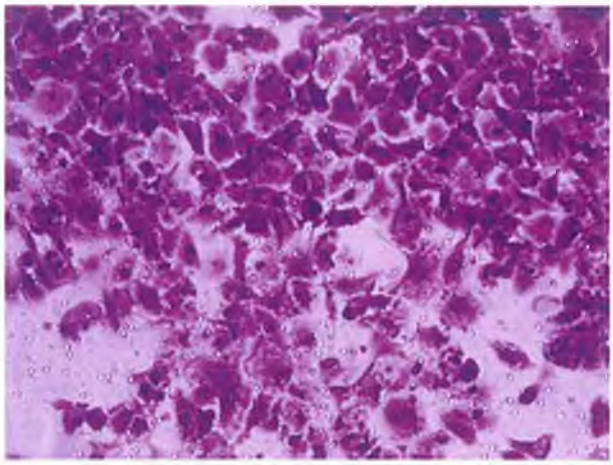

(b)

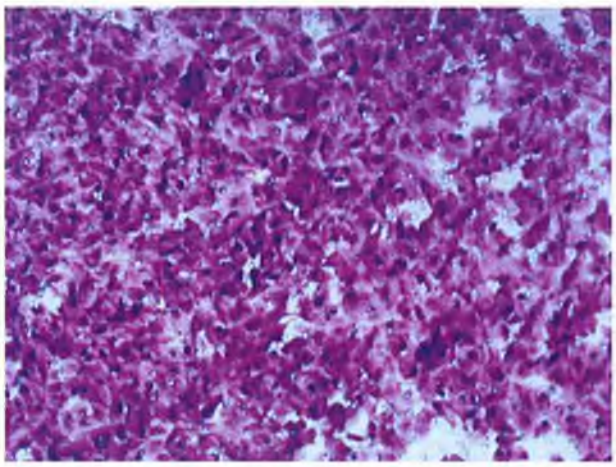

(c)

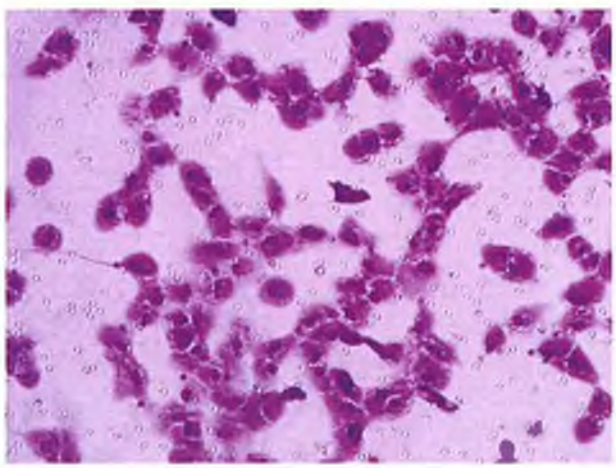

Figure 3.1.14 Invasion of: (a) H1299 parent; (b) H1299-p53 clone 6 and (c) H1299-p53 clone 8

(a)

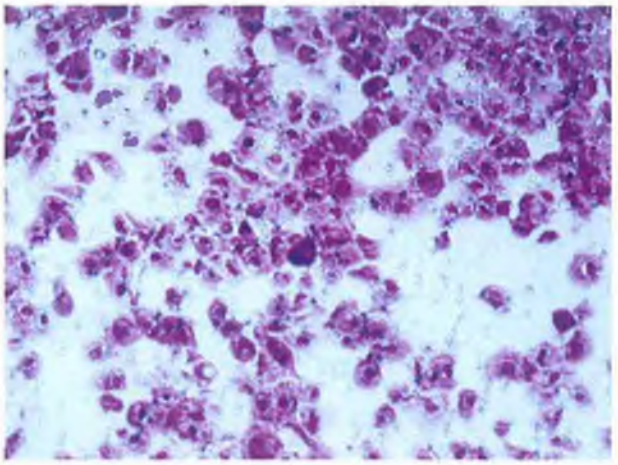

(b)

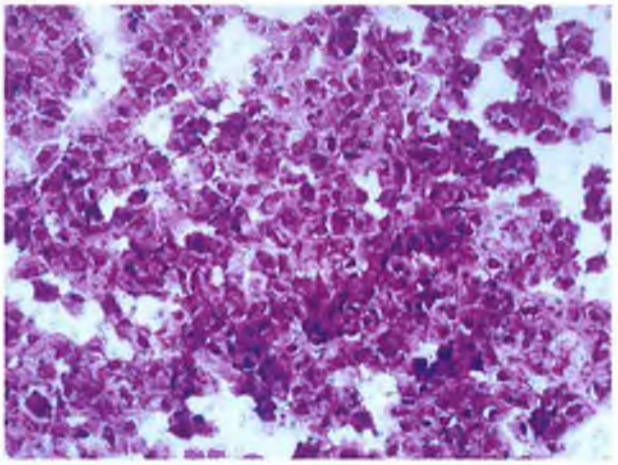

(c)

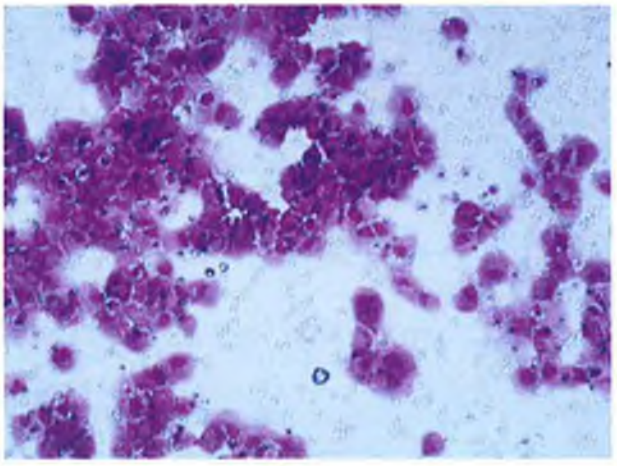

Figure 3.1.15 Invasion of H1299-EV cells: (a) Clone 1; (b) Clone 2 and (c) Clone 3

3.1.11 Microarray analysis of H1299-p53

Since one of the H1299-p53 transfected clones was found to express p53 protein (Figure 3.1.4), it was chosen for microarray analysis. Three samples in triplicate were included in this experiment, H1299, H1299-EV and H1299-p53. For H1299-EV, three separate clones of this cell line were included as replicates. For H1299-p53, triplicate samples of H1299-p53 clone 8 were included.

The genechips used were Affymetrix U133 Plus 2.0 chips (Section 2.11).

3.1.11.1 Quality control

A number of quality control measures are carried out on microarray experiments before gene expression analysis begins. Firstly, a chip information form was filled out for each form. The information from these forms for all of the microarray chips run in this experiment can be seen in Table 3.1.6. For the experiments to be comparable there must be no more than 3-fold difference between the scaling factors for each chip. The lowest scaling factor in this group of chips is 0.632 and the highest is 1.106, which is a fold difference of 1.75.

Another quality control measure taken after the chip is satisfactory is hierarchical clustering. This clusters the samples based on their gene expression, and places the most similar samples in groups together. The hierarchical cluster generated by dChip for this experiment can be seen in Figure 3.1.16. It showed that the parent samples clustered correctly and the H1299-p53 samples clustered correctly but the control transfected H1299-EV samples did not cluster. Despite the result of the clustering, further analysis was carried out using d-chip.

These quality control measures are explained in more detail in Section 3.3.

Table 3.1.6 Quality control on chips from p53 experiment

Sample name	Scaling factor	Noise	Background	% Present	3'/5' Ratio GAPDH
H1299_1	0.867	1.8	52.13	45.9	1
H1299_2	0.729	2.26	66.41	43	0.95
H1299_3	0.847	1.63	49.2	45.1	1.14
H1299_EV_1	0.743	1.8	55.72	47	0.99
H1299_EV_2	0.723	2	62.14	44.4	0.96
H1299_EV_3	1.106	1.32	42.89	42.3	2.19
H1299_p53_1	0.683	2.2	69.53	43.8	0.95
H1299_p53_2	0.632	2.23	68.57	44.7	0.94
H1299_p53_3	0.765	1.94	59.43	44	0.98

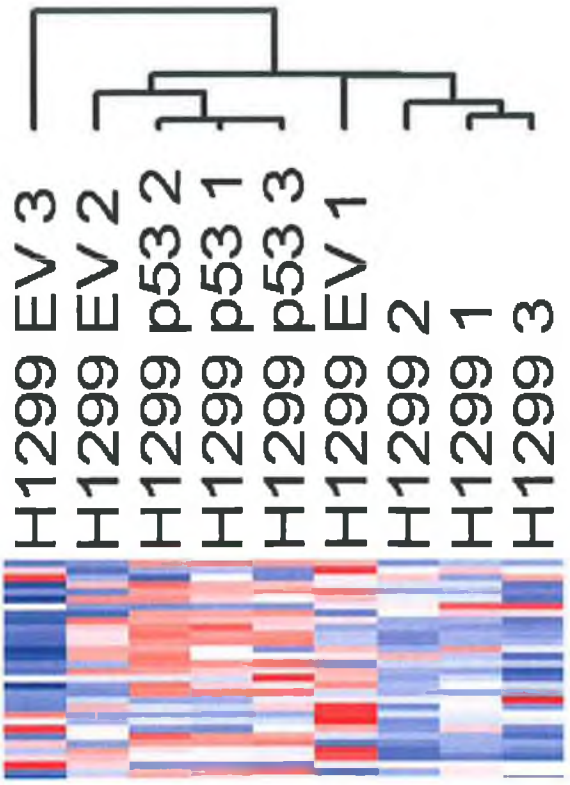

Figure 3.1.16 Hierarchical Cluster of p53 experiment samples

3.1.11.2 Generation of genelists

DChip software was used in the original generation of genelists. Using dChip, H1299 was compared to H1299-EV, and H1299 was compared to H1299-p53. The parameters used were a fold change of 2, a difference of intensity of 100 and a p value of <0.05. The numbers of genes changed in these genelists are shown in Table 3.1.7.

Table 3.1.7 Number of genes differentially regulated

Genelist	No. of genes
H1299 vs H1299-EV	221
H1299 vs H1299-p53	296

These genelists were compared to eliminate genes that were differentially expressed in the control-transfected cells from the p53 genelist. This comparison resulted in a genelist of 254 genes. Of this, 151 were upregulated genes and 104 were downregulated. These genelists are shown in Tables 3.1.8 and 3.1.9. The transfected gene p53, does not appear in these lists. In order to investigate this a genelist was generated in dChip using less stringent filtering criteria of a fold change of 1.2 and a difference in intensities of 50. In this list p53 was detected, however it appeared in both parent and transfected cell lines at intensities of 381 and 293 respectively. This represents a 1.3-fold downregulation of p53 in the transfected cells, which is directly conflicting the results observed earlier in RT-PCR (Figure 3.1.5) and western blotting (Figure 3.1.6). It is possible that the probes on the affymetrix chip are designed to a part of the p53 gene that was not present on the cDNA that was used for transfection, e.g. the untranslated region (UTR). Since the western blotting and RT-PCR results represent repeated experiments with the inclusion of controls, this result should be a true reflection of the p53 status of the transfected cells.

Table 3.1.8 Upregulated genes in H1299-p53

Gene	fold change
Desmoplakin	2.72
Cysteine and glycine-rich protein 1	2.52
Protein tyrosine phosphatase type IVA, member 1	2.25
Methionine adenosyltransferase II, alpha	2.23
Myeloid cell leukemia sequence 1 (BCL2-related)	2.39
Thrombospondin 1	2.92
Thrombospondin 1	5.31
Thrombospondin 1	3.91
Inositol 1,4,5-triphosphate receptor, type 3	2.27
DEAD (Asp-Glu-Ala-Asp) box polypeptide 3, X-linked	2.86
Rho GDP dissociation inhibitor (GDI) beta	6.43
Peptidylprolyl isomerase F (cyclophilin F)	2.54
Transforming growth factor, beta-induced, 68kda	2.3
Chloride intracellular channel 4	3.06
Podocalyxin-like	2.9
Caldesmon 1	2.23
Secreted frizzled-related protein 1	3.02
Laminin, gamma 2	2.53
Guanylate binding protein 1, interferon-inducible, 67kda	2.8
Chromosome 10 open reading frame 69	2.18
PALM2-AKAP2 protein	2.12
Alanyl (membrane) aminopeptidase	2.46
Interleukin 1 receptor, type I	3.99
Lysyl oxidase-like 2	5.32
Metastasis suppressor 1	2.23
Diphtheria toxin receptor	2.71
Death-associated protein kinase 3	2.51
GLI pathogenesis-related 1 (glioma)	2.43
Friend leukemia virus integration 1	2.59
Lysyl oxidase	2.58
SMAD, mothers against DPP homolog 7 (Drosophila)	3.84
Acyl-Coenzyme A oxidase 2, branched chain	2.1
TNF receptor-associated factor 1	2.74
Importin 8	2.11
Protein tyrosine phosphatase, non-receptor type 11 (Noonan syndrome 1)	3.32
Protein tyrosine phosphatase, non-receptor type 11 (Noonan syndrome 1)	2.71
Nucleolar and coiled-body phosphoprotein 1	2.15
Serine (or cysteine) proteinase inhibitor, clade B (ovalbumin), member 8	2.22
Protein tyrosine phosphatase, receptor type, R	3.82
Tropomyosin 1 (alpha)	2.23
Pentaxin-related gene, rapidly induced by IL-1 beta	3.61
Adrenergic, beta-2-, receptor, surface	3.58
V-crk sarcoma virus CT10 oncogene homolog (avian)-like	2.59
Ras-gtpase activating protein SH3 domain-binding protein 2	2.28
Chromosome condensation 1	2.05
BCL2-like 1	2.36
Zinc finger protein 45 (a Kruppel-associated box (KRAB) domain polypeptide)	2.03
Phosphatidylinositol-4-phosphate 5-kinase, type I, alpha	2.03
Secretoglobin, family 1D, member 1	2.2
Fibroblast growth factor 5	2.89
Sin3-associated polypeptide, 18kda	2.04
Inhibitor of DNA binding 1, dominant negative helix-loop-helix protein	2.31

Growth arrest and DNA-damage-inducible, beta	2.34
Annexin A3	2.71
F-box and WD-40 domain protein 11	2.71
Kinesin family member C1	2.28
Synovial sarcoma translocation, chromosome 18	2.15
Insulin-like growth factor binding protein 3	2.47
Peripheral myelin protein 22	3.58
Fibroblast growth factor 5	3.7
Fibroblast growth factor 5	3.62
Baculoviral IAP repeat-containing 3	2.61
Protein tyrosine phosphatase, receptor type, R	3.29
MAX protein	2.04
Notch homolog 2 (Drosophila) /// Notch homolog 2 (Drosophila)	2.07
Phosphatidylinositol-4-phosphate 5-kinase, type I, alpha	3.49
CASP8 and FADD-like apoptosis regulator	2.08
Plasminogen activator, urokinase /// plasminogen activator, urokinase	2.36
Cyclin E2	2.55
Ras homolog gene family, member B	2.04
KIAA0746 protein	2.5
DEAD (Asp-Glu-Ala-Asp) box polypeptide 3, X-linked	2.26
KIAA0286 protein	2.81
Hypothetical protein H41	2.46
Snf2-related CBP activator protein	2.5
Met proto-oncogene (hepatocyte growth factor receptor)	2.9
Dehydrogenase/reductase (SDR family) member 2	2.69
Poliovirus receptor	2.28
Elongation factor, RNA polymerase II, 2	2.15
Microtubule-associated protein 1B	2.04
Hypothetical protein dj462o23.2	2.23
Myotubularin related protein 1	2.1
BCL2-like 1	2.54
Integrin, alpha 6	2.01
Phosphatidylinositol binding clathrin assembly protein	2.05
Lysyl oxidase	2.67
Primase, polypeptide 2A, 58kda	2.35
Chromosome condensation 1	2.23
Gb:AK026847.1 /DB_XREF=gi:10439802 /FEA=mrna /CNT=1	81.68
Phosphoribosylglycinamide formyltransferase,	2.08
Sulfide quinone reductase-like (yeast)	2.06
Calcium/calmodulin-dependent protein kinase II	2.94
Lin-7 homolog C (C. Elegans)	2.12
Erythrocyte membrane protein band 4.1 like 4B	3.08
Tropomodulin 3 (ubiquitous)	2.45
Mitogen-activated protein kinase	2.66
Diphtheria toxin receptor	2.08
Ubiquitin-fold modifier 1	2.3
Paraspeckle component 1	2.31
Potassium channel tetramerisation domain containing 5	2
Chromosome 6 open reading frame 166	2.03
Dual specificity phosphatase 23	2.34
Guanylate binding protein 3	2.54
Normal mucosa of esophagus specific 1	4.18
Calcium binding protein 39	2.18
Dnaj (Hsp40) homolog, subfamily C, member 5	2.25

Eukaryotic translation initiation factor 4E binding protein 2	2.05
Monoglyceride lipase	2.36
Myosin VB	2.44
Breast cancer membrane protein 101	3.69
Protocadherin 18	2.23
HIV-1 rev binding protein 2	2.51
Purine-rich element binding protein B	2.08
Chromosome 6 open reading frame 105	3.08
Ring finger protein (C3HC4 type) 159	2.08
Transcribed locus, highly similar to NP_058593.1	2.03
Dimethylarginine dimethylaminohydrolase 1	2.78
MRNA; cdna dkfzp564c0762 (from clone dkfzp564c0762)	2.09
Gb:AI361034 /DB_XREF=gi:4112655 /DB_XREF=qy03e10.x1	2.13
Gb:AA805622 /DB_XREF=gi:2874372 /DB_XREF=oc19b11.s1	3.1
Hypothetical LOC388480	2.11
Guanylate binding protein 1, interferon-inducible, 67kda	3.27
Suppressor of Ty 16 homolog (S. Cerevisiae)	2.14
TNF receptor-associated factor 1	2.9
Hypothetical protein LOC285550	2.51
Transferrin receptor (p90, CD71)	3.44
Membrane associated DNA binding protein	2.61
Grpe-like 2, mitochondrial (E. Coli)	3.12
UL16 binding protein 2	2.27
Homo sapiens, clone IMAGE:3866695, mrna	2.21
Zinc finger protein 566	2.08
Ras-gtpase-activating protein SH3-domain-binding protein	2.54
Microfibrillar-associated protein 3	2.93
Neuron navigator 3	2.5
Desmoglein 2	2.6
Dimethylarginine dimethylaminohydrolase 1	4.03
Ras homolog gene family, member B	3.19
Zinc finger protein 146	2.17
Dnaj (Hsp40) homolog, subfamily C, member 14	2.51
Inositol polyphosphate-5-phosphatase, 40kda	2.72
Primase, polypeptide 2A, 58kda	2.07
Fucosyltransferase 8 (alpha (1,6) fucosyltransferase)	2.97
Hypothetical protein HSPC129	2.32
V-ets erythroblastosis virus E26 oncogene homolog 1 (avian)	2.56
F-box and leucine-rich repeat protein 21	3.89
RNA binding motif protein 14	2.56
Keratin associated protein 2-4	4.11
Rho GDP dissociation inhibitor (GDI) beta	8.13
Solute carrier family 16 (monocarboxylic acid transporters), member 1	2.28
Catenin (cadherin-associated protein), alpha 1, 102kda	2.37
Gb:BC029166.1 /DB_XREF=gi:23272920 /TID=Hs2.385583.1 /CNT=2	2.07

Table 3.1.9 Downregulated genes in H1299-p53

Gene	Fold change
SH3 domain binding glutamic acid-rich protein like	-2.08
SH3 domain binding glutamic acid-rich protein like	-2.18
Insulin induced gene 1	-2.19
Transducin (beta)-like 1X-linked	-2.32
Sterol regulatory element binding transcription factor 1	-2.81
Periplakin	-4.64
Special AT-rich sequence binding protein 1	-2.45
Latrophilin 1	-3.62
Arginase, type II	-3.42
Neurofilament, heavy polypeptide 200kda	-3.61
Insulin receptor substrate 1	-2.57
O-6-methylguanine-DNA methyltransferase	-2.11
Dual-specificity tyrosine-(Y)-phosphorylation regulated kinase 1B	-2.33
Chromosome X open reading frame 34	-2.03
Carboxypeptidase M	-2.35
Cyclin-dependent kinase inhibitor 2A (melanoma, p16, inhibits CDK4)	-2.04
Phosphatidylethanolamine N-methyltransferase	-2.31
Nuclear factor of activated T-cells 5, tonicity-responsive	-3.15
Tetratricopeptide repeat domain 3	-2.22
Fatty acid desaturase 1	-2
Protein kinase C binding protein 1	-2.11
Paternally expressed 3	-10.83
Acetylserotonin O-methyltransferase-like	-2.22
Nuclear receptor subfamily 2, group F, member 1	-2.85
Carboxylesterase 2 (intestine, liver)	-2.08
Protein tyrosine phosphatase type IVA, member 3	-3.9
Secreted phosphoprotein 1	-5.87
V-rel reticuloendotheliosis viral oncogene homolog A	-2.03
RPL13-2 pseudogene	-2.22
Prostate tumor overexpressed gene 1	-2.23
Fatty acid synthase	-2.05
Lipin 1	-2.16
Chromodomain helicase DNA binding protein 9	-2.25
Troponin T1, skeletal, slow	-2.08
F-box and leucine-rich repeat protein 7	-2.54
Transducin (beta)-like 1X-linked	-2.03
Pleckstrin homology domain containing, family C member 1	-2.08
Calreticulin	-2.19
Potassium voltage-gated channel, subfamily G, member 1	-2.85
Likely ortholog of mouse zinc finger protein EZI	-2.15
Sma4	-2.14
Olfactory receptor, family 7, subfamily E, member 18 pseudogene	-2.05
Zinc finger protein 395	-2.25
Dnaj (Hsp40) homolog, subfamily D, member 1	-9.13
Host cell factor C1 regulator 1 (XPO1 dependant)	-2.04
Dapper homolog 1, antagonist of beta-catenin (xenopus)	-3.89
Dipeptidase 3	-6.15
Regulator of G-protein signalling 17	-2.93
Chemokine-like factor	-2.04
Nucleosomal binding protein 1	-5.5
SH2 domain containing 3A	-2.95
Neurofilament, heavy polypeptide 200kda	-3.38

Cluster Incl. AA669799:ag36c04.s1 Homo sapiens cdna, 3 end	-2.22
Acetylserotonin O-methyltransferase-like	-2
Host cell factor C1 regulator 1 (XPO1 dependant)	-2.38
Latrophilin 1	-2.03
Thyroid hormone receptor associated protein 3	-2.55
Kiaa1333	-2.81
Gb:AA827878 /DB_XREF=gi:2900241 /DB_XREF=od56g09.s1	-2.58
Gb:AF113016.1 /DB_XREF=gi:6642755 /FEA=flmrna /CNT=30	-4.28
Nucleoporin like 1	-2.07
Metastasis associated lung adenocarcinoma transcript 1 (non-coding RNA)	-3.09
Likely ortholog of rat vacuole membrane protein 1	-3.87
Nuclear factor I/A	-2.43
RAB3D, member RAS oncogene family	-2.04
Rho gtpase activating protein 18	-2.09
KIAA1280 protein	-2.51
KIAA1160 protein /// RAB43, member RAS oncogene family	-2.15
Solute carrier family 25 (mitochondrial carrier; phosphate carrier), member 23	-2.31
Mitogen-activated protein kinase kinase 7	-2.05
Retinoic acid induced 1	-2.16
Metastasis associated lung adenocarcinoma transcript 1 (non-coding RNA)	-3.15
Hypothetical protein BC001096	-2.1
Staufen, RNA binding protein, homolog 2 (Drosophila)	-2.87
Gb:AI694536 /DB_XREF=gi:4971876 /DB_XREF=wd72d12.x1	-2.12
Spermatogenesis associated 11	-2.03
Zinc finger protein 595	-5.87
Hypothetical protein BC014339	-2.14
6-phosphofructo-2-kinase/fructose-2,6-biphosphatase 4	-2.11
Myo-inositol 1-phosphate synthase A1	-2.66
Gb:AI566130 /DB_XREF=gi:4524582 /DB_XREF=tn53g07.x1	-2.15
Hypothetical protein FLJ37659	-112.09
Eomesodermin homolog (Xenopus laevis)	-4.12
Chromosome 10 open reading frame 75	-2.11
MRNA; cdna dkfzp434l201 (from clone dkfzp434l201)	-8.75
Pyruvate dehydrogenase phosphatase isoenzyme 2	-5.55
Gb:AF152528.1 /DB_XREF=gi:5457102 /FEA=mrna /CNT=1	-2.92
CDNA: FLJ23566 fis, clone LNG10880	-2.36
Carboxypeptidase M	-2.08
Shugoshin-like 2 (S. Pombe)	-2.15
Hypothetical protein LOC150763	-2.62
Carboxypeptidase M	-2.51
Cyclin-dependent kinase inhibitor 2B (p15, inhibits CDK4)	-2.71
Hypothetical gene LOC133874	-3.32
Gb:AW083849 /DB_XREF=gi:6039001 /DB_XREF=xc46a12.x1	-2.28
Gb:AV651242 /DB_XREF=gi:9872256 /DB_XREF=AV651242	-5.65
Gb:AW270845 /DB_XREF=gi:6657875 /DB_XREF=xs04h08.x1	-2.3
Carboxypeptidase M	-2.18
Gb:AI418253 /DB_XREF=gi:4264184 /DB_XREF=tf74b09.x1	-2.59
Carboxypeptidase M	-2.67
Chromosome 14 open reading frame 62	-4.61
Gb:AK057525.1 /DB_XREF=gi:16553266 /TID=Hs2.401310.1 /CNT=6	-2.72
Hypothetical gene supported by AK056786	-3.05

3.2 Pulse selection of cell lines

Four different lung cancer cell lines were chosen for the drug treatment (Table 3.2.1). The cell lines include two adenocarcinoma (AC) and two large cell carcinoma (LCC) cell lines. They were pulse-selected with taxol and carboplatin representing two drugs, which are used clinically for treating this type of cancer. The concentrations of each drug used for pulse selection can be seen in section 2.6.

Table 3.2.1 List of lung cancer cell lines and drugs used for the pulse-selections

Cell line	Cell type	Drugs used
A549	Adenocarcinoma	taxol, carboplatin
SKLU-1	Adenocarcinoma	taxol, carboplatin
NCI-H1299 (H1299)	Large cell carcinoma	taxol, carboplatin
NCI-H460 (H460)	Large cell carcinoma	taxol, carboplatin

Table 3.2.2 Concentrations for pulse-selection

Cell Line	Taxol (ng/ml)	Carboplatin (μg/ml)
A549	150	100
H1299	150	50
SKLU-1	10	10
H460	50	50

3.2.1 Determination of sensitivity of the parent cell lines to chemotherapeutic agents

The parent cell lines were analysed using an *in vitro* toxicity assay to determine the IC50 (drug concentration killing half of the cell population) of the following chemotherapeutic drugs: adriamycin, taxol, carboplatin, cisplatin, 5-fluorouracil, VP-16 and vincristine. This was carried out as described in Section 2.4.

Cell line	Adriamycin (ng/ml)	5-Fluoruracil (ng/ml)	Taxol (ng/ml)	Taxotere (ng/ml)
A549	17.3 ± 0.2	150.9 ± 13.8	1.1 ± 0.1	0.8 ± 0.9
SKLU-1	27.1 ± 0.4	1223.3 ± 73.7	1.2 ± 0.1	-
H1299	30.3 ± 0.9	152.1 ± 15.2	4 ± 0.3	0.8 ± 0.1
H460	11.1 ± 1.6	188.7 ± 17	4.4 ± 0.2	0.8 ± 0.2

Cell line	Vincristine (ng/ml)	VP-16 (ng/ml)	Carboplatin (μg/ml)	Cisplatin (ng/ml)
A549	3.7 ± 05	117.3 ± 18	5.9 ± 0.2	584.4 ± 32.3
SKLU-1	0.7 ± 0.3	115.7 ± 5.9	2.8 ± 0.2	405.7 ± 21.2
H1299	2.4 ± 0.1	111.1 ± 12.3	3.7 ± 0.6	436.8 ± 29.6
H460	3.7 ± 0.6	78.8 ± 8.6	2.4 ± 0.2	250.3 ± 29.7

Table 3.2.3 IC50s of parent cell lines to a number of chemotherapy drugs (Results are expressed as IC50 ± SD, n=3)

Table 3.2.3 shows the IC50 concentrations for the parent cell lines. There is a considerable difference in sensitivity to the panel of drugs between each cell line and even between the same cell types. For example A549 is about twice as resistant to carboplatin compared to SKLU-1, whereas SKLU-1 is 8-fold more resistant to 5-fluorouracil compared to A549. Similarly within the group of large cell carcinomas, H1299 is more resistant to adriamycin and the platinum agents than H460.

3.2.2 Changes in resistance to chemotherapeutic drugs in selected variants

Pulse selection of the above cell lines with taxol and carboplatin resulted in the establishment of eight novel cell lines. These were denoted "-tax" for the taxol selected cells, and "-cpt" for the carboplatin selected cells. SKLU-1 was very sensitive to repeated drug treatment and pulse selection at high kill concentration resulted in total cell death after three pulses. Therefore, pulse selection was performed at a much lower concentration, which resulted in less cell death for the first three pulses and after that gave a 50% kill. These concentrations can be seen in Table 3.2.1.

All pulse-selected cell lines exhibited at least a 2-fold increase in resistance to the selecting drug. This level of resistance is relatively low compared to the high levels of resistance that can be achieved by a continuous treatment with the selecting chemotherapy drug. In the clinical setting patients receive chemotherapy treatment once every 1-3 weeks, therefore a weekly drug treatment for 4 hours (pulse selection) is more related to the *in vivo* situation. A number of the newly established cell lines exhibited multidrug resistance, becoming resistant to compounds other than the selecting drug. In general, cells pulsed with carboplatin show similar levels of cross-resistance to cisplatin, both platinum-based drugs.

3.2.2.1 Changes in resistance in A549 pulse-selected variants

The IC50 values for the A549 pulse-selected variants can be seen in Table 3.2.4. Fold resistance information and p values are shown in Table 3.2.5 and Figure 3.2.1. A549-tax shows statistically significant increases in resistance to adriamycin, taxol, carboplatin, 5-FU, VP-16 and vincristine. These are low-level resistances, with the greatest change evident in resistance to taxol and VP-16. The only significant change in resistance observed in A549-cpt is a 0.5-fold resistance (or 2-fold increase in sensitivity) to taxol. This cell lines also displays changes in resistance to carboplatin and cisplatin, but these were not found to be statistically significant.

Table 3.2.4 IC50s of A549 variants

	A549	A549-tax	A549-cpt
Adriamycin (ng/ml)	17.3 ± 0.2	31.9 ± 4.9	13.3 ± 1.8
Taxol (ng/ml)	1.1 ± 0.1	6 ± 0.5	0.5 ± 0.1
Taxotere (ng/ml)	0.8 ± 0.9	1.5 ± 0.2	0.3 ± 0.1
Carboplatin (μg/ml)	5.9 ± 0.2	7.3 ± 0.3	9.6 ± 2.2
Cisplatin (ng/ml)	584.4 ± 32.3	517.6 ± 21.5	1377 ± 427.4
5-FU (ng/ml)	150.9 ± 13.8	290.5 ± 10.2	204.6 ± 26.5
VP-16 ng/ml)	117.3 ± 18	484.5 ± 81.4	106 ± 11.5
Vincristine (ng/ml)	3.7 ± 0.5	6 ± 0.2	4.4 ± 0.9

(Results are expressed as IC50 ± SD, n=3)

Table 3.2.5 Fold resistance of A549 pulse-selected variants

Chemotherapeutic agent	A549	A549-tax	P value A549-tax	A549-cpt	P value A549-cpt
Adriamycin	1	1.8*	0.035	0.8	0.055
Taxol	1	5.5***	0.003	0.5***	0.002
Taxotere	1	1.8	0.365	0.3	0.397
Carboplatin	1	1.3***	0.004	1.6	0.102
Cisplatin	1	0.9*	0.049	2.4	0.084
5-FU	1	1.9***	0.0002	1.4	0.053
VP-16	1	4.1*	0.013	0.9	0.421
Vincristine	1	1.6**	0.007	1.2	0.338

* p value <0.05

** p value <0.01

*** p value <0.005

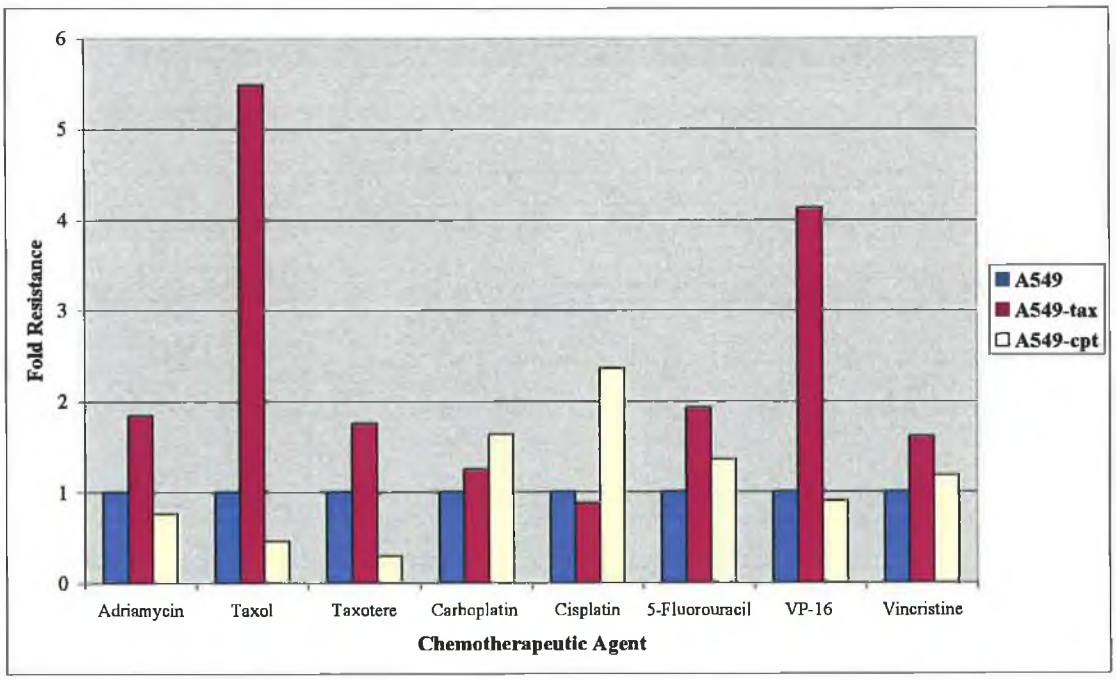

Figure 3.2.1 Fold resistance of A549 pulse-selected variants

3.2.2.2 Changes in resistance in H1299 pulse-selected variants

The IC50 values for the H1299 pulse-selected variants can be seen in Table 3.2.6. Fold resistance information and p values are shown in Table 3.2.7 and Figure 3.2.2.

H1299-tax shows significant resistance to taxol, taxotere, carboplatin, 5-FU and vincristine. The greatest fold change was observed in taxol and taxotere, as was expected.

H1299-cpt shows significant resistance to taxol, carboplatin, cisplatin and VP-16. The most interesting increases in resistance are to carboplatin and cisplatin, however the resistance is very low at 2-fold and 1.5-fold respectively.

Table 3.2.6 IC50s of H1299 variants

	H1299	H1299-tax	H1299-cpt
Adriamycin (ng/ml)	30.3 ± 0.9	29.8 ± 1.3	27.4 ± 1.7
Taxol (ng/ml)	4 ± 0.3	17.7 ± 0.7	4.7 ± 0.3
Taxotere (ng/ml)	0.8 ± 0.1	1.9 ± 0.2	0.5 ± 0.2
Carboplatin (μg/ml)	3.7 ± 0.6	6.2 ± 0.5	7.5 ± 0.9
Cisplatin (ng/ml)	436.8 ± 29.6	654.9 ± 196.2	673.1 ± 86.4
5-FU (ng/ml)	152.1 ± 15.2	270 ± 10	148 ± 2.1
VP-16 (ng/ml)	111.1 ± 12.3	122.4 ± 19.3	156.4 ± 9.6
Vincristine (ng/ml)	2.4 ± 0.1	5.4 ± 1	1.8 ± 0.3

(Results are expressed as IC50 ± SD, n=3)

Table 3.2.7 Fold resistance of H1299 pulse-selected variants

Chemotherapeutic agent	H1299	H1299-tax	P value H1299-tax	H1299-cpt	P value H1299-tax
Adriamycin	1	1	0.620	0.9	0.074
Taxol	1	4.4***	0.0003	1.2*	0.045
Taxotere	1	2.5***	0.002	0.6	0.062
Carboplatin	1	1.7***	0.004	2**	0.007
Cisplatin	1	1.5	0.192	1.5*	0.031
5-FU	1	1.8**	0.001	1	0.693
VP-16	1	1.1	0.448	1.4**	0.008
Vincristine	1	2.3*	0.031	0.8*	0.045

* p value <0.05

** p value <0.01

*** p value <0.005

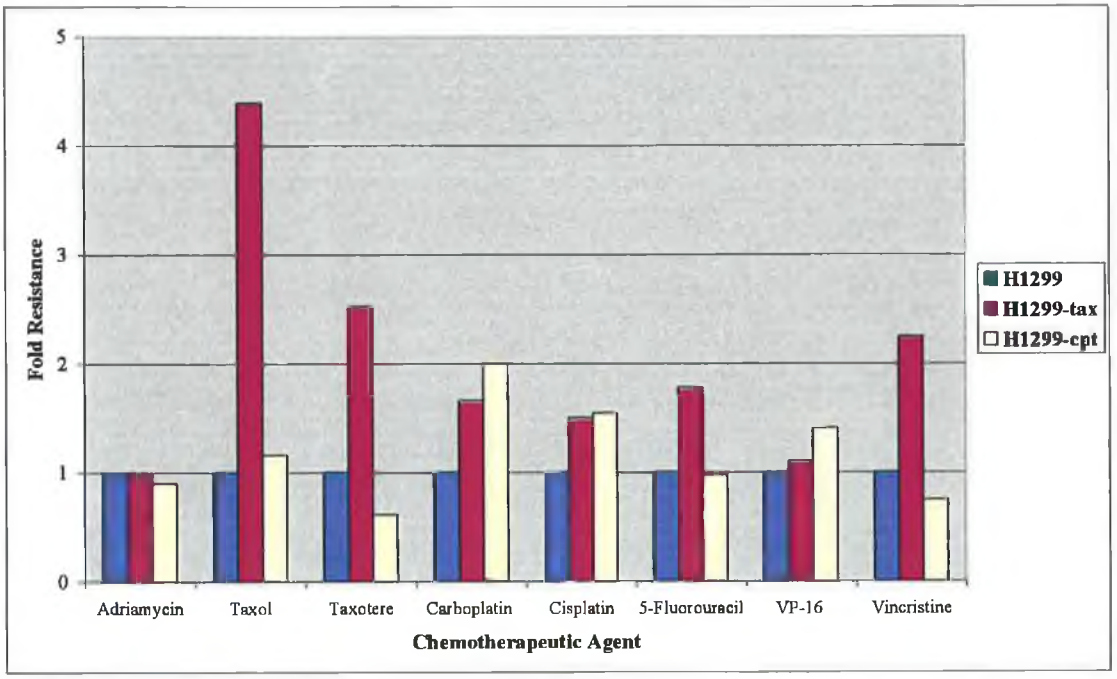

Figure 3.2.2 Fold resistance of H1299 pulse-selected variants

3.2.2.3 Changes in resistance in H460 pulse-selected variants

The IC50 values for the H460 pulse-selected variants can be seen in Table 3.2.8. Fold resistance information and p values are shown in Table 3.2.9 and Figure 3.2.3.

H460-tax shows a significant increase in resistance of 2.4-fold to taxol, and 2.8-fold to taxotere. Interestingly, there is a decrease in sensitivity to carboplatin in this cell line.

H460-cpt displays significant increases in resistance to taxol, carboplatin and vincristine. Unexpectedly, the greatest change in resistance was to vincristine at 2.9-fold.

Table 3.2.8 IC50s of H460 variants

	H460	H460-tax	H460-cpt
Adriamycin (ng/ml)	11.1 ± 1.6	9.9 ± 0.5	11 ± 0.5
Taxol (ng/ml)	4.4 ± 0.2	10.8 ± 0.3	7 ± 0.3
Taxotere (ng/ml)	0.8 ± 0.2	2.3 ± 0.3	1.9 ± 0.9
Carboplatin (μg/ml)	2.4 ± 0.2	2 ± 0.1	5.6 ± 0.9
Cisplatin (ng/ml)	250.3 ± 29.7	163.3 ± 94.1	413 ± 266.4
5-FU (ng/ml)	188.7 ± 17	201 ± 12.2	166.7 ± 22.3
VP-16 (ng/ml)	78.8 ± 8.6	77.1 ± 4.6	68.3 ± 3.6
Vincristine (ng/ml)	3.7 ± 0.6	9.1 ± 5.2	10.6 ± 1.2

(Results are expressed as IC50 ± SD, n=3)

Table 3.2.9 Fold resistance of H460 pulse-selected variants

Chemotherapeutic agent	H460	H460-tax	P value H460-tax	H460-cpt	P value H460-cpt
Adriamycin	1	0.9	0.344	1	0.925
Taxol	1	2.4***	0.0001	1.6***	0.0005
Taxotere	1	2.8***	0.003	2.3	0.178
Carboplatin	1	0.8*	0.023	2.3*	0.024
Cisplatin	1	0.7	0.246	1.6	0.401
5-FU	1	1.1	0.370	0.9	0.250
VP-16	1	1	0.858	0.9	0.157
Vincristine	1	2.5	0.208	2.9***	0.003

* p value <0.05

** p value <0.01

*** p value <0.005

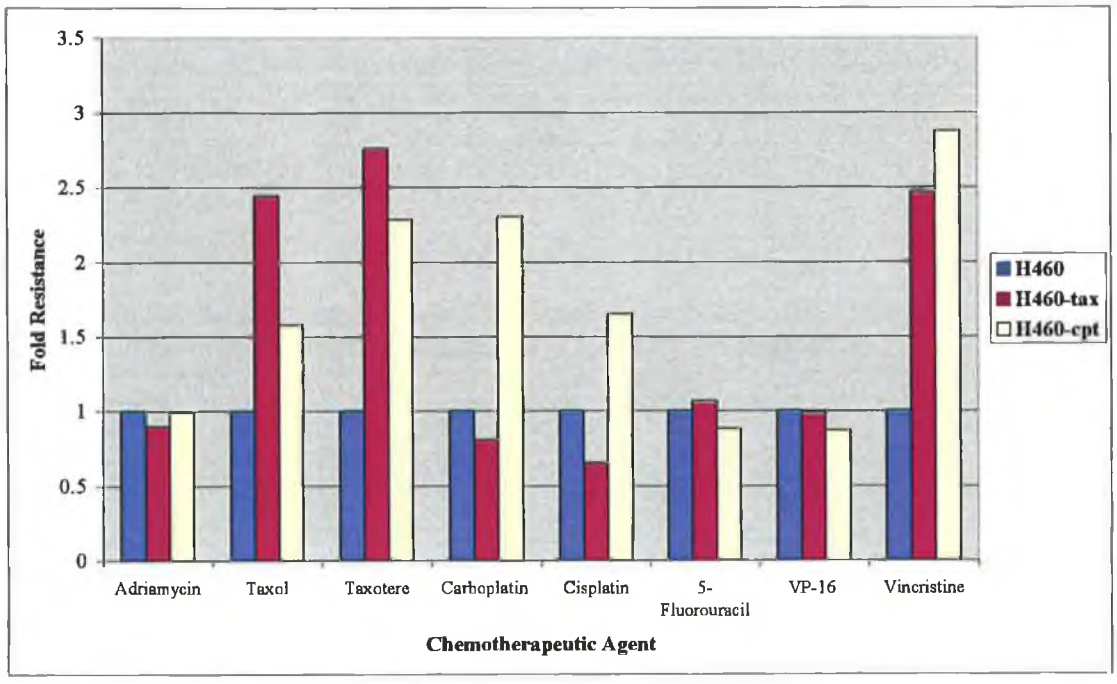

Figure 3.2.3 Fold resistance of H460 pulse-selected variants

3.2.2.4 Changes in resistance in SKLU1 pulse-selected variants

The IC50 values for the SKLU1 pulse-selected variants can be seen in Table 3.2.10. Fold resistance information and p values are shown in Table 3.2.11 and Figure 3.2.4. SKLU1-tax shows increases in resistance to adriamycin (2.1-fold), taxol (5-fold), cisplatin (1.4-fold) and VP-16 (1.4-fold).

SKLU1-cpt displays significant increases in resistance to adriamycin, taxol, carboplatin, cisplatin and VP-16. Although this cell line was pulsed with carboplatin, it shows an 8.5-fold increase in resistance to taxol and only a 1.4-fold increase in resistance to carboplatin.

Table 3.2.10 IC50s of SKLU-1 variants

	SKLU-1	SKLU-1-tax	SKLU-1-cpt
Adriamycin (ng/ml)	27.1 ± 0.4	55.8 ± 5.1	78 ± 10.8
Taxol (ng/ml)	1.2 ± 0.1	6.2 ± 0.5	10.5 ± 0.6
Carboplatin (μg/ml)	2.8 ± 0.2	3.7 ± 0.9	4 ± 0.2
Cisplatin (ng/ml)	405.7 ± 21.2	566 ± 46.3	1176.7 ± 75.1
5-FU (ng/ml)	1223.3 ± 73.7	1210 ± 215.2	553.3 ± 7.6
VP-16 (ng/ml)	115.7 ± 5.9	162 ± 17.1	239.7 ± 12.6
Vincristine (ng/ml)	0.7 ± 0.3	1.3 ± 0.1	1 ± 0.3

(Results are expressed as IC50 ± SD, n=3)

Table 3.2.11 Fold resistance of SKLU1 pulse-selected variants

Chemotherapeutic agent	SKLU1	SKLU1-tax	P value SKLU1-tax	SKLU1-cpt	P value SKLU1-cpt
Adriamycin	1	2.1**	0.010	2.9*	0.014
Taxol	1	5***	0.003	8.5***	0.001
Carboplatin	1	1.3	0.209	1.4***	0.001
Cisplatin	1	1.4*	0.014	2.9***	0.002
5-FU	1	1	0.927	0.5***	0.004
VP-16	1	1.4*	0.032	2.1***	0.001
Vincristine	1	1.8	0.058	1.4	0.265

* p value <0.05

** p value <0.01

*** p value <0.005

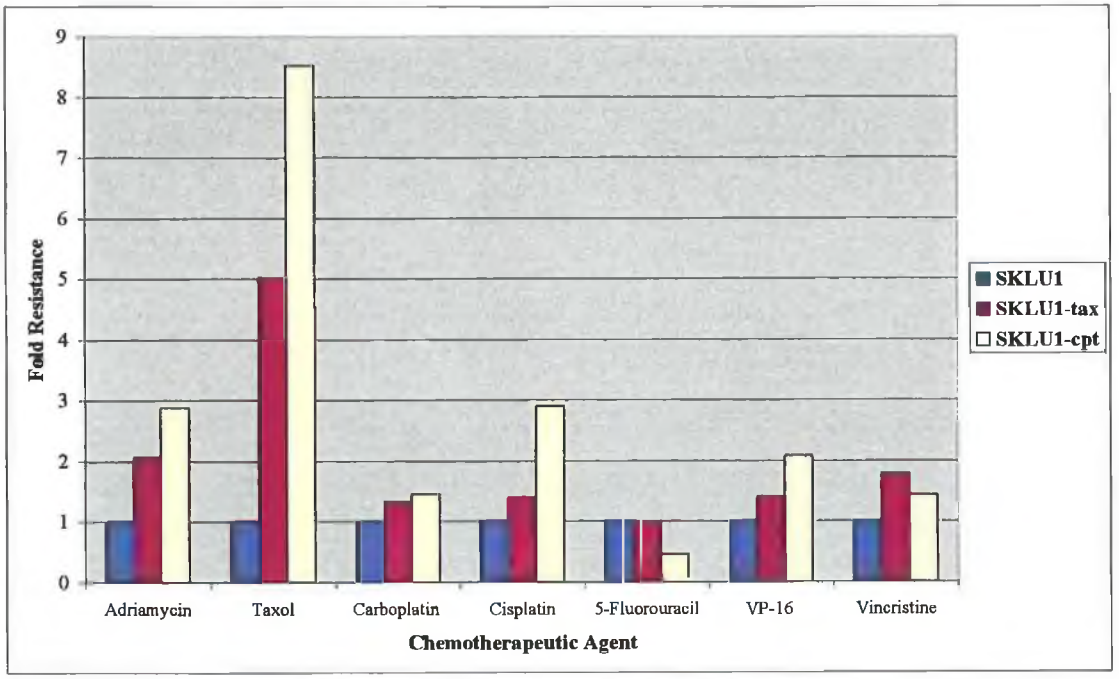

Figure 3.2.4 Fold resistance of SKLU1 pulse-selected variants

3.2.3 Invasion assays

Invasion assays were used to determine invasion ability of a cell line *in vitro*. The cells are placed on artificial extracellular matrix (ECM) which is coated onto a porous membrane and inserted into a 24-well plate. Cells are considered invasive when they are able to migrate through the ECM gel and the porous membrane and subsequently attach to the underside of the membrane within 24 hours. Some cell lines are capable of detaching from the insert and attaching to the bottom of the 24-well plate. These cells are termed superinvasive.

3.2.3.1 Invasion of parent cell lines

The invasive abilities of the four parent cell lines used in this study are demonstrated in Figures 3.2.5-3.2.8. There was increasing invasion ability in the parent cell lines as follows: H460; A549; SKLU-1 and H1299. Additionally a certain cell population of SKLU-1 (Figure 3.2.7b) and H1299 (Figure. 3.2.8b) displayed the ability to super-invade. The images presented are representative of at least three separate experiments, are at a magnification of 10X and are stained with crystal violet (Section 2.7).

(a)

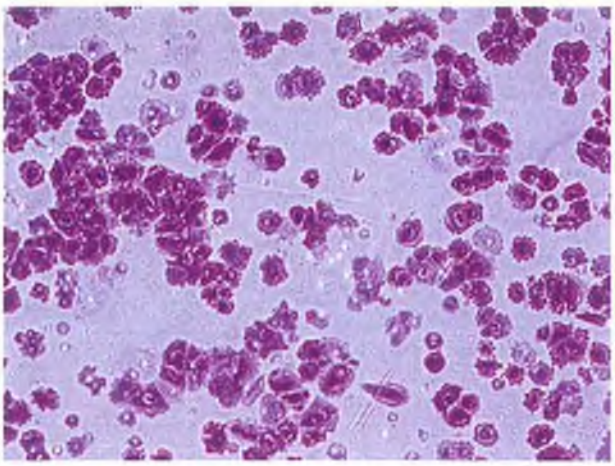

Figure 3.2.5 Invasion of H460

(b)

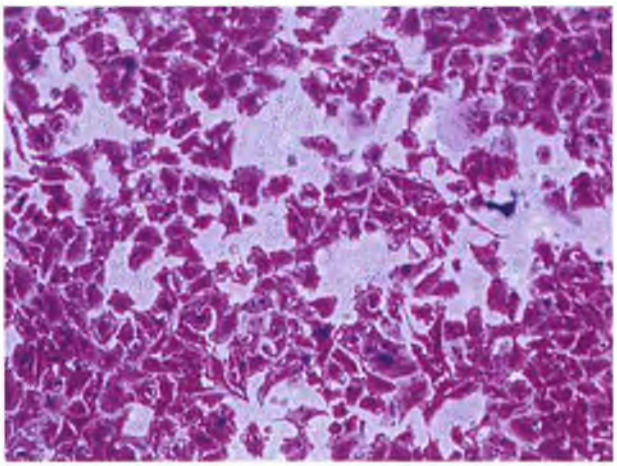

Figure 3.2.6 Invasion of A549

(a)

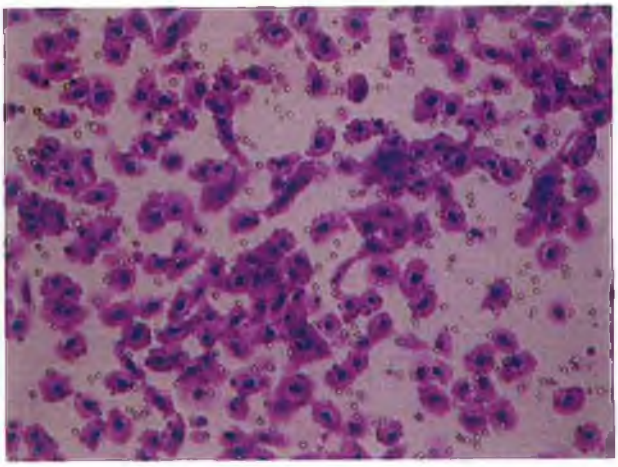

(b)

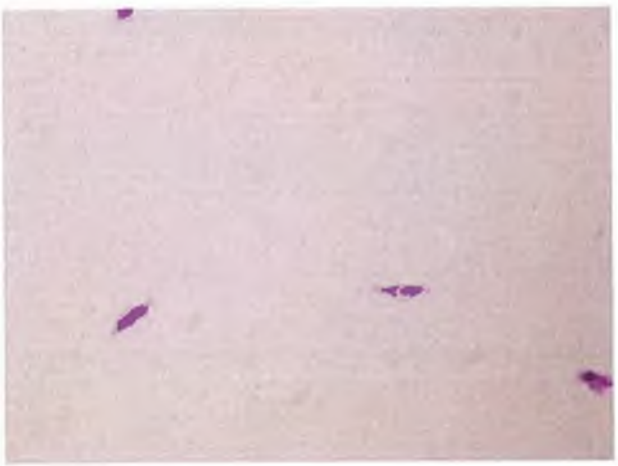

Figure 3.2.7 Invasion and superinvasion of SKLU1

(a)

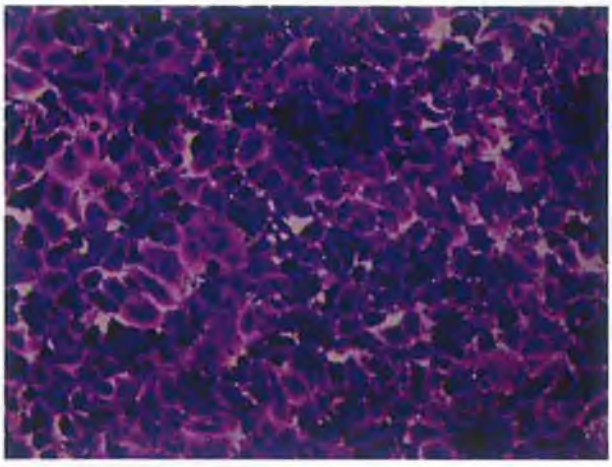

(b)

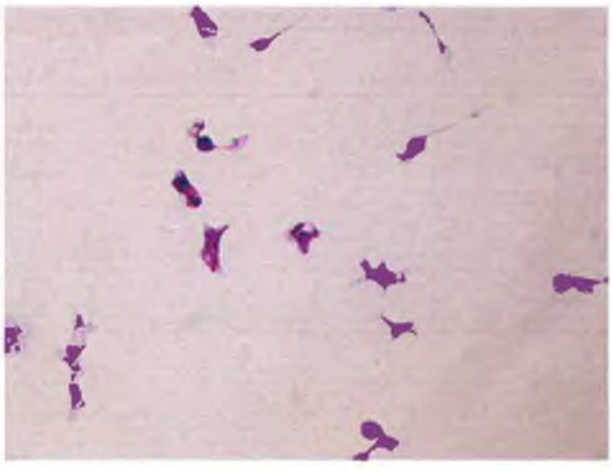

Figure 3.2.8 Invasion (a) and superinvasion (b) of H1299

3.2.3.2 Changes in invasion capacity after pulse-selection

The H460 parent line was the least invasive cell line used in this study. After pulse selecting the cells for taxol and carboplatin, both variants showed decreases in invasion activity (Figure 3.2.10). This invasion was quantified by counting the number of invading cells. Figure 3.2.9 shows the decrease of invasion the pulse-selected H460 variants.

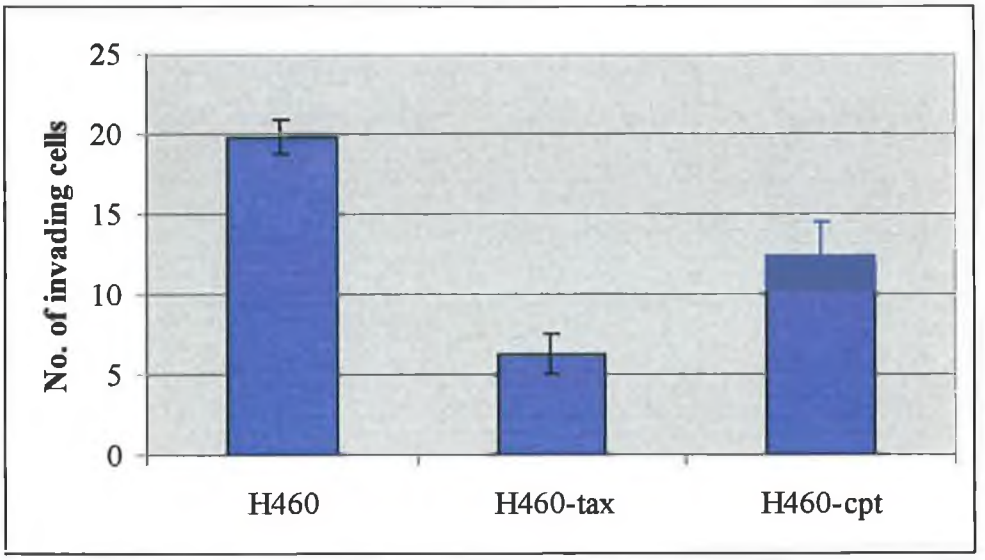

Figure 3.2.9 Quantified invasion of H460 variants

(a)

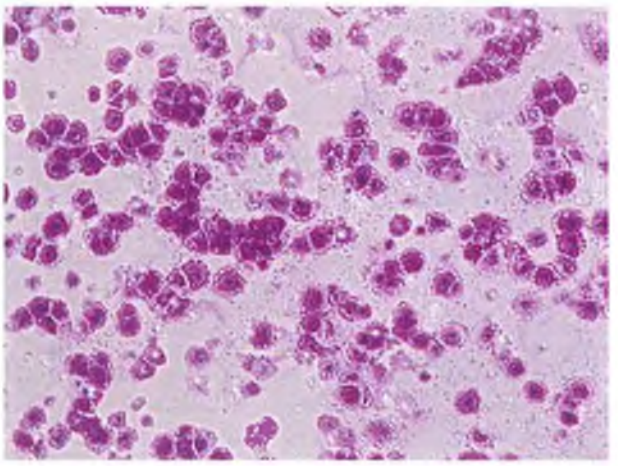

(b)

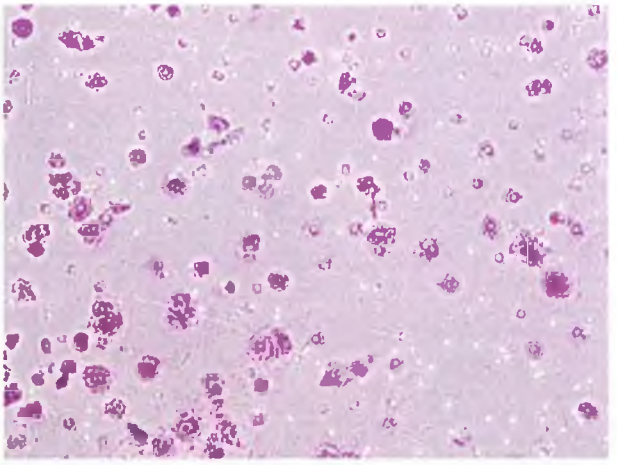

(c)

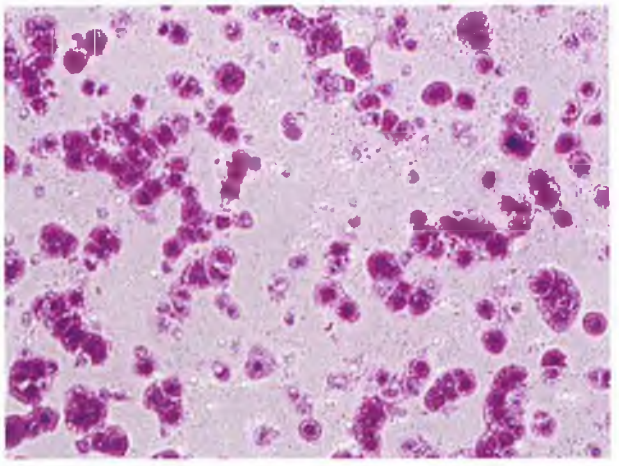

Figure 3.2.10 Invasion of (a) H460, (b) H460-tax and (c) H460-cpt

The parental A549 cells showed a significant ability to invade (Figure 3.2.12). The taxol-selected cells showed slightly increased invasion, whereas the selection with carboplatin show considerably decreased invasion activity (Figure 3.2.11). The latter cells also differ morphologically from the parent cells having become larger and elongated.

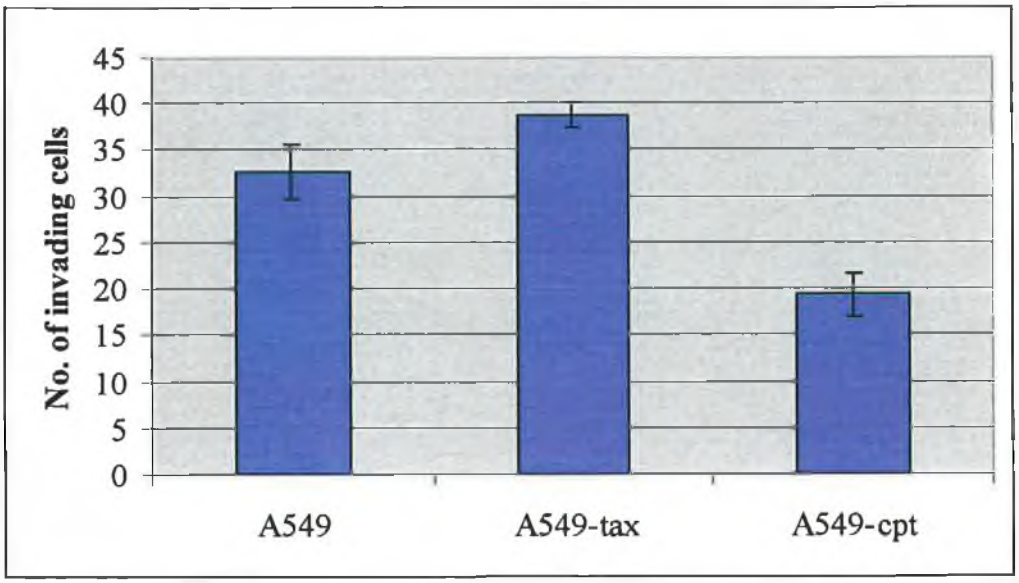

Figure 3.2.11 Quantified invasion of A549 variants

(a)

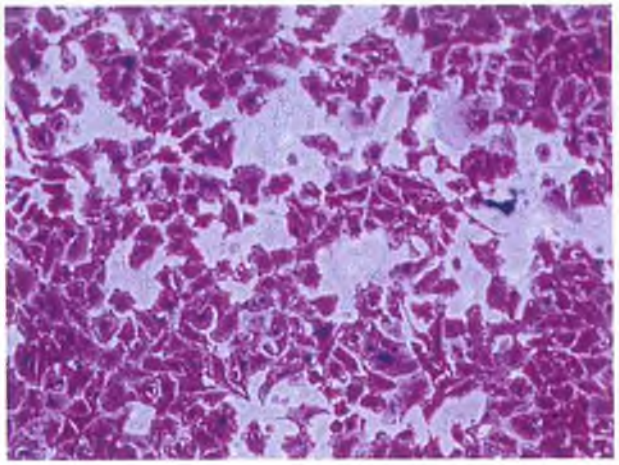

(b)

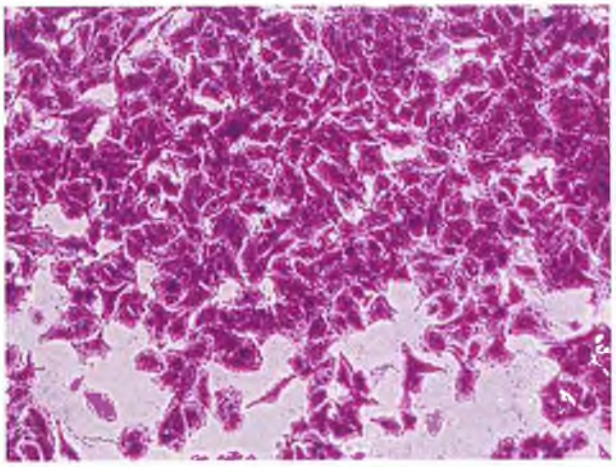

(c)

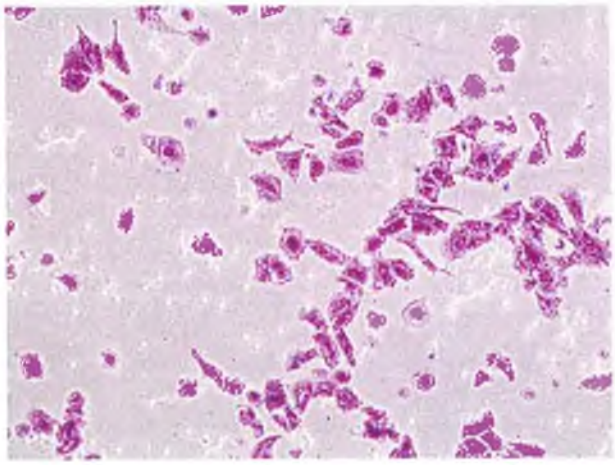

Figure 3.2.12 Invasion of (a) A549, (b) A549-tax and (c) A549-cpt

SKLU-1 parent cells were invasive and a few cells also super-invaded. In contrast to the results mentioned above, pulse-selected variants of SKLU1 were less invasive than the parent cell line (Figures 3.2.13 and 3.2.14).

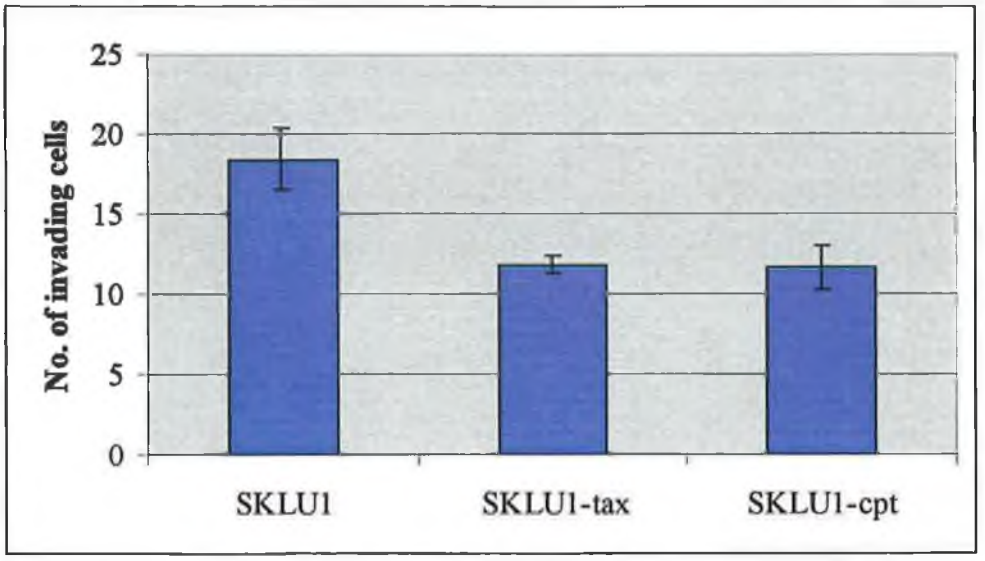

Figure 3.2.13 Quantified invasion of SKLU1 variants

(a)

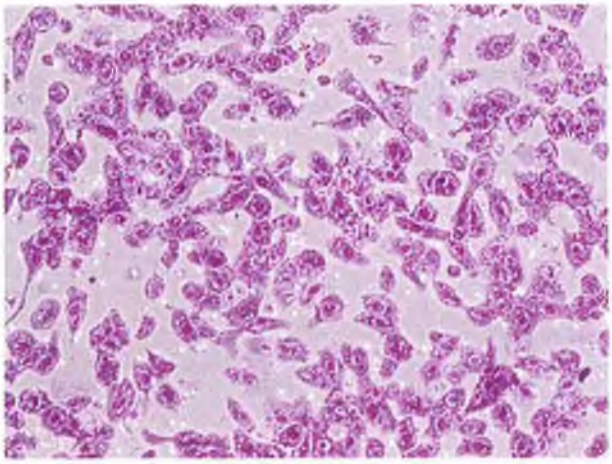

(b)

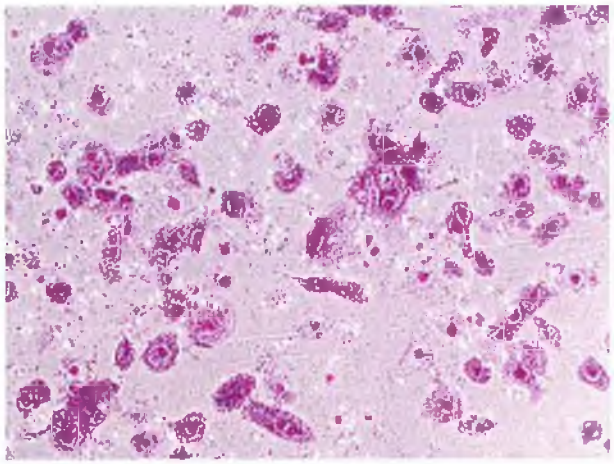

(c)

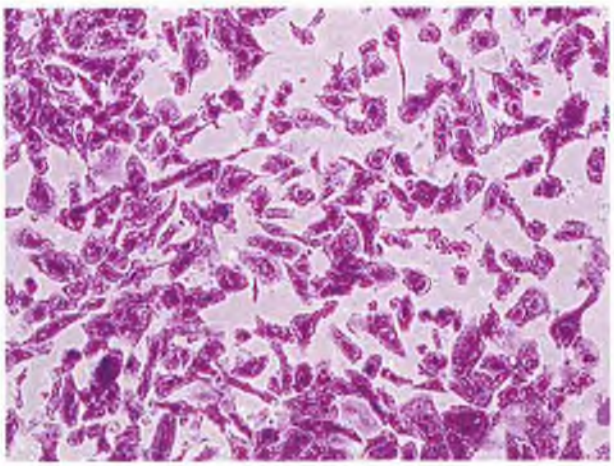

Figure 3.2.14 Invasion of (a) SKLU1, (b) SKLU1-tax and (c) SKLU1-cpt

H1299 parent was the most invasive and superinvasive cell line used in this project. After taxol-selection the invasion capacity slightly increased, whereas the carboplatin-selected cells showed a decrease in invasion activity (Figures 3.2.15 and 3.2.16), similar to what was seen with A549 cells.

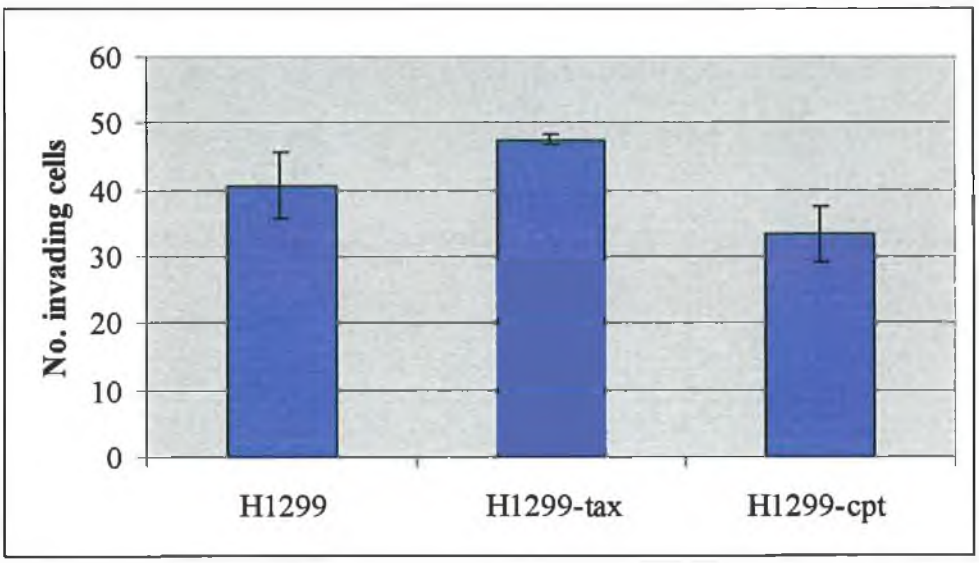

Figure 3.2.15 Quantified invasion of H1299 variants

(a)

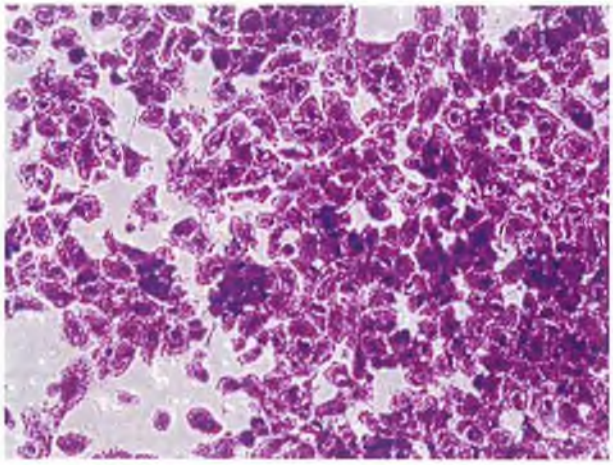

(b)

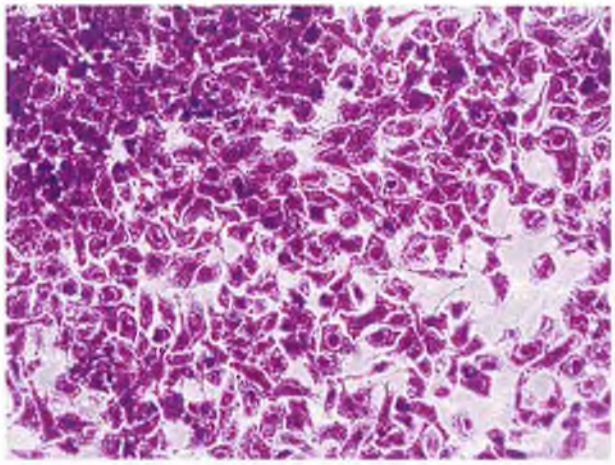

(c)

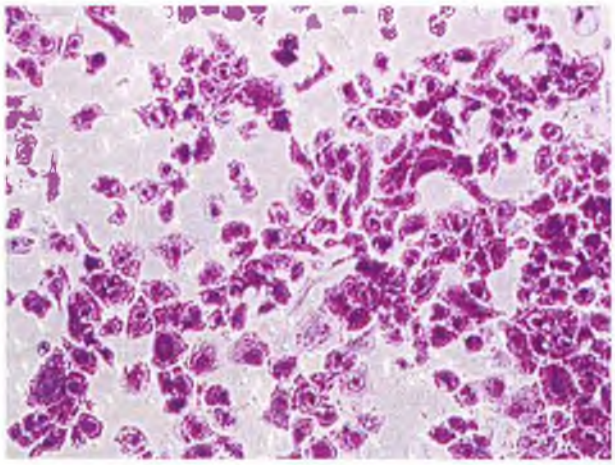

Figure 3.2.16 Invasion of (a) H1299, (b) H1299-tax and (c) H1299-cpt

3.2.4 Pgp expression

Pgp expression was detected in cell lines using western blotting. Only one of the cell lines, H1299, was found to express the protein. Figure 3.2.17 shows that P-gp was up-regulated in H1299-tax relative to H1299.

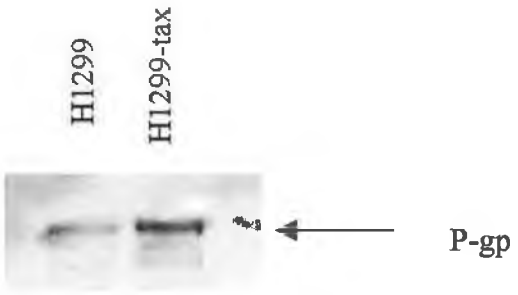

Figure 3.2.17 P-gp expression in selected cell lines

3.2.5 MRP1 expression

MRP1 protein was detected in the cell lines (Figure 3.2.18). A549 parental cells express high levels of the protein, which seems to remain relatively unchanged in the pulse-selected variants. In H1299 cells, MRP1 protein is expressed at a very low level in the H1299-cpt cell line. All of the H460 cell lines express MRP1, with less expression in the selected variants compared to the parent cell line. SKLU1 parent cells express very low levels of MRP1, whereas the protein is much more abundant in SKLU1-tax and especially SKLU1-cpt.

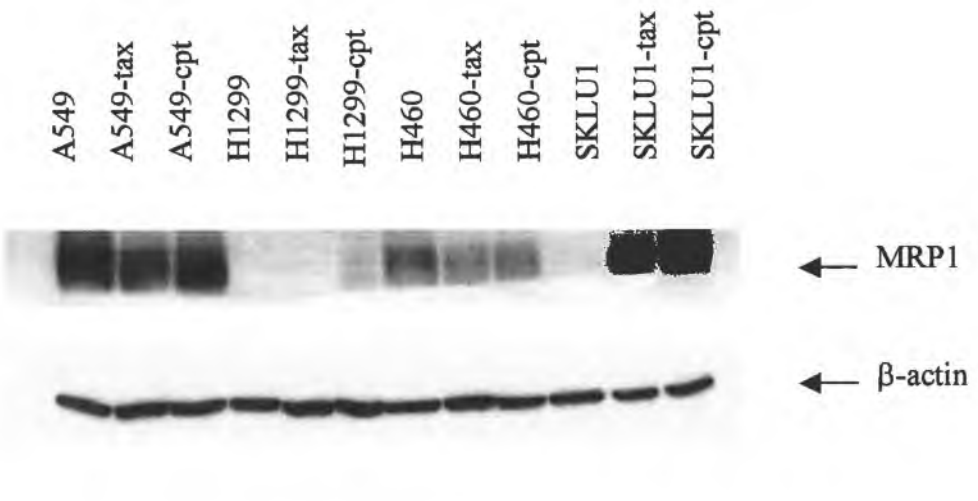

Figure 3.2.18 MRP1 expression in selected cell lines

3.2.6 Combination assays

Toxicity assays were carried out in all cell lines with a combination of adriamycin and the NSAID sulindac, an MRP1 inhibitor or a combination of taxol with GF120918, a Pgp inhibitor. A summary of the results observed in all combination assays can be seen in Table 3.2.12.

Table 3.2.12 Summary of effects observed in combination assays

Cell line	Sulindac and adriamycin	GF120918 and taxol
A549	++	-
A549-tax	++	+
A549-cpt	++	-
H1299	-	++
H1299-tax	-	+
H1299-cpt	+	++
SKLU1	-	-
SKLU1-tax	-	-
SKLU1-cpt	-	-
H460	++	-
H460-tax	-	-
H460-cpt	++	+

++ definite effect; + some effect; - no effect

3.2.6.1 Adriamycin and sulindac in A549

There was some synergy observed between adriamycin and sulindac in A549 cells. MRP1 protein was expressed in this cell line (see section 3.2.5). The greatest effect was observed at 20μg/ml sulindac combined with adriamycin (Figure 3.2.19). In A549-tax (Figure 3.2.20), while there is still an effect of combining the two drugs, it is much less than that observed in the parent. Figure 3.2.21 shows the effects of this combination in A549-cpt. MRP1 is more highly expressed in this cell line, so it is unsurprising that the effect of combining sulindac with adriamycin is greatest here.

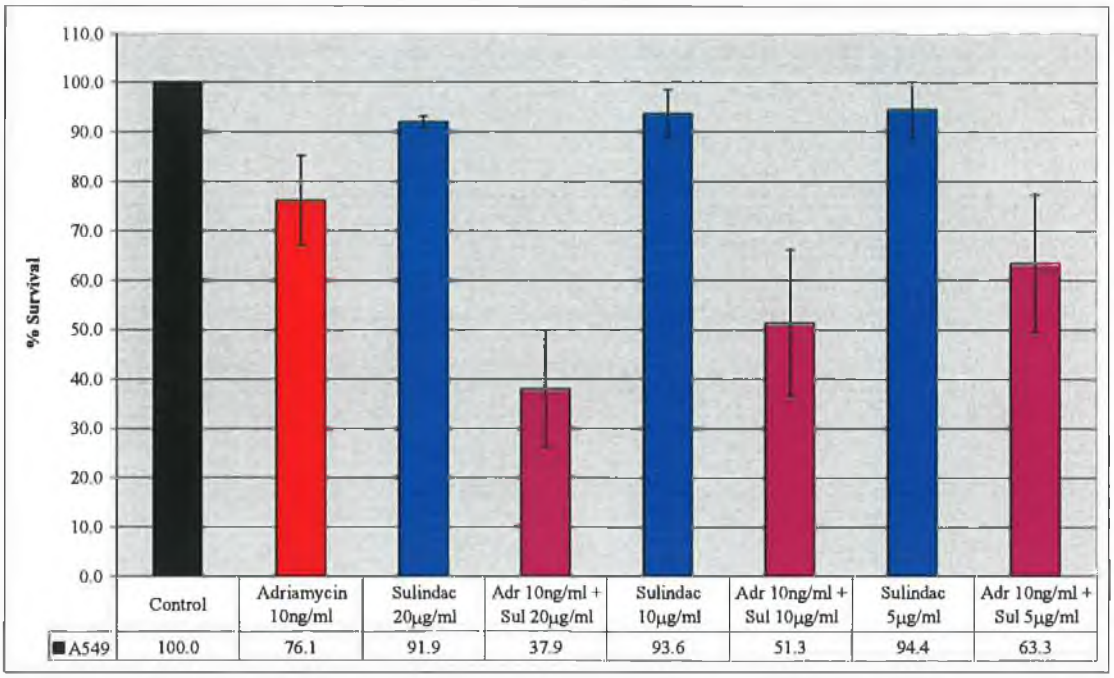

Figure 3.2.19 Adriamycin and sulindac combination in A549

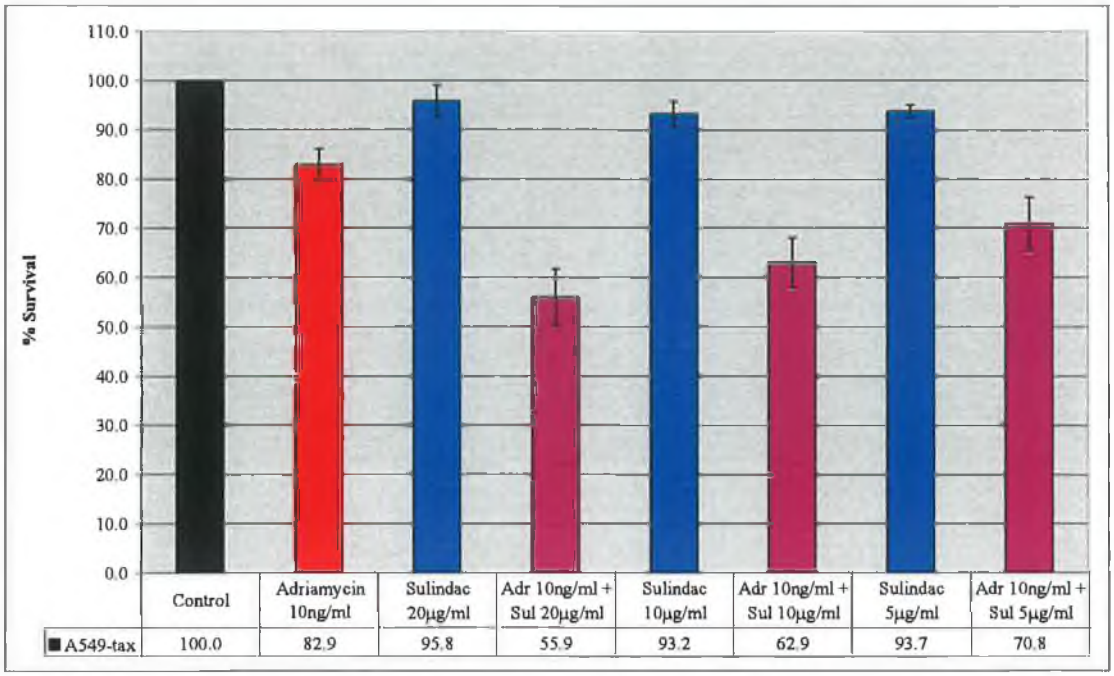

Figure 3.2.20 Adriamycin and sulindac combination in A549-tax

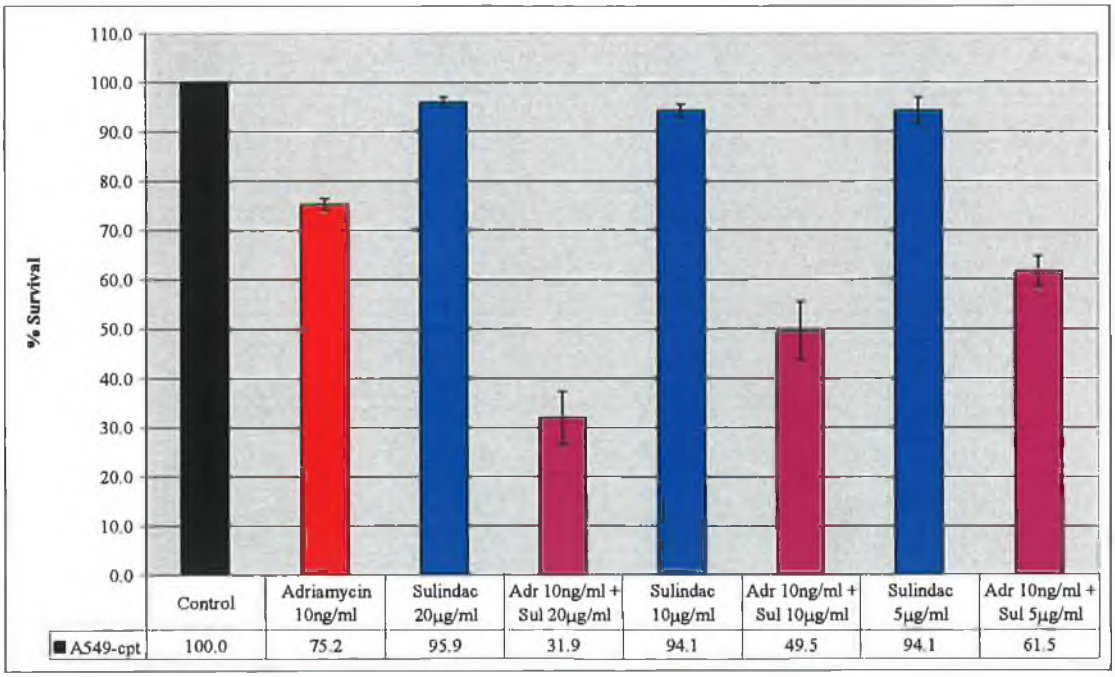

Figure 3.2.21 Adriamycin and sulindac combination in A549-cpt

3.2.6.2 Adriamycin and sulindac in H1299

The combination of adriamycin and sulindac in H1299, H1299-tax and H1299-cpt is shown in Figures 3.2.22, 3.2.23 and 3.2.24 respectively. MRP1 is expressed at very low levels in these cell lines (Figure 3.2.5). No strong effect of this combination is seen in any of the cell lines.

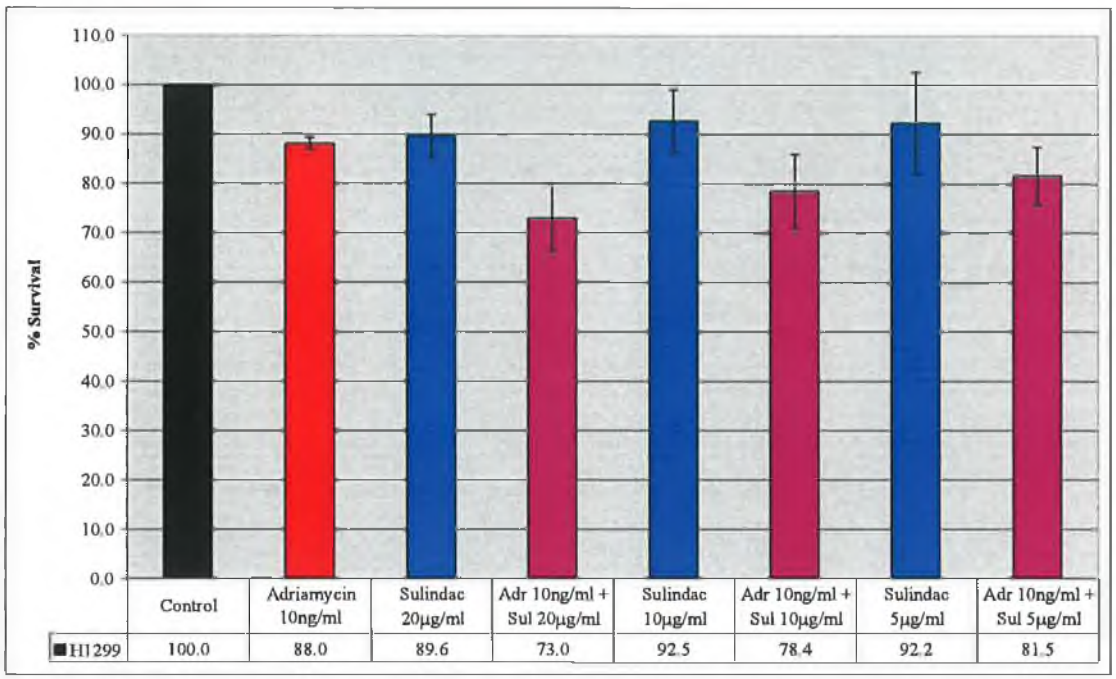

	Control	Adriamycin 10ng/ml	Sulindac 20µg/ml	Adr 10ng/ml + Sul 20µg/ml	Sulindac 10µg/ml	Adr 10ng/ml + Sul 10µg/ml	Sulindac 5µg/ml	Adr 10ng/ml + Sul 5µg/ml
H1299	100.0	88.0	89.6	73.0	92.5	78.4	92.2	81.5

Figure 3.2.22 Adriamycin and sulindac combination in H1299

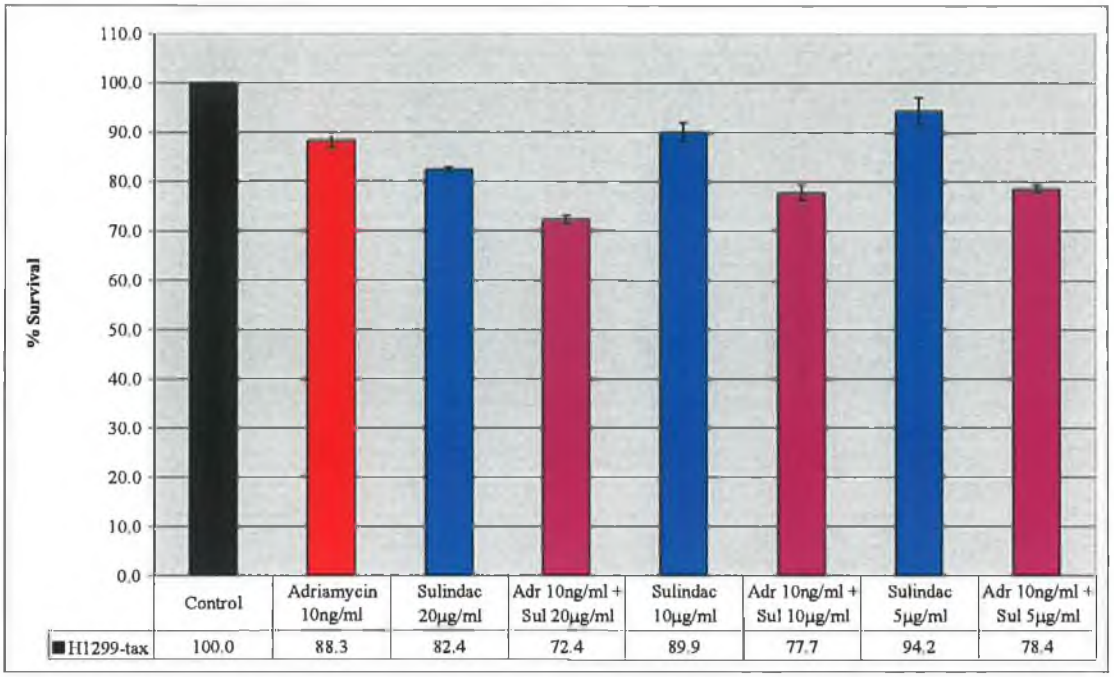

Figure 3.2.23 Adriamycin and sulindac combination in H1299-tax

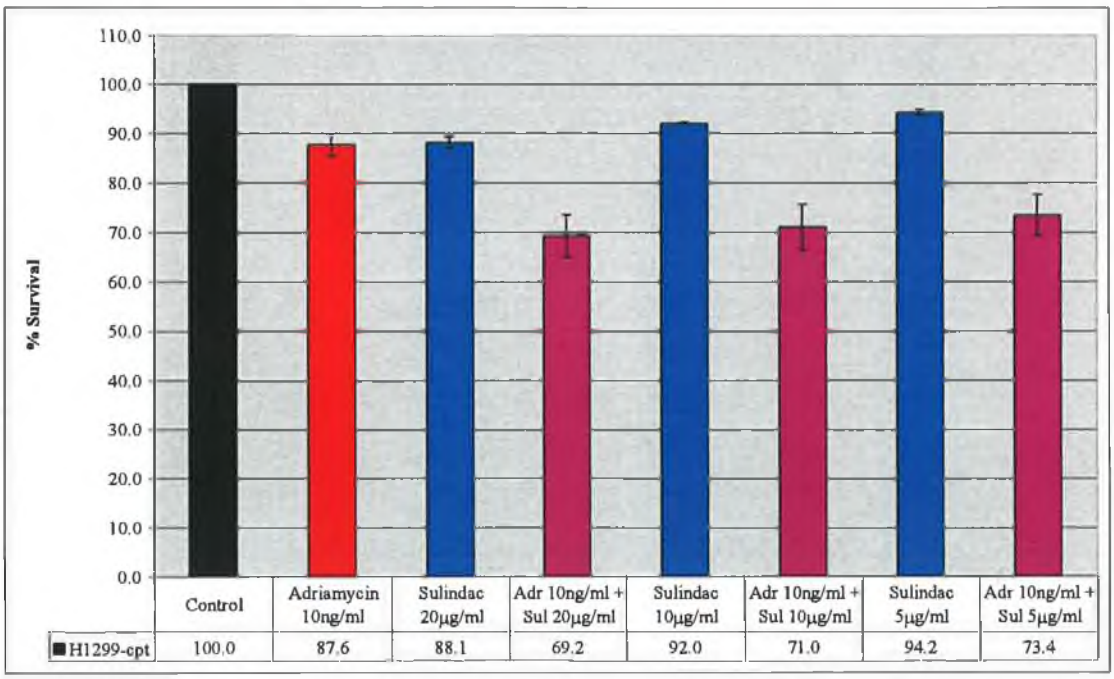

Figure 3.2.24 Adriamycin and sulindac combination in H1299-cpt

3.2.6.3 Adriamycin and sulindac in SKLU1

The effect of combining adriamycin and sulindac is SKLU1, SKLU1-tax and SKLU1-cpt is shown in Figures 3.2.25, 3.2.26 and 3.2.27 respectively. The relationship between adriamycin and sulindac in the SKLU1 cell lines seemed to be additive. There was no difference observed in the behaviour of the drug combination in the resistant cell lines compared to the parent cell line, despite an increase in MRP1 expression in the selected variants.

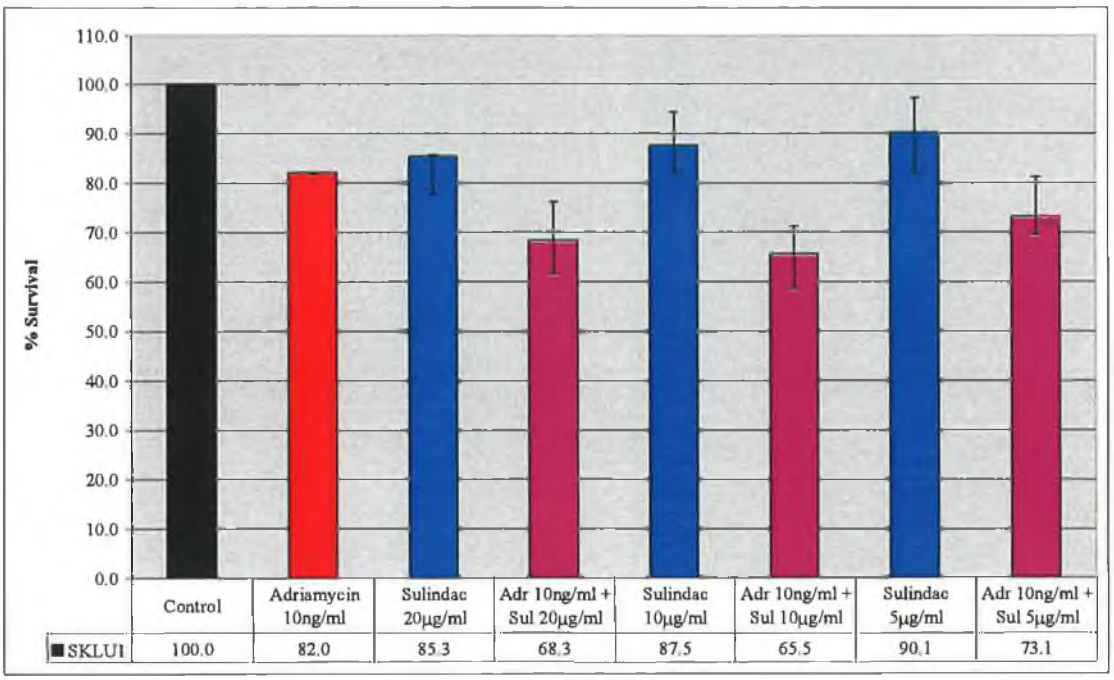

Figure 3.2.25 Adriamycin and sulindac combination in SKLU1

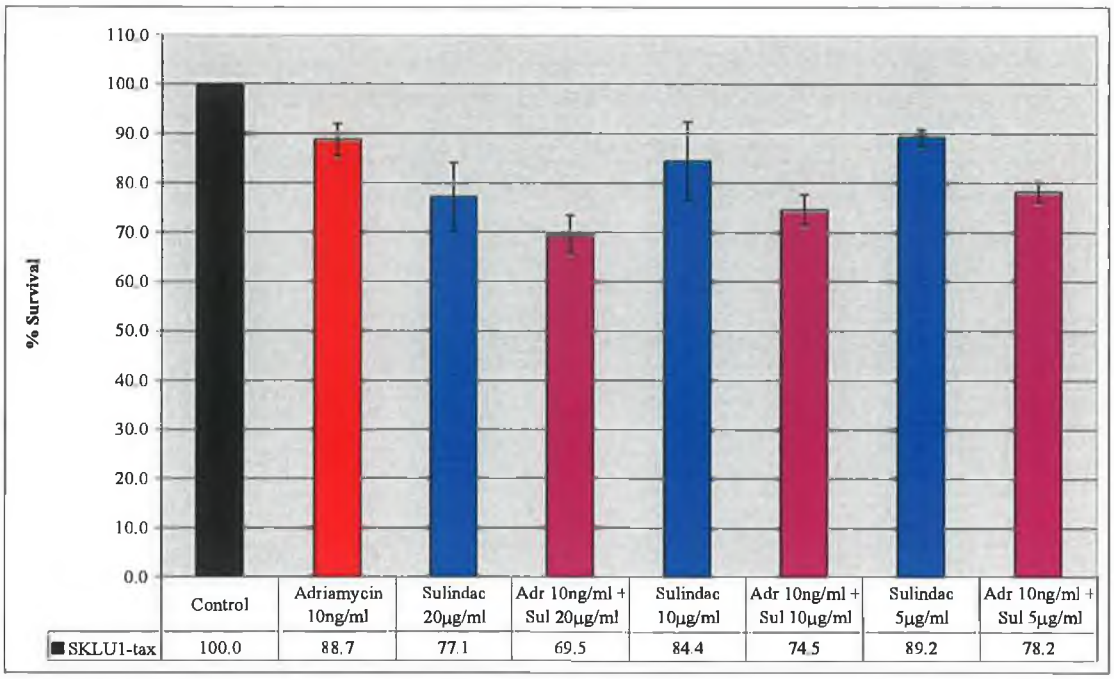

Figure 3.2.26 Adriamycin and sulindac combination in SKLU1-tax

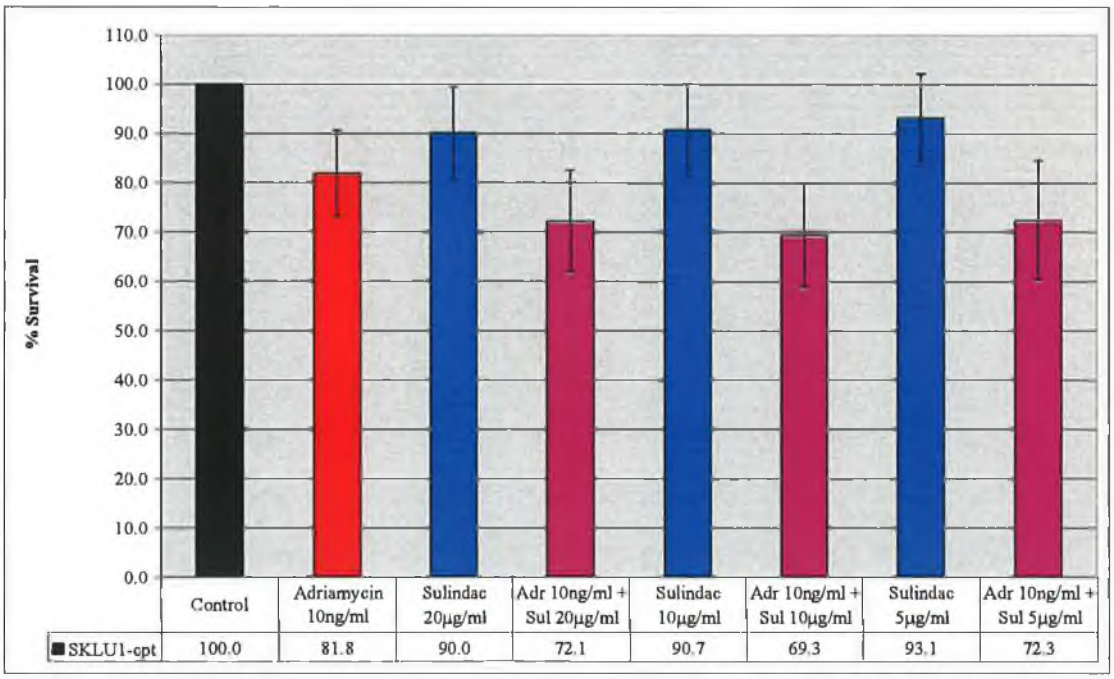

Figure 3.2.27 Adriamycin and sulindac combination in SKLU1-cpt

3.2.6.4 Adriamycin and sulindac in H460

The effect of combining adriamycin and sulindac is H460, H460-tax and H460-cpt is shown in Figures 3.2.28, 3.2.29 and 3.2.30 respectively. There is a slight increase in effect of the combination in H460 and H460-cpt. This effect is not observed in H460-tax, which correlated to MRP1 expression, since MRP1 appears to be downregulated in H460-tax compared to H460.

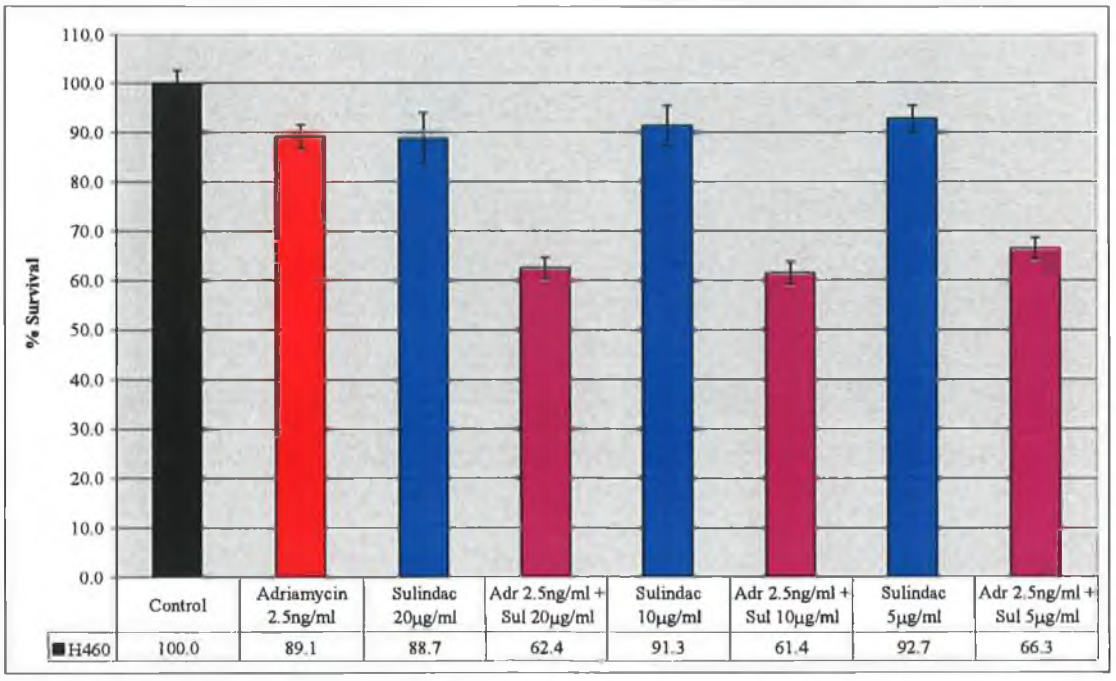

Figure 3.2.28 Adriamycin and sulindac combination in H460

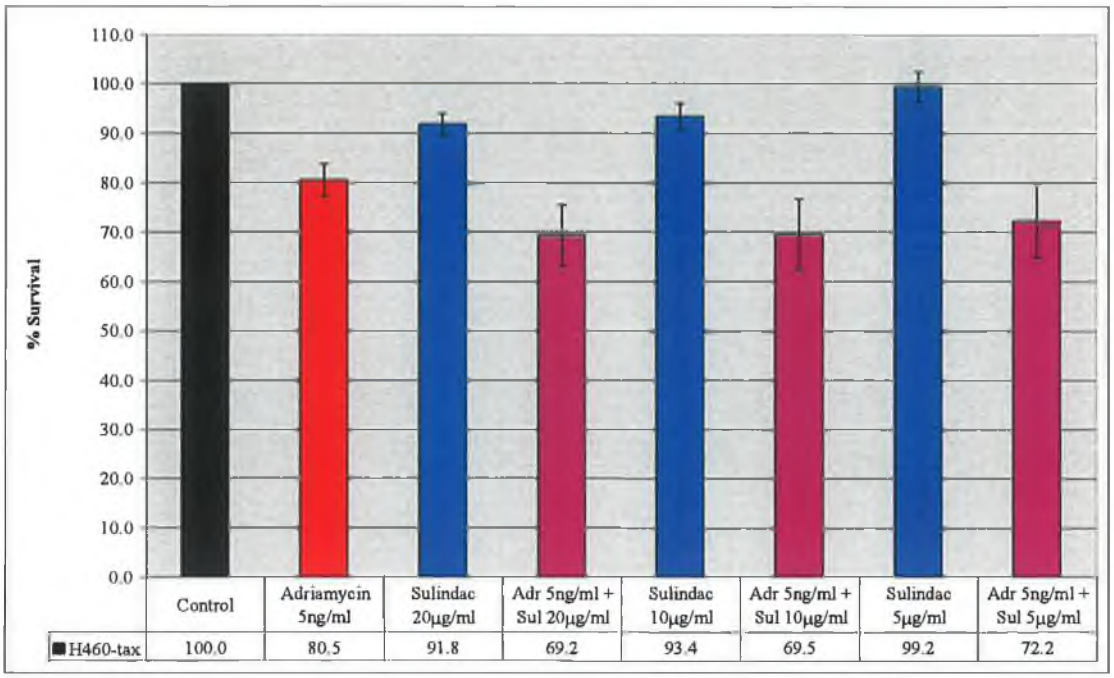

Figure 3.2.29 Adriamycin and sulindac combination in H460-tax

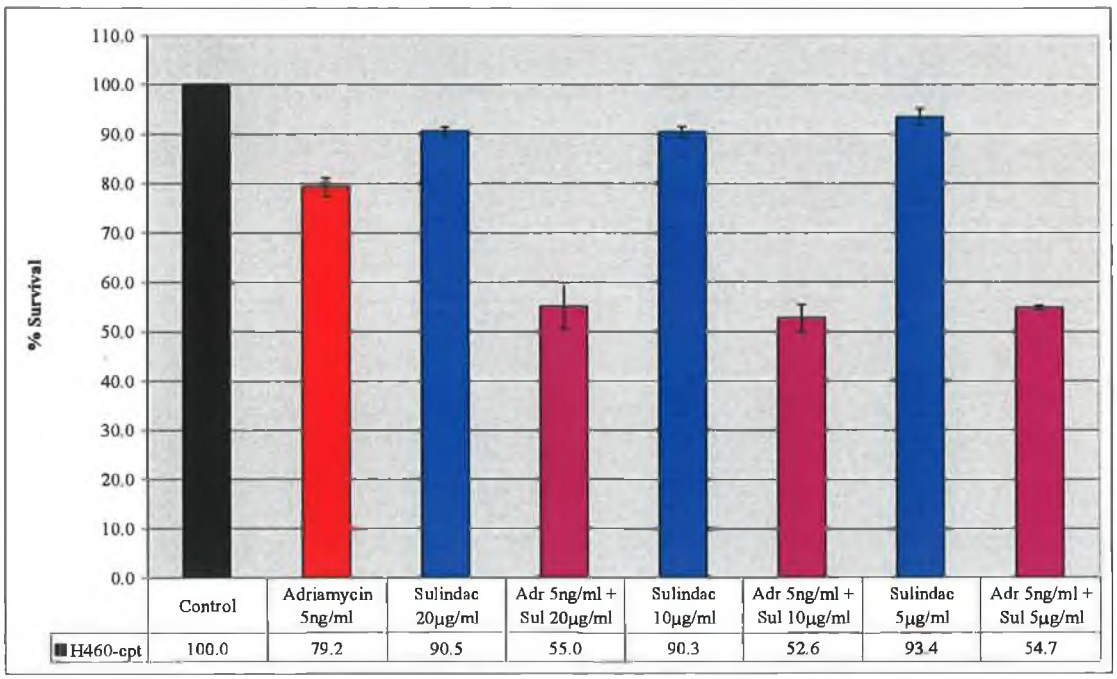

Figure 3.2.30 Adriamycin and sulindac combination in H460-cpt

3.2.6.5 Taxol and GF120918 in A549

The effect of the combination of taxol with the P-gp inhibitor GF120918 (Elacridar) in the cell lines A549, A549-tax and A549-cpt (Figures 3.2.31, 3.2.32 and 3.2.33) was investigated. This combination did not result in synergism in the A549 or A549-cpt cells. P-gp expression was not detected by western blotting. There appears to be a slight combination effect in A549-tax.

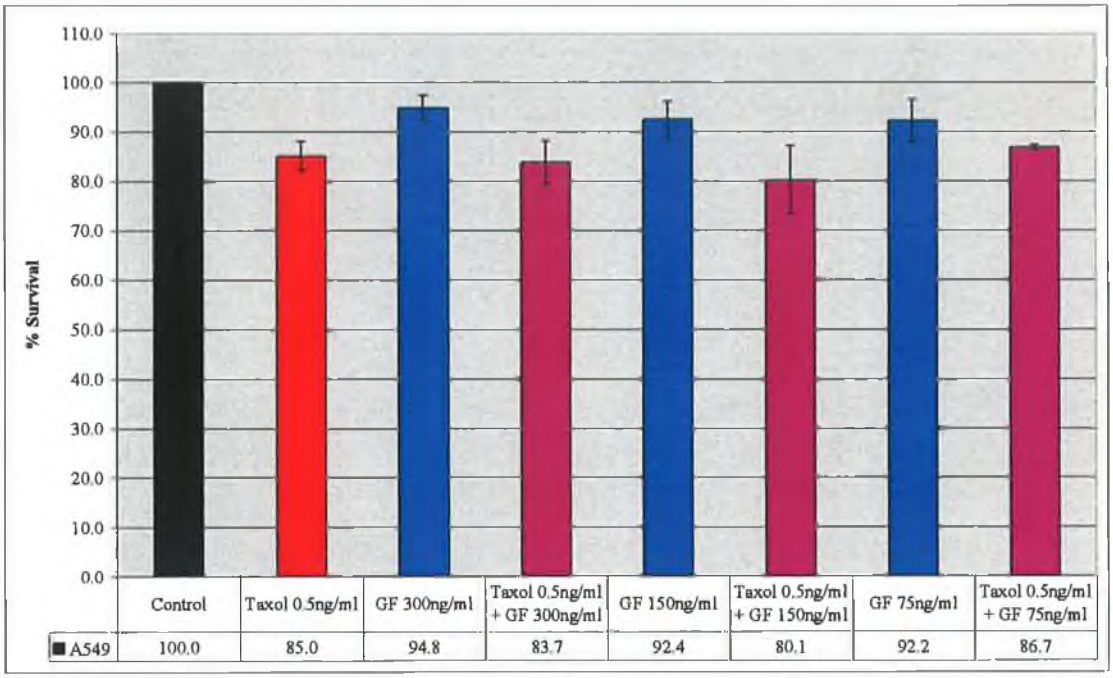

Figure 3.2.31 Taxol and GF120918 combination in A549

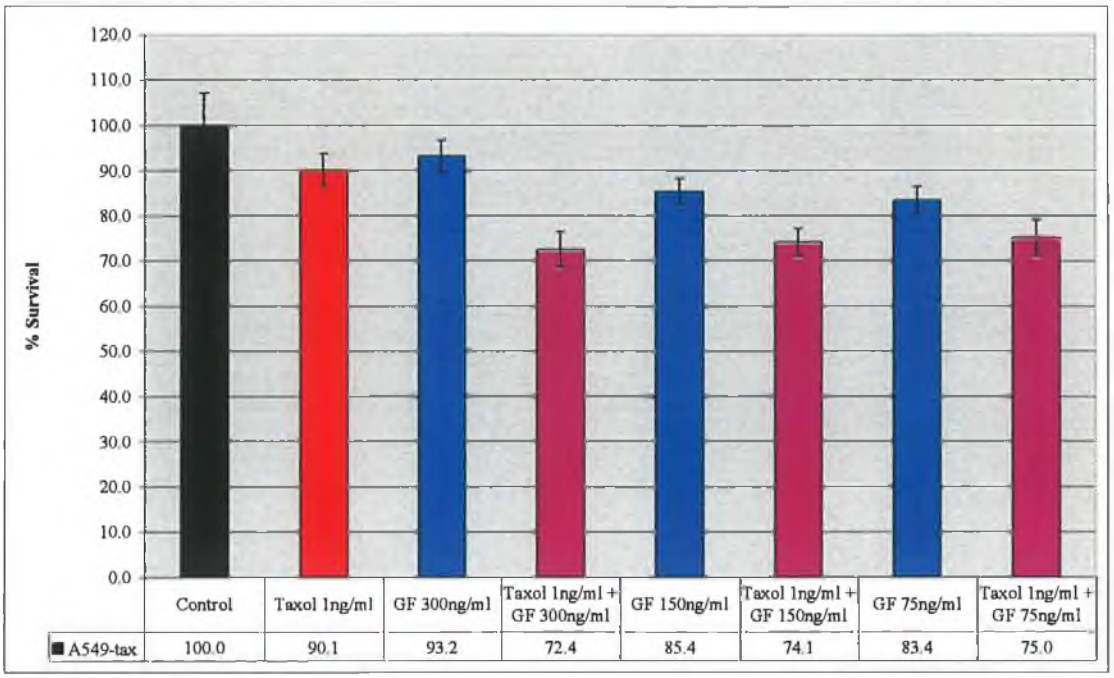

Figure 3.2.32 Taxol and GF120918 combination in A549-tax

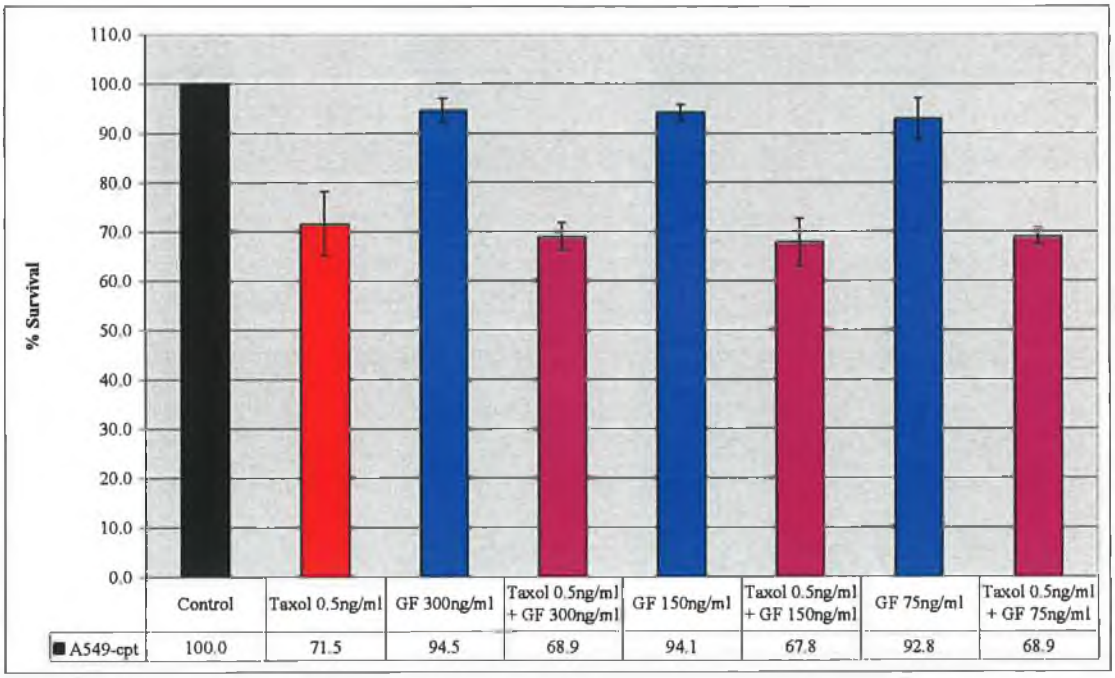

Figure 3.2.33 Taxol and GF120918 combination in A549-cpt

3.2.6.6 Taxol and GF120918 in H1299

The effect of the combination of taxol with the P-gp inhibitor GF120918 in the cell lines H1299, H1299-tax and H1299-cpt (Figures 3.2.34, 3.2.35 and 3.2.36). Synergy was observed between these two drugs in the H1299 cell lines and this was expected since P-gp is expressed in these cell lines (Section 3.2.4). Interestingly, there is less of an effect in H1299-tax than in the parent, despite the fact that this cell line expresses more P-gp.

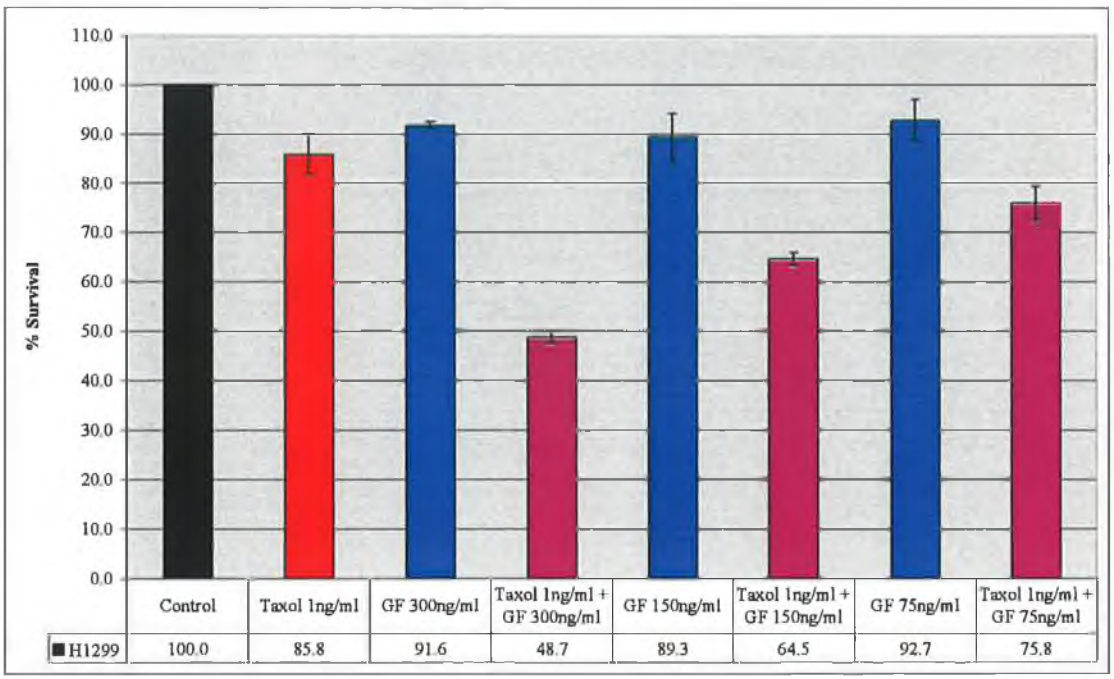

Figure 3.2.34 Taxol and GF120918 combination in H1299

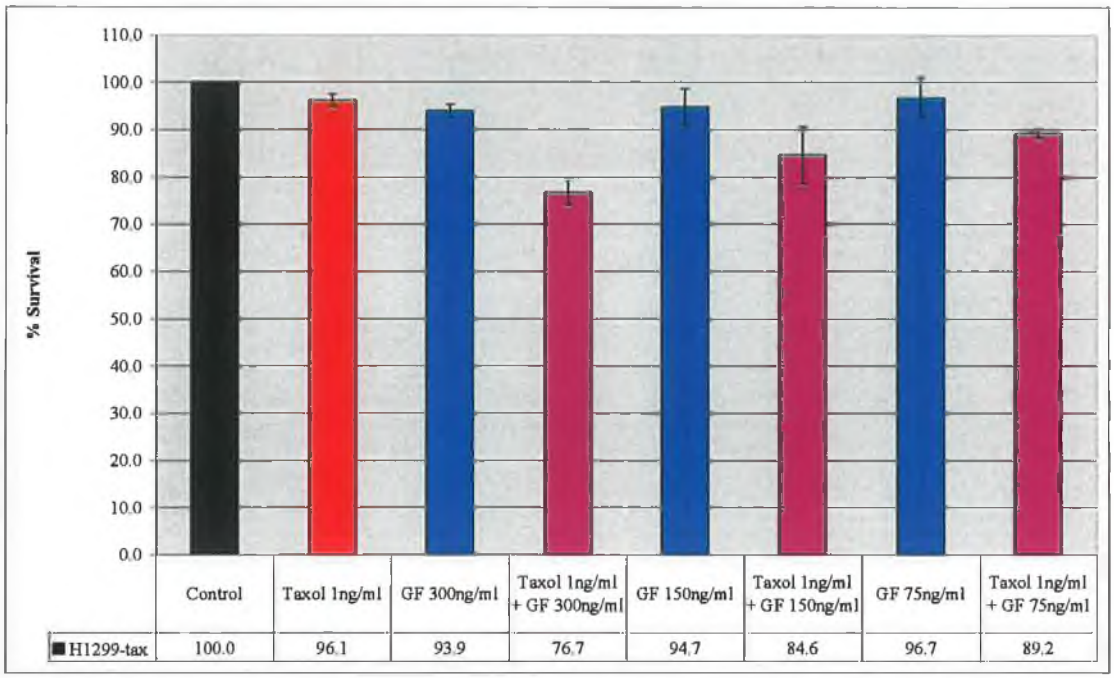

Figure 3.2.35 Taxol and GF120918 combination in H1299-tax

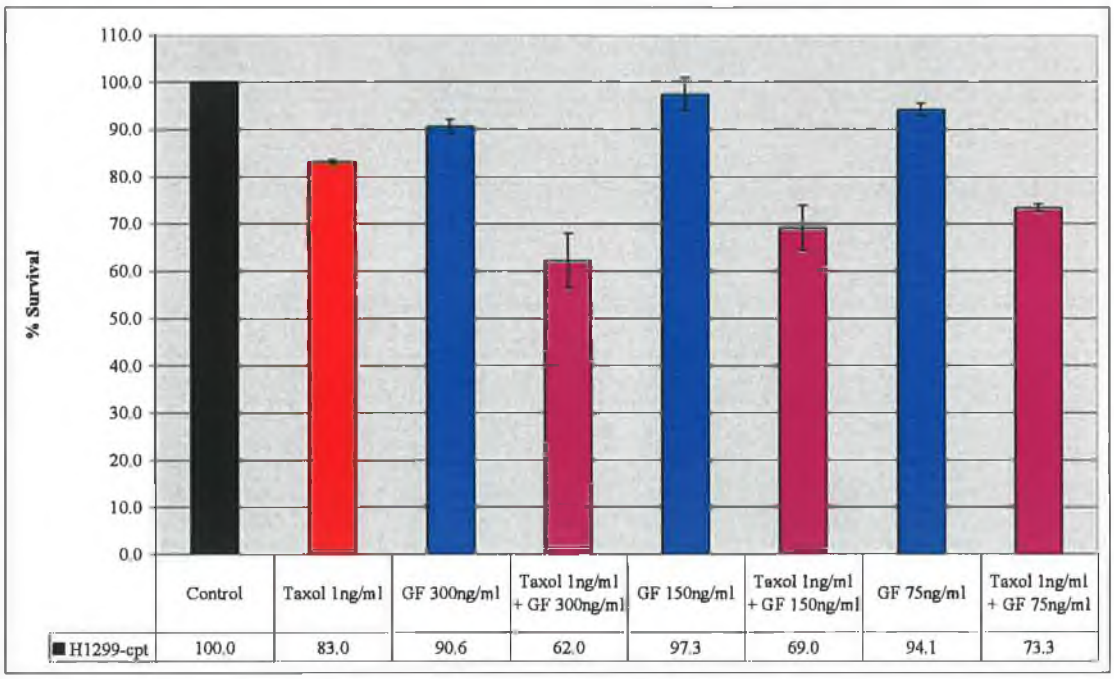

Figure 3.2.36 Taxol and GF120918 combination in H1299-cpt

3.2.6.7 Taxol and GF120918 in SKLU1

The effect of the combination of taxol with the P-gp inhibitor GF120918 in the cell lines SKLU1, SKLU1-tax and SKLU1-cpt (Figures 3.2.37, 3.2.38 and 3.2.39) shows no positive effect with the combination of taxol and GF120918 in SKLU1 cells. The taxol resistant variant showed only additive effects when treated with the combination. These results suggest low or no presence of P-gp in these cell lines and is consistent with western blotting results.

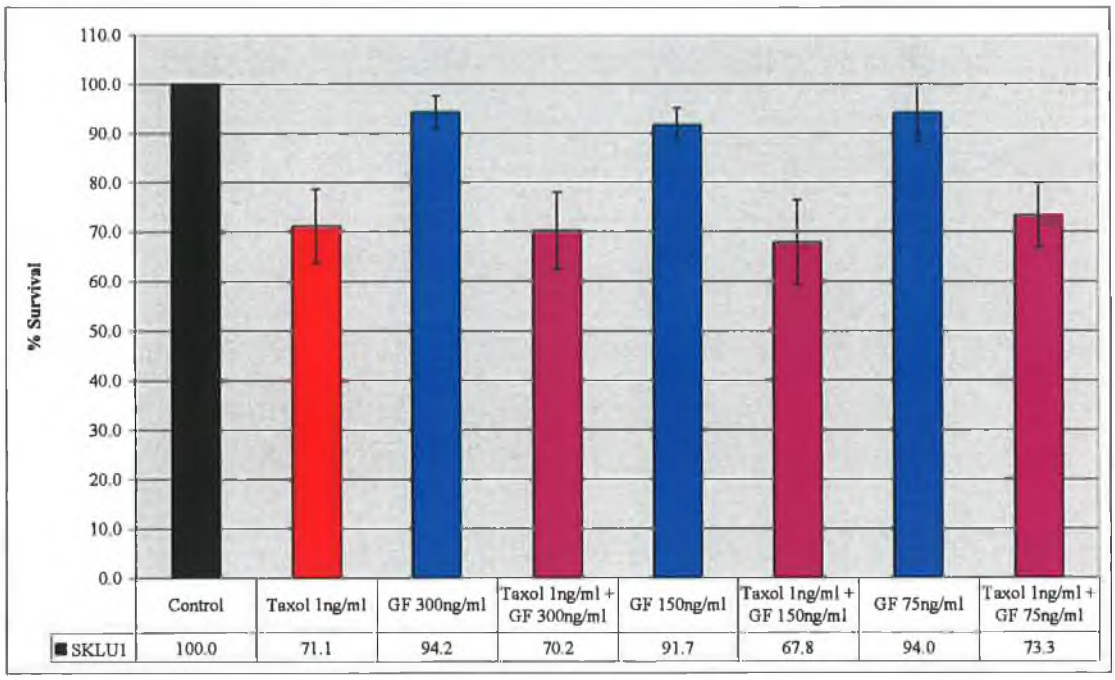

Figure 3.2.37 Taxol and GF120918 combination in SKLU1

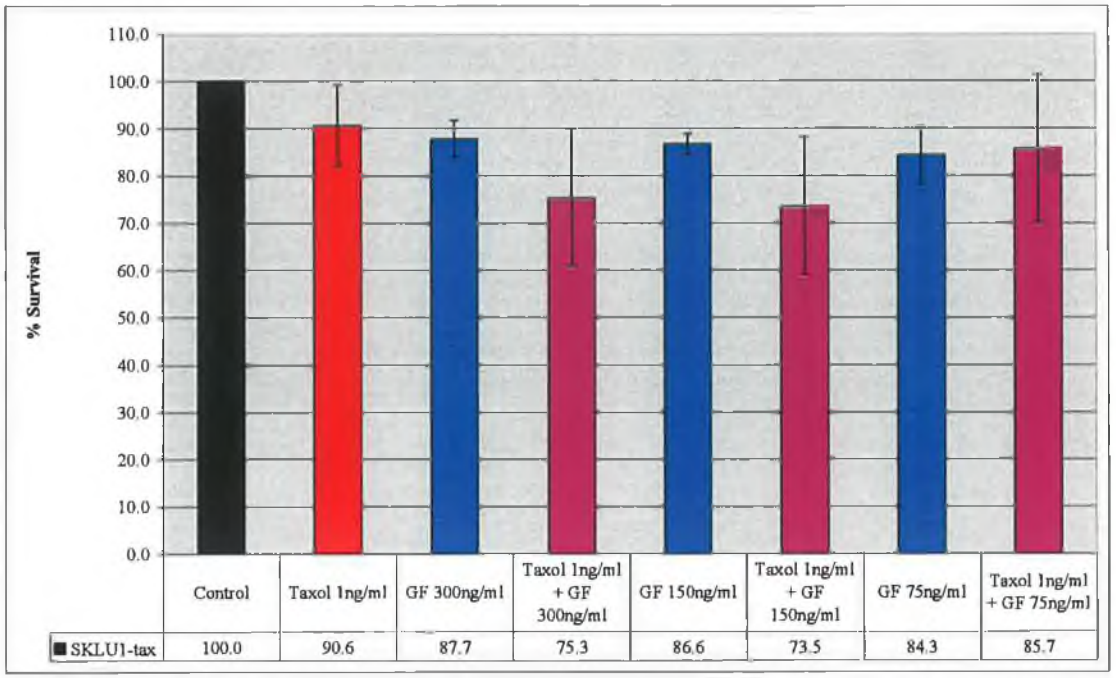

Figure 3.2.38 Taxol and GF120918 combination in SKLU1-tax

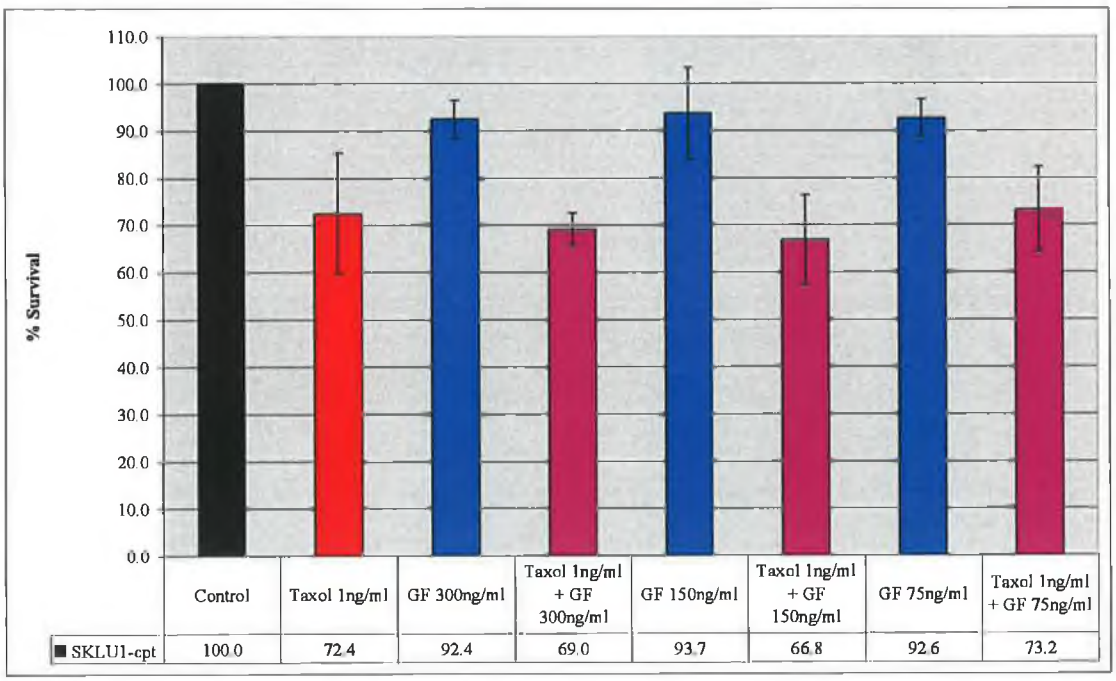

Figure 3.2.39 Taxol and GF120918 combination in SKLU1-cpt

3.2.6.8 Taxol and GF120918 in H460

The effect of the combination of taxol with the P-gp inhibitor GF120918 in the cell lines H460, H460-tax and H460-cpt (Figures 3.2.40, 3.2.41 and 3.2.42) was investigated. Combination of taxol and GF120918 in H460 cells appeared to result in an additive effect, with some possible synergy in the carboplatin-resistant cell line, which is unusual. The taxol-resistant variant behaves similarly to the parent cell line.

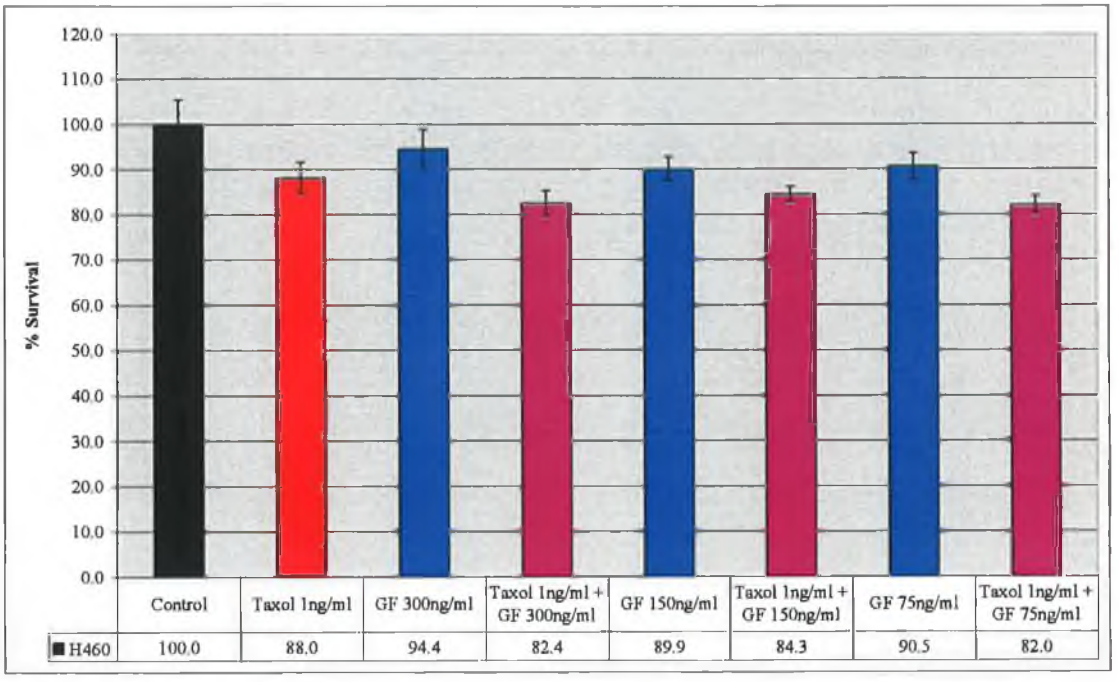

Figure 3.2.40 Taxol and GF120918 combination in H460

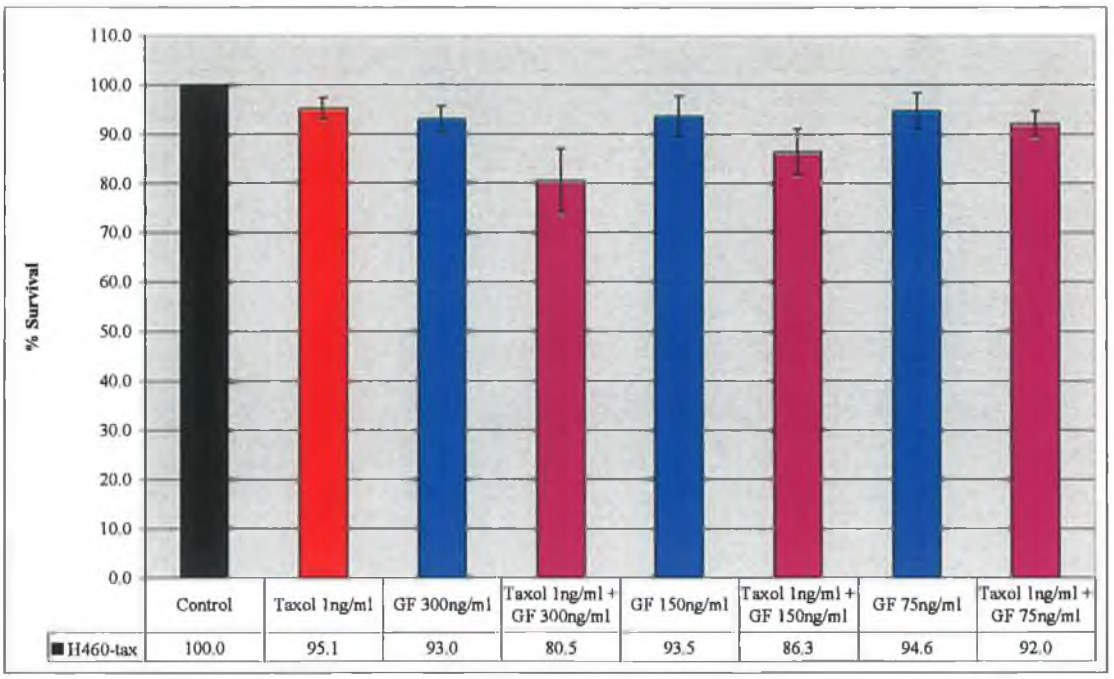

Figure 3.2.41 Taxol and GF120918 combination in H460-tax

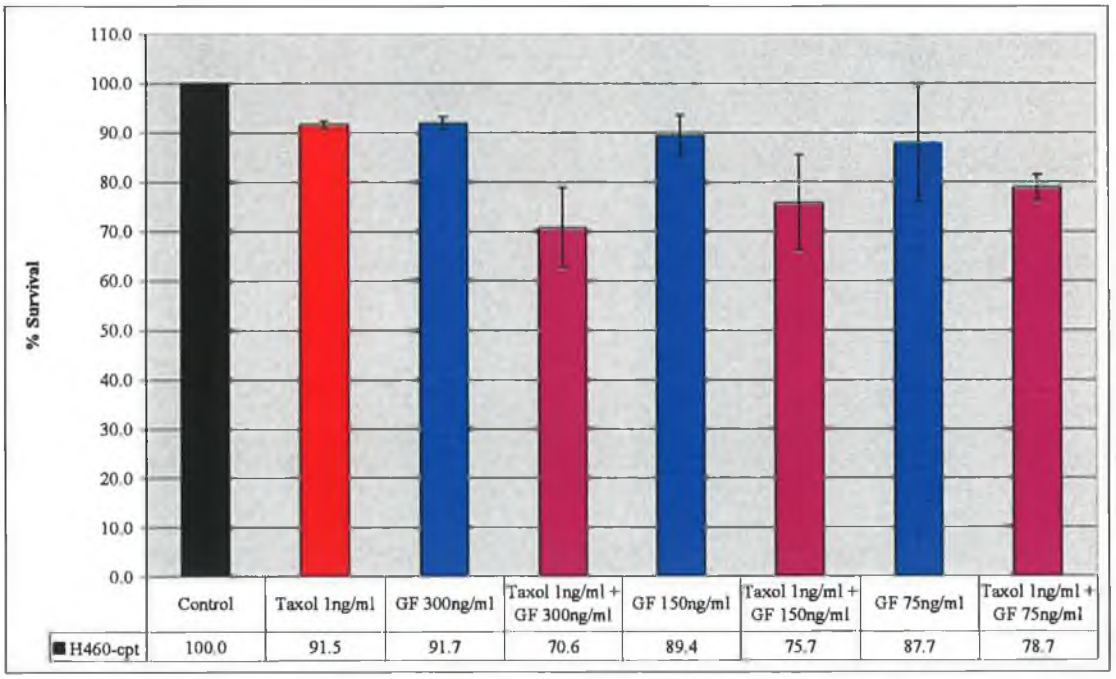

Figure 3.2.42 Taxol and GF120918 combination in H460-cpt

3.3 Microarray analysis of Taxol selections

3.3.1 RNA Quality

RNA integrity was examined using the Agilent Bioanalyser at two points in the microarray experiments (Section 2.11.2). Firstly the purity of isolated RNA was determined prior to sample processing. An example of this bioanalyser trace can be seen in Figure 3.3.1 (a). Intact 28S and 18S ribosomal RNA bands, which indicate good quality RNA, were observed in all samples. Secondly, the yield and size distribution of transcripts of biotin-labelled cRNA were analysed. An example of this bioanalyser trace can be seen in Figure 3.3.1 (b).

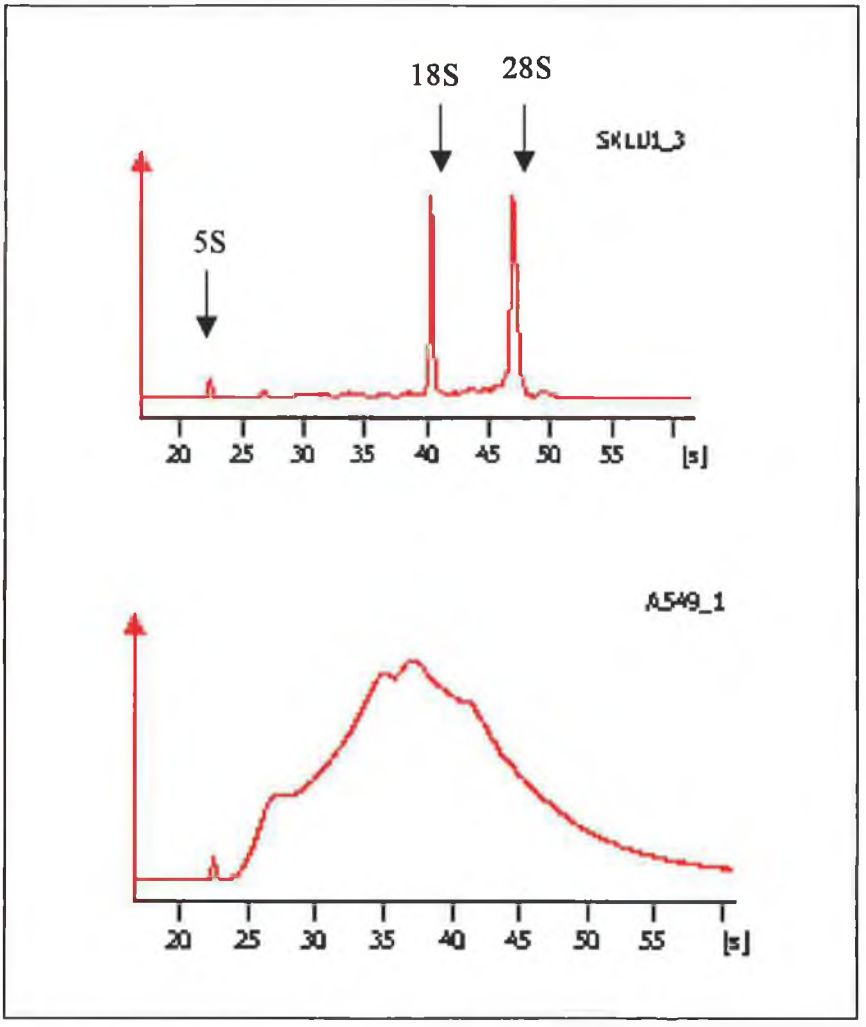

Figure 3.3.1 Example of Bioanalyzer traces of (a) initial isolated RNA and (b) Biotin-labeled cRNA after IVT.

3.3.2 GeneChip Quality Control

A number of quality control measures are carried out on microarray experiments before gene expression analysis begins. These were generated by GCOS in a report file (*rpt). A chip information form was filled out for each chip summarising this information. The information from these forms for all of the microarray chips run in this experiment can be seen in Table 3.3.1.

3.3.2.1 Scale factor

Each array has varying image intensity, and this intensity, or brightness, is measured by the "scaling factor". In order to make an accurate comparison of multiple sets of array data the intensities of the arrays were brought to the same level. This process was performed by GCOS® (GeneChip Operating Software) using a mathematical technique known as 'scaling'. Scaling worked by calculating the overall intensity of an array and averaging every probe set on the array (with the exception of the top and bottom 2% of the probe set intensities). The average intensity of the array was then multiplied by the scaling factor to ensure that all of the intensities on the given array went up or down to a similar degree. Scaling allowed normalisation of several experiments to one target intensity. For the experiments to be comparable, there must be no more than 3 fold difference between the scaling factors for each chip. The lowest scaling factor in this group of chips is 0.688 and the highest is 1.132, which is a fold difference of 1.6.

3.3.2.2 Noise

"Noise" measured the pixel-to-pixel variation of probe cells on the array. It was caused by small variations in the digital signal observed by the scanner as it sampled the array surface. As each scanner has a unique electrical noise associated with its operation, noise values among scanners vary. Therefore arrays that were scanned on the same scanner were expected to have similar noise values. All of the noise values for this set of arrays were between 1.5 and 2.3.

3.3.2.3 Background

Affymetrix have found that typical background values range from 20 to 100 and that arrays being compared should have similar background. The background values ranged from 47 to 66 for this set of arrays, which is acceptable. High background is usually caused by ethanol carryover during sample processing.

3.3.2.4 Present call

The percentage of genes present relates to the number of probe sets present relative to the total number of probe sets on the array. Replicate samples should have similar percentage present and normally vary between 40-60% for cell line samples. All of the replicates were within 5% of each other, ranging from 42.3-45.9%.

3.3.2.5 3':5' ratio

All of the arrays used actin and GAPDH to assess RNA sample and assay quality by having probes specific for the 3', middle and 5'end of these genes. The ratio of signal intensity from 3' probes to 5'probes was a measure of the number of cDNA synthesis reactions that went to completion. A ratio of 1 indicated full length transcript and was considered ideal. A cut-off value of 3 was applied, values above 3 indicated that some of the sensitivity of the assay had been lost. The range of 3':5' ratios in these experiments was 0.93-1.14.

3.3.2.6 Hybridisation controls

Spiked cRNAs were used as hybridization controls. BioB, bioC and bioD represent genes in the biotin synthesis family of *E.coli*, and Cre is the recombinase gene from the P1 bacteriophage. They were spiked in increasing concentrations and the average difference values were expected to be present in increasing amounts, B being the least and Cre the most. Chips passed QC if the BioB control was deemed "present" by GCOS.

3.3.2.7 Visual examination

After scanning the array chips were inspected for the presence of image artefacts. These include spots or regions on the chip with unusually high or low intensity, scratches or overall background. All of the chips used passed visual inspection.

3.3.2.8 Quality control by hierarchical clustering

Another quality control measure taken after the chip is satisfactory is hierarchical clustering. This clusters the samples based on their gene expression, and places the most similar samples in groups together. The hierarchical cluster generated by dChip for this experiment can be seen in Figure 3.3.2. The triplicate samples all cluster together, as expected. After this, the cell lines cluster together, with the parent cell lines being most similar to their taxol-resistant variant. The cluster also shows A549 and H460 to be the most similar of the cell lines, with H1299 being the most different from the group of cell lines. These are represented by a tree where the length of the branches reflect the degree of similarity between the objects

Table 3.3.1 Quality control on chips from taxol experiment

Sample name	Scaling factor	Noise	Background	% Present	3'/5' Ratio GAPDH
H1299_1	0.867	1.8	52.13	45.9	1
H1299_2	0.729	2.26	66.41	43	0.95
H1299_3	0.847	1.63	49.2	45.1	1.14
H1299_Tax 1	0.943	1.85	55.74	44.1	0.99
H1299_Tax 2	0.798	1.74	51.75	45.3	0.97
H1299_Tax 3	0.878	1.62	48.21	44.8	0.96
A549_1	1.132	1.61	48.23	43	1.11
A549_2	1.071	1.74	52.29	42.3	1.08
A549_3	0.814	1.71	50.21	45.1	1.12
A549_Tax 1	0.822	1.83	52.76	44.7	0.96
A549_Tax 2	0.985	1.76	51.78	43.1	1
A549_Tax 3	0.86	1.83	54.26	43.2	0.97
H460_1	0.858	1.66	48.68	43.3	0.93
H460_2	0.872	1.58	47.13	44.2	0.99
H460_3	1.039	1.59	48.12	42.7	1.06
H460_Tax 1	0.712	1.78	52.25	43.9	0.93
H460_Tax 2	0.8	1.79	52.17	45.4	0.94
H460_Tax 3	0.782	1.88	55.95	42.4	0.97
SKLU1_1	0.874	1.56	47.35	44.1	0.92
SKLU1_2	0.688	1.9	57.2	44.3	0.89
SKLU1_3	0.702	1.96	60.01	45.1	0.87
SKLU1_Tax 1	0.721	1.98	60.31	46.7	0.97
SKLU1_Tax 2	0.897	1.68	51.76	46.5	0.95
SKLU1_Tax 3	0.849	1.65	51.58	47	0.92

Figure 3.3.2 Hierarchical Cluster of parent and taxol samples

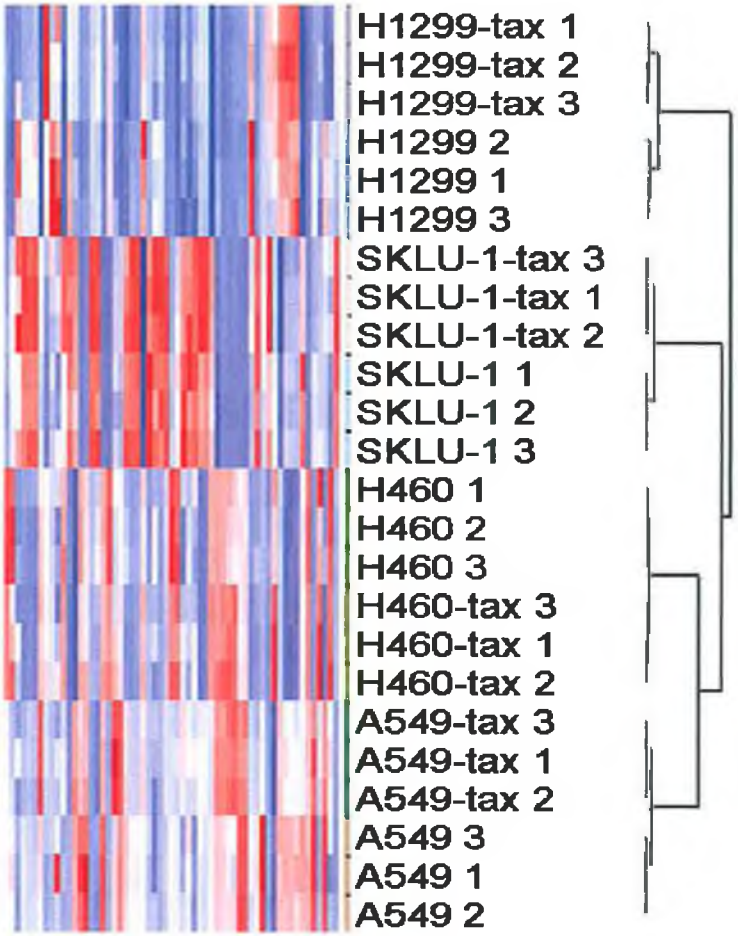
H1299-tax 1
H1299-tax 2
H1299-tax 3
H1299 2
H1299 1
H1299 3
SKLU-1-tax 3
SKLU-1-tax 1
SKLU-1-tax 2
SKLU-1 1
SKLU-1 2
SKLU-1 3
H460 1
H460 2
H460 3
H460-tax 3
H460-tax 1
H460-tax 2
A549-tax 3
A549-tax 1
A549-tax 2
A549 3
A549 1
A549 2

3.3.3 Genelists

Since the samples clustered as anticipated, gene expression analysis continued. DChip software was used in the original generation of genelists. Using dChip, each parent triplicate was compared to the triplicate of its taxol-resistant variant. The parameters used were a fold change of 1.2, a difference of intensity of 100 and a p value of ≤ 0.05. The numbers of genes changed in the taxol-resistant cell lines compared to the parent are shown in Table 3.3.2. The H460 cell line result stands out since only 829 genes were differentially regulated compared to nearly 3000 genes in all the other cell lines.

Table 3.3.2 Number of genes differentially expressed in parent vs taxol genelists

Genelist	No. of genes
A549 – parent vs taxol	2779
H1299 – parent vs taxol	3329
H460 – parent vs taxol	829
SKLU1 – parent vs taxol	2970

The next step in the analysis was comparison of these genelists. This was carried out using Microsoft Access. When all four gene lists were compared, nineteen genes were shown to be common (Table 3.3.3). Two genes from this list were upregulated in all four cell lines. These genes are ATP-binding cassette, sub-family B (MDR/TAP), member 1 also known as Mdr1 and phosphoglucomutase-2. These genes are highlighted in Table 3.3.3. Mdr1 is highly upregulated (from 2 – 9 fold), while phosphoglucomutase-2 is 1.2 fold upregulated in all the cell lines. No genes were downregulated in all four cell lines.

Table 3.3.3 List of genes significantly up- or down-regulated in all of the taxol selections compared to parent cell lines

Gene	A549	H1299	H460	SKLU1
CD59 antigen p18-20	-1.43	-1.69	-1.33	1.26
interleukin 1 receptor, type I	-1.34	3.12	-2.1	1.72
insulin-like growth factor binding protein 6	-1.83	-3.59	-1.45	1.55
5'-nucleotidase, ecto (CD73)	-2.87	-1.37	-2.89	1.21
B-cell CLL/lymphoma 3	1.43	-2.18	-1.75	2.55
tumor necrosis factor receptor superfamily, member 1A	-1.38	-1.38	-1.29	1.26
Paraneoplastic antigen MA2	-1.48	2.65	1.69	-6.43
ATP-binding cassette, sub-family B (MDR/TAP), member 1	**9.07**	**2.7**	**6.62**	**8.7**
phosphoribosylglycinamide formyltransferase	1.3	1.59	1.3	-1.48
vascular endothelial growth factor	1.39	-1.58	-1.56	2.82
A kinase (PRKA) anchor protein (gravin) 12	1.8	-1.98	2.28	2.53
Chromosome 14 open reading frame 78	-1.3	-2.71	-1.67	1.34
collagen, type VI, alpha 1	-1.89	-1.7	-1.86	1.56
G protein-coupled receptor 48	-1.56	2.56	-1.34	-1.54
FXYD domain containing ion transport regulator 5	-1.82	-2.9	-1.57	2.05
tissue inhibitor of metalloproteinase 2	-4.18	-1.44	-1.32	1.61
mitogen-inducible gene 6	1.44	-1.64	-1.72	-1.5
phosphoglucomutase 2	**1.24**	**1.2**	**1.21**	**1.27**
tissue inhibitor of metalloproteinase 2	-3.64	-1.46	-1.37	1.46

Genelists were then generated that represented genes up- or down-regulated in three of the four cell lines. The number of genes in each of these genelists is shown in Table 3.3.4.

Table 3.3.4 Number of genes differentially regulated in three of four cell lines

Genelist	No. genes
A549 + H1299 + H460	69
A549 + H1299 + SKLU1	162
A549 + H460 + SKLU1	48
H1299 + H460 + SKLU1	60

These genelists were compared and this resulted in two genelists, one of upregulated genes and one of down regulated genes. Table 3.3.5 shows the upregulated genes. Thirty-two genes were upregulated significantly in three of the four taxol-resistant cell lines. Table 3.3.6 shows the downregulated genes. Forty-two genes were significantly downregulated in three of the four taxol-resistant cell lines.

Table 3.3.5 List of genes significantly upregulated in three of four taxol selected cell lines compared to parent cells

Gene	A549	H1299	H460	SKLU1
A kinase (PRKA) anchor protein (gravin) 12	1.8		2.28	2.53
phosphoglucomutase 2	1.24	1.2	1.21	1.27
hypothetical protein DKFZp762C1112	1.36		1.23	1.3
heat shock 70kDa protein 9B (mortalin-2)	1.22	1.26	1.23	
caldesmon 1	1.46	2.03	1.69	
ATP-binding cassette, sub-family E (OABP), member 1	1.22	1.26	1.38	
crystallin, zeta (quinone reductase)	1.59	1.49	1.25	
ATP-binding cassette, sub-family F (GCN20), member 2	1.22	1.77	1.26	
inhibitor of DNA binding 3,	1.28	2.74	2.32	
ATP-binding cassette, sub-family B (MDR/TAP), member 1	9.07	2.7	6.62	8.7
phosphoribosylglycinamide formyltransferase,	1.3	1.59	1.3	
mitochondrial ribosomal protein L42	1.32	1.2	1.22	
TIA1 cytotoxic granule-associated RNA binding protein	1.41	1.58		1.38
LIM protein (similar to rat protein kinase C-binding enigma)	1.52	1.5		2.56
GULP, engulfment adaptor PTB domain containing 1	1.21	1.71		1.55
cytochrome b-5	1.3	1.37		1.53
Bernardinelli-Seip congenital lipodystrophy 2 (seipin)	1.25	1.81		1.42
tissue factor pathway inhibitor 2	1.93	1.44		8.01
LIM protein (similar to rat protein kinase C-binding enigma)	1.43	1.45		2.23
zinc finger protein 238	1.62	1.39		1.33
stromal cell protein	1.25	1.28		1.26
hypothetical protein FLJ10656	1.5	1.65		1.45
similar to signal peptidase complex (18kD)	1.26	1.47		1.59
chromosome 20 open reading frame 30	1.23	1.53		1.35
hypothetical protein FLJ20421	1.44	1.35		1.65
chromobox homolog 4 (Pc class homolog, Drosophila)	1.21	1.41		1.41
CDNA FLJ33420 fis, clone BRACE2020028	1.25	1.67		1.85
RAB27B, member RAS oncogene family	1.54	2.17		2.15
influenza virus NS1A binding protein		1.37	1.25	1.33
Transcribed locus, weakly similar to NP_079012.2		1.45	1.37	3.51

Table 3.3.6 List of genes significantly downregulated in three of four taxol selected cell lines compared to parent cells

Gene	A549	H1299	H460	SKLU1
serine (or cysteine) proteinase inhibitor,	-1.24		-1.36	-1.49
G protein-coupled receptor 56	-1.55		-2.95	-1.82
testis derived transcript (3 LIM domains)	-1.26		-1.32	-2.45
G protein-coupled receptor 48	-1.56		-1.34	-1.54
plasminogen activator	-1.39	-3.81	-1.56	
zinc finger protein 36, C3H type-like 1	-1.56	-1.67	-1.42	
CD59 antigen p18-20	-1.43	-1.69	-1.33	
epithelial membrane protein 1	-6.22	-2.37	-1.86	
fascin homolog 1	-1.29	-2.56	-1.29	
S100 calcium binding protein A13	-1.27	-1.56	-1.38	
solute carrier family 16 member 3	-19.5	-1.66	-1.52	
insulin-like growth factor binding protein 6	-1.83	-3.59	-1.45	
5'-nucleotidase, ecto (CD73)	-2.87	-1.37	-2.89	
potassium intermediate subfamily N, member 4	-1.68	-4.28	-1.87	
cysteine-rich protein 1 (intestinal)	-2.61	-30.87	-3.45	
carbonyl reductase 3	-1.63	-1.68	-1.54	
tumor necrosis factor receptor superfamily, member 1A	-1.38	-1.38	-1.29	
Microtubule-associated protein 1B	-1.49	-1.58	-1.37	
Chromosome 14 orf 78	-1.3	-2.71	-1.67	
collagen, type VI, alpha 1	-1.89	-1.7	-1.86	
solute carrier family 16 member 3	-31.72	-1.73	-1.43	
EF hand domain containing 2	-1.6	-2.21	-1.45	
FXYD domain containing ion transport regulator 5	-1.82	-2.9	-1.57	
tissue inhibitor of metalloproteinase 2	-4.18	-1.44	-1.32	
SH3-domain kinase binding protein 1	-1.82	-1.37	-1.25	
solute carrier family 2 (facilitated glucose transporter), member 1	-1.51	-1.35		-1.8
myristoylated alanine-rich protein kinase C substrate	-1.3	-1.86		-1.45
laminin, gamma 2	-3.55	-23.11		-1.66
plasminogen activator, urokinase	-1.54	-2.79		-1.73
follistatin-like 1	-1.29	-7.44		-1.49
PTEN induced putative kinase 1	-1.89	-1.7		-1.34
connective tissue growth factor	-1.36	-2.37		-1.43
histone 1, H2bk	-1.31	-1.23		-1.65
frizzled homolog 2 (Drosophila)	-1.63	-1.73		-1.43
ribonuclease P 40kDa subunit	-1.39	-1.42		-1.47
kinesin 2 60/70kDa	-1.45	-1.78		-1.35
PTEN-like phosphatase	-1.25	-1.6		-1.64
tissue factor pathway inhibitor		-108.5	-1.36	-1.98
chromosome 6 open reading frame 145		-1.56	-1.86	-1.36
Tissue factor pathway inhibitor		-122.41	-1.22	-1.48
mitogen-inducible gene 6		-1.64	-1.72	-1.5

3.3.4 Upregulated genes in all four taxol selections

As mentioned above (Section 3.3.2), only two genes were upregulated in all four taxol-resistant cell lines. Figure 3.3.2 shows the relationship between Mdr1 expression and the level of taxol resistance displayed by the cells. There is no obvious trend, with the least resistant cell line, A549, having the largest fold increase in Mdr1 expression.

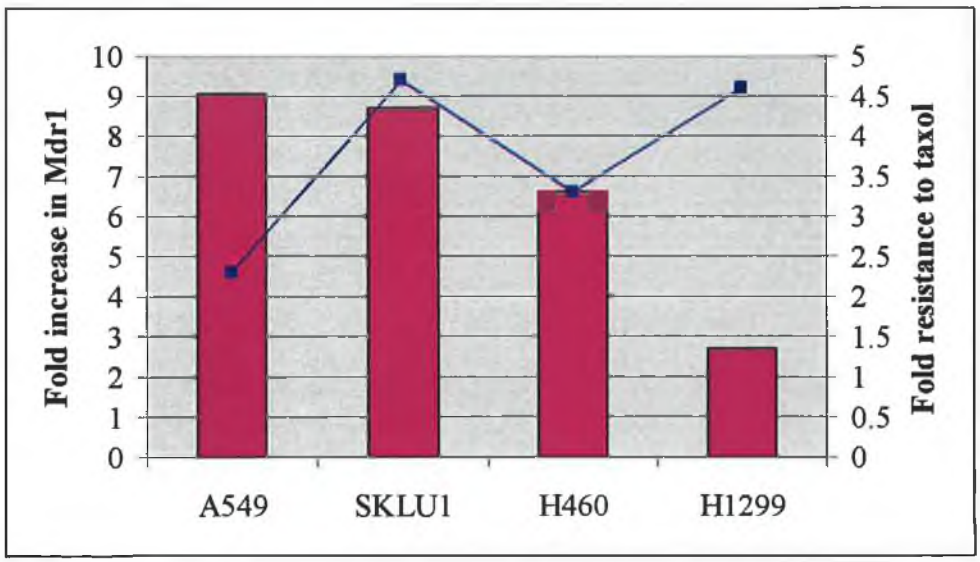

Figure 3.3.2 Relationship between taxol resistance and Mdr1 expression

3.3.5 Choice of genes for further analysis

Analysis of the genelists in Microsoft Access led to a genelist of interesting genes from this study of seventy-four genes (Thirty-two upregulated and forty-to downregulated, Section 3.3.4). This had to be narrowed down to a manageable number of genes to be analysed further. This was achieved by two methods. Firstly, any unannotated or poorly annotated genes were removed. Secondly the list was shortened by magnitude of fold change. The resulting genelist of "target genes" can be seen in Table 3.3.7.

Table 3.3.7 Fold changes in target genes chosen for further study

Gene name	A549	H1299	H460	SKLU1
Epithelial membrane protein 1	-6.22	-2.37	-1.86	
Cysteine-rich protein 1	-2.61	-30.87	-3.45	
Follistatin-like 1	-1.29	-7.44		-1.49
Connective tissue growth factor	-1.36	-2.37		-1.43
Insulin-like growth factor binding protein 6	-1.83	-3.59	-1.45	
Crystallin, zeta	1.59	1.49	1.25	
ATP-binding cassette, sub-family B (MDR/TAP), member 1	9.07	2.7	6.62	8.7
Inhibitor of DNA binding 3	1.28	2.74	2.32	
GULP1	1.21	1.71		1.55
Stromal cell protein	1.25	1.28		1.26

3.3.6 Expression of target genes

In the following results are presented as average intensity ± standard deviation of the three replicates for each sample.

Table 3.3.8 shows the intensity of expression for each of the target genes in A549 and A549-taxol. The gene with the highest fold change in this system is ABCB1 (Figure 3.3.3). However this gene is expressed at very low levels in both cell lines relative to the expression of some of the other genes. For example, CRYZ has less than a 2-fold increase in expression, but the difference in intensity in this gene from A549 to A549-taxol is over 1000.

In Table 3.3.9 the intensity of expression for each of the target genes in H1299 and H1299-taxol is shown. CRIP1 displays the highest fold change in these cell lines, with a 30-fold decrease in H1299-taxol compared to H1299 (Figure 3.3.4). It is interesting to note that ABCB1 (P-gp) is expressed at a higher intensity in H1299 parent cells than in any of the other parent cell lines, although it remains at a relatively low intensity.

The intensity of expression for each of the target genes in H460 and H460-taxol is shown in Table 3.3.10. Only six of the ten target genes were differentially expressed in this system. ABCB1 shows the greatest fold change in H460-tax compared to H460 (Figure 3.3.5). H460-taxol cells appear to have the largest expression of ABCB1 of all the cell lines tested.

ABCB1 is again the gene with the greatest fold change in SKLU1-taxol cells compared to SKLU1 with an almost 9-fold change in intensity (Figure 3.3.6). Table 3.3.11 shows the intensity of expression for each of the target genes in these cell lines. Only five of the ten target genes were differentially expressed in these cell lines.

Table 3.3.8 Expression of target genes in A549 and A549-tax

Gene	*A549 expression*	*A549-tax expression*
EMP1	257 ± 22	41 ± 14
CRIP1	2458 ± 55	942 ± 68
FSTL1	1339 ± 46	1035 ± 73
CTGF	556 ± 33	409 ± 38
IGFBP 6	1762 ± 65	961 ± 41
CRYZ	1731 ± 54	2755 ± 89
ABCB1	14 ± 10	123 ± 12
ID3	2949 ± 55	3770 ± 176
GULP	777 ± 38	941 ± 28
SCP	665 ± 37	829 ± 28

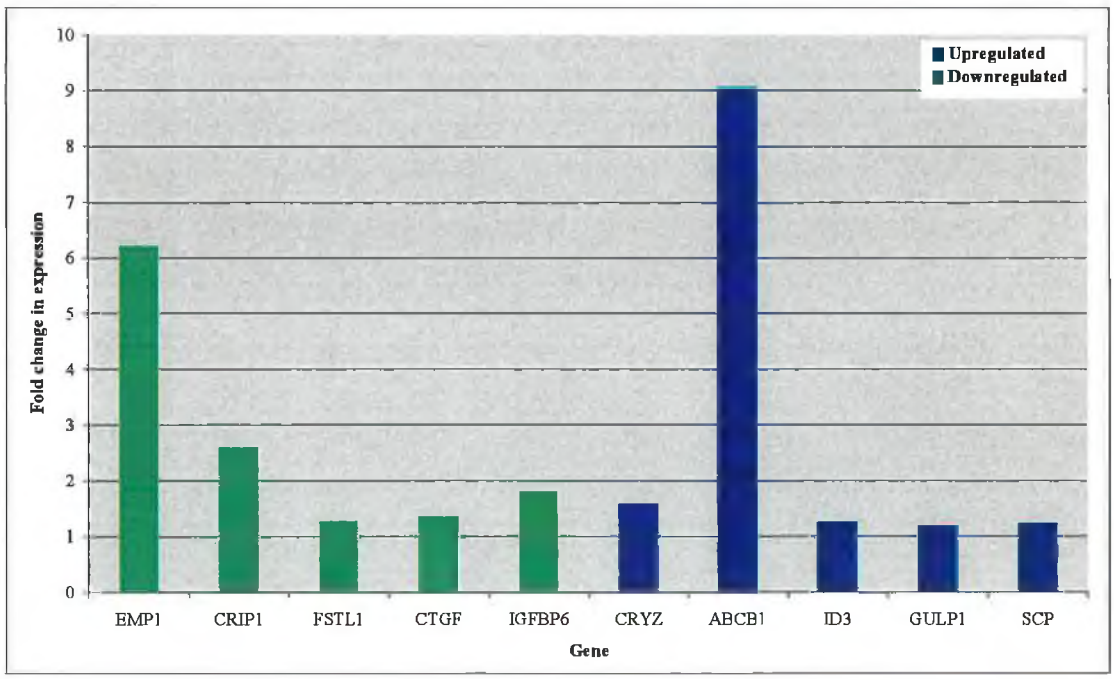

Figure 3.3.3 Fold change in expression of target genes in A549-taxol

Table 3.3.9 Expression of target genes in H1299 and H1299-tax

Gene	*H1299 expression*	*H1299-tax expression*
EMP1	2688 ± 131	1134 ± 80
CRIP1	361 ± 18	12 ± 17
FSTL1	335 ± 27	45 ± 19
CTGF	1546 ± 129	654 ± 25
IGFBP 6	169 ± 17	47 ± 8
CRYZ	806 ±39	1204 ± 44
ABCB1	62 ± 7	167 ± 12
ID3	684 ± 36	1878 ± 156
GULP	482 ± 60	825 ± 20
SCP	886 ± 62	1137 ± 22

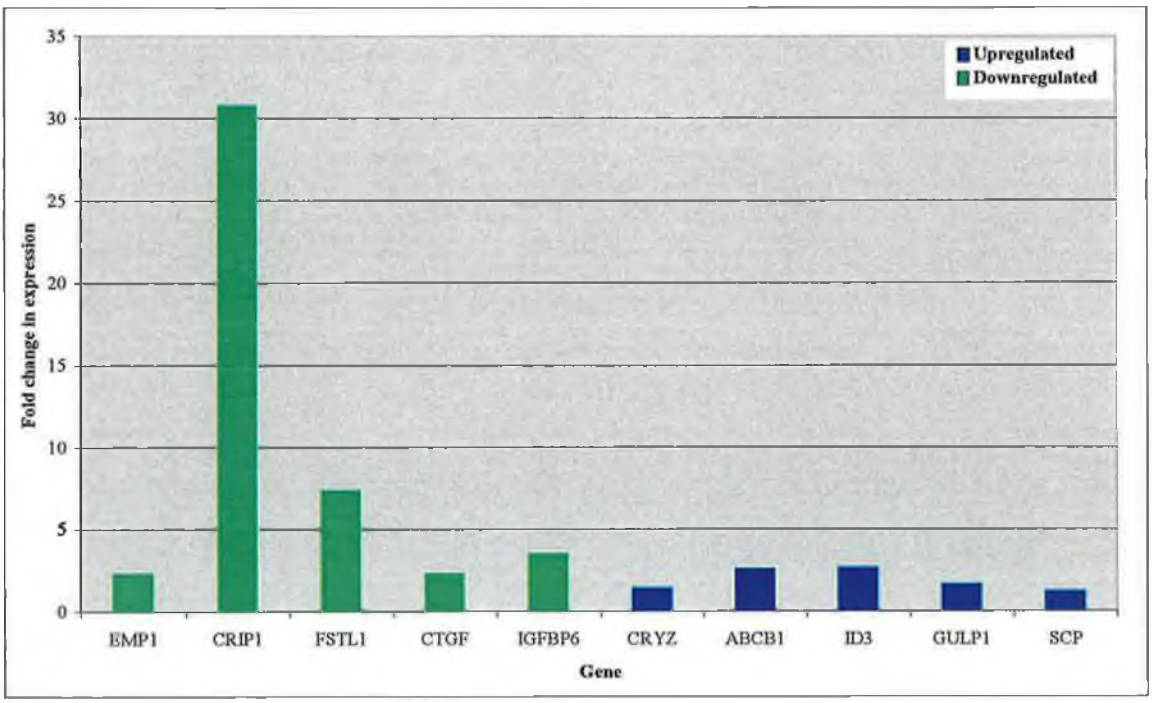

Figure 3.3.4 Fold change in expression of target genes in H1299-taxol

Table 3.3.10 Expression of target genes in H460 and H460-tax

Gene	*H460 expression*	*H460-tax expression*
EMP1	352 ± 26	190 ± 19
CRIP1	2393 ± 238	693 ± 58
IGFBP 6	407 ± 24	280 ± 11
CRYZ	431 ± 16	538 ± 19
ABCB1	46 ± 6	306 ± 13
ID3	556 ± 60	1290 ± 81

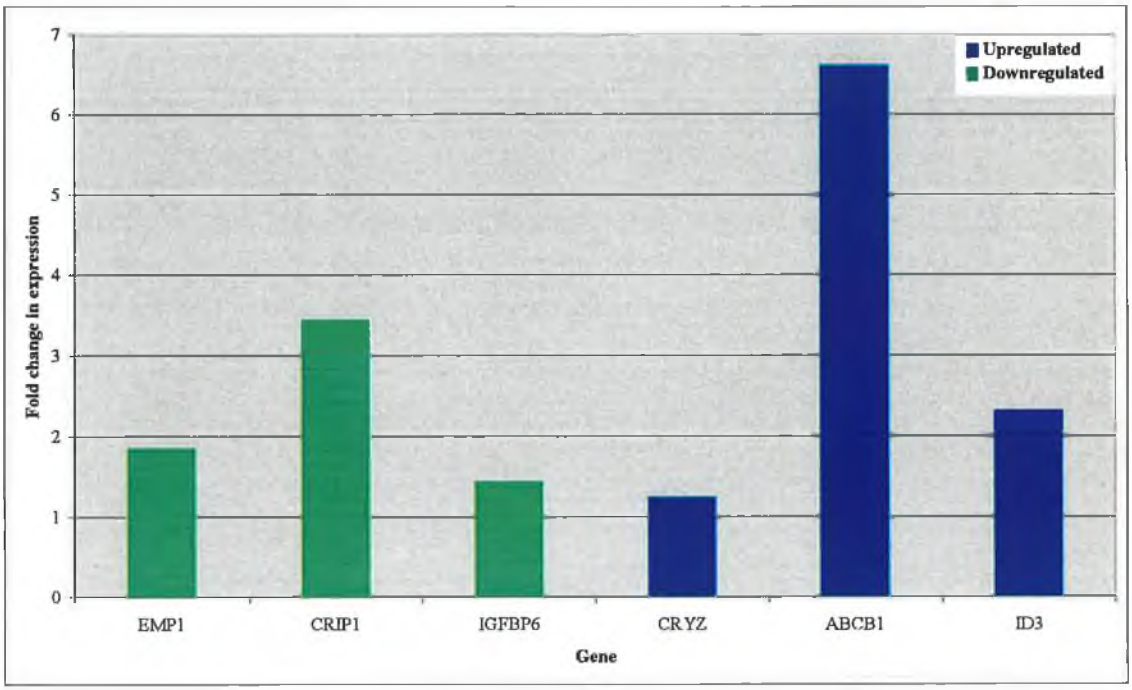

Figure 3.3.5 Fold change in expression of target genes in H460-taxol

Table 3.3.11 Expression of target genes in SKLU1 and SKLU1-tax

Gene	*SKLU1 expression*	*SKLU1-tax expression*
FSTL1	3373 ± 151	2270 ± 78
CTGF	1894 ± 130	1323 ± 51
ABCB1	15 ± 8	128 ± 8
GULP	311 ± 34	480 ± 23
SCP	497 ± 11	626 ± 17

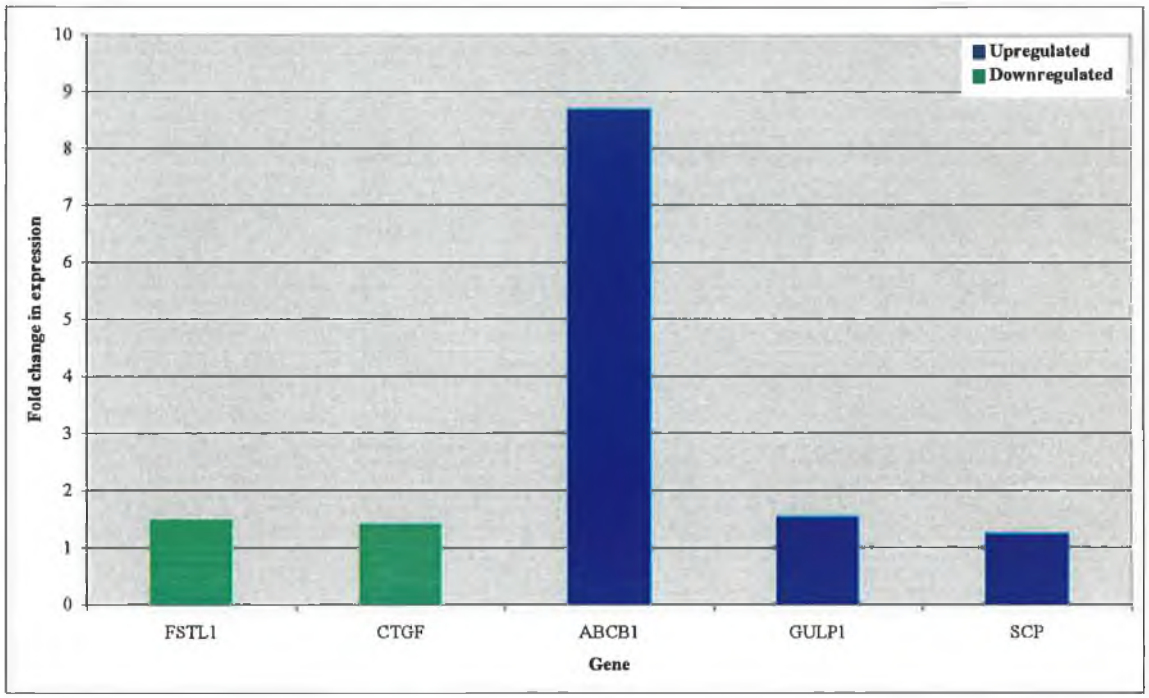

Figure 3.3.6 Fold change in expression of target genes in SKLU1-taxol

3.3.7 Pathway Analysis of target genes

Pathway analysis on the ten target genes was carried out using Pathway Assist. The genelist was imported to the programme and from this information common pathways were built. Genelists to be studied in Pathway Assist were imported in the form of *txt files. PathwayAssist is a product aimed at the visualisation and analysis of biological pathways, gene regulation networks and protein interaction maps. It comes with a comprehensive database that gives a snapshot of all information available in PubMed, with the focus on pathways and cell signalling networks. PathwayAssist worked by identifying relationships among genes, small molecules, cell objects and processes and built pathways based on these relationships. Figure 3.3.7 shows how the ten genes are linked through common pathways. The genes coloured blue are the upregulated target genes and the genes coloured green are the downregulated target genes. The pink genes are the specified links from pathway assist.

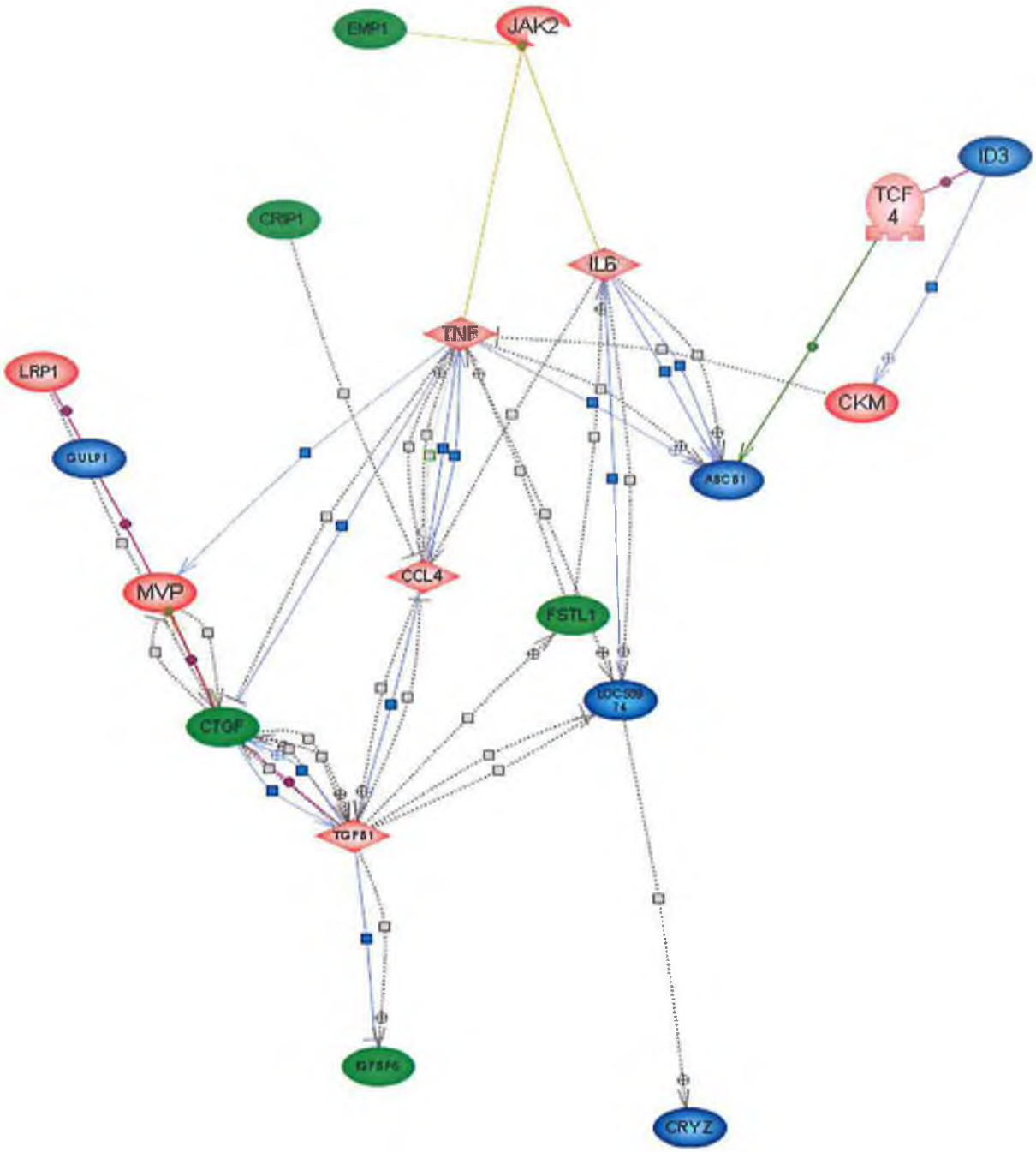

Figure 3.3.7 Common pathways of target genes

Table 3.3.12 Abbreviations from common pathway (Figure3.3.7)

Abbreviation	Gene name
ID3	Inhibitor of DNA-binding 3
ABCB1	ABC sub-family B member 1 (Mdr1)
Loc55974	Stromal cell protein (SCP)
CRYZ	Crystallin, zeta (quinone reductase)
GULP1	Engulfment adapter protein
EMP1	Epithelial membrane protein 1
CRIP1	Cystein rich intestinal protein 1
CTGF	Connective tissue growth factor
FSTL1	Follistatin-like 1
IGFBP6	Insulin-like growth factor receptor binding protein 6
JAK2	Janus kinase 2
TCF4	Transcription factor 4
IL6	Interleukin 6
TNF	Tumour necrosis factor
CCL4	Chemokine ligand 4
MVP	Major vault protein
LRP1	Low density lipoprotein-related protein 1
TGFβ1	Transforming growth factor, beta 1
CKM	Creatine Kinase

3.4 RNA interference

Ten targets were chosen from microarray studies on taxol-selected cell lines. Five of these targets were found to be upregulated in association with taxol resistance and five to be downregulated in association with taxol resistance. The targets are shown below. Two pre-designed siRNAs from Ambion were tested for each target. The cell lines chosen for the study were A549 and H1299 and their taxol-resistant variants.

3.4.1 Details of targets

Upregulated targets:

- ABCB1 (p-glycoprotein)
- ID3 (Inhibitor of DNA binding 3)
- GULP1 (engulfment factor)
- SCP (Stromal cell protein)
- CRYZ (Quinone reductase)

It was expected that an increase in sensitivity to taxol would be observed in the **taxol resistant cell lines** after transfection with siRNAs to the above genes.

Downregulated targets:

- EMP1 (Epithelial membrane protein 1)
- CRIP1 (Cysteine-rich intestinal protein 1)
- FSTL1 (Follistatin-like 1)
- CTGF (Connective tissue growth factor)
- IGFBP6 (Insulin-like growth factor binding protein 6)

It was expected that an increase in resistance to taxol would be observed in the **parental cell lines** after transfection with siRNAs to the above genes, since they are expressed at a lower level in the taxol-resistant cells.

3.4.2 Effects of siRNA transfection on proliferation

In order to determine if transfection of a given siRNA had an effect on the sensitivity of a cell line to a chemotherapeutic agent, it was important to ensure that the transfection did not have an effect on the proliferation of the cells. Kinesin was included as a positive control. This gene plays an important role in cell division, so transfection of kinesin siRNA results in cell cycle arrest. Figures 3.4.1 and 3.4.2 show the effect of siRNA transfection of the targets in A549 and A549-tax cells respectively. Figures 3.4.3 and 3.4.4 show the effect of siRNA transfection of the targets in H1299 and H1299-tax cells respectively. Most of the siRNAs had little or no effect on the proliferation of the cell lines. However, a number of the siRNAs affected proliferation of the cell lines. In A549 and A549-tax, transfection of IGFBP6 siRNA (2) led to a considerable increase in proliferation. In H1299-tax, transfection of SCP siRNA (1) led to a considerable decrease in proliferation.

Transfection of siRNAs to specific genes was expected to transiently silence the target gene. Therefore, only modest phenotypic effects were expected with these experiments, since the protein would only be downregulated for a short period of time, and there would not be a total downregulation of protein.

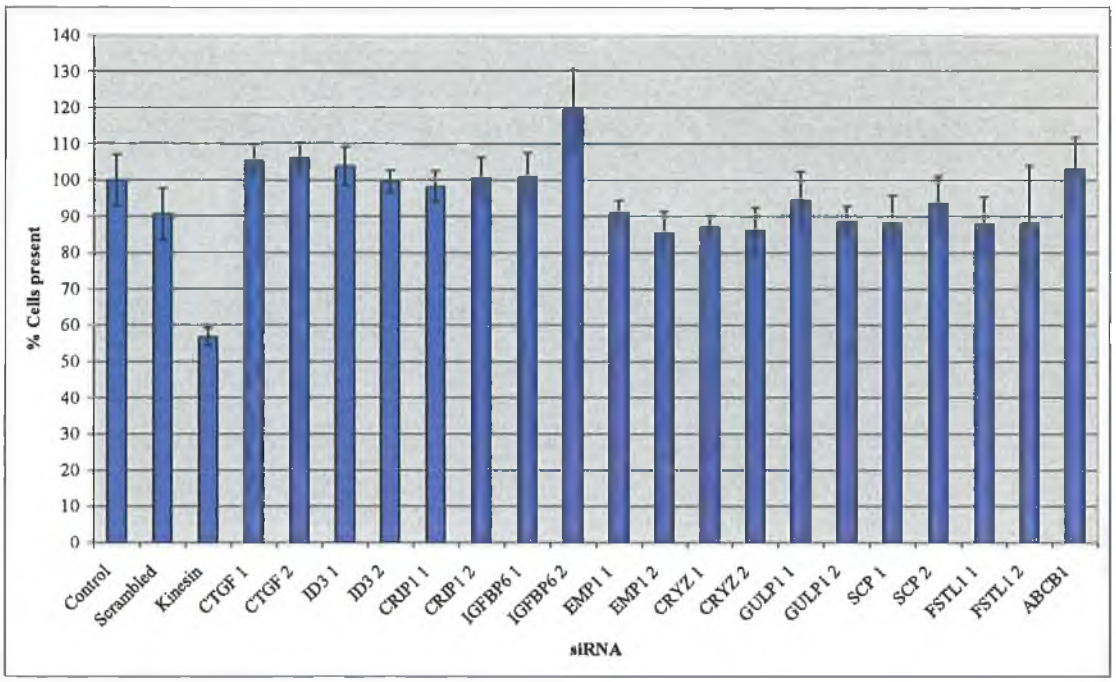

Figure 3.4.1 Effect of siRNA transfection on proliferation of A549 cells

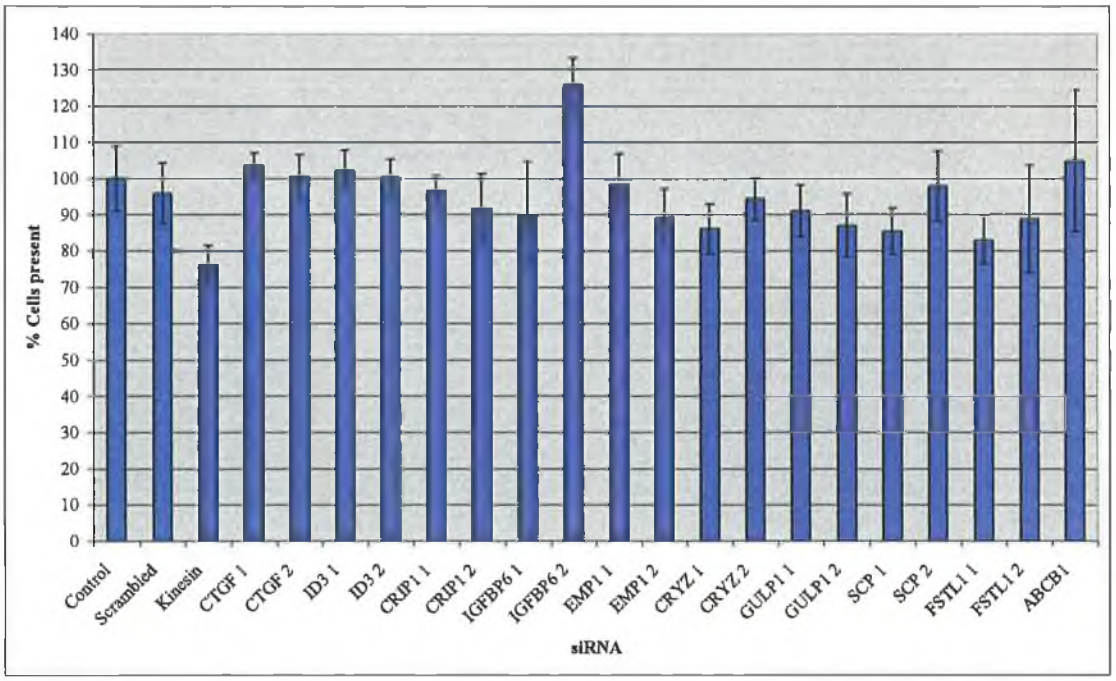

Figure 3.4.2 Effect of siRNA transfection on proliferation of A549-tax cells

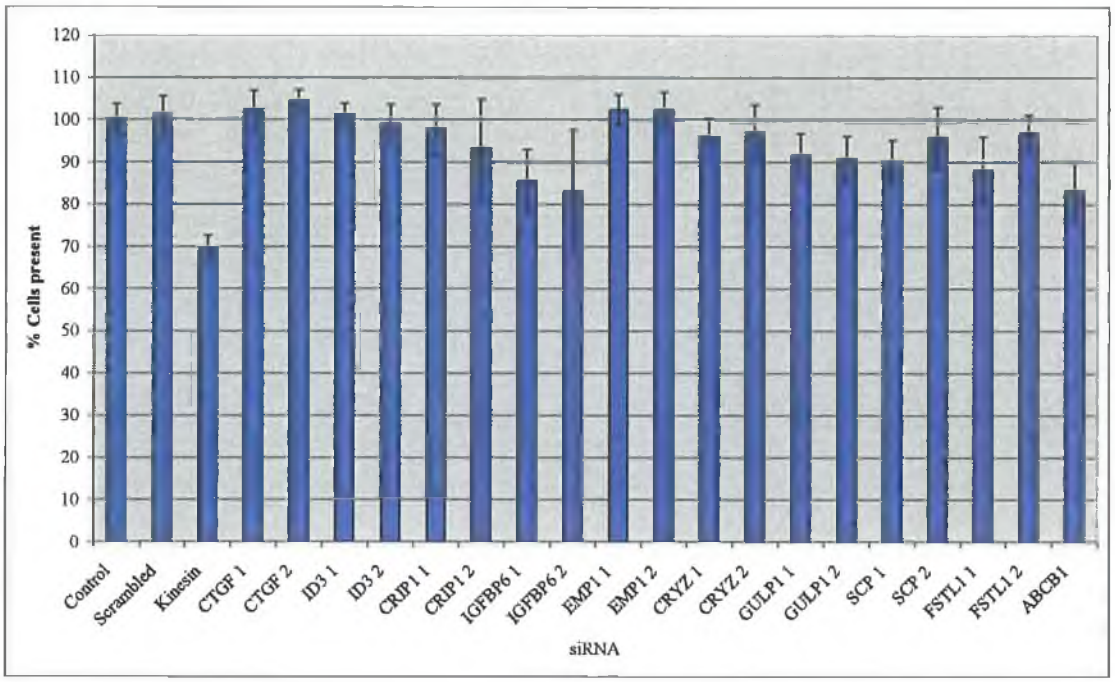

Figure 3.4.3 Effect of siRNA transfection on proliferation of H1299 cells

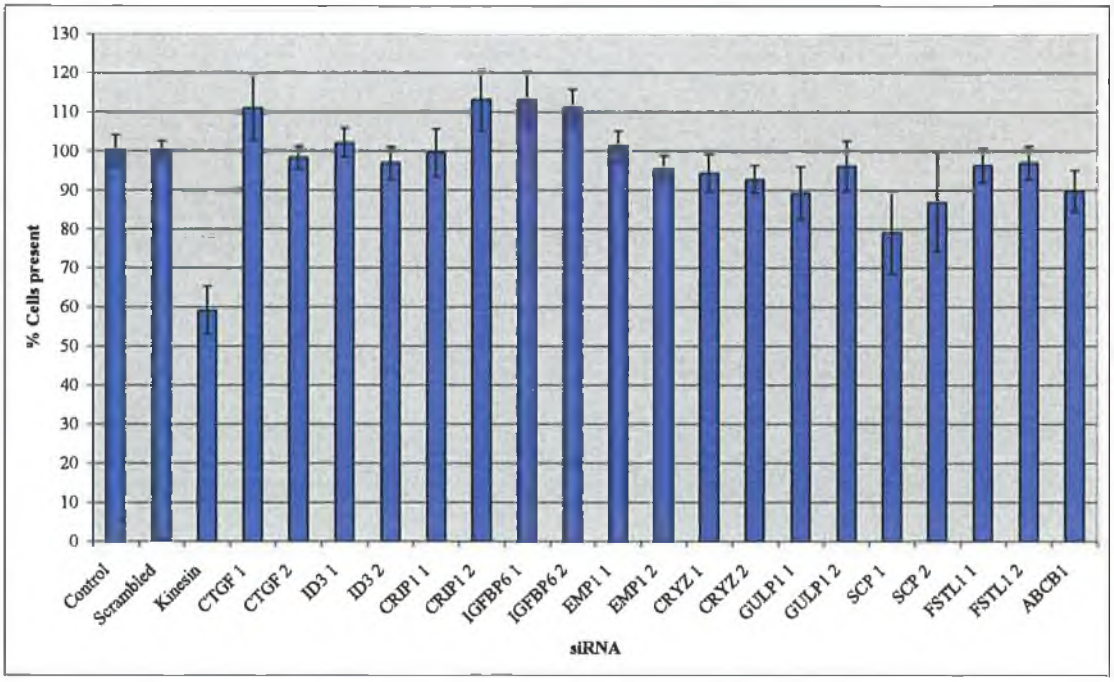

Figure 3.4.4 Effect of siRNA transfection on proliferation of H1299-tax cells

3.4.3 Effects of siRNA transfection on sensitivity to taxol

After determining the effect of transfection of the target genes siRNAs on proliferation, the role of these genes in determining sensitivity to taxol was investigated. Two siRNAs for each target gene were transfected into A549, A549-tax, H1299 and H1299-tax. The effect of the these siRNA transfections on taxol sensitivity was determined as described in Section 2.13.3. In each experiment, a control of either transfection reagent or a scrambled siRNA transfection was included to ensure that the effect was due to the gene being targeted. A summary of the results obtained can be seen in Table 3.4.1. More detailed results from each transfection follow in subsequent sections.

Table 3.4.1 Summary of results from transfection of target genes siRNA

Gene	A549	A549-tax	H1299	H1299-tax
ABCB1	-	+	+	+
ID3	+	-	+	-
CRYZ	-	-	-	+
GULP1	-	-	-	+
SCP	-	-	-	-
CTGF	-	-	-	-
CRIP1	+	+	-	-
IGFBP6	+	-	+	-
EMP1	+	+	-	-
FSTL1	+	+	-	-

+ Indicates that an effect was observed

- Indicates that no effect was observed

3.4.3.1 Effect of transfection of ABCB1 siRNA

ABCB1 is a gene whose protein product is P-gp, the multidrug resistance protein. Transfection of ABCB1 siRNA has no effect on the sensitivity to taxol in A549 cells (Figure 3.4.5). However there is a slight increase in sensitivity of taxol in transfected A549-tax cells (Figure 3.4.6). This increase is relatively small considering that microarray analysis of these cells shows a 9-fold increase in Mdr1 in the taxol-selected cells. Transfection of ABCB1 siRNA resulted in a slight increase in sensitivity to taxol in H1299 parent cells (Figure 3.4.7). The effect is much more significant in the taxol-selected cells (Figure 3.4.8), which were shown to have almost a 3-fold increase in Mdr1 by microarray analysis.

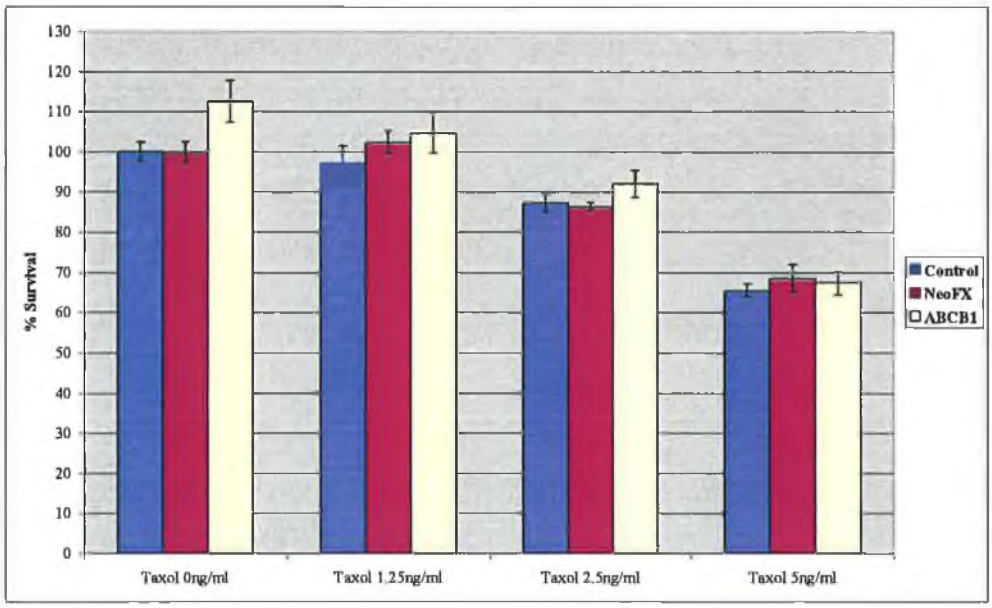

Figure 3.4.5 Effect of transfection of ABCB1 siRNA in A549 cells

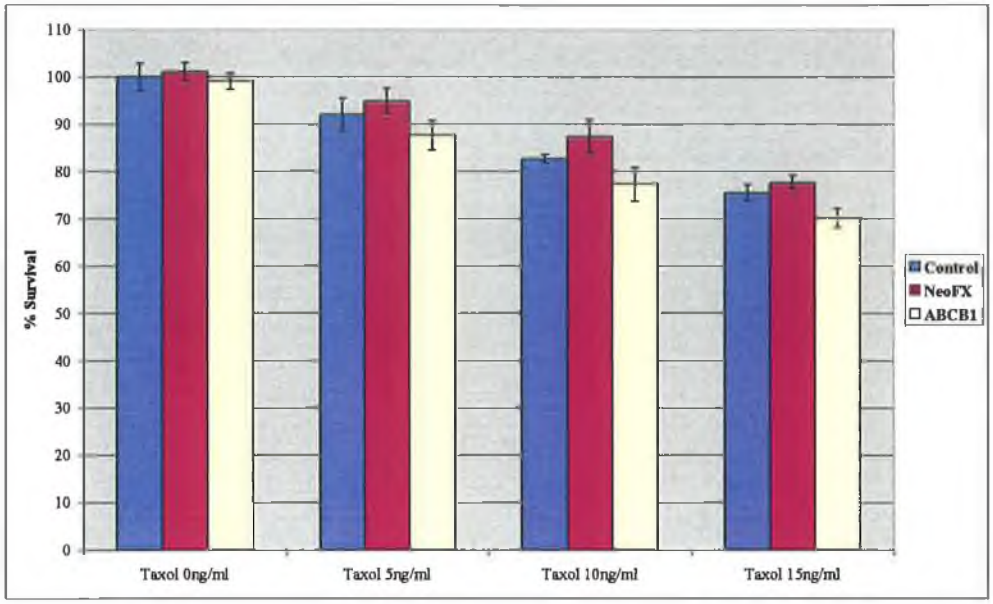

Figure 3.4.6 Effect of transfection of ABCB1 siRNA in A549-taxol cells

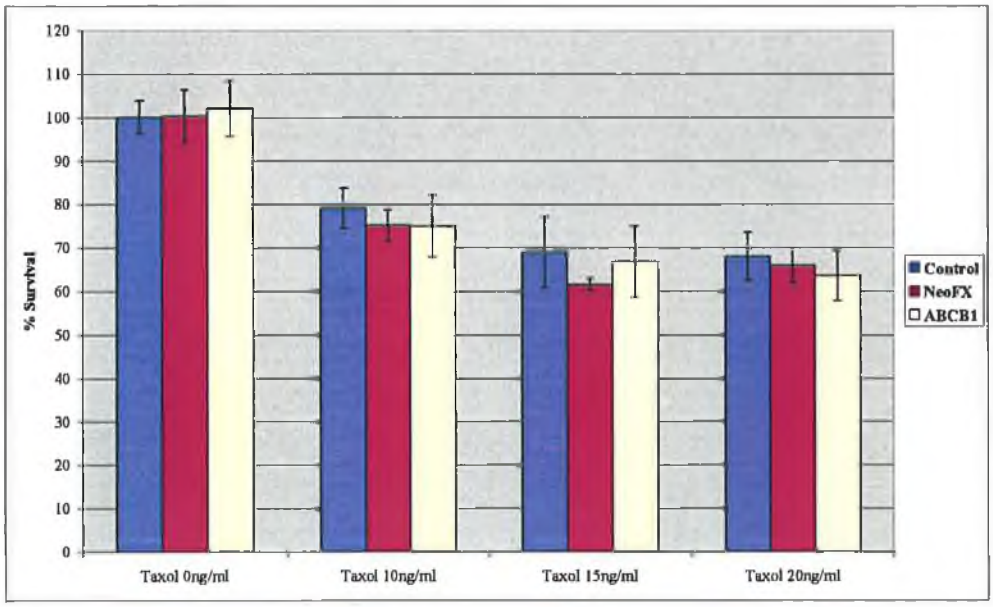

Figure 3.4.7 Effect of transfection of ABCB1 siRNA in H1299 cells

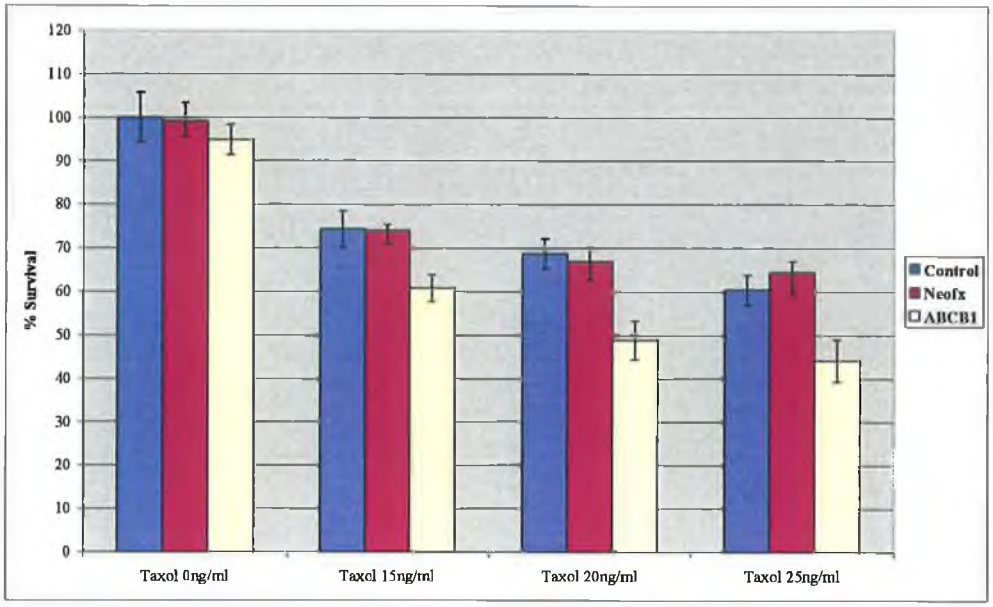

Figure 3.4.8 Effect of transfection of ABCB1 siRNA in H1299-taxol cells

3.4.3.2 Effect of transfection of ID3 siRNA

ID3 is Inhibitor of DNA-binding 3. ID3 was upregulated approximately 1.3-fold in taxol resistant cells by the microarray analysis. In A549 there is an increase in sensitivity to taxol after transfection with ID3 siRNA (Figures 3.4.9). There might also be slight sensitisation in A549-tax (Figure 3.4.10). ID3 was approximately 3-fold upregulated in H1299-tax compared to the parent cells by the microarray analysis. Transfection of ID3 siRNA led to a slight increase in sensitivity to taxol in the parent cells (Figure 3.4.11), but appeared not to have an effect in H1299-tax (Figure 3.4.12).

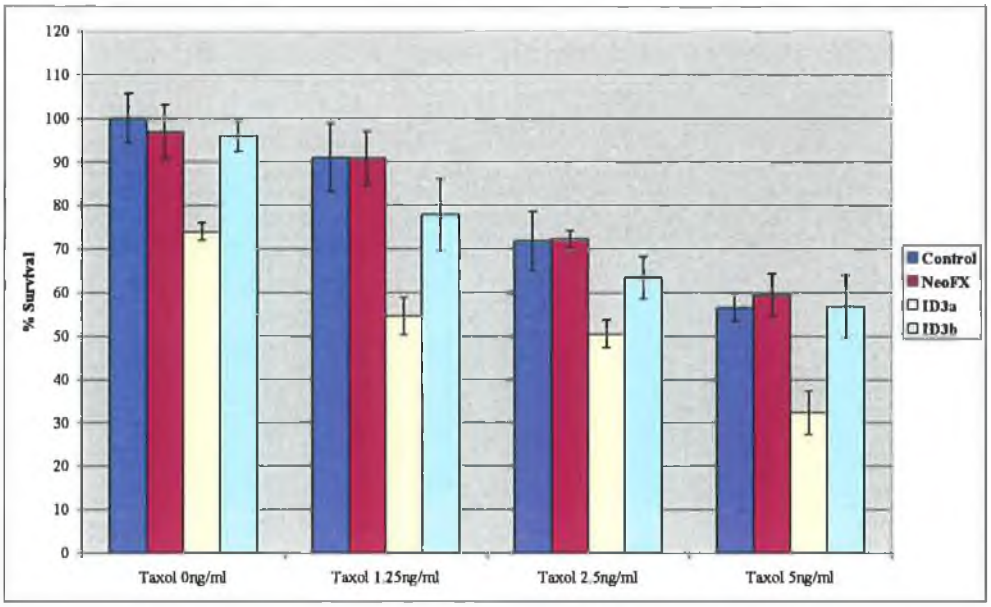

Figure 3.4.9 Effect of transfection of ID3 siRNA in A549 cells

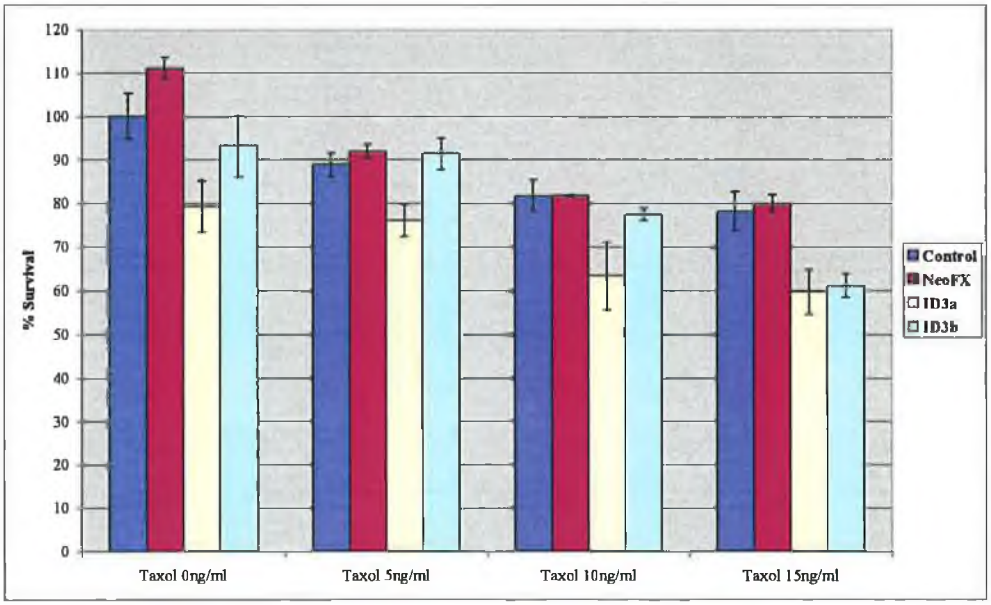

Figure 3.4.10 Effect of transfection of ID3 siRNA in A549-tax cells

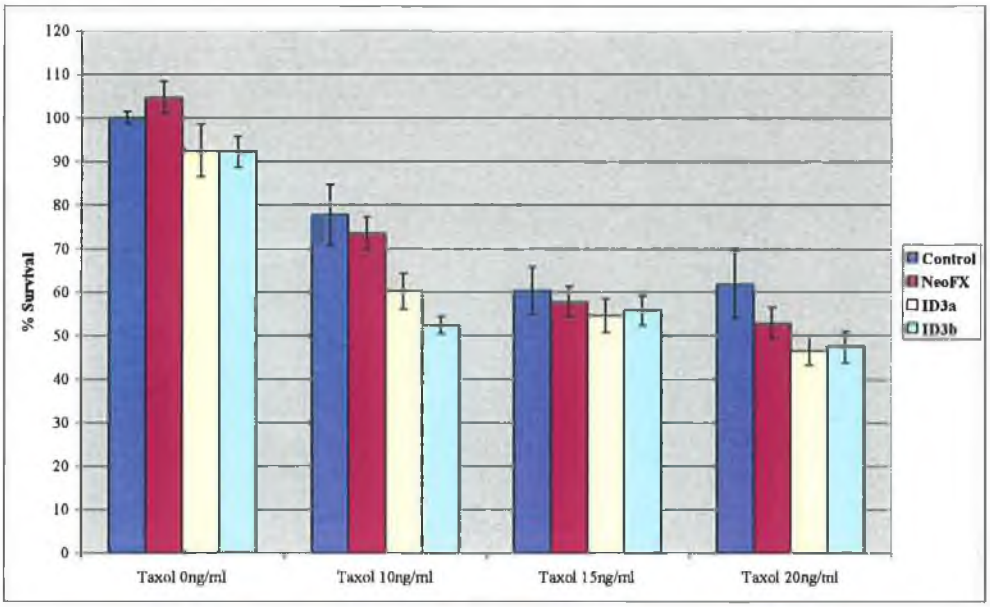

Figure 3.4.11 Effect of transfection of ID3 siRNA in H1299 cells

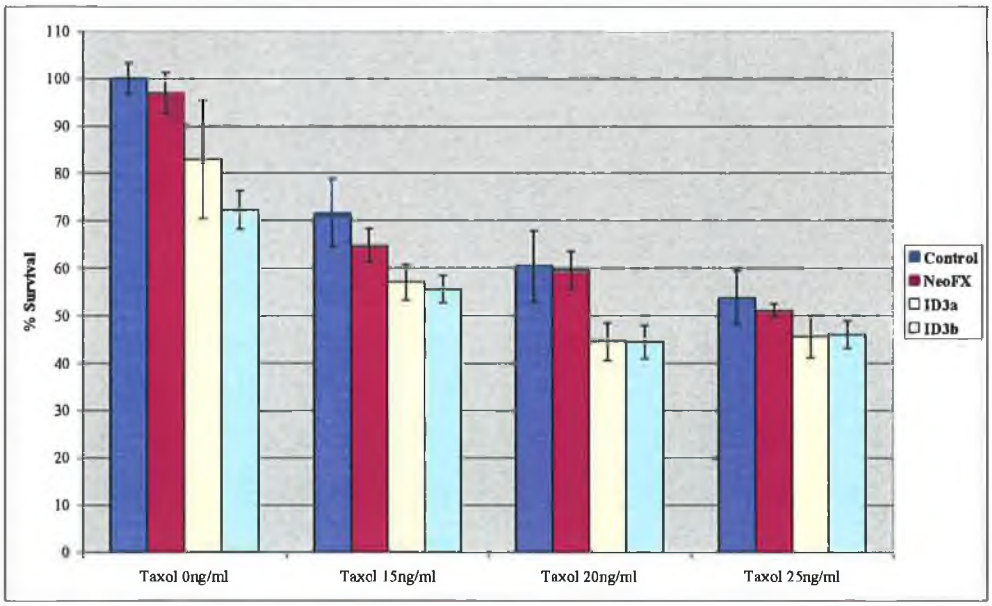

Figure 3.4.12 Effect of transfection of ID3 siRNA in H1299-tax cells

3.4.3.3 Effect of transfection of CRYZ siRNA

CRYZ is crystallin, zeta or quinone reductase. CRYZ was upregulated in taxol-selected cells. Transfection of CRYZ siRNA in A549 and A549-tax had no significant effect on sensitivity to taxol in either parental or selected cell lines (Figures 3.4.13 and 3.4.14). CRYZ is 1.5 fold upregulated in H1299-tax compared to the parent cell line. Transfection of CRYZ siRNA resulted in a slight increase in sensitivity to taxol at 10ng/ml in the parent cells (Figure 3.4.15). The effect is difficult to see at other concentrations and does not appear in the taxol selected cells (Figure 3.4.16)

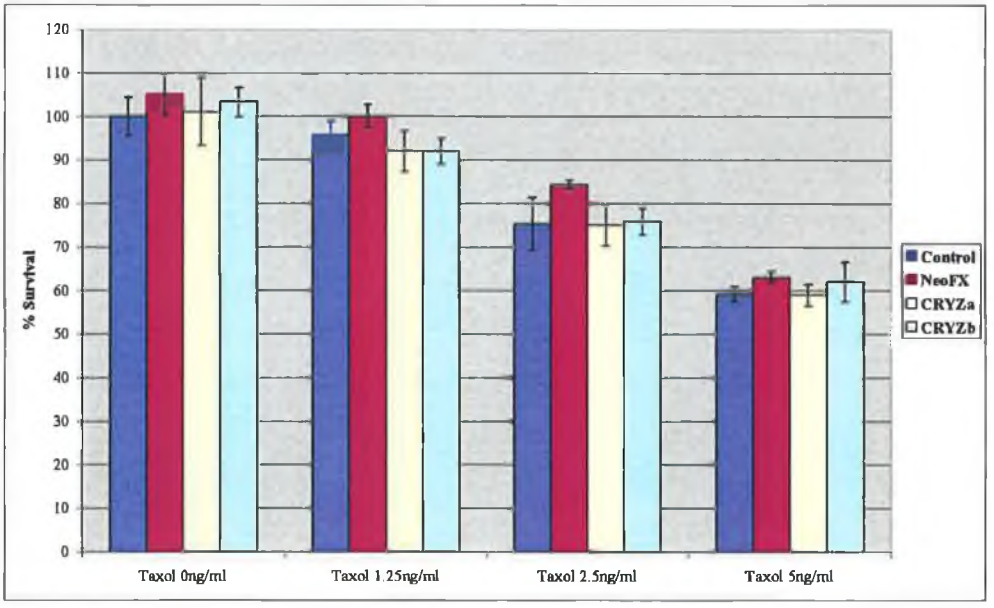

Figure 3.4.13 Effect of siRNA transfection of CRYZ in A549 cells

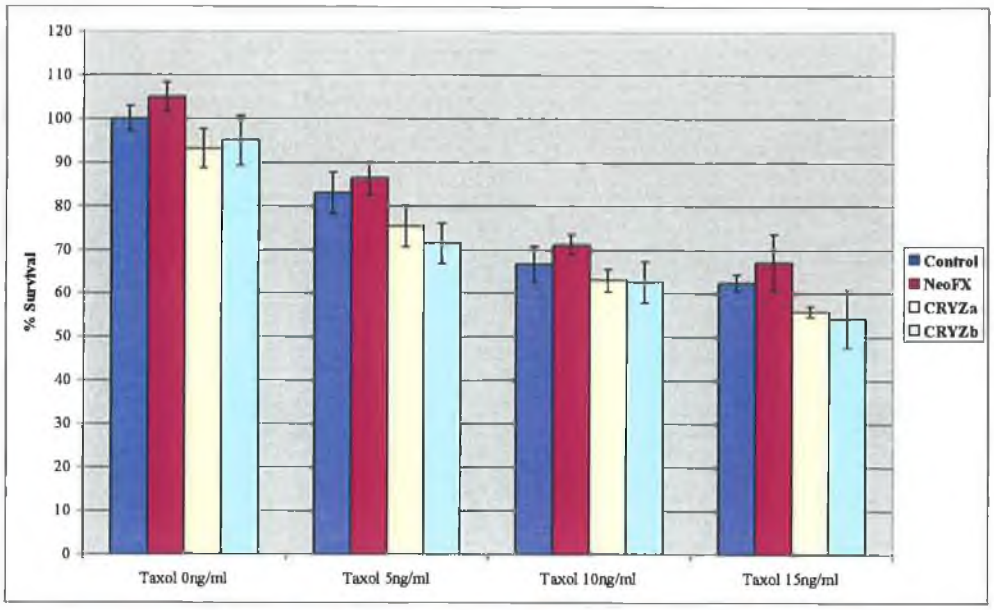

Figure 3.4.14 Effect of transfection of CRYZ siRNA in A549-tax cells

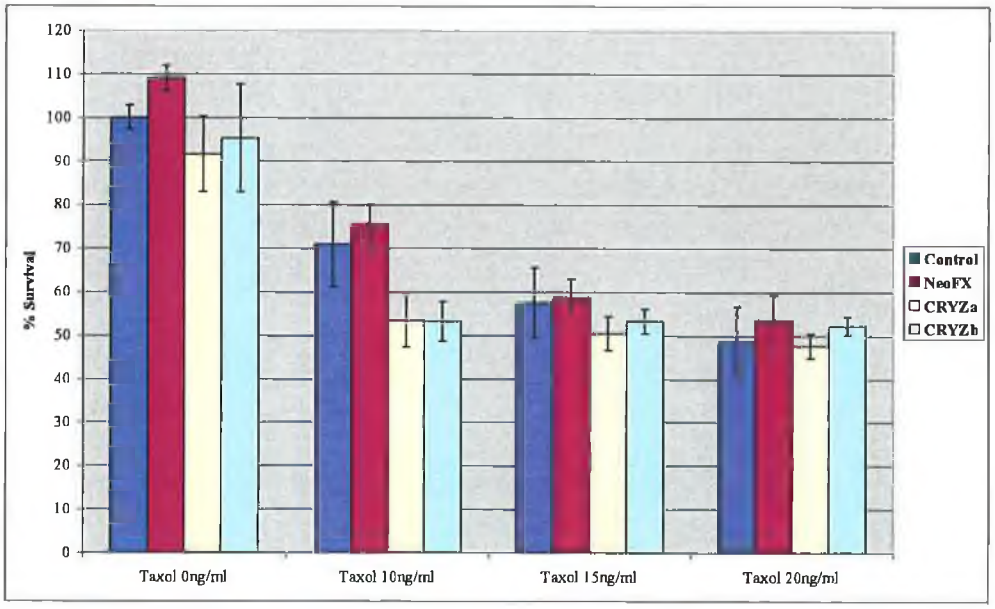

Figure 3.4.15 Effect of transfection of CRYZ siRNA in H1299 cells

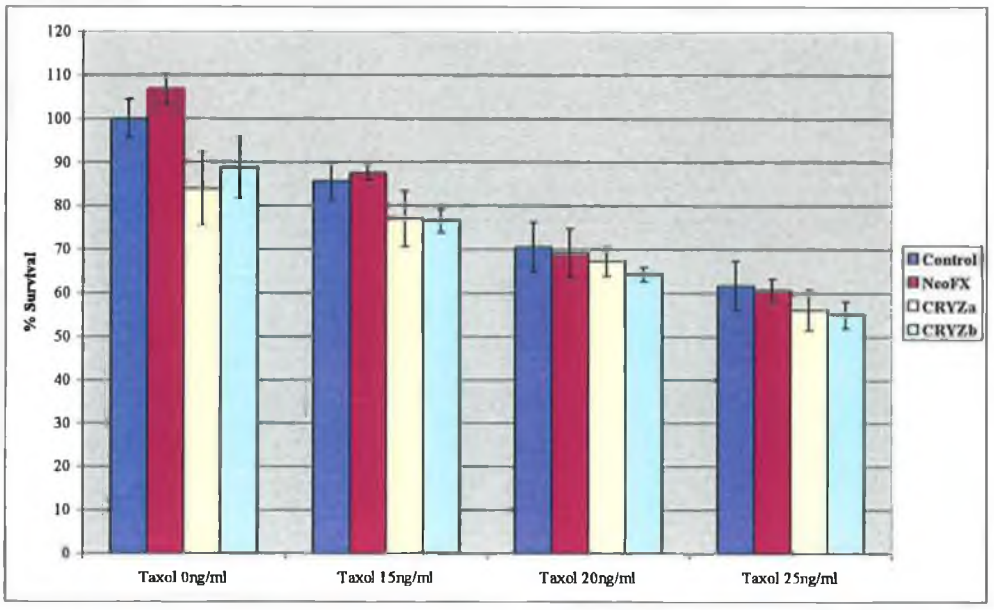

Figure 3.4.16 Effect of transfection of CRYZ siRNA in H1299-tax cells

3.4.3.4 Effect of transfection of GULP1 siRNA

GULP1 is an engulfment factor. GULP1 is upregulated in the taxol-selected A549 cells compared to parent A549, but had no effect on taxol sensitivity in either cell line (Figures 3.4.17 and 3.4.18). GULP1 is upregulated in taxol resistant H1299 cells. No major change in sensitivity was observed in the parent cell line transfected with GULP1 siRNA (Figure 3.4.19). However, an increase in sensitivity was noted in the H1299-tax cell line (Figure 3.4.20).

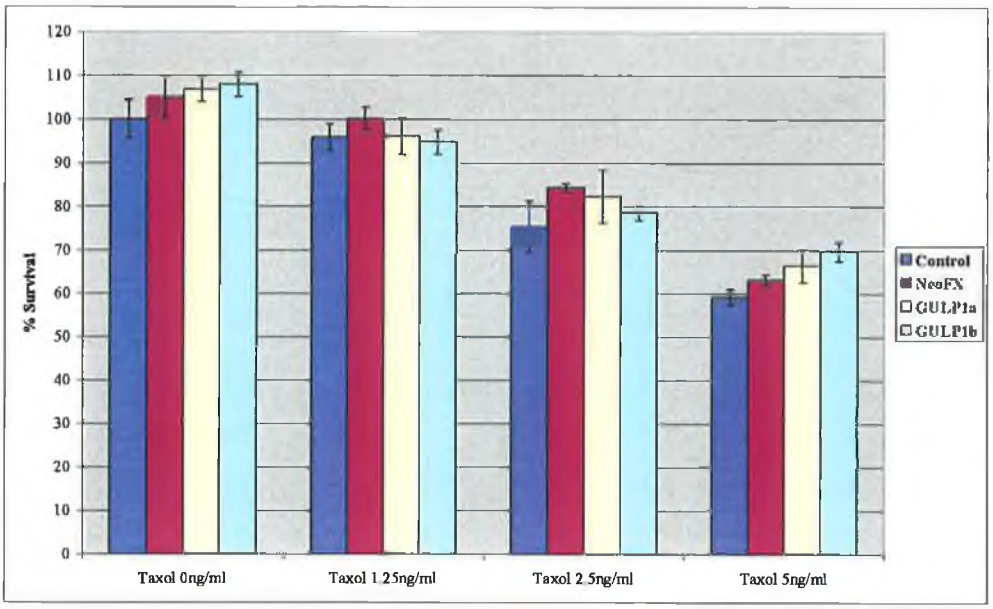

Figure 3.4.17 Effect of transfection of GULP1 siRNA in A549 cells

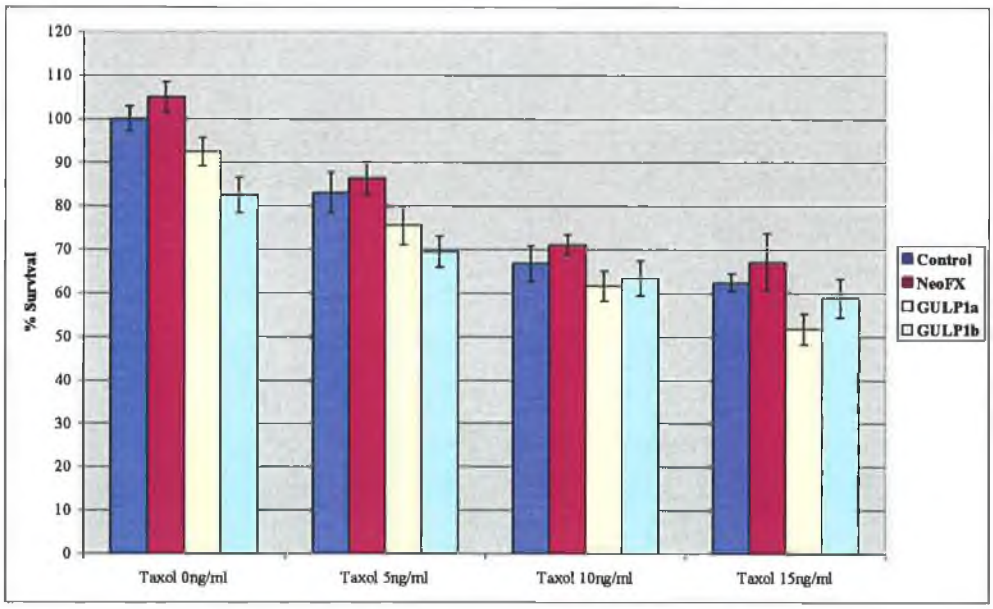

Figure 3.4.18 Effect of transfection of GULP1 siRNA in A549-tax cells

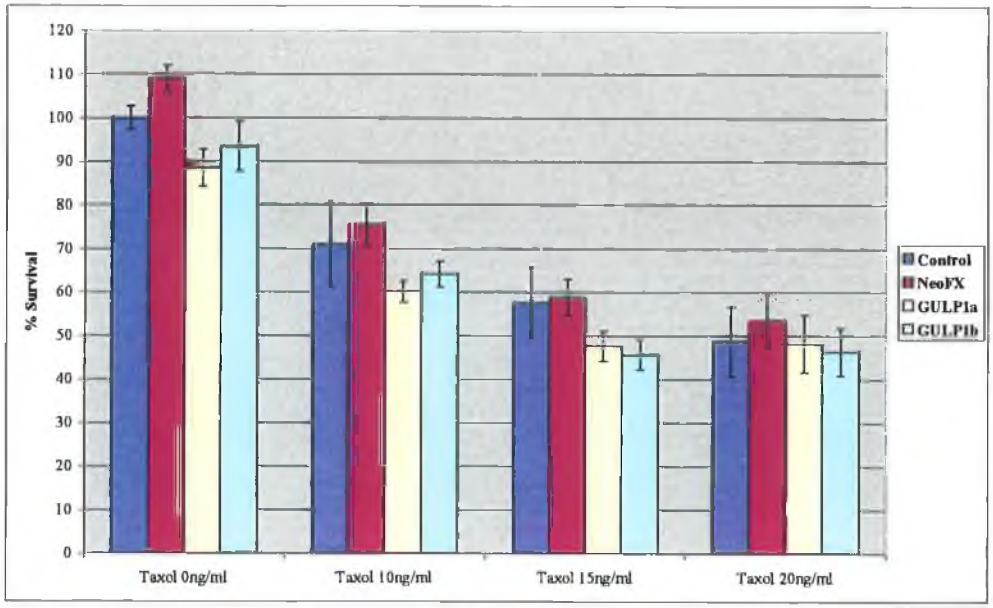

Figure 3.4.19 Effect of transfection of GULP1 siRNA in H1299 cells

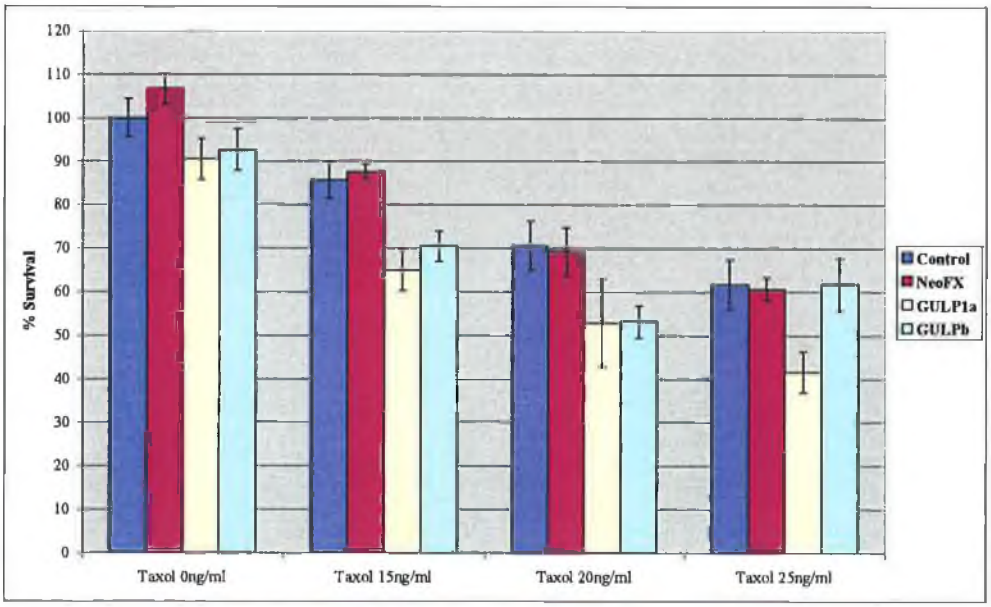

Figure 3.4.20 Effect of transfection of GULP1 siRNA in H1299-tax cells

3.4.3.5 Effect of transfection of SCP siRNA

SCP is stromal cell protein. SCP was upregulated in the taxol-selected A549 cells compared to A549, but had no effect on taxol sensitivity in either parent or resistant cell line (Figures 3.4.21 and 3.4.22). SCP was upregulated in H1299-tax cells, but had no effect on taxol sensitivity in either parent or resistant cell line (Figures 3.4.23 and 3.4.24).

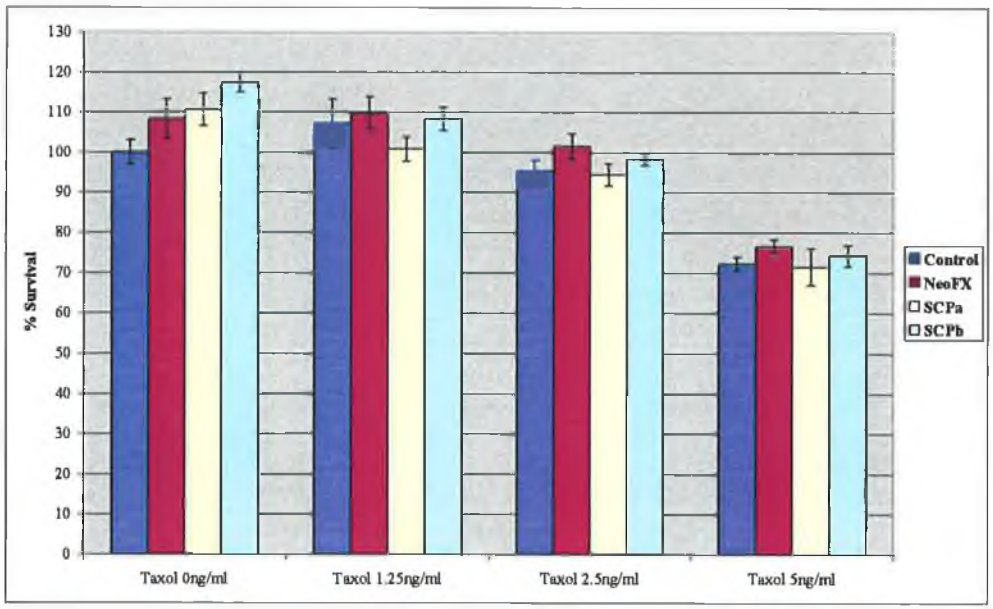

Figure 3.4.21 Effect of transfection of SCP siRNA in A549 cells

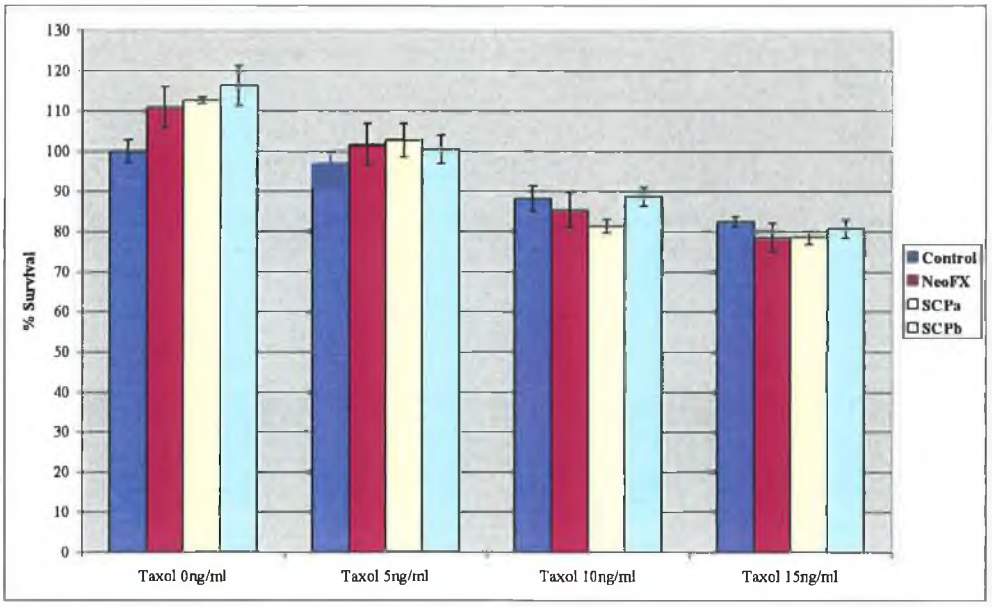

Figure 3.4.22 Effect of transfection of SCP siRNA in A549-tax cells

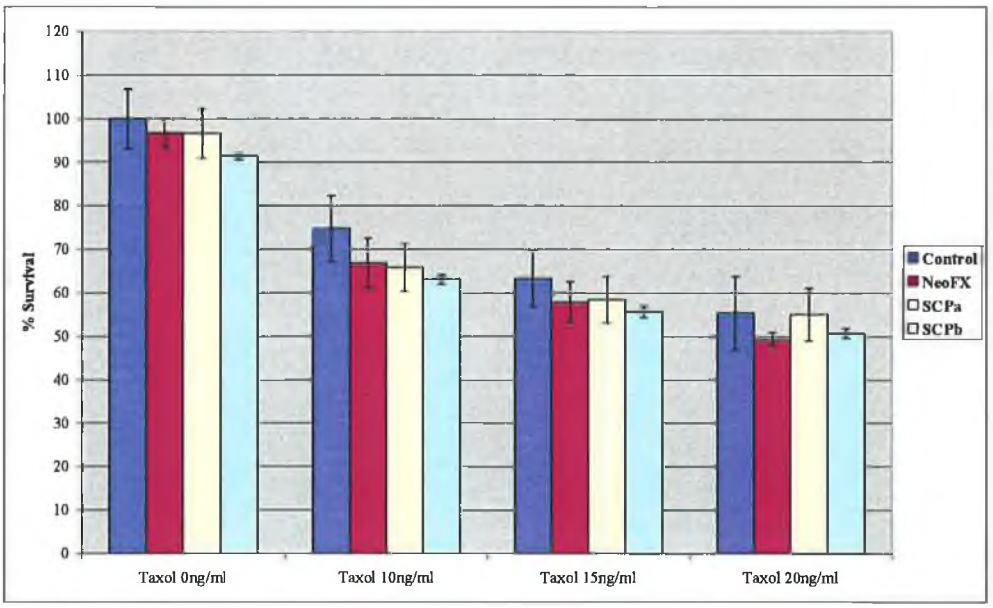

Figure 3.4.23 Effect of transfection of SCP siRNA in H1299 cells

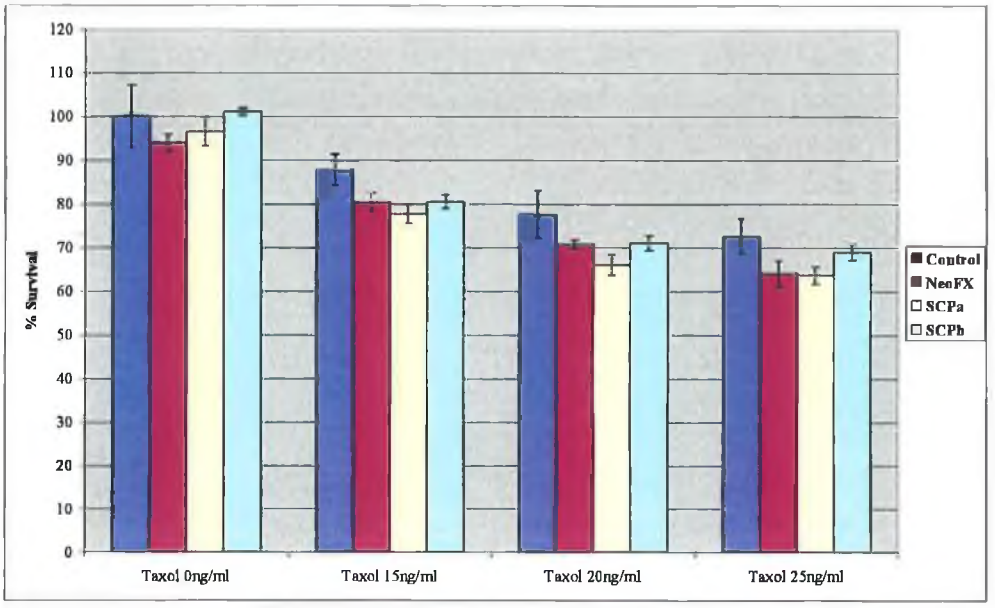

Figure 3.4.24 Effect of transfection of SCP siRNA in H1299-tax cells

3.4.3.6 Effect of transfection of CTGF siRNA

CTGF is connective tissue growth factor. CTGF was downregulated in the taxol-selected variant of A549. The transfection of CTGF siRNA had very little effect on either the parent or selected cell line (Figures 3.4.25 and 3.4.26). CTGF was 2-fold downregulated in H1299-tax compared to parent cells. Transfection of one of the siRNAs for CTGF resulted in a small increase in resistance to taxol in the parent cells (Figure 3.4.27), which would be expected. However, the other siRNA did not show this effect. The transfection of CTGF siRNA in H1299-tax did not change the sensitivity of the cells to taxol (Figure 3.4.28).

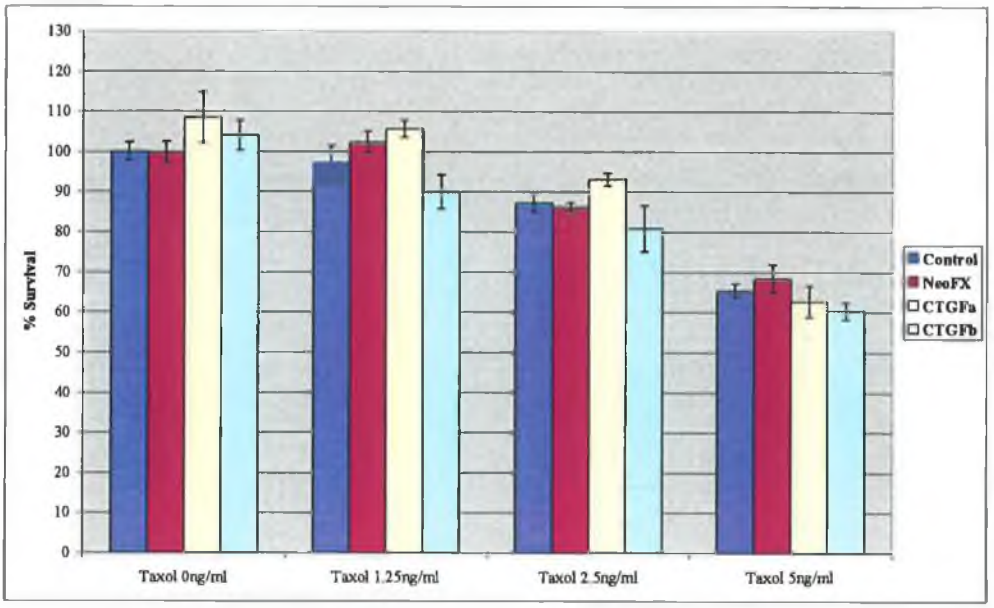

Figure 3.4.25 Effect of transfection of CTGF siRNA in A549 cells

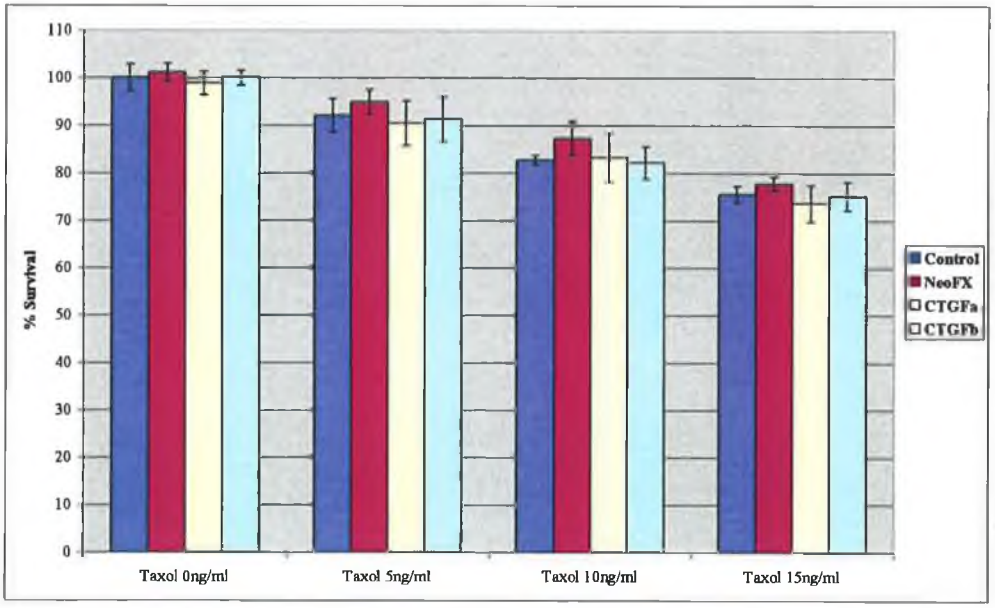

Figure 3.4.26 Effect of transfection of CTGF siRNA in A549-tax cells

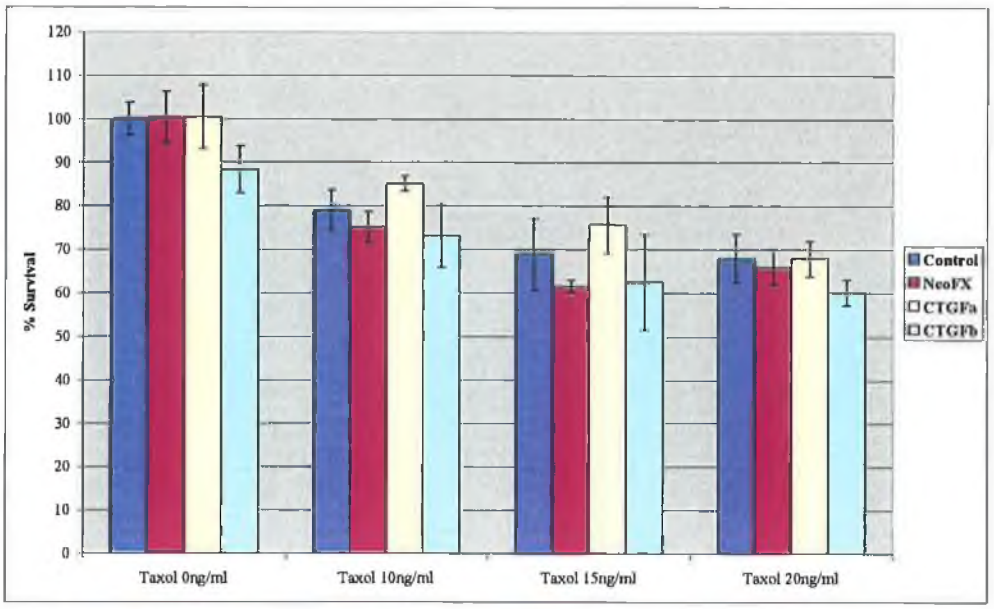

Figure 3.4.27 Effect of transfection of CTGF siRNA in H1299 cells

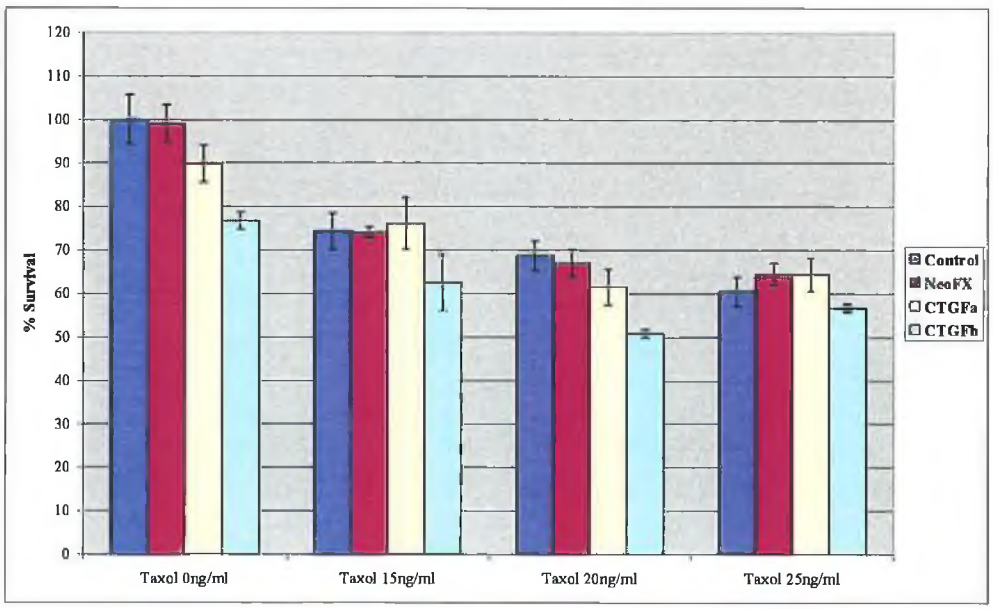

Figure 3.4.28 Effect of transfection of CTGF siRNA in H1299-tax cells

3.4.3.7 Effect of transfection of CRIP1 siRNA

CRIP1 is cysteine-rich intestinal protein 1. CRIP1 was almost 3-fold downregulated in A549-tax compared to parent cells. In both parent and taxol-selected cells transfection of CRIP1 siRNA led to an increase in resistance (Figures 3.4.29 and 3.4.30). H1299-tax cells displayed a very large (30-fold) decrease in CRIP1 compared to the parent cells. Unlike A549 cells, siRNA transfection of CRIP1 did not lead to an increase in resistance (Figures 3.4.31 and 3.4.32). This is surprising considering the large fold change compared to the much lower fold change in A549. This result illustrates that there are probably multiple genes involved in taxol resistance and that the pathways in different cell types are different, so that changing levels of a protein is enough to change sensitivity to taxol in one cell line but not another.

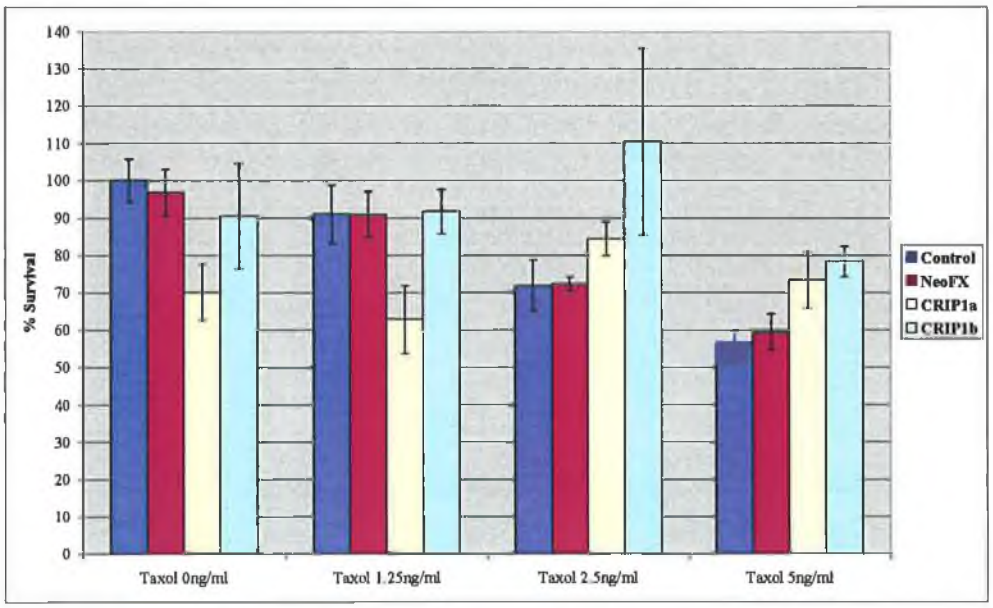

Figure 3.4.29 Effect of transfection of CRIP1 siRNA in A549 cells

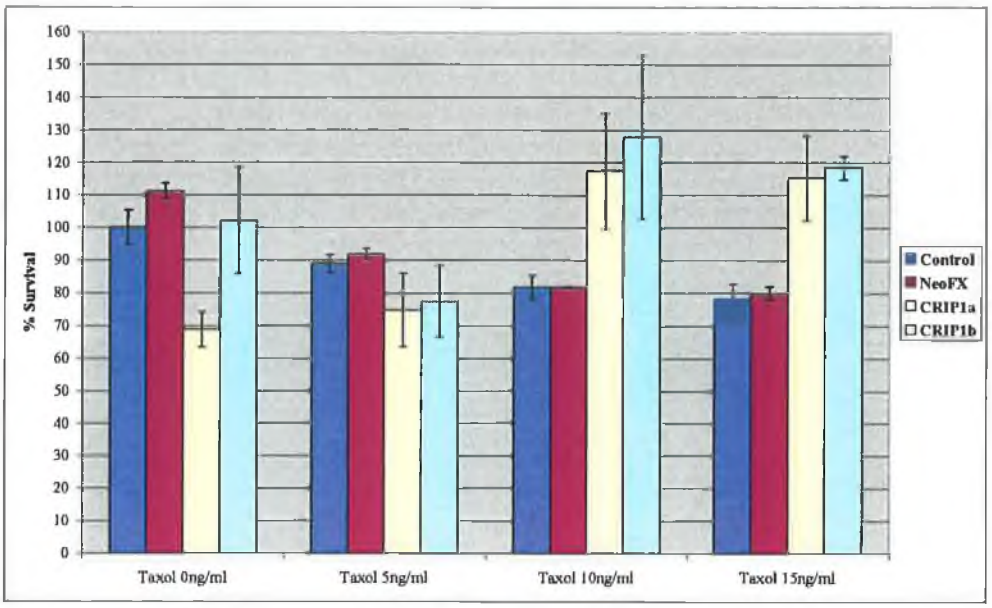

Figure 3.4.30 Effect of transfection of CRIP1 siRNA in A549-tax cells

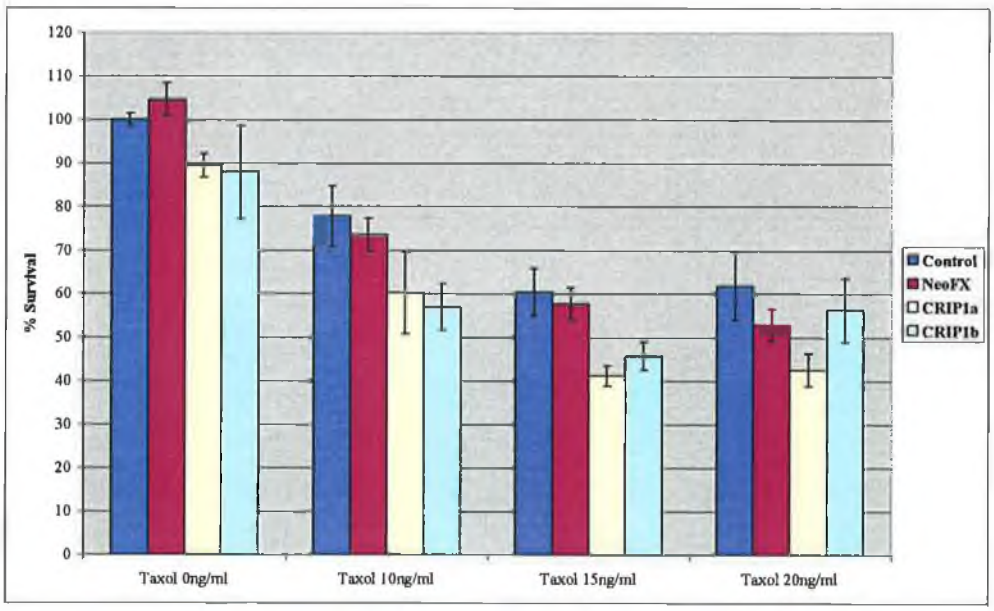

Figure 3.4.31 Effect of transfection of CRIP1 siRNA in H1299 cells

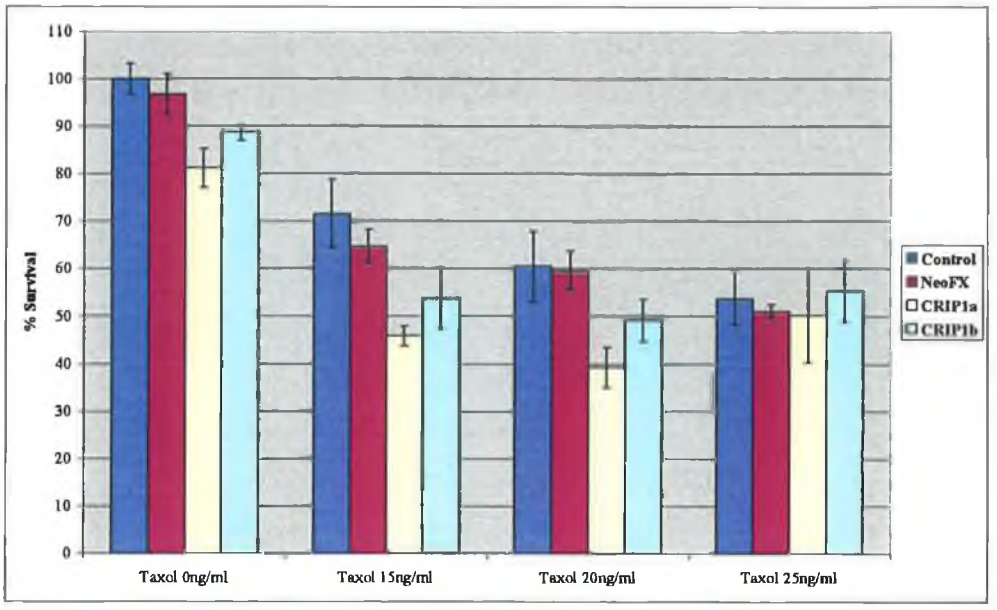

Figure 3.4.32 Effect of transfection of CRIP1 siRNA in H1299-tax cells

3.4.3.8 Effect of transfection of IGFBP6 siRNA

IGFBP6 is Insulin-like growth factor receptor binding protein 6. IGFBP6 was down-regulated in taxol-resistant A549 and H1299 cells. Transfection of IGFBP6 siRNA had no effect on taxol sensitivity in either A549-tax or H1299-tax (Figures 3.4.34 and 3.4.36). In the parent cell lines, there may be a slight increase in sensitivity to taxol. transfection of IGFBP6 siRNA caused an increase in survival in the control cells. Taking this into consideration, there seems to be an effect in the parent cells after transfection of IGFBP6 siRNA (Figures 3.4.33 and 3.4.35).

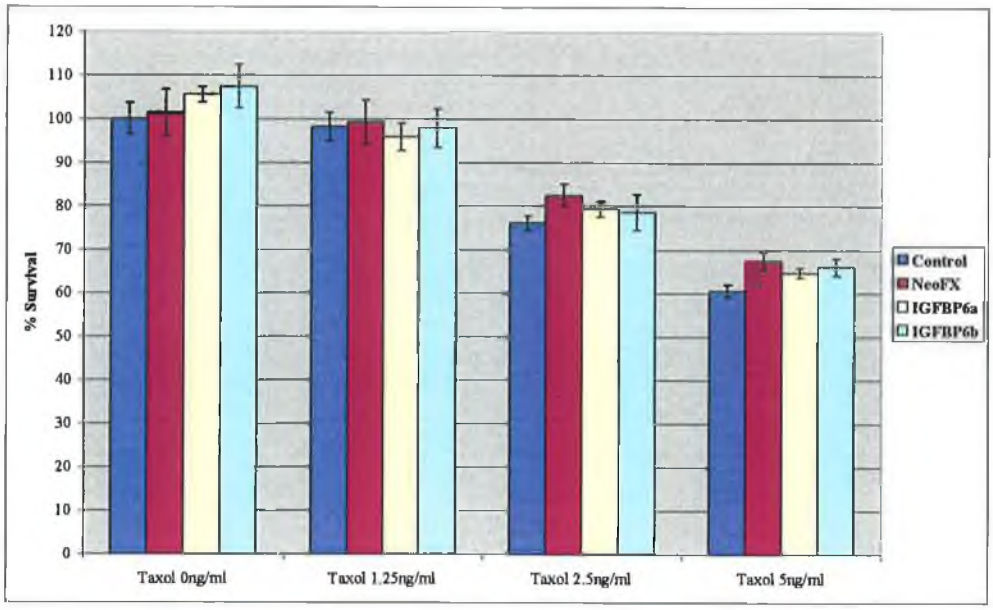

Figure 3.4.33 Effect of transfection of IGFBP6 siRNA in A549 cells

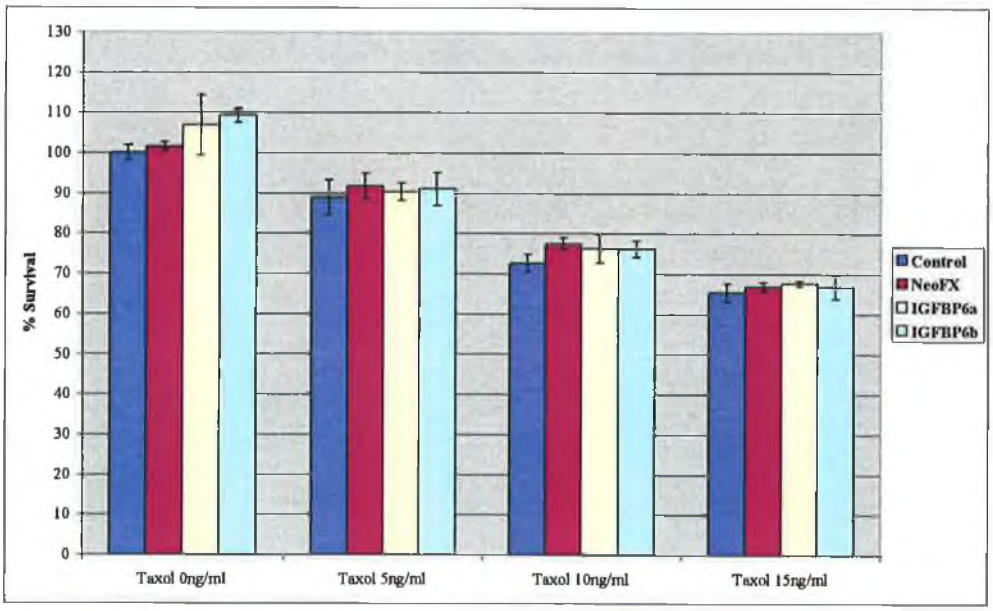

Figure 3.4.34 Effect of transfection of IGFBP6 siRNA in A549-tax cells

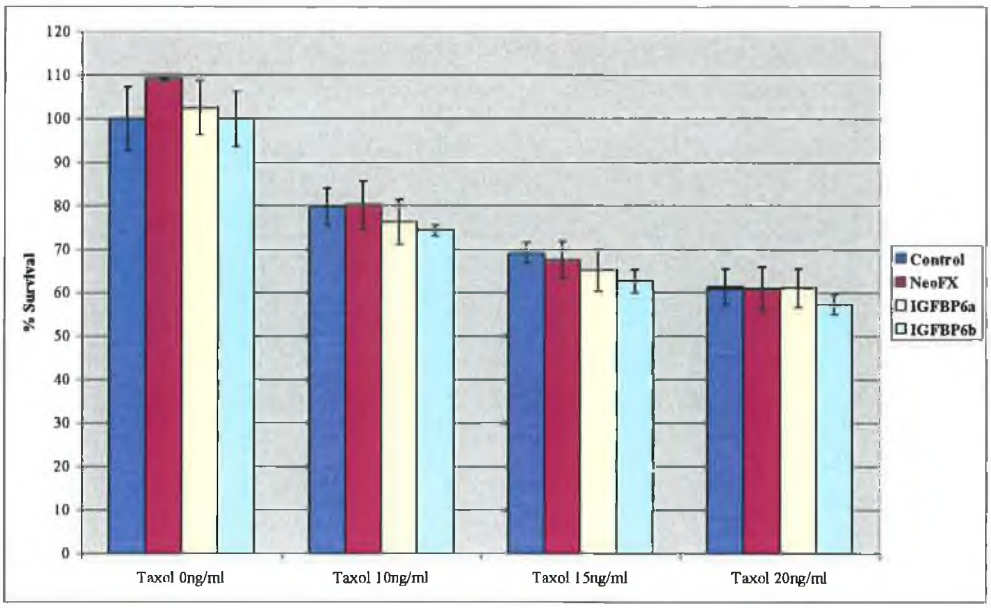

Figure 3.4.35 Effect of transfection of IGFBP6 siRNA in H1299 cells

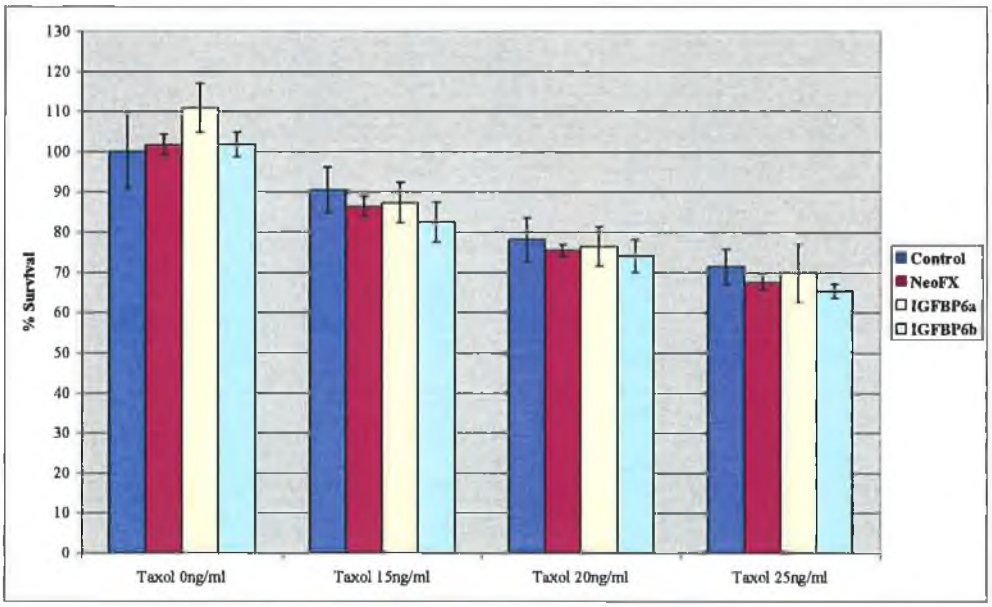

Figure 3.4.36 Effect of transfection of IGFBP6 siRNA in H1299-tax cells

3.4.3.9 Effect of transfection of EMP1 siRNA

EMP1 is epithelial membrane protein 1. EMP1 is downregulated 6-fold in A549-tax compared to parent cells. Despite this, there was no change in sensitivity to taxol in either cell lines at low taxol concentration (Figures 3.4.37 and 3.4.38). At the highest concentration of taxol, there appears to be an increase in sensitivity, most noticeably in the parent cells. This increase in sensitivity is the opposite effect than expected, since EMP1 was found to be downregulated in taxol-resistant cells. EMP1 is downregulated 2-fold in H1299-tax cells compared to parent cells. The transfection of EMP1 siRNA had no effect on taxol sensitivity in either cell line (Figures 3.4.39 and 3.4.40).

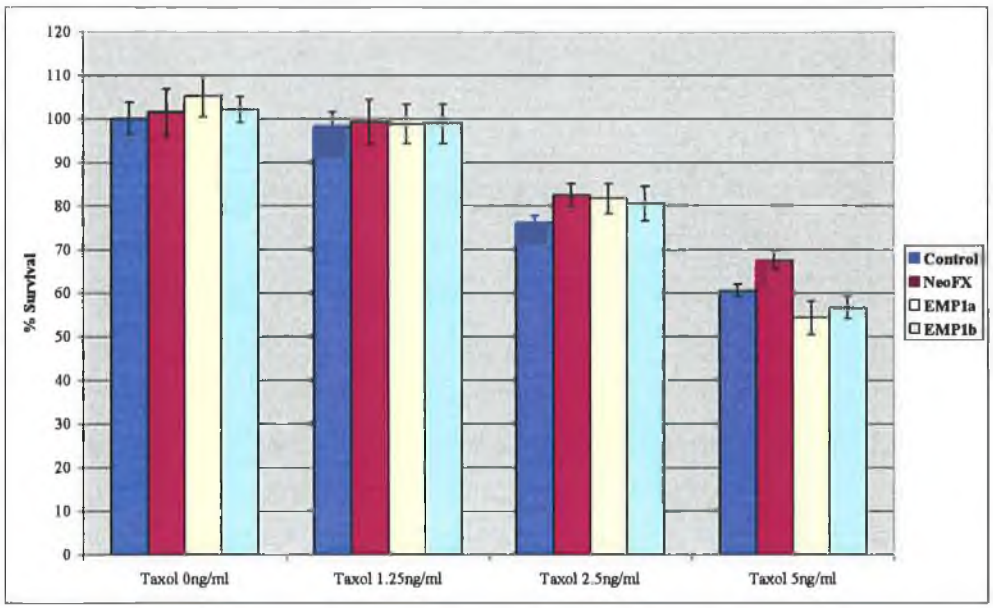

Figure 3.4.37 Effect of transfection of EMP1 siRNA in A549 cells

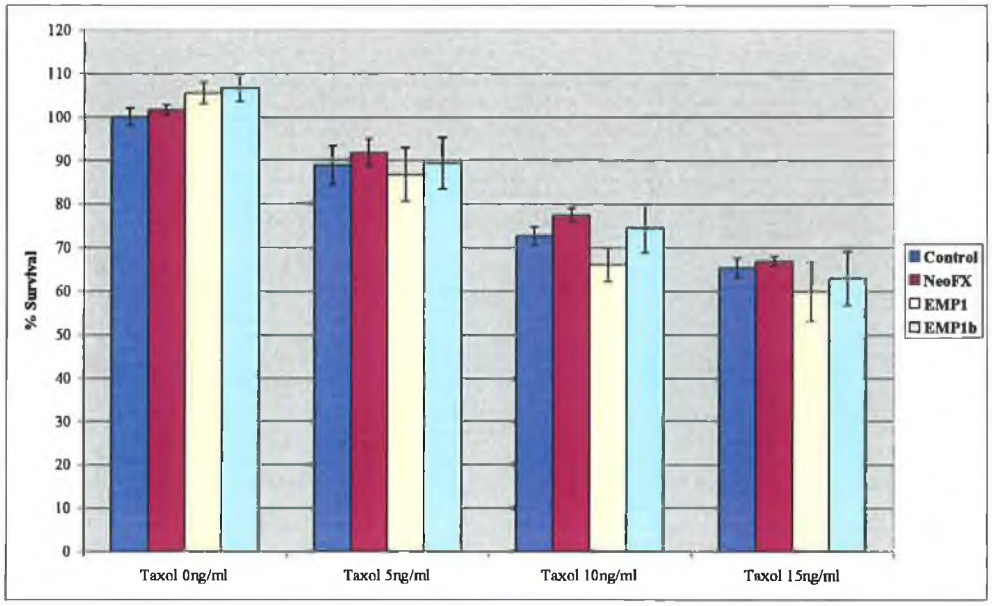

Figure 3.4.38 Effect of transfection of EMP1 siRNA in A549-tax cells

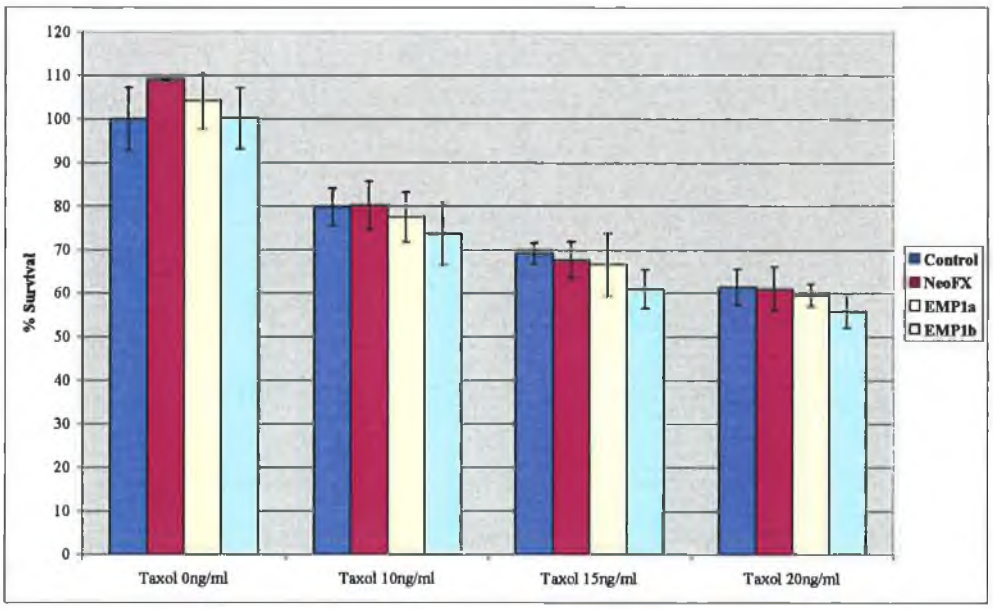

Figure 3.4.39 Effect of transfection of EMP1 siRNA in H1299 cells

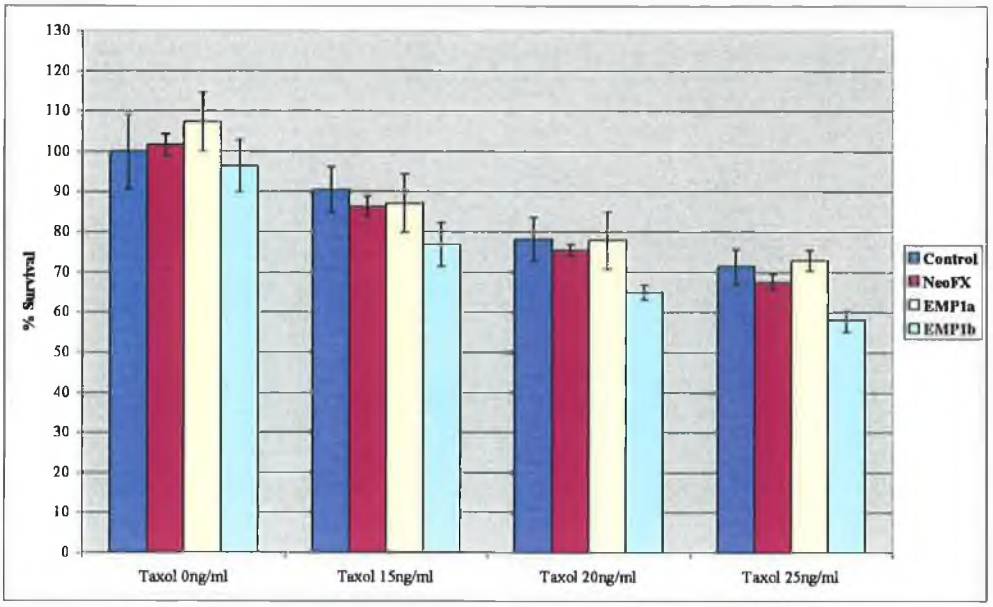

Figure 3.4.40 Effect of transfection of EMP1 siRNA in H1299-tax cells

3.4.3.10 Effect of transfection of FSTL1 siRNA

FSTL1 is follistatin-like 1. FSTL1 was found by microarray analysis to be downregulated in A549-tax compared to the parent cell line. Conversely, transfection of FSTL1 siRNA led to an increase in sensitivity of both parent and taxol-selected cells at high taxol concentrations (Figures 3.4.41 and 3.4.42). FSTL1 was found by microarray analysis to be downregulated 7.5-fold in H1299-tax compared to the parent cell line. Transfection of FSTL1 siRNA did not notably affect taxol sensitivity in either H1299 or H1299-tax (Figures 3.4.43 and 3.4.44).

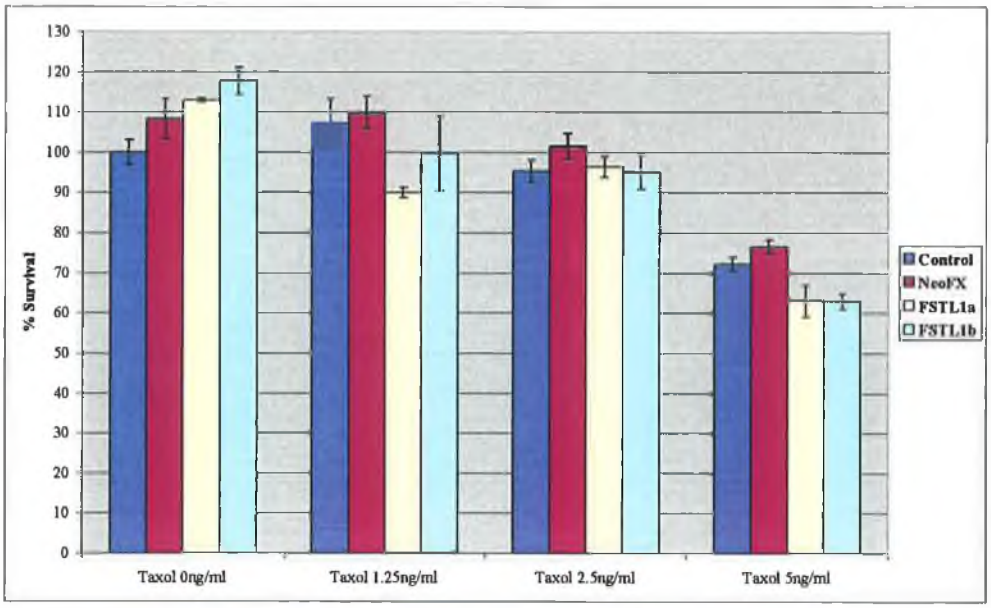

Figure 3.4.41 Effect of transfection of FSTL1 siRNA in A549 cells

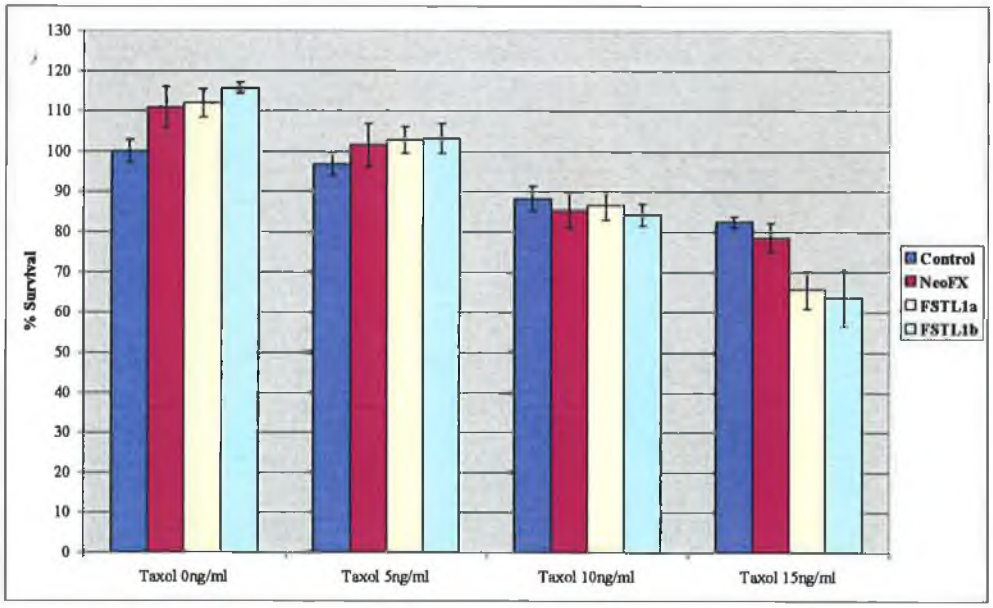

Figure 3.4.42 Effect of transfection of FSTL1 siRNA in A549-tax cells

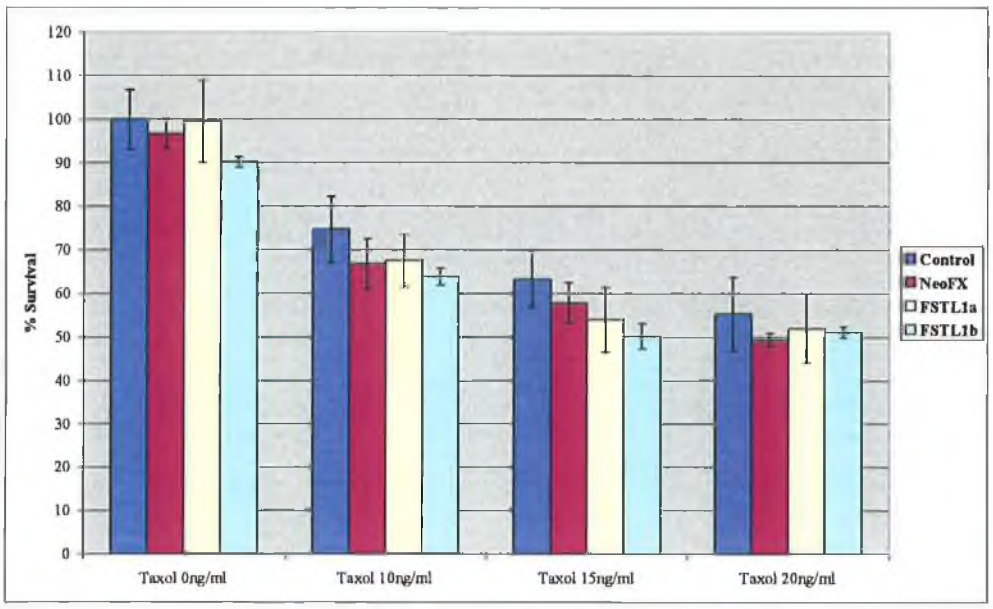

Figure 3.4.43 Effect of transfection of FSTL1 siRNA in H1299 cells

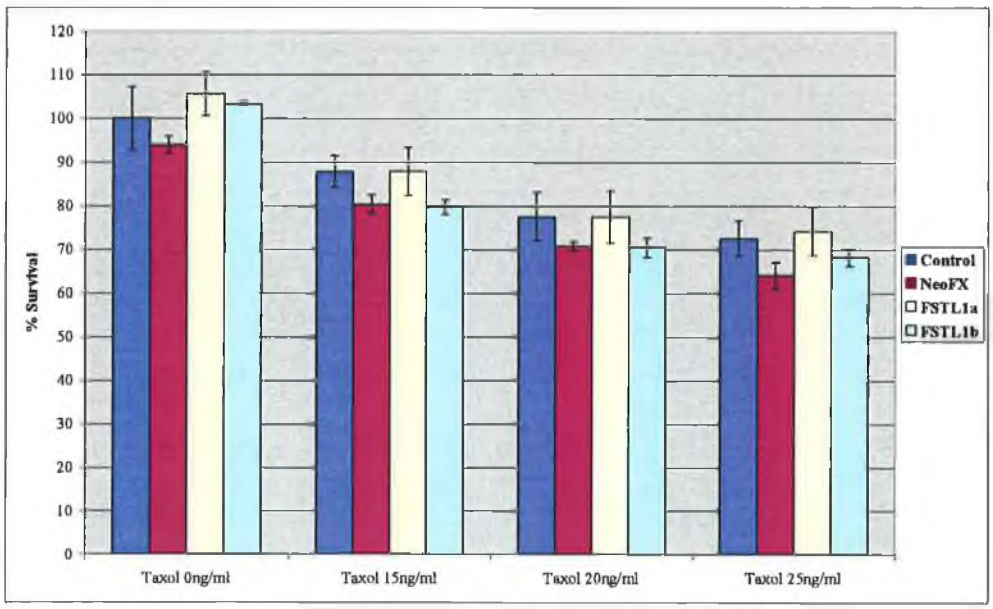

Figure 3.4.44 Effect of transfection of FSTL1 siRNA in H1299-tax cells

3.5 Further analysis of target genes

Three of the ten targets chosen for siRNA analysis were chosen for further analysis based on the results from Section 3.4. The three targets were ABCB1, ID3 and CRIP1. Both ABCB1 and ID3 were upregulated in the taxol-selected cell lines and siRNA-mediated silencing of these genes led to an increase in sensitivity to taxol. CRIP1 was downregulated in the taxol-selected cell lines and silencing of CRIP1 led to a decrease in sensitivity to taxol in A549 cell lines.

3.5.1 ABCB1

Transfection of ABCB1 siRNA resulted in the greatest change in sensitivity to taxol, especially in the H1299-tax cell line (Section 3.4.3). H1299 and H1299-tax are the only cell lines in this study that express detectable levels of P-gp (Section 3.1.4). Transfection of ABCB1 siRNA was tested for its effect on sensitivity to taxotere, adriamycin and carboplatin in the cell lines H1299, H1299-tax, H460 and H460-tax, and to taxotere and carboplatin in A549 and A549-tax. The results are shown in figures 3.5.1-3.5.16. These results are summarised in Table 3.5.2.

Table 3.5.2 Summary of effects of transfection of ABCB1 siRNA

Cell line	*Taxotere*	*Adriamycin*	*Carboplatin*
H1299	No change	Small ↑ resistance	No change
H1299-tax	↑ sensitivity	No change	No change
A549	No change	ND	No change
A549-tax	Small ↑ sensitivity	ND	No change
H460	No change	No change	No change
H460-tax	Small ↑ sensitivity	No change	No change

ND – not done

Transfection of ABCB1 siRNA into the taxol resistant cell lines: A549-tax (Figure 3.5.4); H1299-tax (Figure 3.5.2) and H460-tax (Figure 3.5.6) resulted in an increase in sensitivity to taxotere. This was expected and paralleled the results found with taxol. In H1299 cells, there was a decrease in sensitivity to adriamycin with transfection of ABCB1 siRNA (Figure 3.5.7). The results obtained for adriamycin sensitivity after transfection with ABCB1 siRNA were surprising, since adriamycin is a P-gp substrate, similar results to those obtained for taxol and taxotere would have been expected. No effects were seen in any of the cell lines in carboplatin sensitivity after transfection of ABCB1 siRNA. This was expected since carboplatin is not a substrate for P-gp.

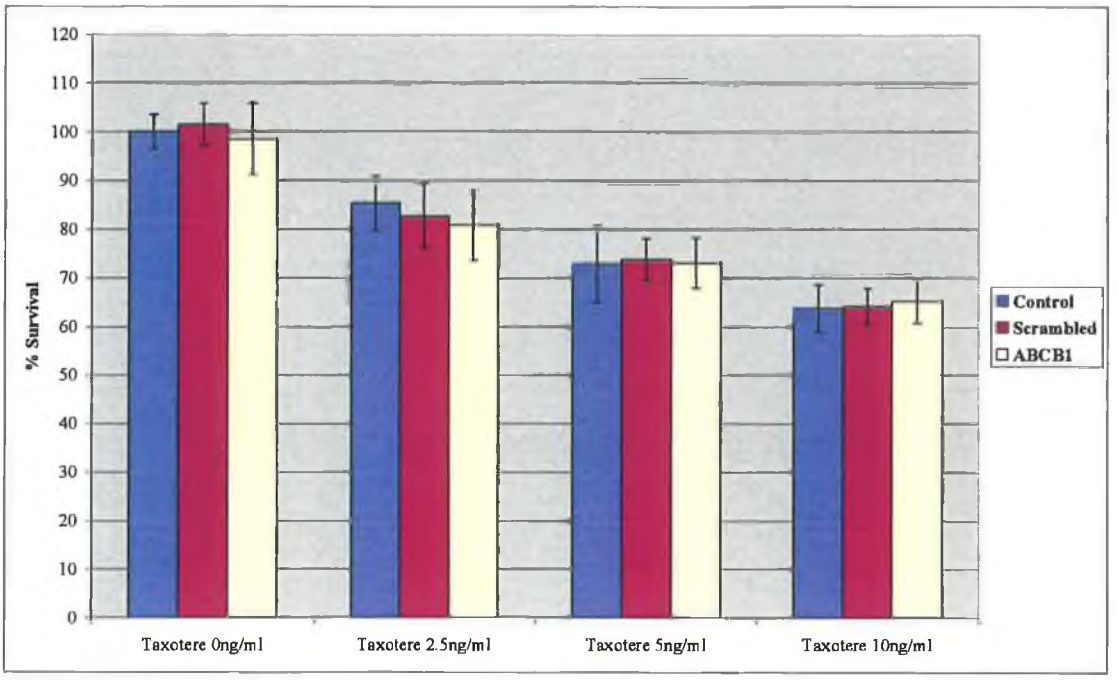

Figure 3.5.1 Effect of transfection of ABCB1 siRNA on taxotere sensitivity in H1299 cells

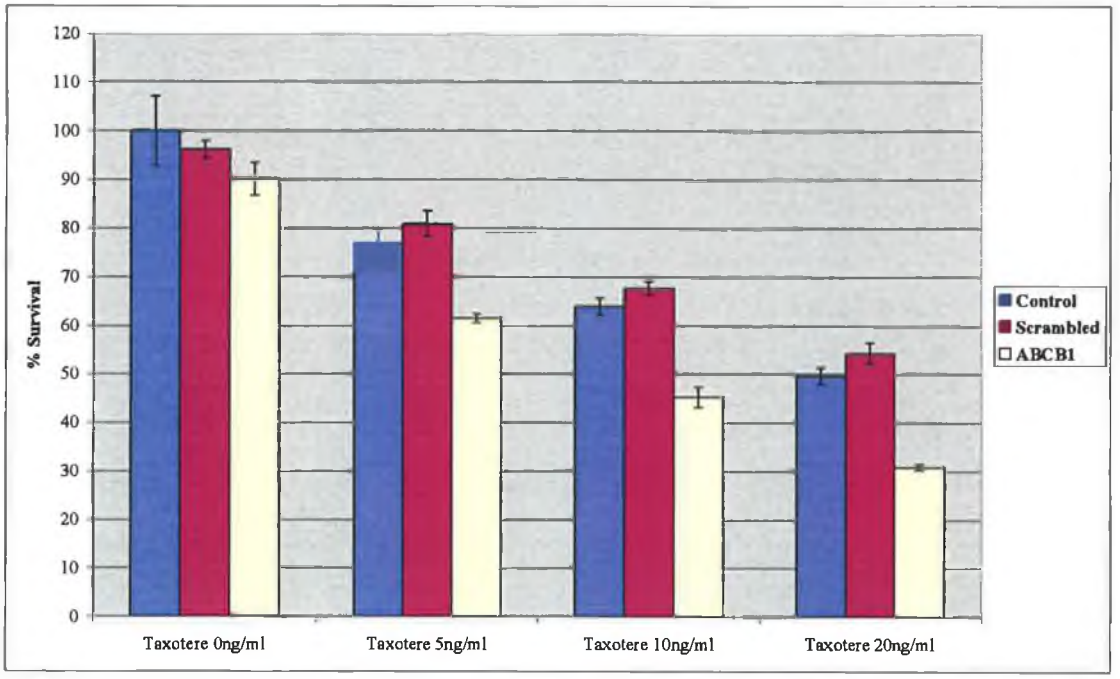

Figure 3.5.2 Effect of transfection of ABCB1 siRNA on taxotere sensitivity in H1299-tax cells

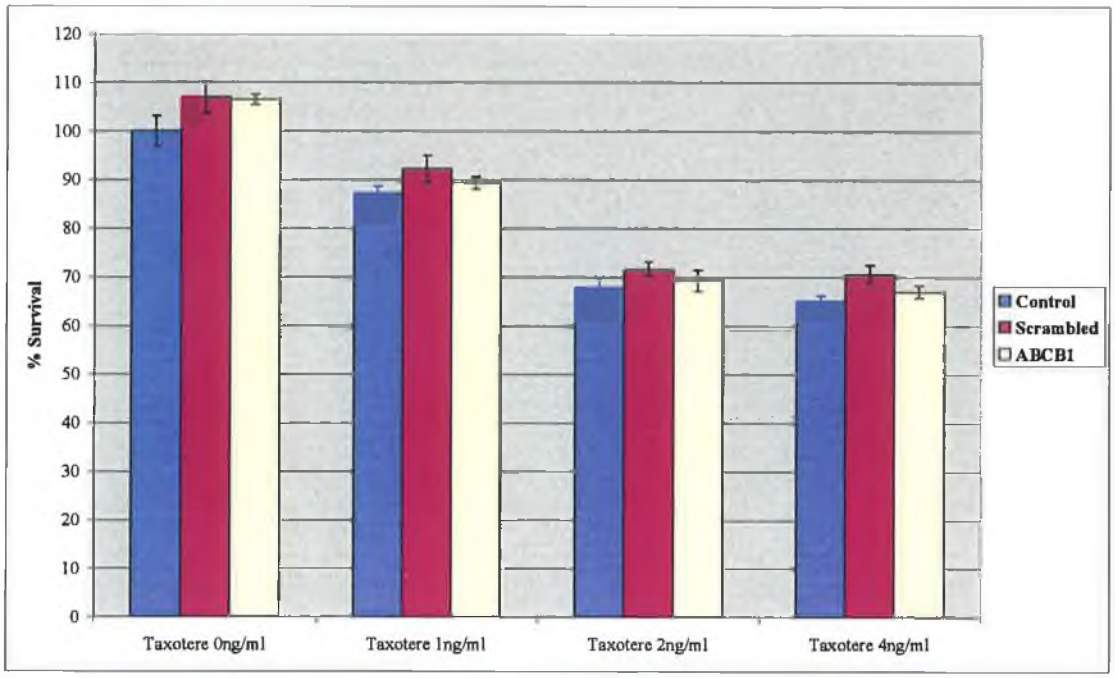

Figure 3.5.3 Effect of transfection of ABCB1 siRNA on taxotere sensitivity in A549 cells

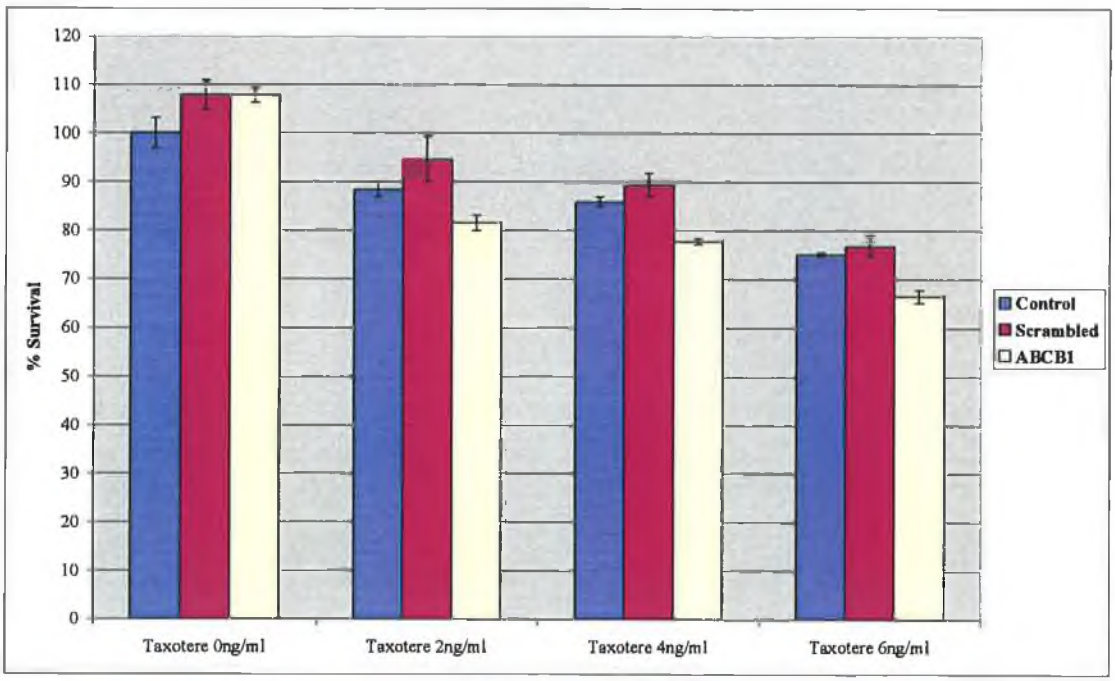

Figure 3.5.4 Effect of transfection of ABCB1 siRNA on taxotere sensitivity in A549-tax cells

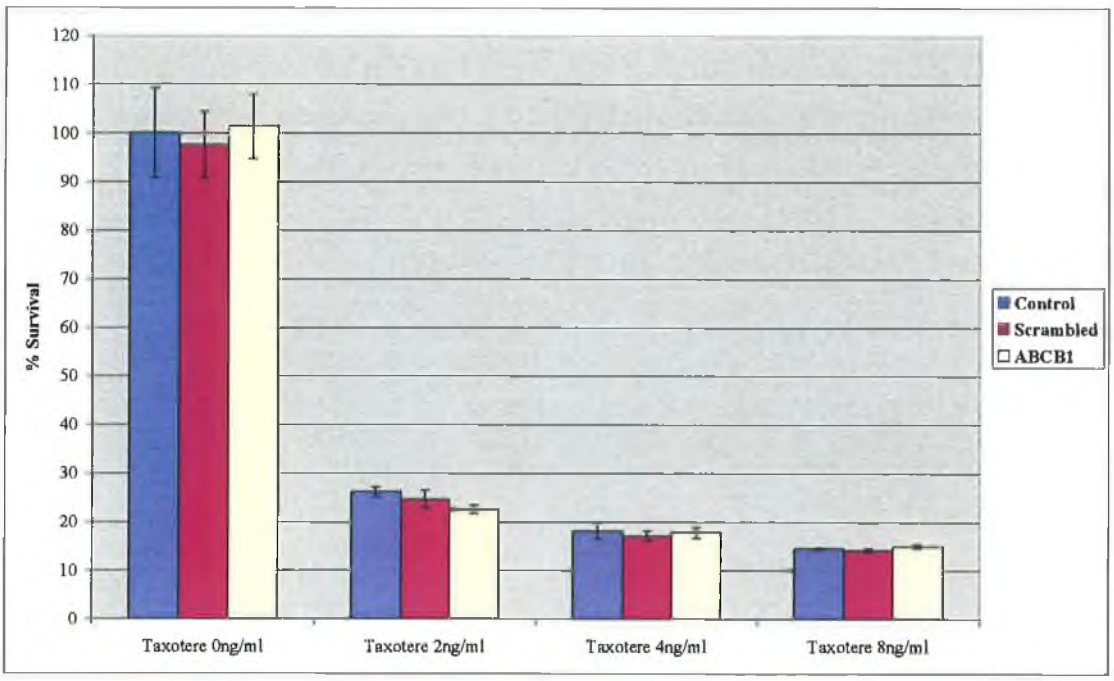

Figure 3.5.5 Effect of transfection of ABCB1 siRNA on taxotere sensitivity in H460 cells

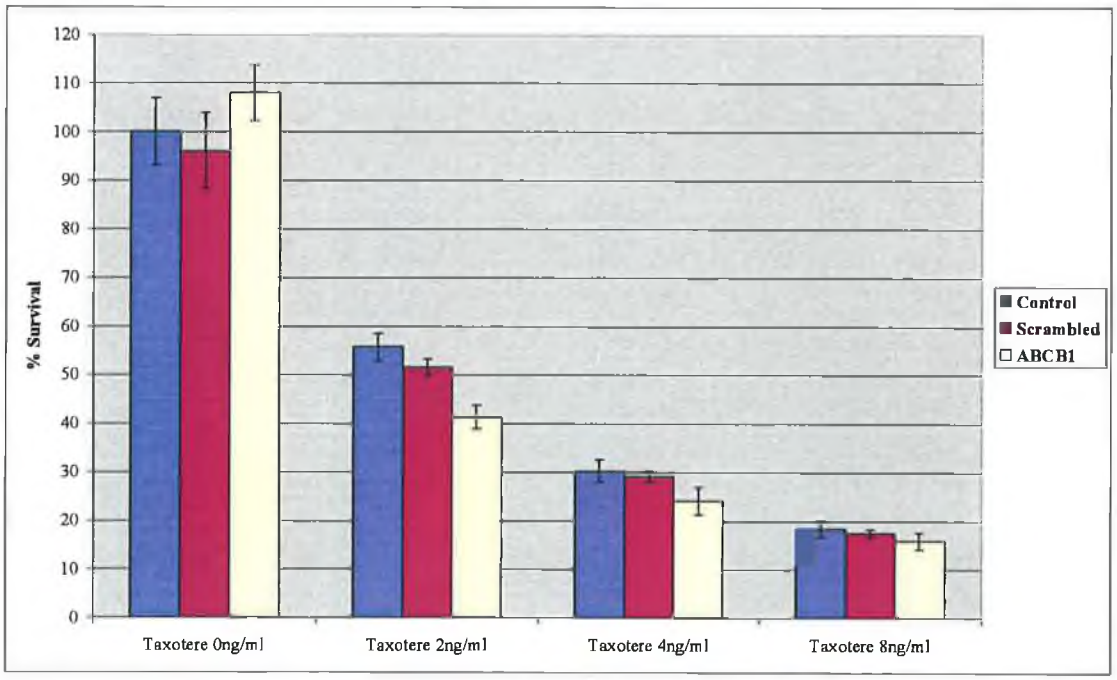

Figure 3.5.6 Effect of transfection of ABCB1 siRNA on taxotere sensitivity in H460-tax cells

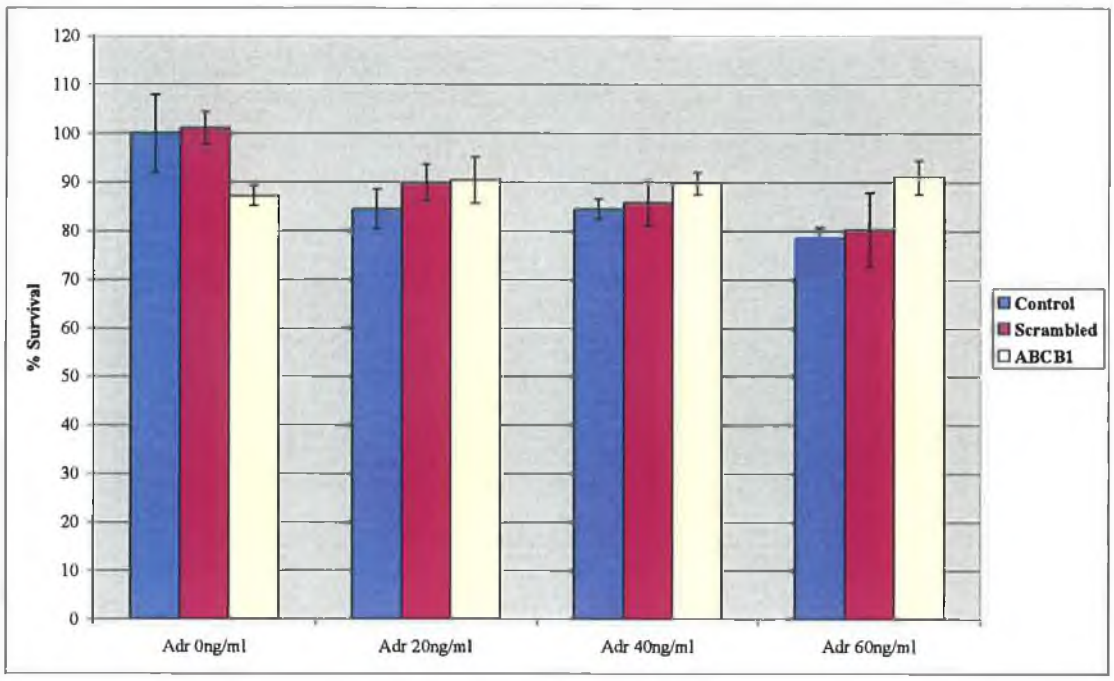

Figure 3.5.7 Effect of transfection of ABCB1 siRNA on adriamycin sensitivity in H1299 cells

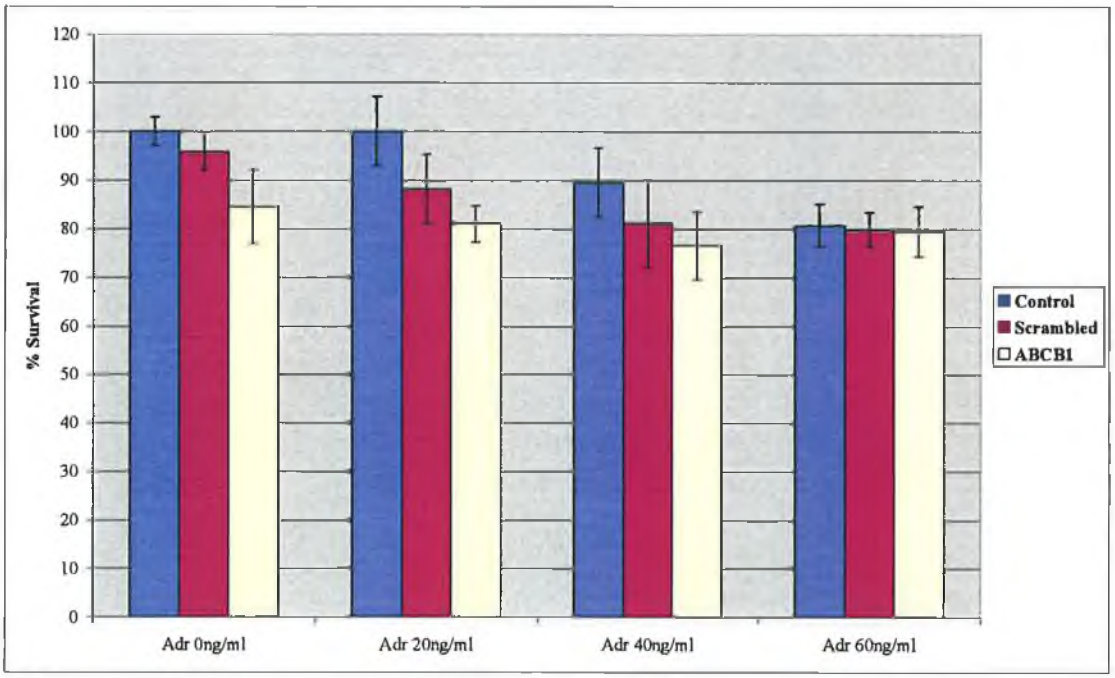

Figure 3.5.8 Effect of transfection of ABCB1 siRNA on adriamycin sensitivity in H1299-tax cells

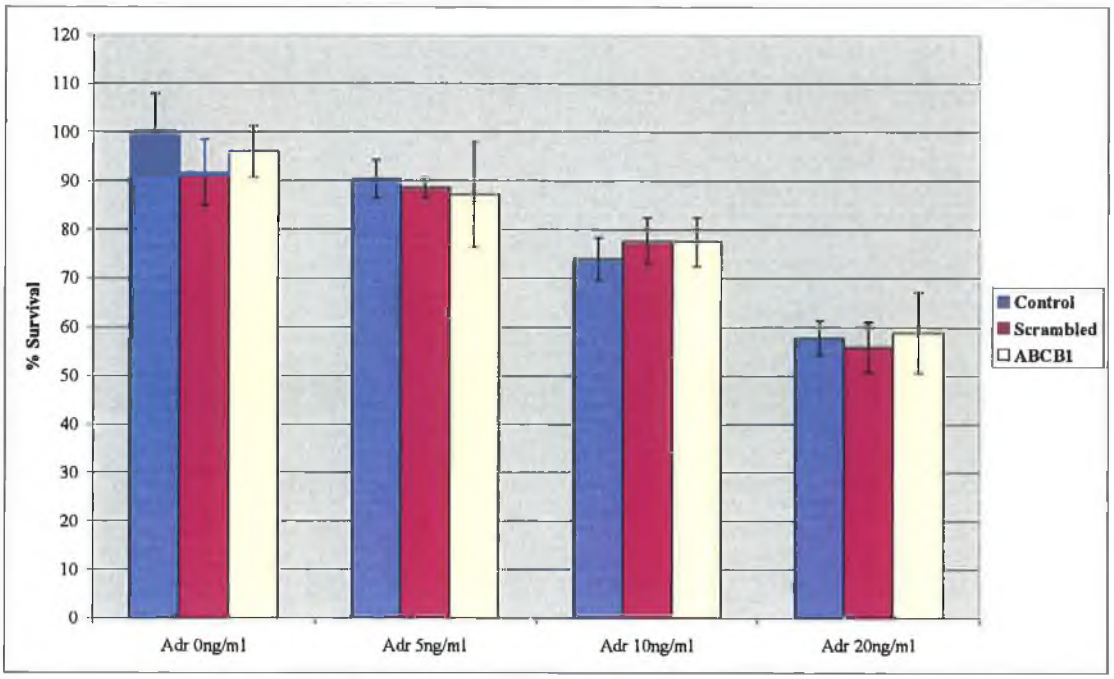

Figure 3.5.9 Effect of transfection of ABCB1 siRNA on adriamycin sensitivity in H460 cells

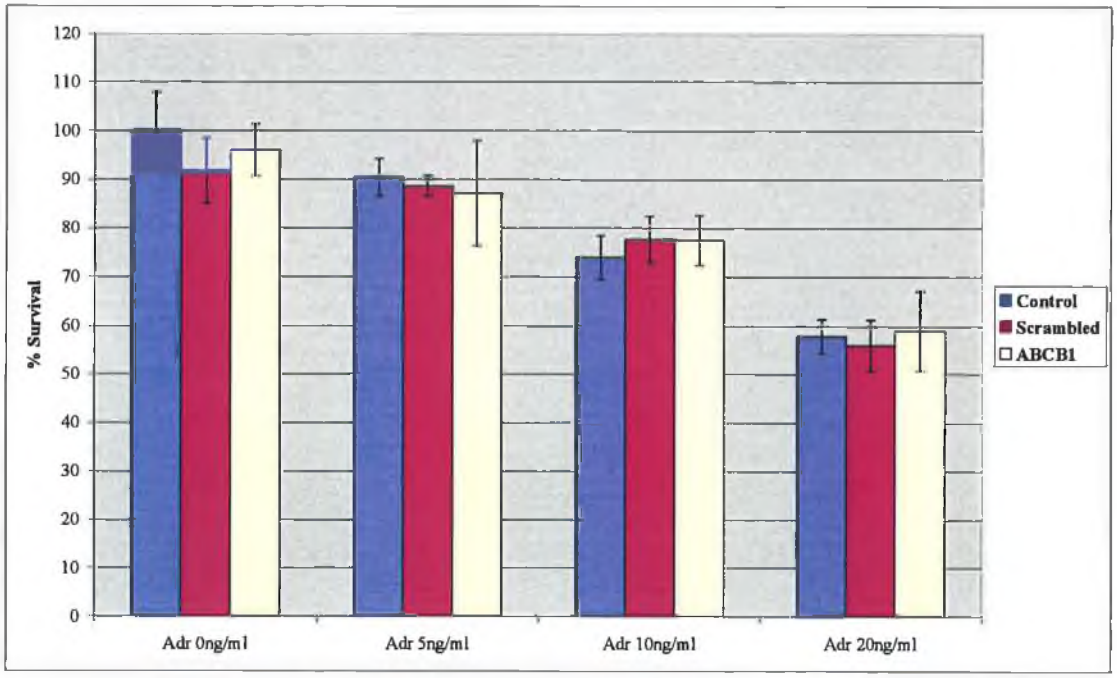

Figure 3.5.10 Effect of transfection of ABCB1 siRNA on adriamycin sensitivity in H460-tax cells

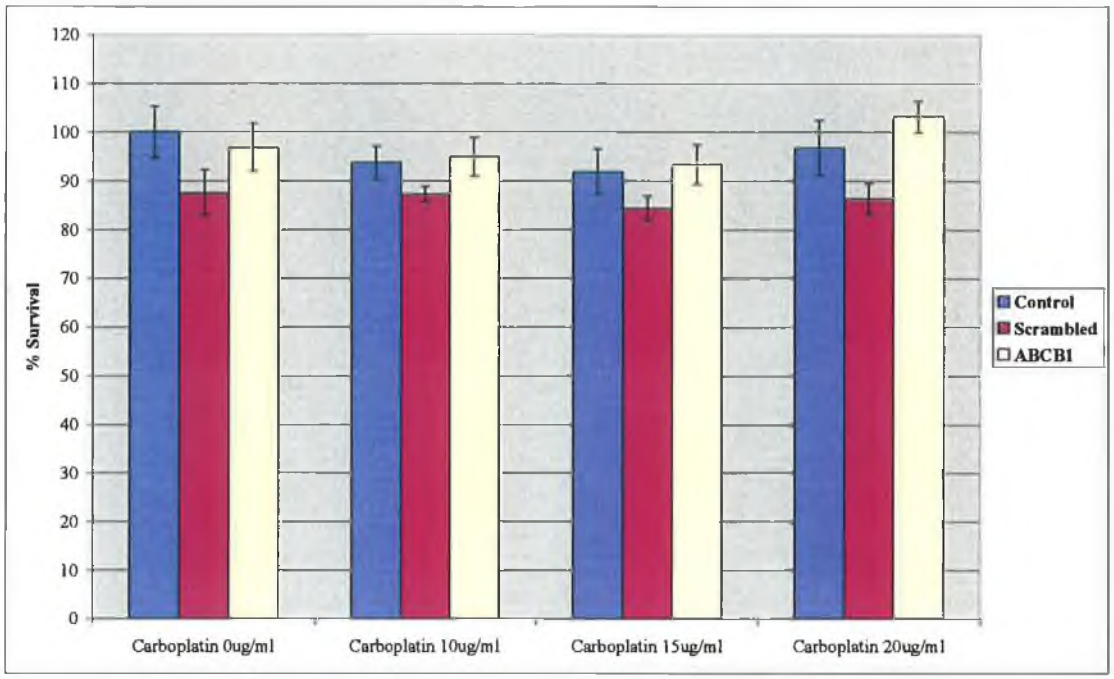

Figure 3.5.11 Effect of transfection of ABCB1 siRNA on carboplatin sensitivity in H1299 cells

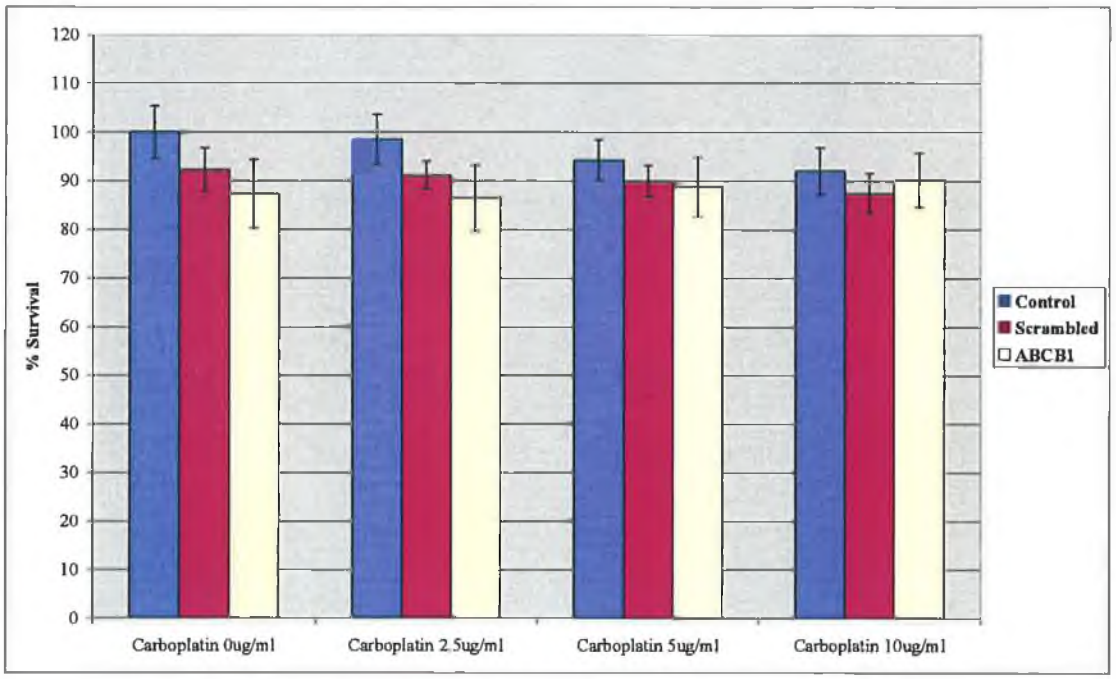

Figure 3.5.12 Effect of transfection of ABCB1 siRNA on carboplatin sensitivity in H1299-tax cells

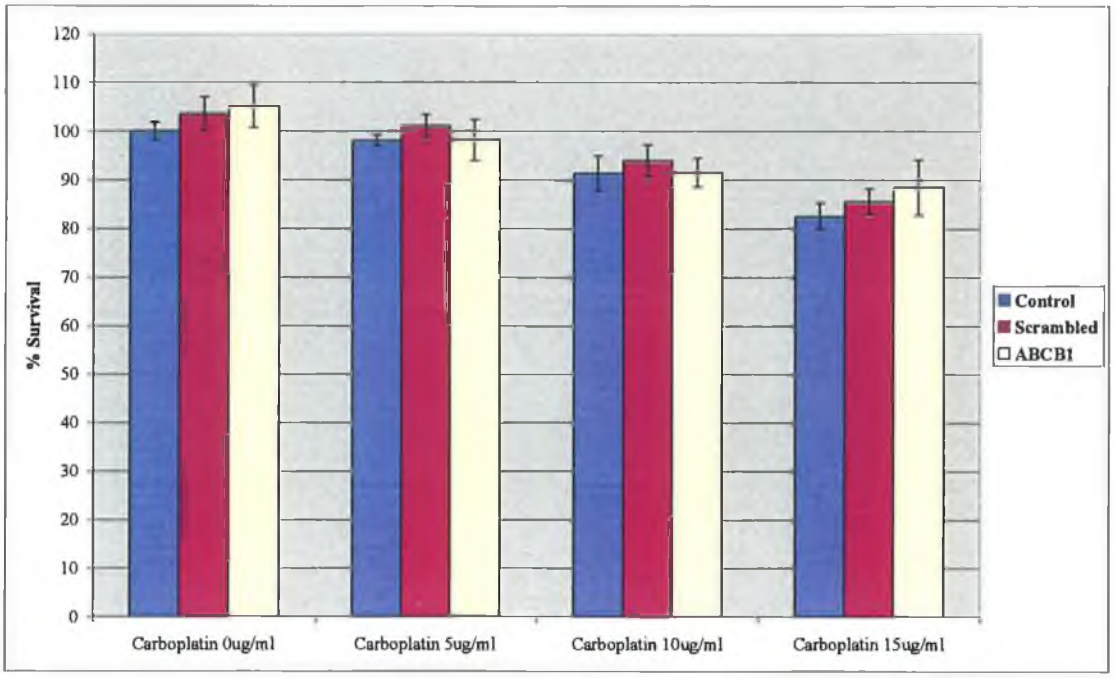

Figure 3.5.13 Effect of transfection of ABCB1 siRNA on carboplatin sensitivity in A549 cells

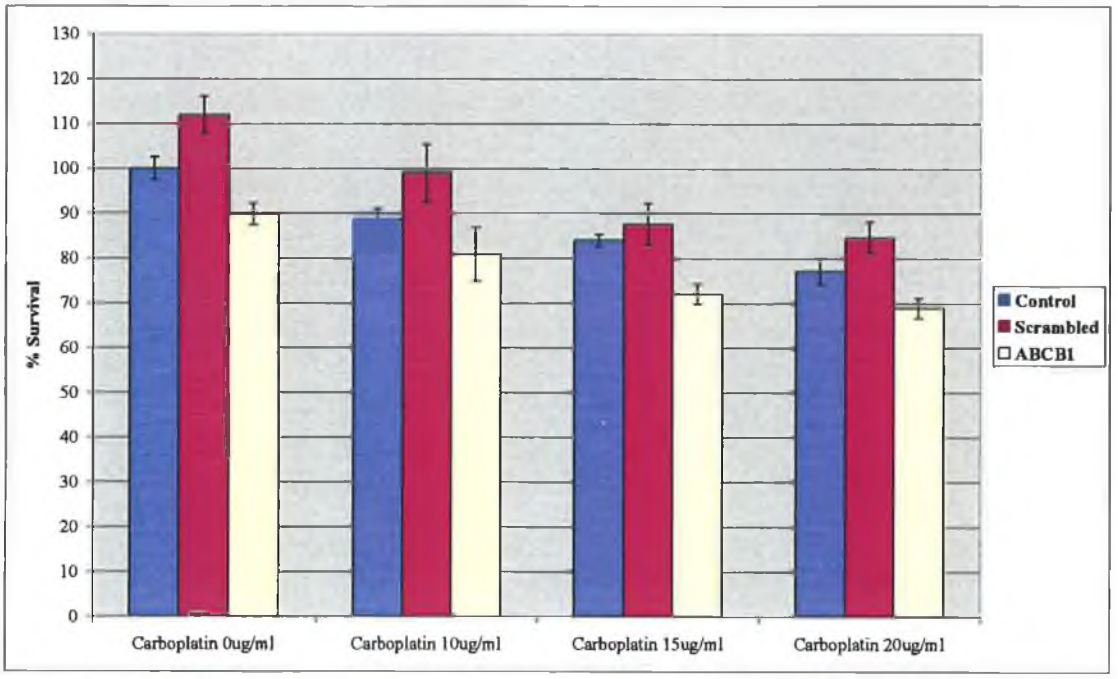

Figure 3.5.14 Effect of transfection of ABCB1 siRNA on carboplatin sensitivity in A549-tax cells

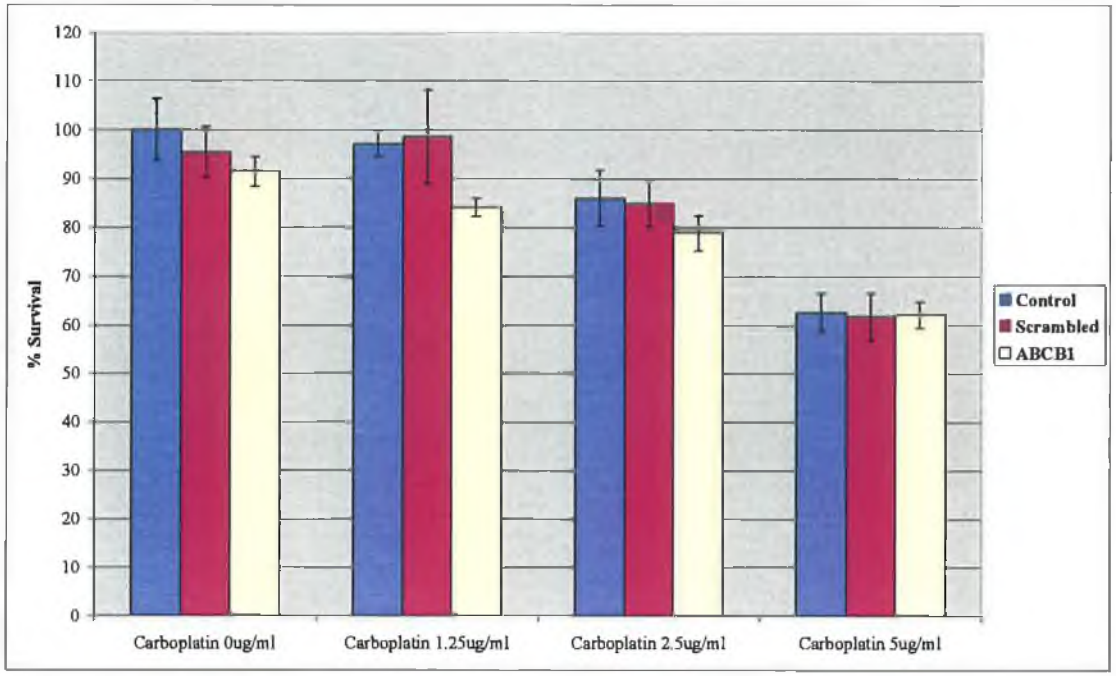

Figure 3.5.15 Effect of transfection of ABCB1 siRNA on carboplatin sensitivity in H460 cells

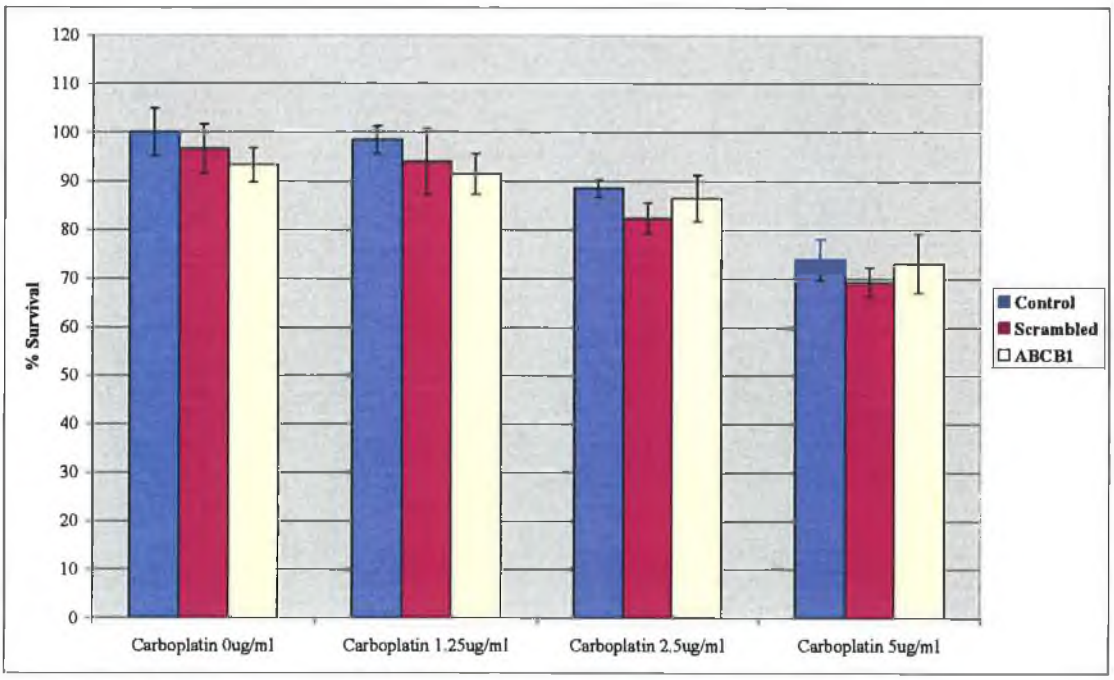

Figure 3.5.16 Effect of transfection of ABCB1 siRNA on carboplatin sensitivity in H460-tax cells

3.5.2 ID3

Silencing of this gene resulted in an increase in sensitivity to taxol. This was observed in all the cell lines tested. Silencing of this gene was tested for its effect on sensitivity to taxotere, adriamycin and carboplatin in the cell lines H1299, H1299-tax, A549, A549-tax, H460 and H460-tax. The results are shown in Figures 3.5.19-3.5.1.34. These results are summarised in Table 3.5.2.

Table 3.5.2 Summary of effects of transfection of ID3 siRNA

Cell line	*Taxotere*	*Adriamycin*	*Carboplatin*
H1299	Small ↑ sensitivity	No change	Small ↑ resistance
H1299-tax	No change	No change	Small ↑ resistance
A549	No change	ND	Small ↑ sensitivity
A549-tax	No change	ND	No change
H460	No change	No change	No change
H460-tax	No change	No change	No change

ND – not done

H1299 and H1299-tax (Figures 3.5.19 and 3.5.20) show an increase in sensitivity to taxotere with silencing of ID3. There was little or no effect observed in the other cell lines. There was no effect on the sensitivity observed in any of the cell lines to adriamycin after transfection with ID3 siRNA.

Silencing of ID3 resulted in an increase in sensitivity to carboplatin in A549 (Figure 3.5.31). Interestingly, there was a decrease in sensitivity to carboplatin observed in H1299 (Figure 3.5.29) and H1299-tax (Figure 3.5.30).

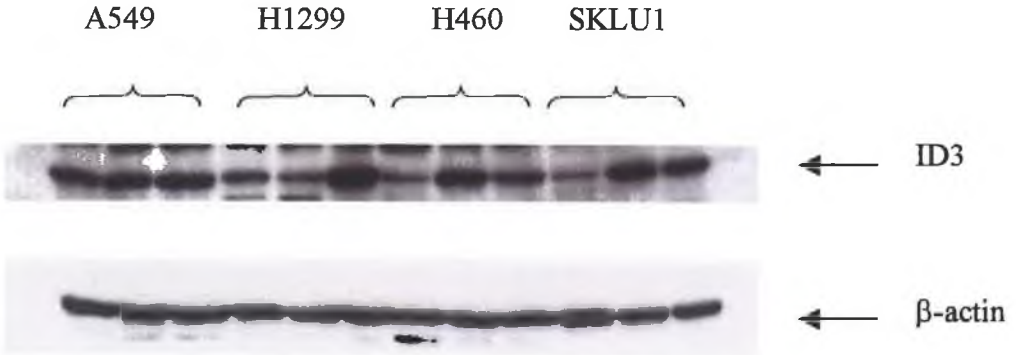

Figure 3.5.17 Expression of ID3 protein in selected cell lines
(each cell line samples in the order: parent; -tax; -cpt)

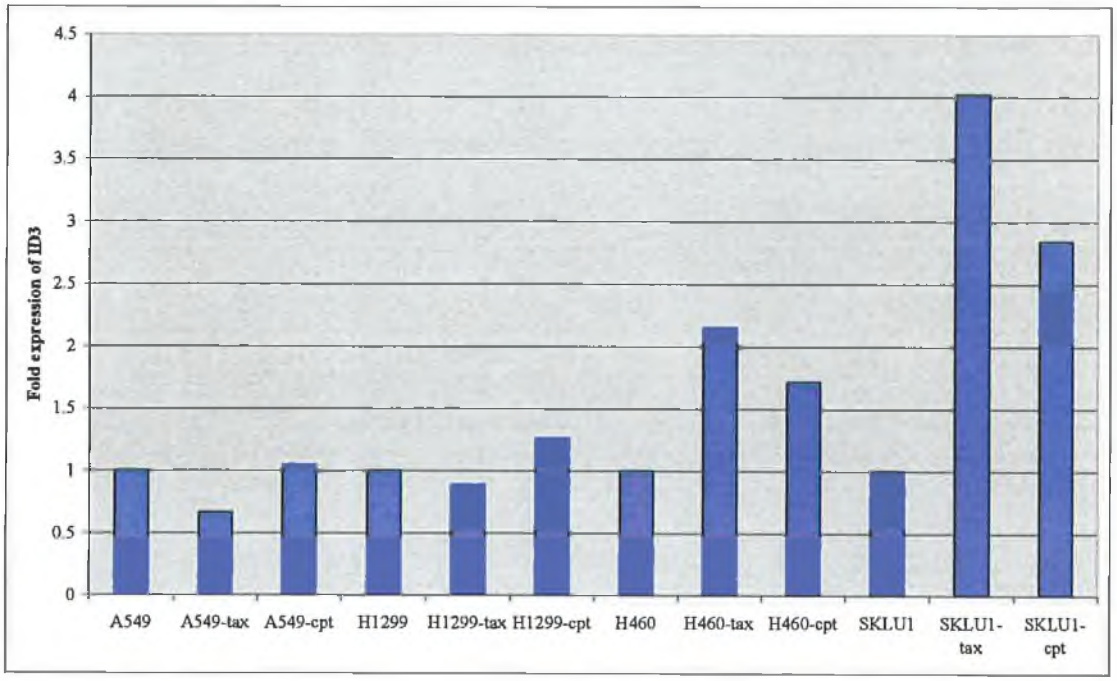

Figure 3.5.18 Densitometry showing fold expression of ID3

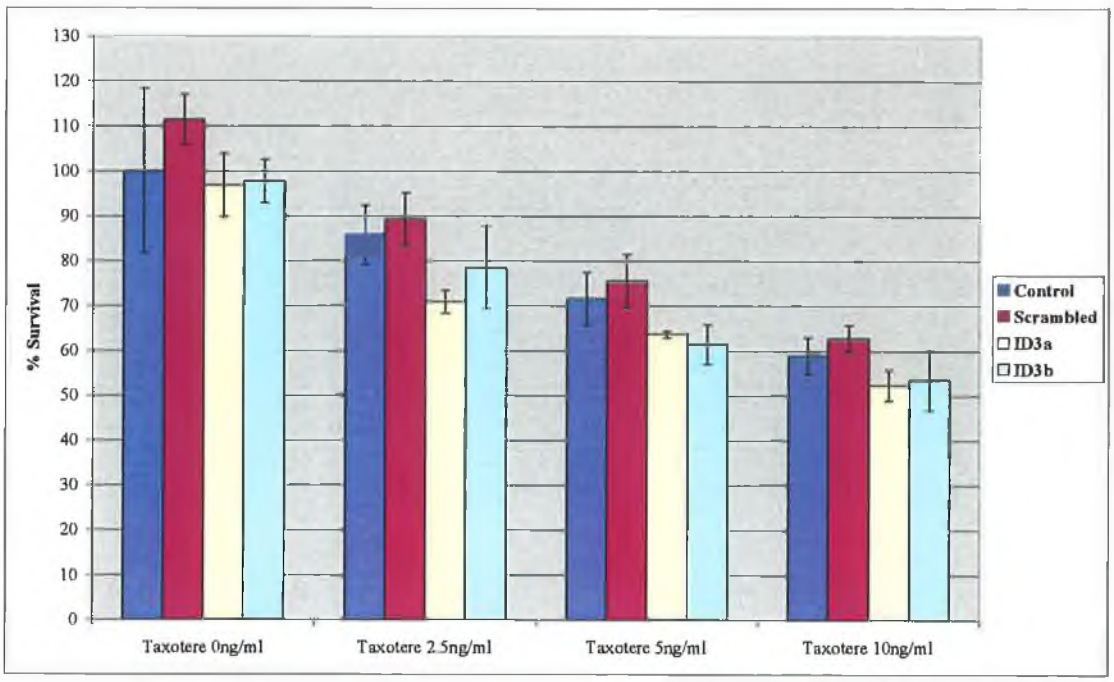

Figure 3.5.19 Effect of transfection of ID3 siRNA on taxotere sensitivity in H1299 cells

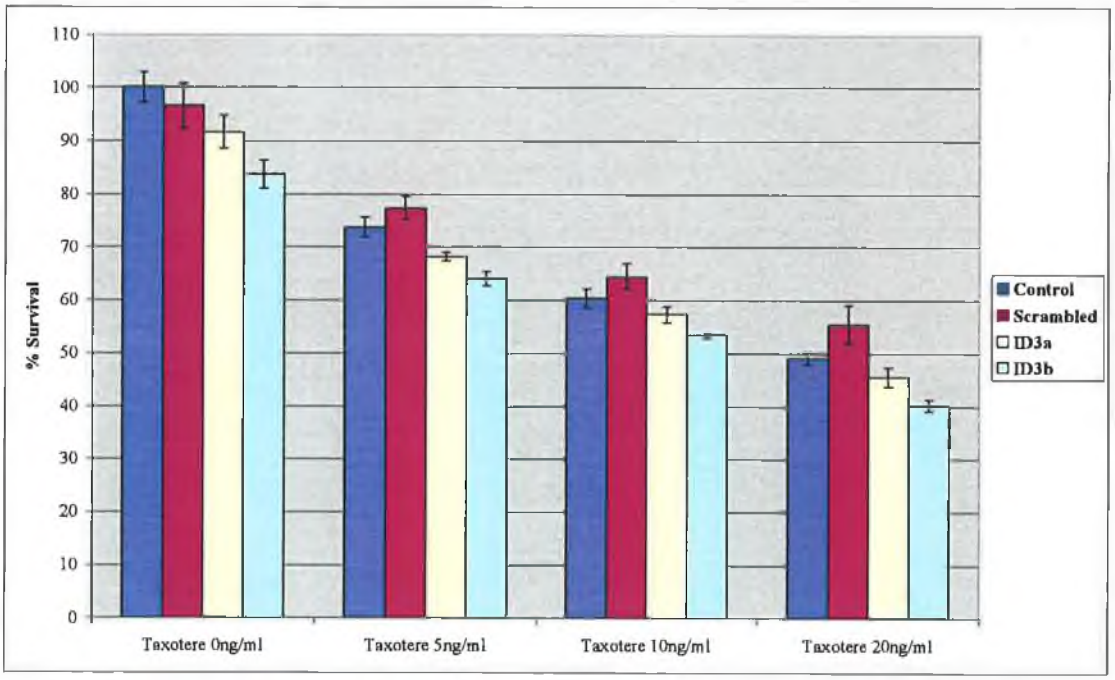

Figure 3.5.20 Effect of transfection of ID3 siRNA on taxotere sensitivity in H1299-tax cells

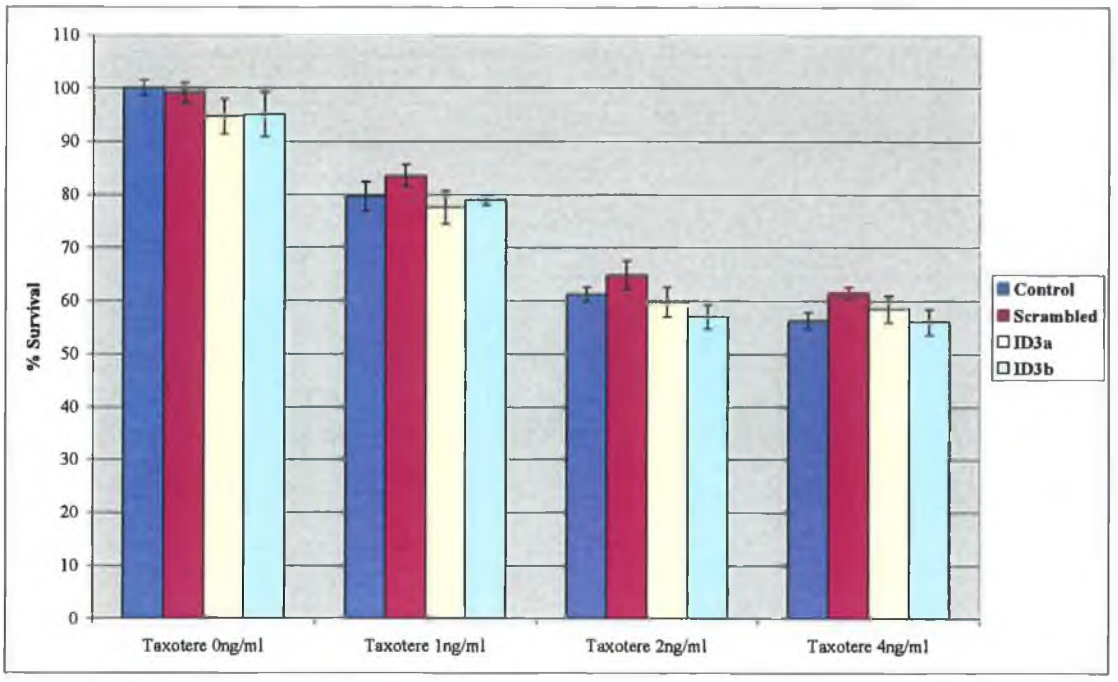

Figure 3.5.21 Effect of transfection of ID3 siRNA on taxotere sensitivity in A549 cells

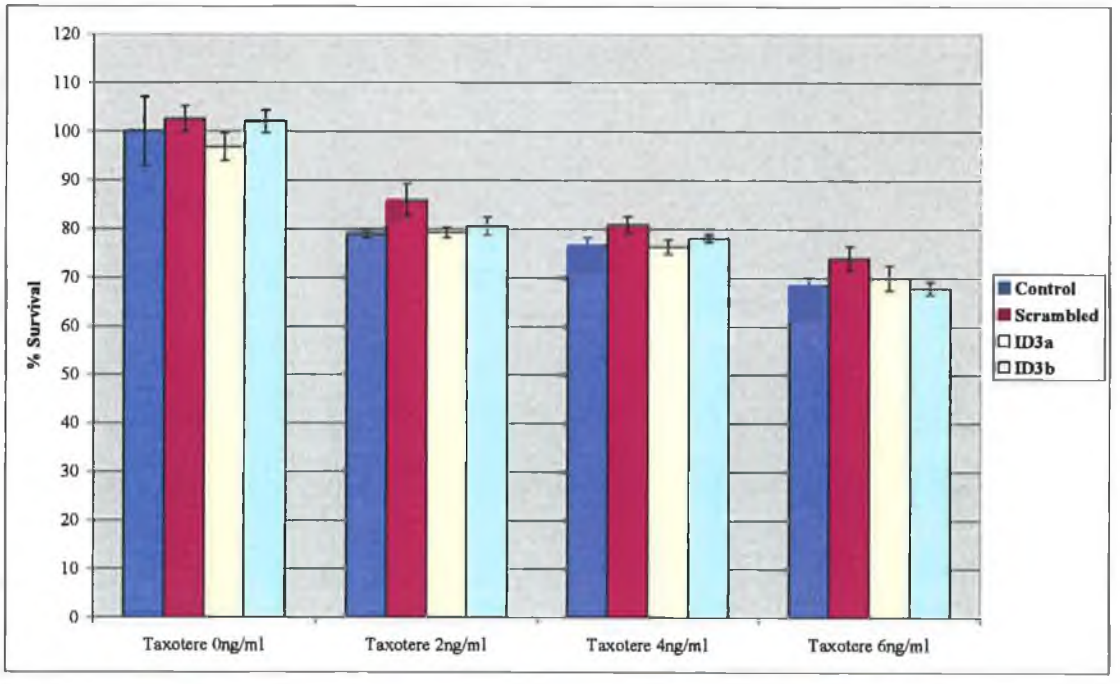

Figure 3.5.22 Effect of transfection of ID3 siRNA on taxotere sensitivity in A549-tax cells

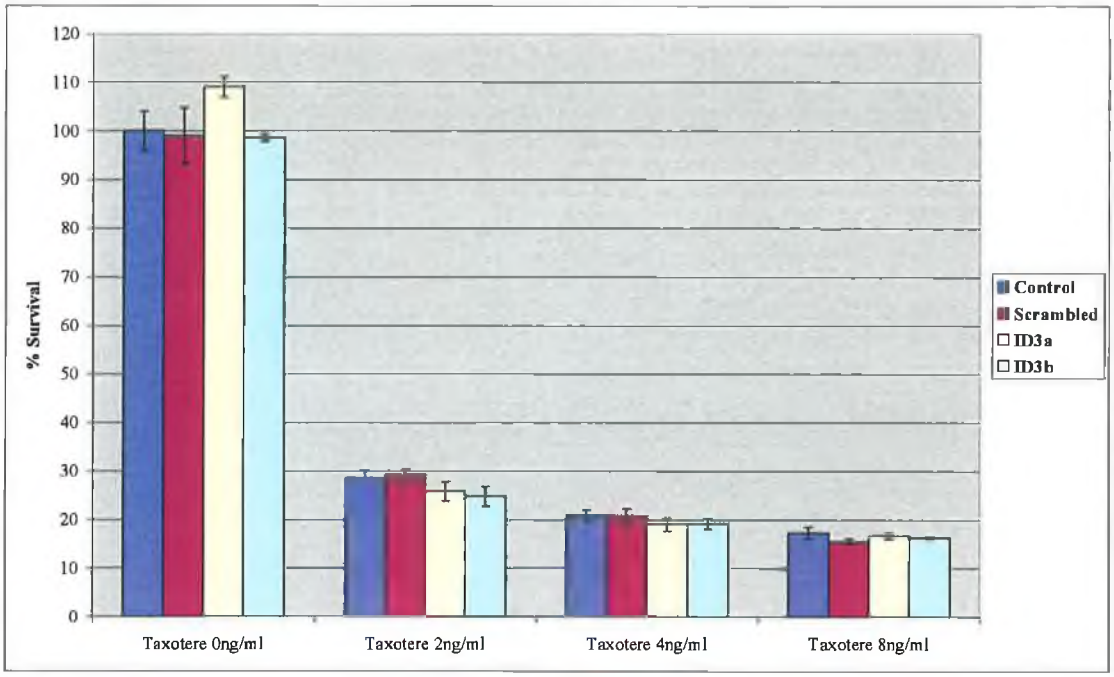

Figure 3.5.23 Effect of transfection of ID3 siRNA on taxotere sensitivity in H460 cells

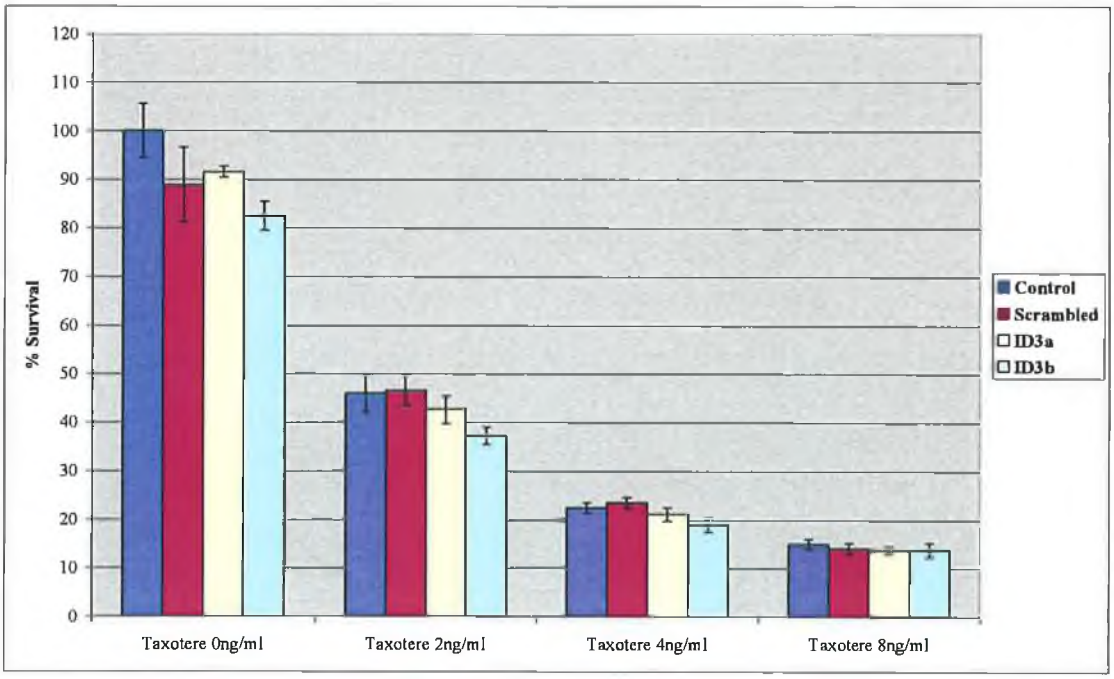

Figure 3.5.24 Effect of transfection of ID3 siRNA on taxotere sensitivity in H460-tax cells

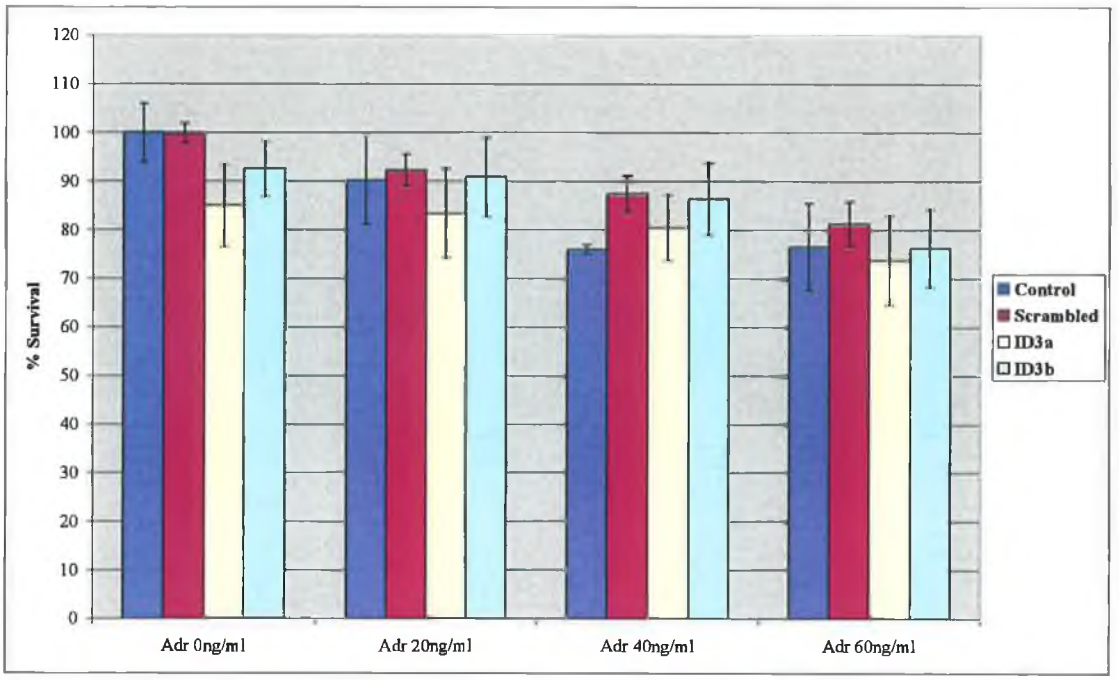

Figure 3.5.25 Effect of transfection of ID3 siRNA on adriamycin sensitivity in H1299 cells

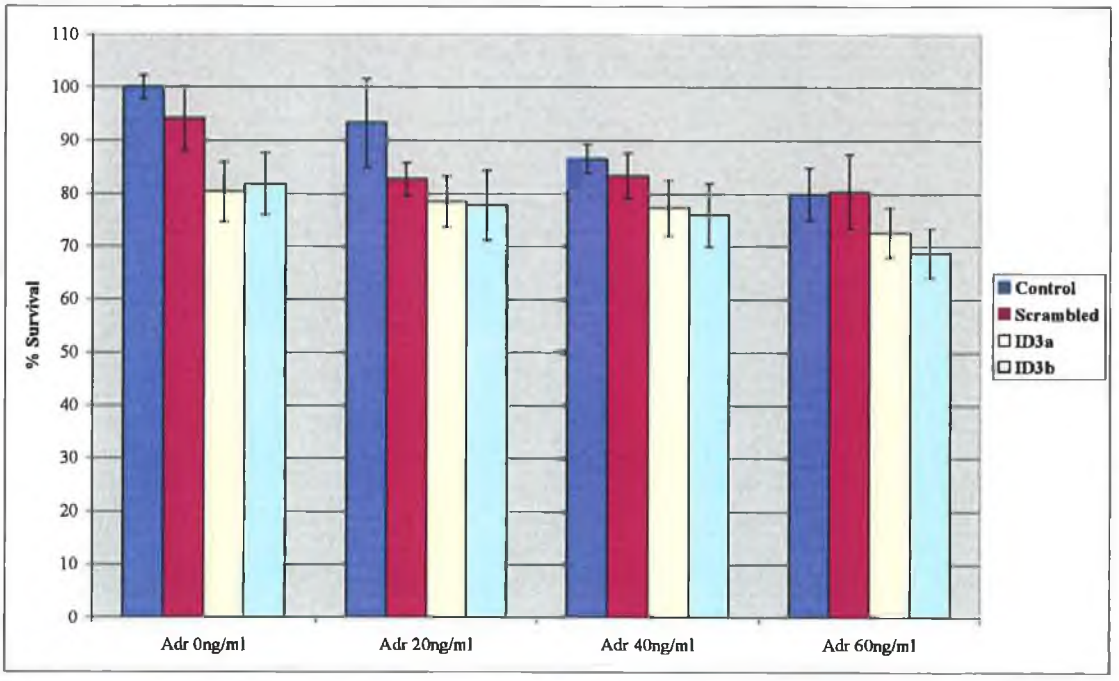

Figure 3.5.26 Effect of transfection of ID3 siRNA on adriamycin sensitivity in H1299-tax cells

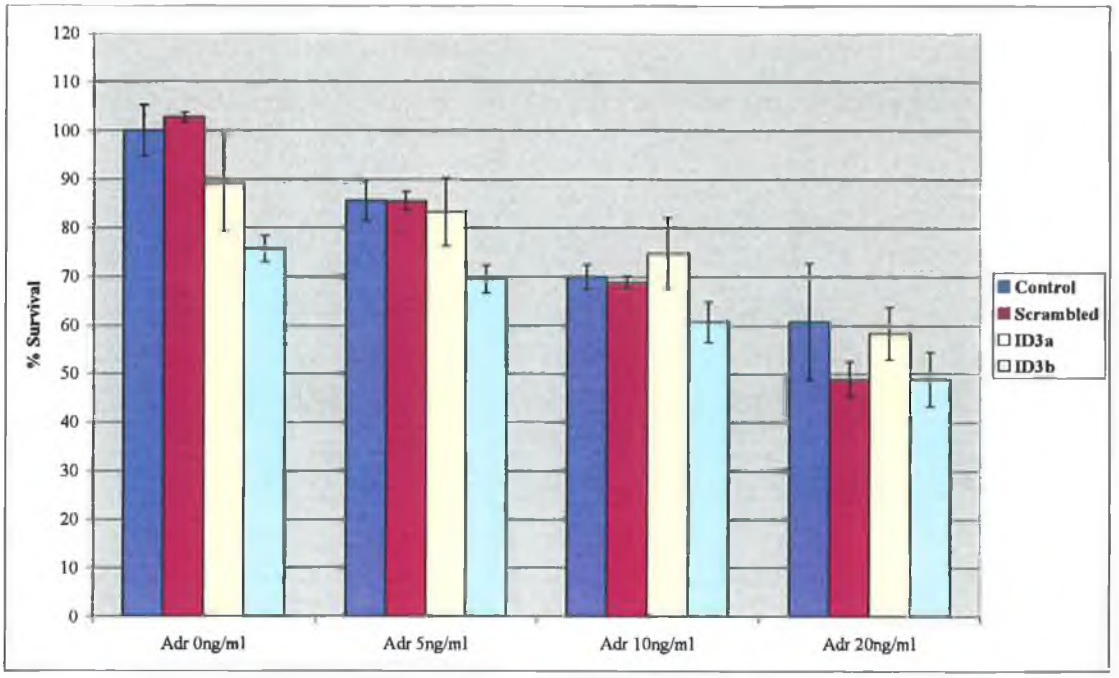

Figure 3.5.27 Effect of transfection of ID3 siRNA on adriamycin sensitivity in H460 cells

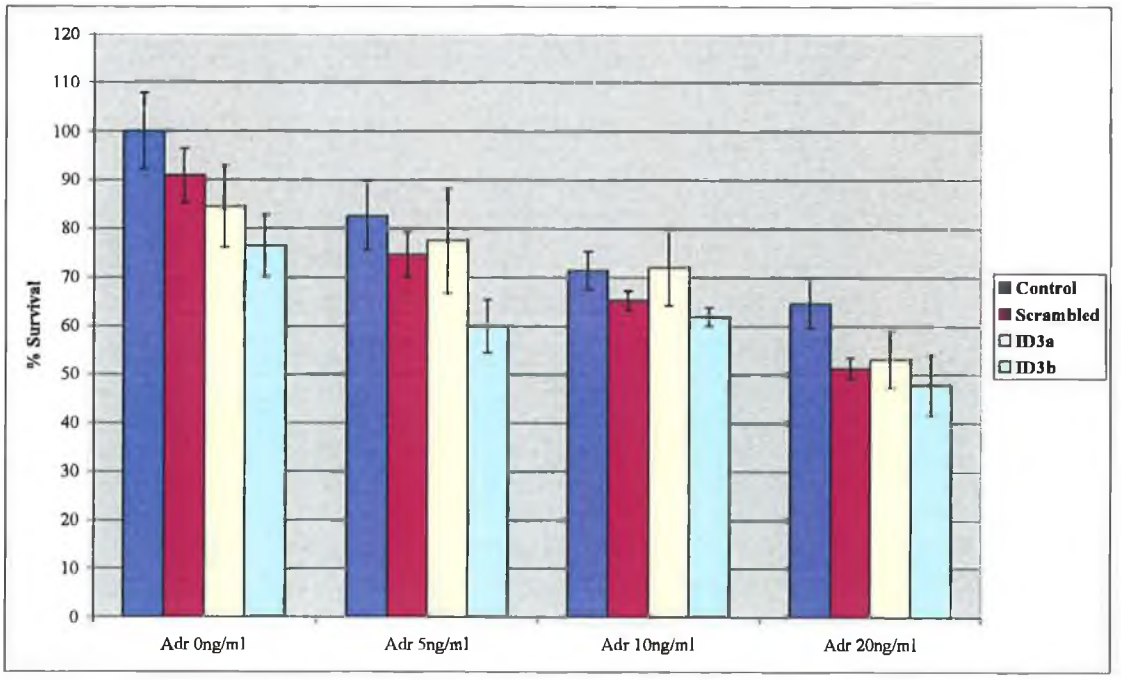

Figure 3.5.28 Effect of transfection of ID3 siRNA on adriamycin sensitivity in H460-tax cells

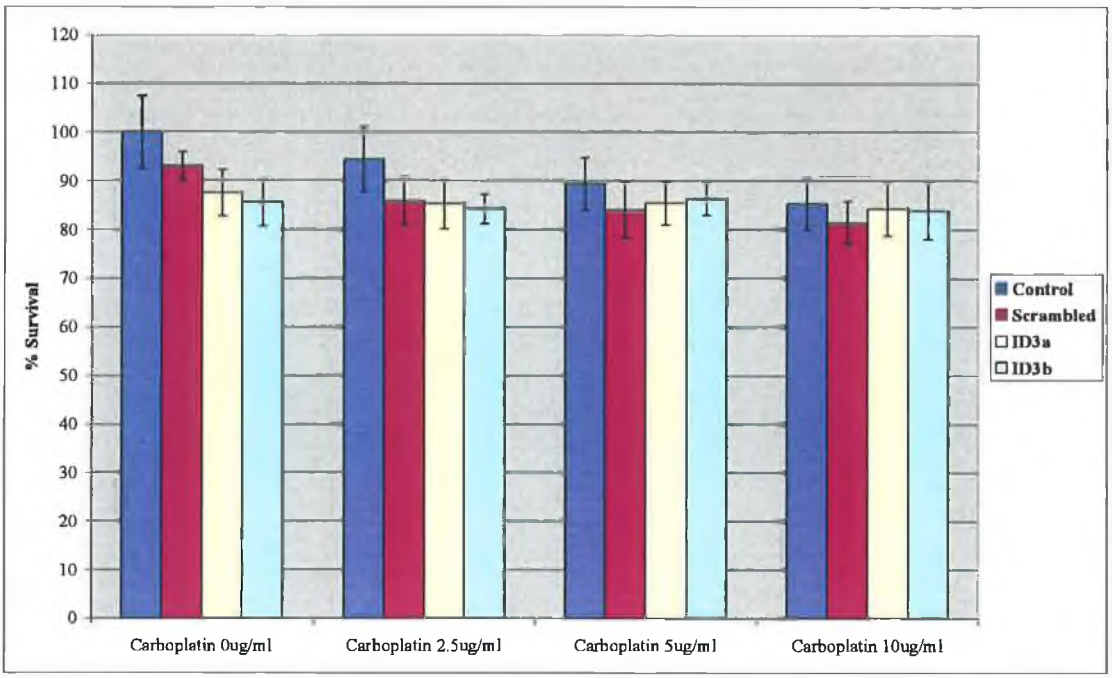

Figure 3.5.29 Effect of transfection of ID3 siRNA on carboplatin sensitivity in H1299 cells

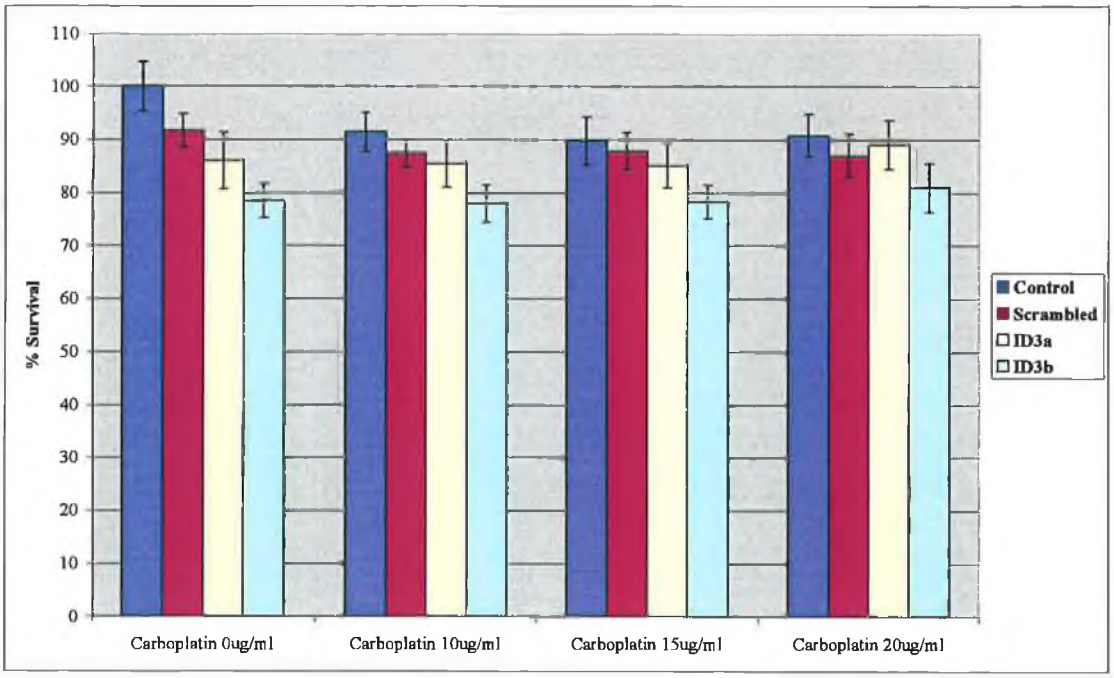

Figure 3.5.30 Effect of transfection of ID3 siRNA on carboplatin sensitivity in H1299-tax cells

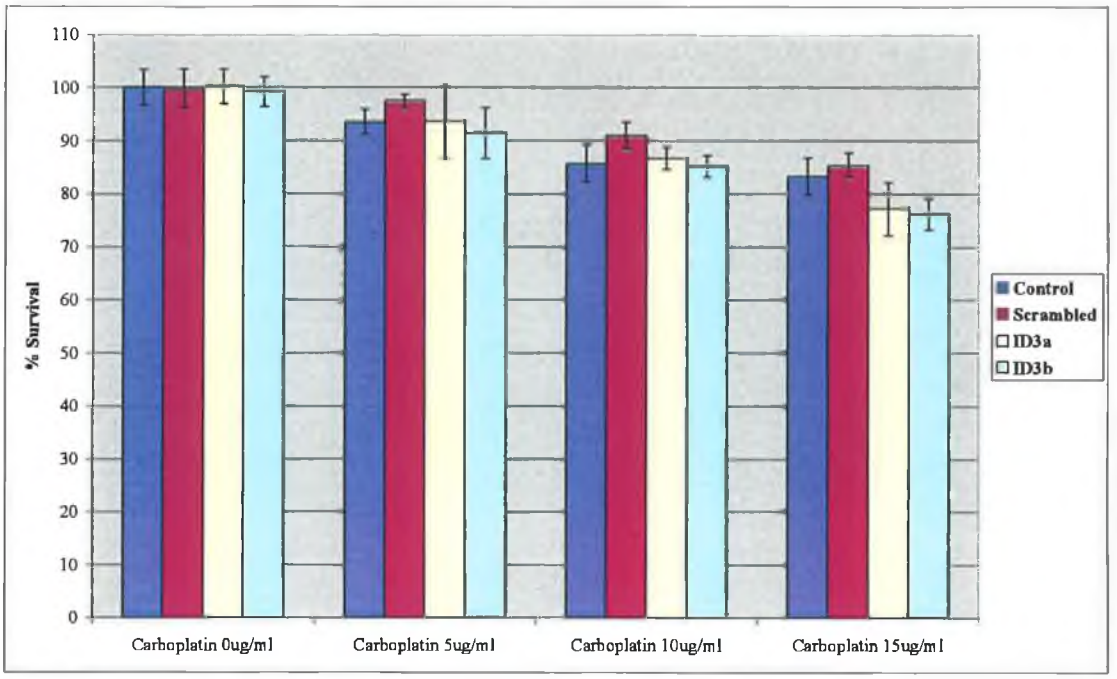

Figure 3.5.31 Effect of transfection of ID3 siRNA on carboplatin sensitivity in A549 cells

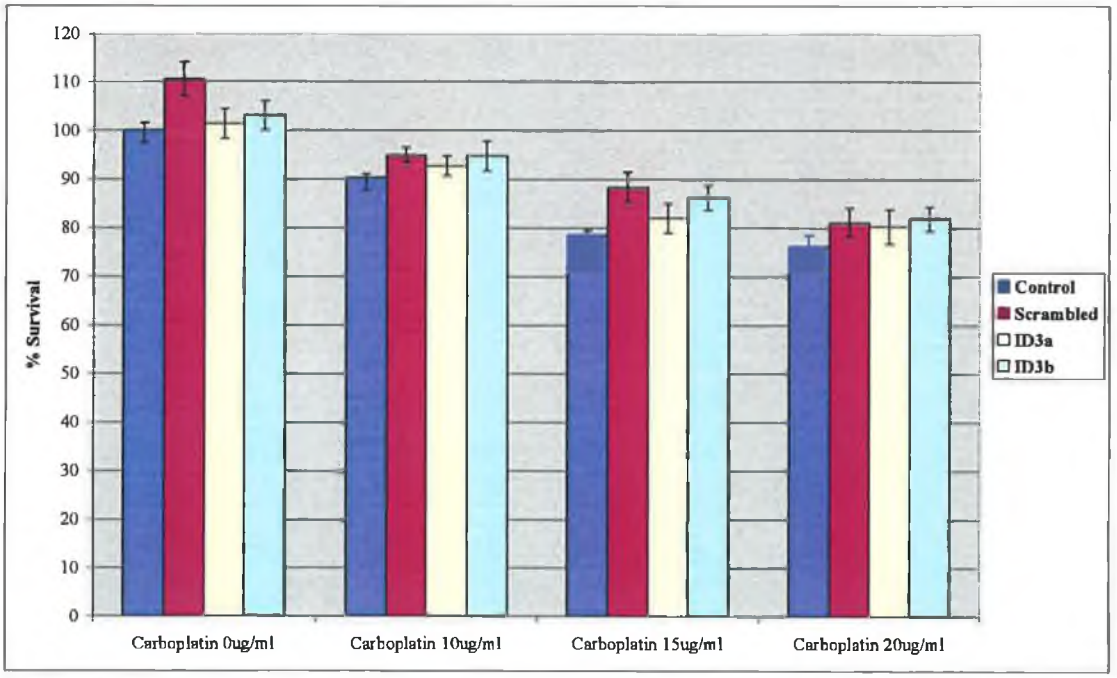

Figure 3.5.32 Effect of transfection of ID3 siRNA on carboplatin sensitivity in A549-tax cells

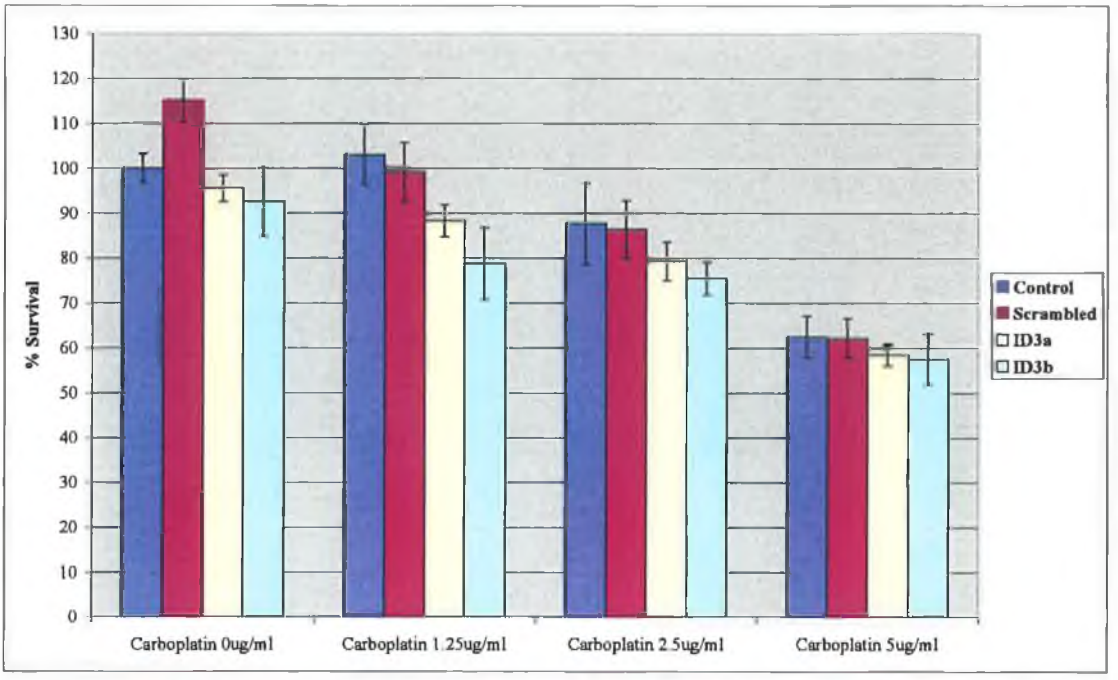

Figure 3.5.33 Effect of transfection of ID3 siRNA on carboplatin sensitivity in H460 cells

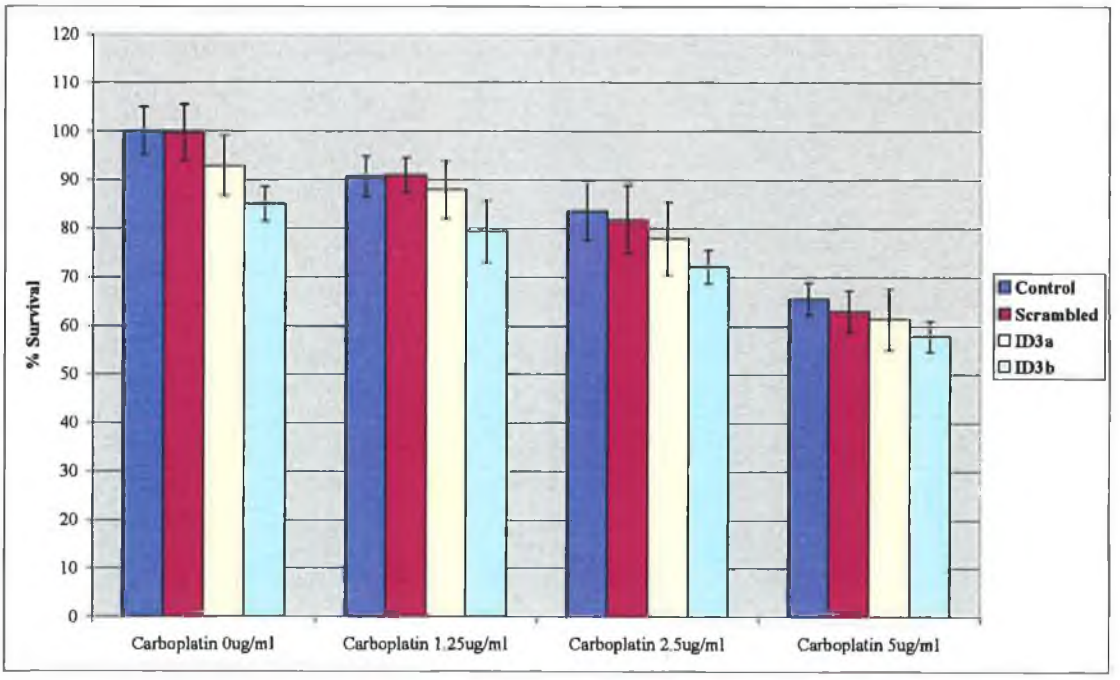

Figure 3.5.34 Effect of transfection of ID3 siRNA on carboplatin sensitivity in H460-tax cells

3.5.3 CRIP1

Transfection of CRIP1 siRNA resulted in a decrease in sensitivity to taxol. This effect was only seen in the A549 parental and taxol-resistant cells. The effect on sensitivity to taxotere, adriamycin and carboplatin in the cell lines H1299, H1299-tax, A549, A549-tax, H460 and H460-tax was tested after transfection with CRIP1 siRNA. The results are shown in Figures 3.5.37-3.5.1.52. These results are summarised in Table 3.5.3.

Table 3.5.3 Summary of effects of transfection of CRIP1 siRNA

Cell line	*Taxotere*	*Adriamycin*	*Carboplatin*
H1299	Small ↑ sensitivity	Small ↑ resistance	↑ resistance
H1299-tax	↑ sensitivity	No change	Small ↑ resistance
A549	Small ↑ sensitivity	ND	Small ↑ sensitivity
A549-tax	Small ↑ sensitivity	ND	Small ↑ resistance
H460	No change	Small ↑ resistance	No change
H460-tax	No change	Small ↑ resistance	No change

ND – not done

H1299 (Figure 3.5.37), H1299-tax (Figure 3.5.38), A549 (Figure 3.5.39) and A549-tax (Figure 3.5.40) all showed an increase in sensitivity to taxotere after transfection with CRIP1 siRNA. This was unexpected, especially in A549 cells considering that the opposite effect was observed in taxol sensitivity.

A decrease in adriamycin sensitivity was observed in H1299 (Figure 3.5.43) and H460 (3.5.45) after transfection with CRIP1 siRNA.

Similarly, a decrease in sensitivity to carboplatin was observed in H1299 (Figure 3.5.47), H1299-tax (Figure 3.5.48) and A549-tax (Figure 3.5.50) after siRNA transfection with CRIP1. In contrast, there was a small increase in sensitivity to carboplatin observed in A549 (Figure 3.5.49).

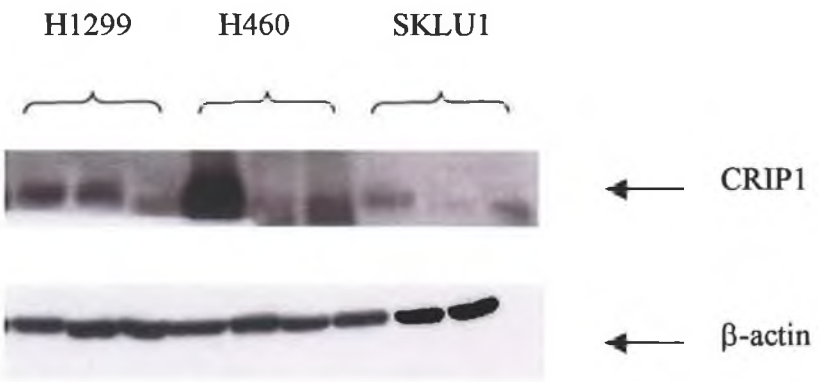

Figure 3.5.35 Expression of CRIP1 protein in selected cell lines
(each cell line samples in the order: parent; -tax; -cpt)

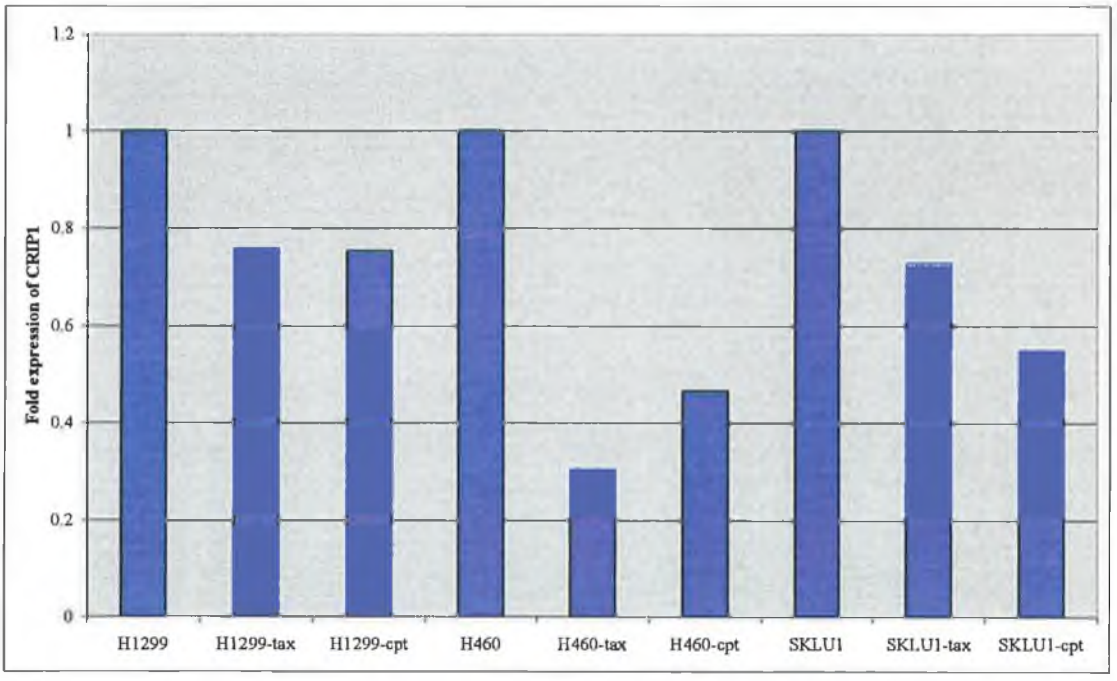

Figure 3.5.36 Densitometry showing fold expression of CRIP1

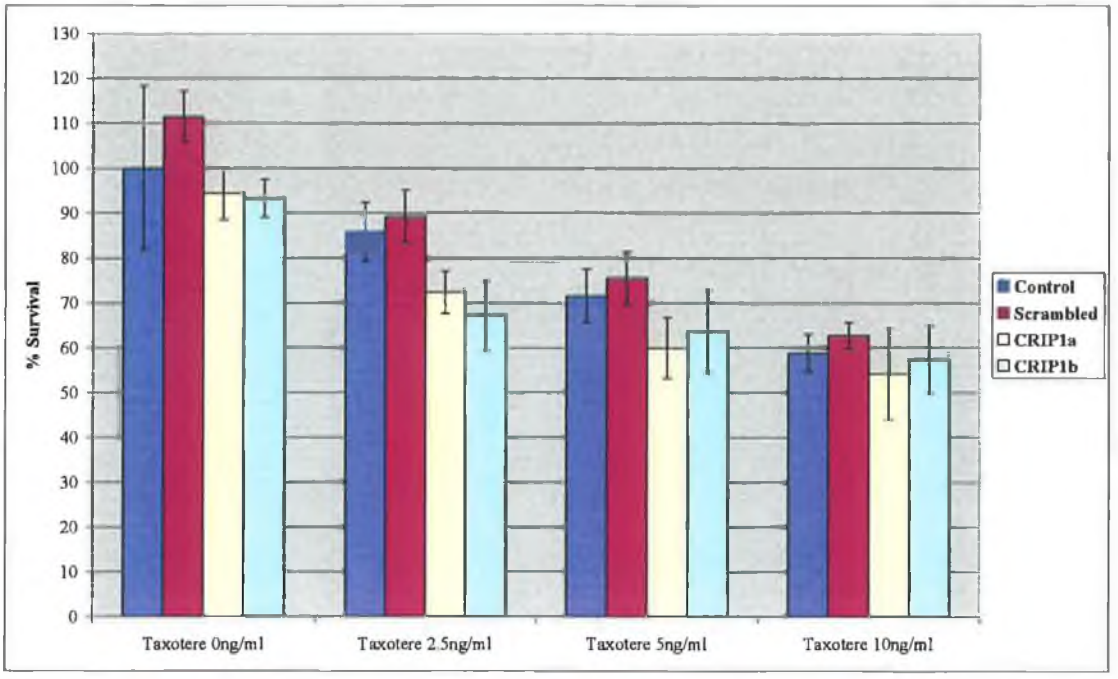

Figure 3.5.37 Effect of transfection of CRIP1 siRNA on taxotere sensitivity in H1299 cells

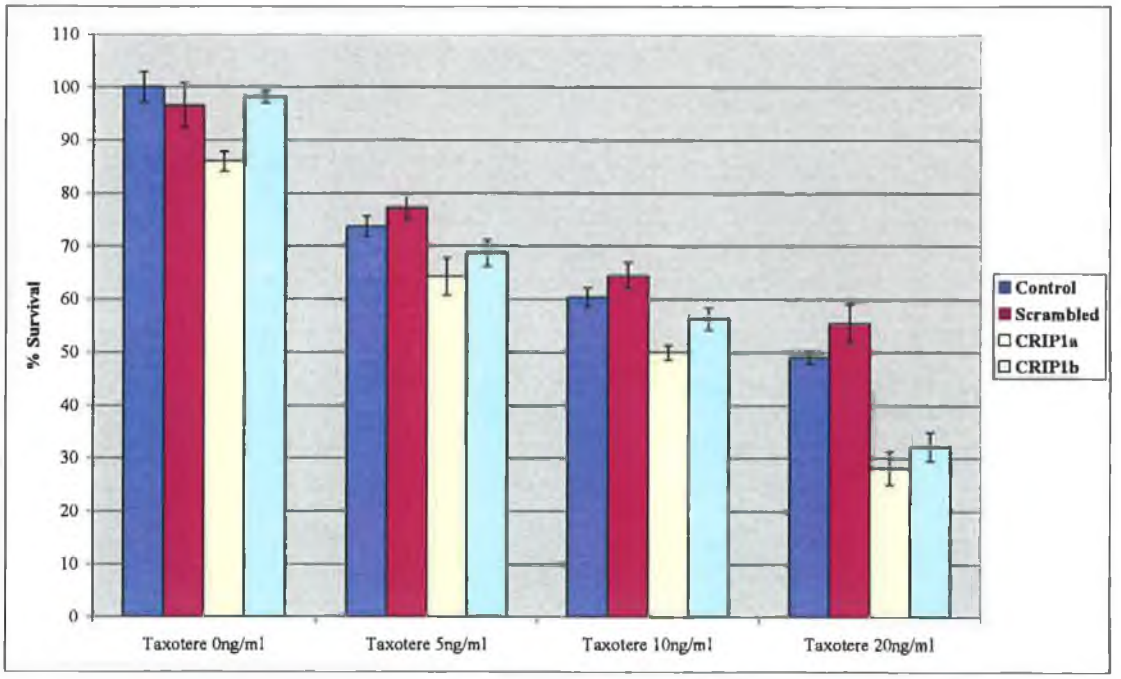

Figure 3.5.38 Effect of transfection of CRIP1 siRNA on taxotere sensitivity in H1299-tax cells

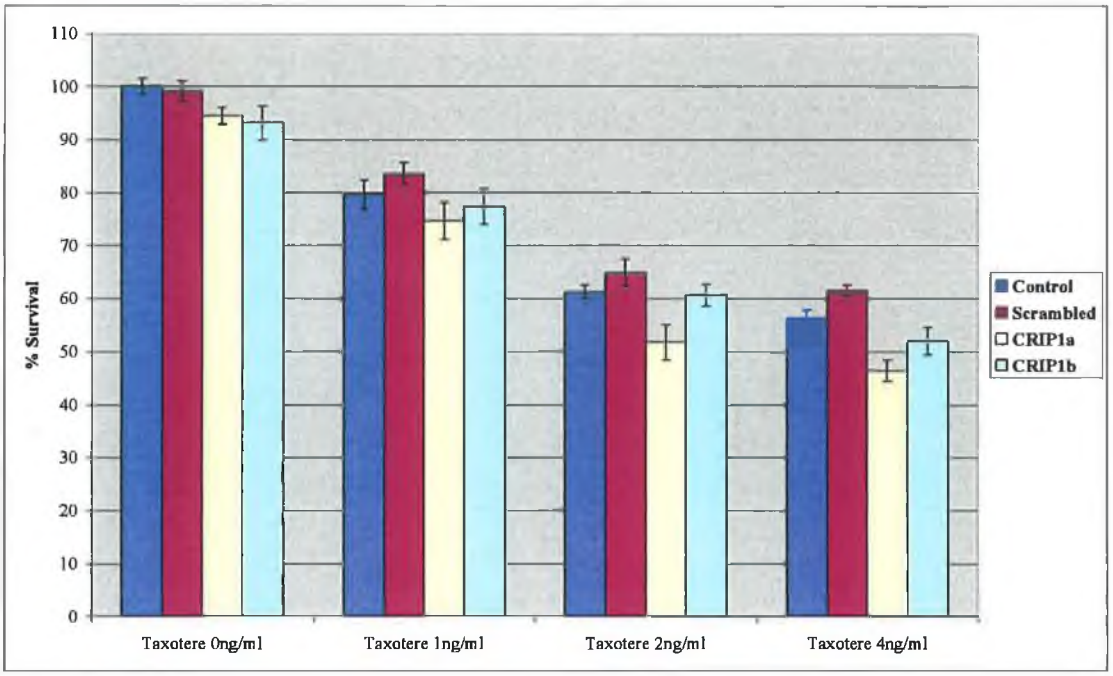

Figure 3.5.39 Effect of transfection of CRIP1 siRNA on taxotere sensitivity in A549 cells

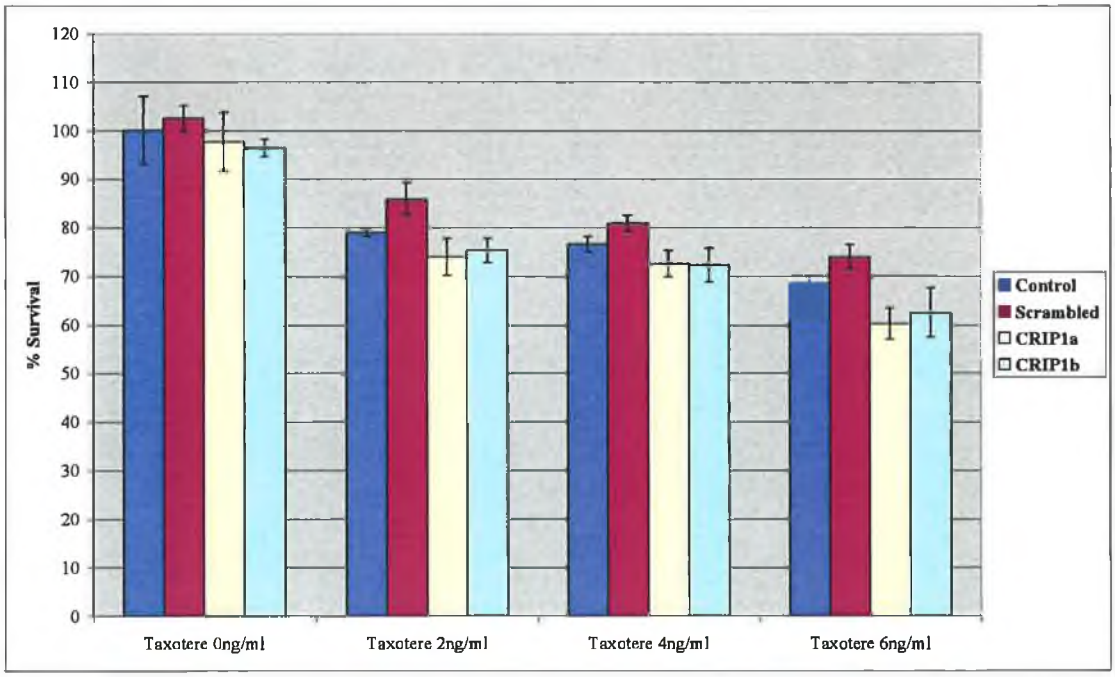

Figure 3.5.40 Effect of transfection of CRIP1 siRNA on taxotere sensitivity in A549-tax cells

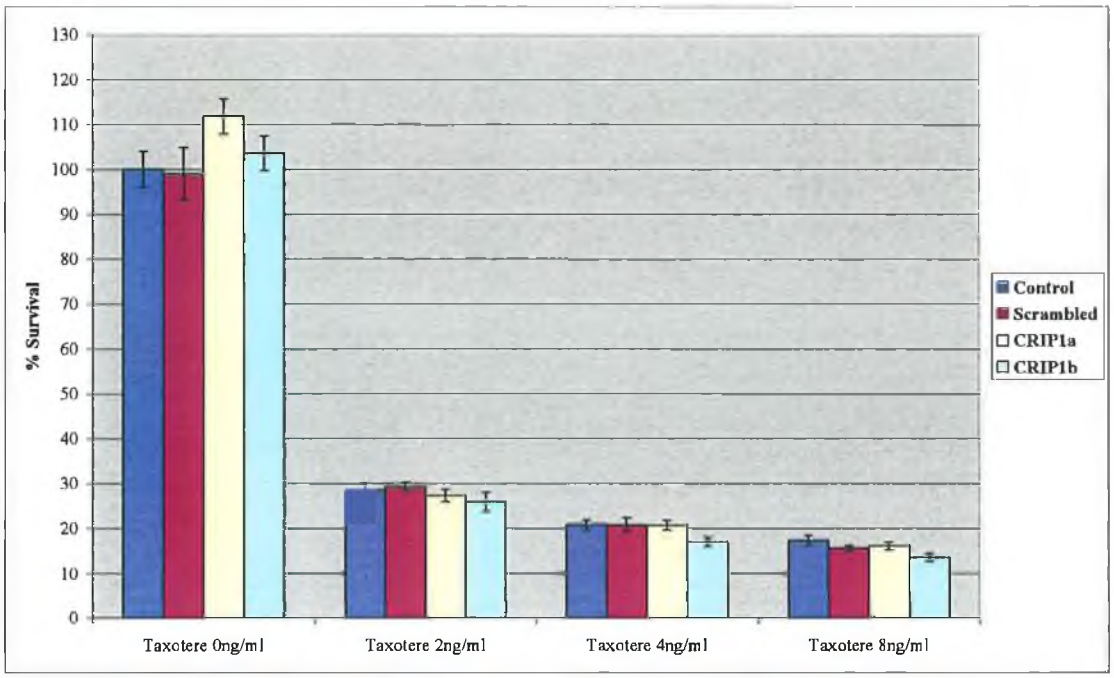

Figure 3.5.41 Effect of transfection of CRIP1 siRNA on taxotere sensitivity in H460 cells

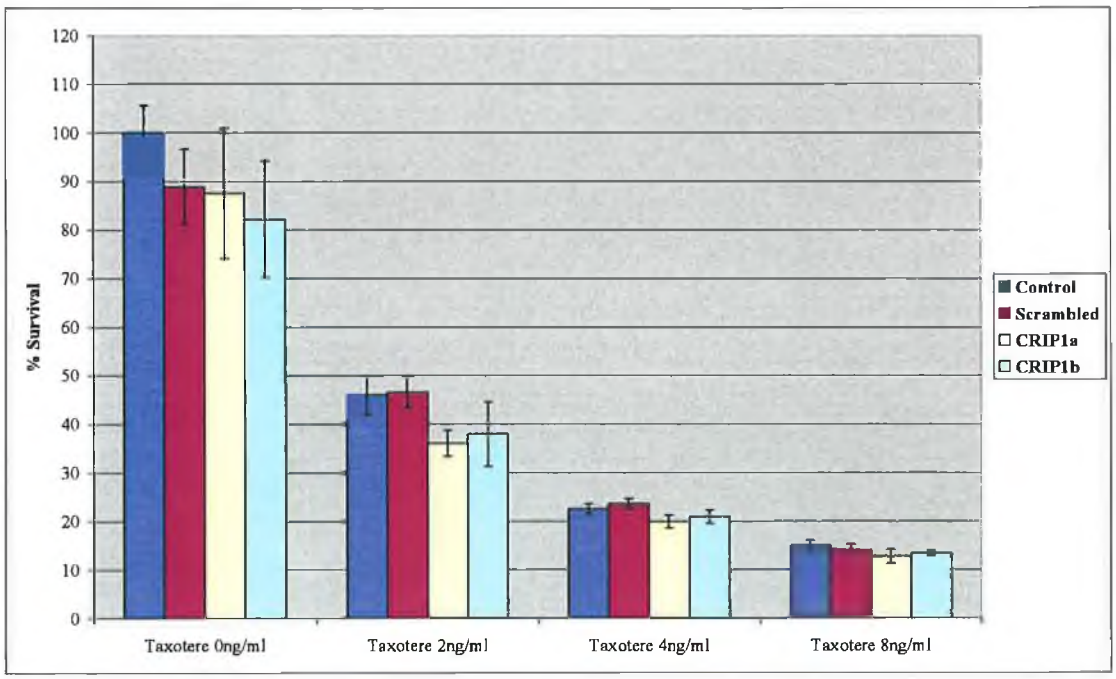

Figure 3.5.42 Effect of transfection of CRIP1 siRNA on taxotere sensitivity in H460-tax cells

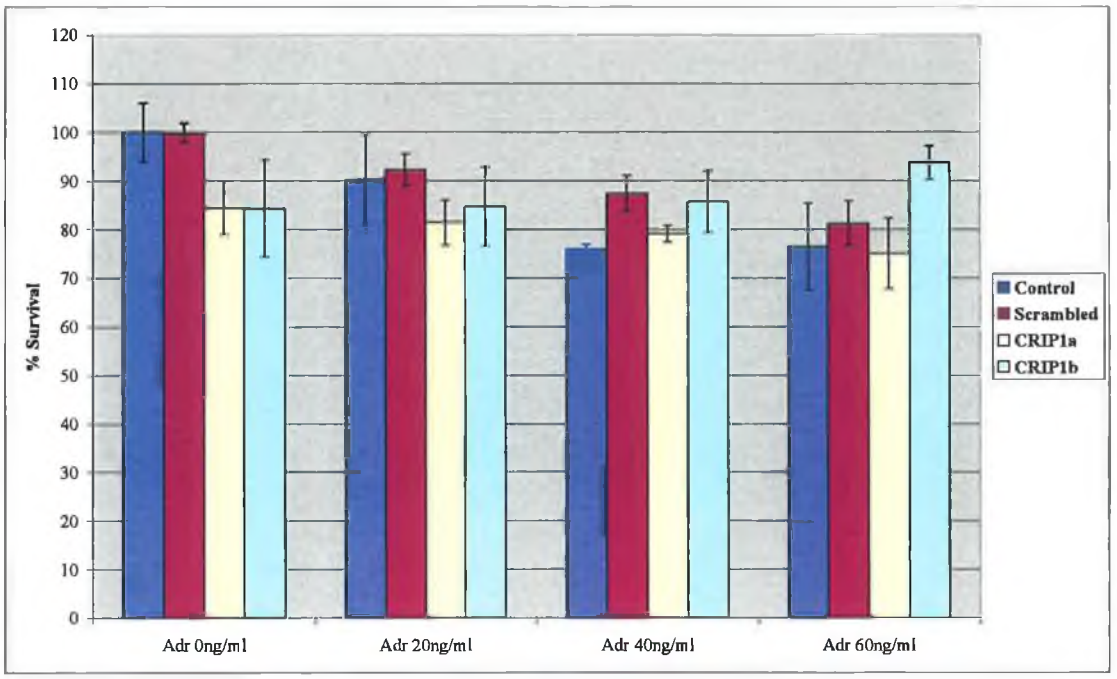

Figure 3.5.43 Effect of transfection of CRIP1 siRNA on adriamycin sensitivity in H1299 cells

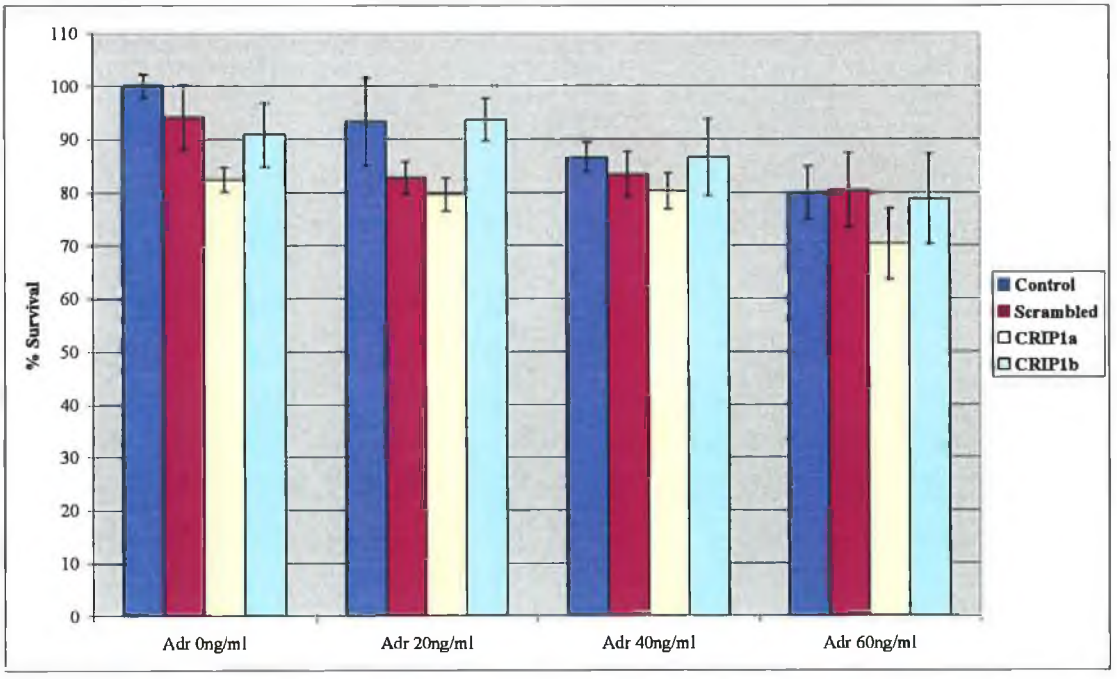

Figure 3.5.44 Effect of transfection of CRIP1 siRNA on adriamycin sensitivity in H1299-tax cells

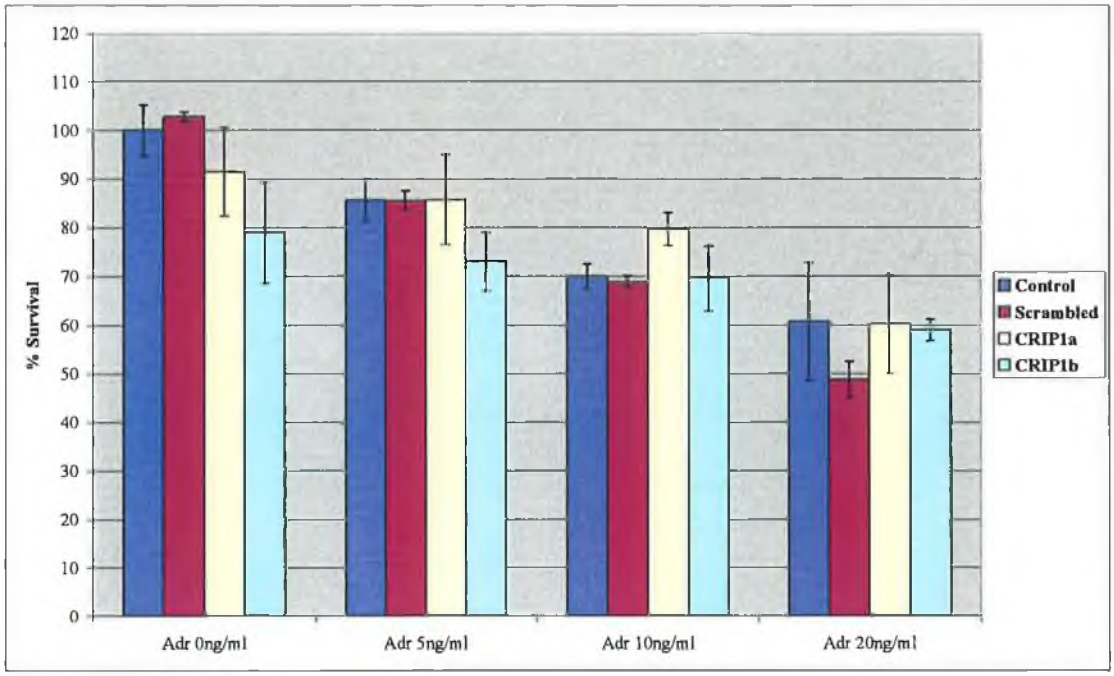

Figure 3.5.45 Effect of transfection of CRIP1 siRNA on adriamycin sensitivity in H460 cells

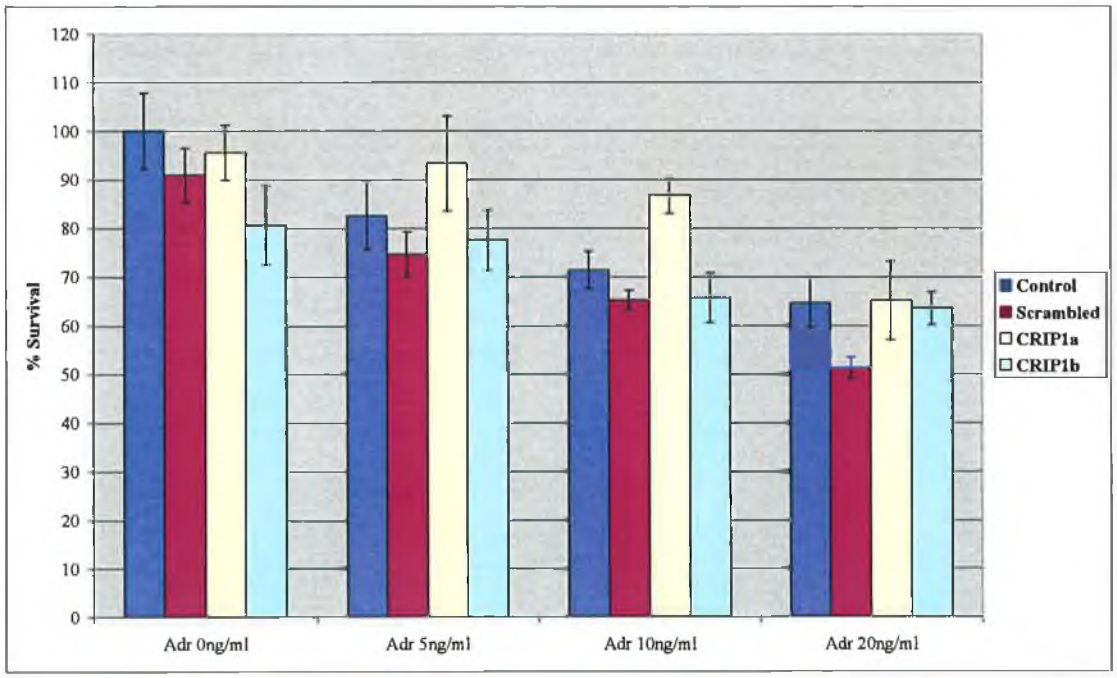

Figure 3.5.46 Effect of transfection of CRIP1 siRNA on adriamycin sensitivity in H460-tax cells

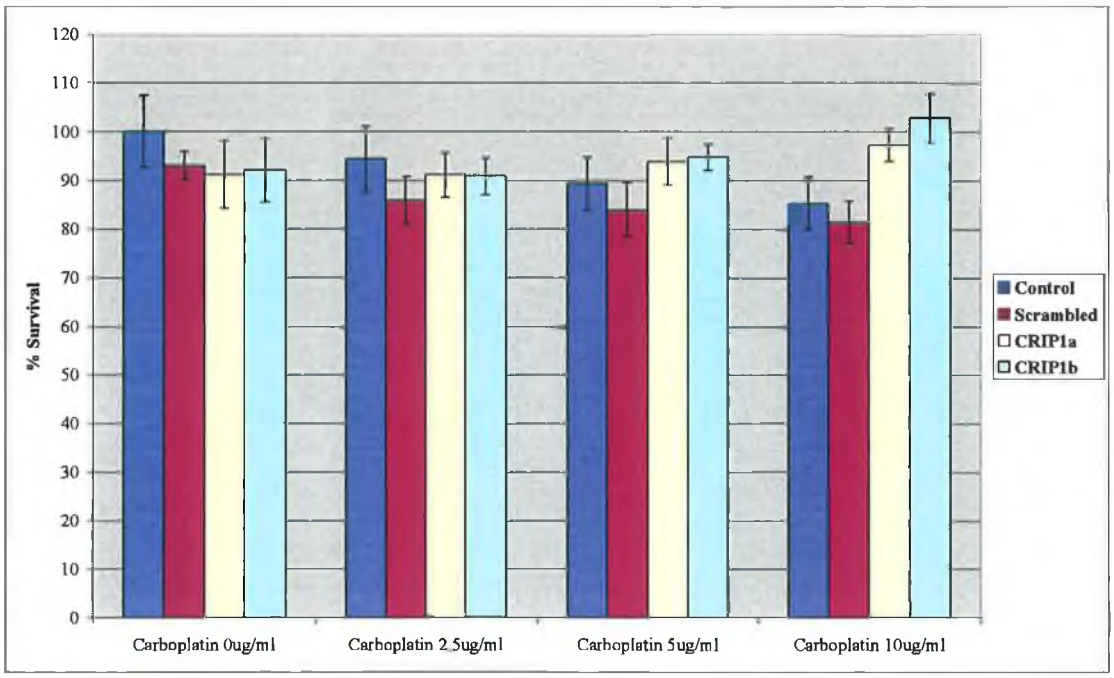

Figure 3.5.47 Effect of transfection of CRIP1 siRNA on carboplatin sensitivity in H1299 cells

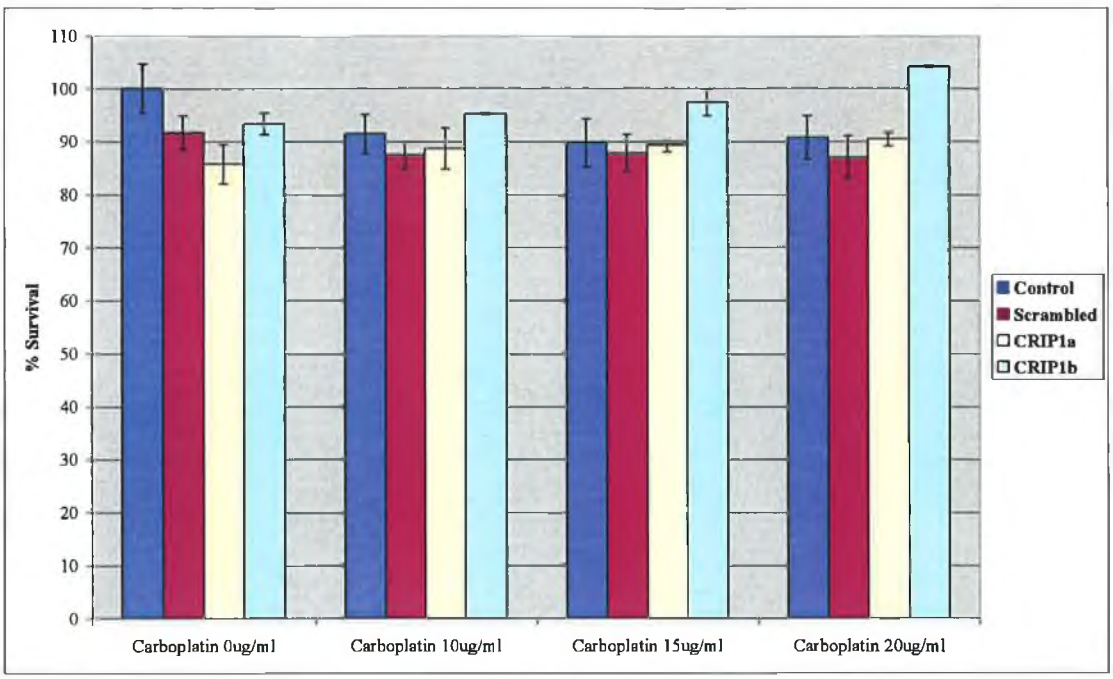

Figure 3.5.48 Effect of transfection of CRIP1 siRNA on carboplatin sensitivity in H1299-tax cells

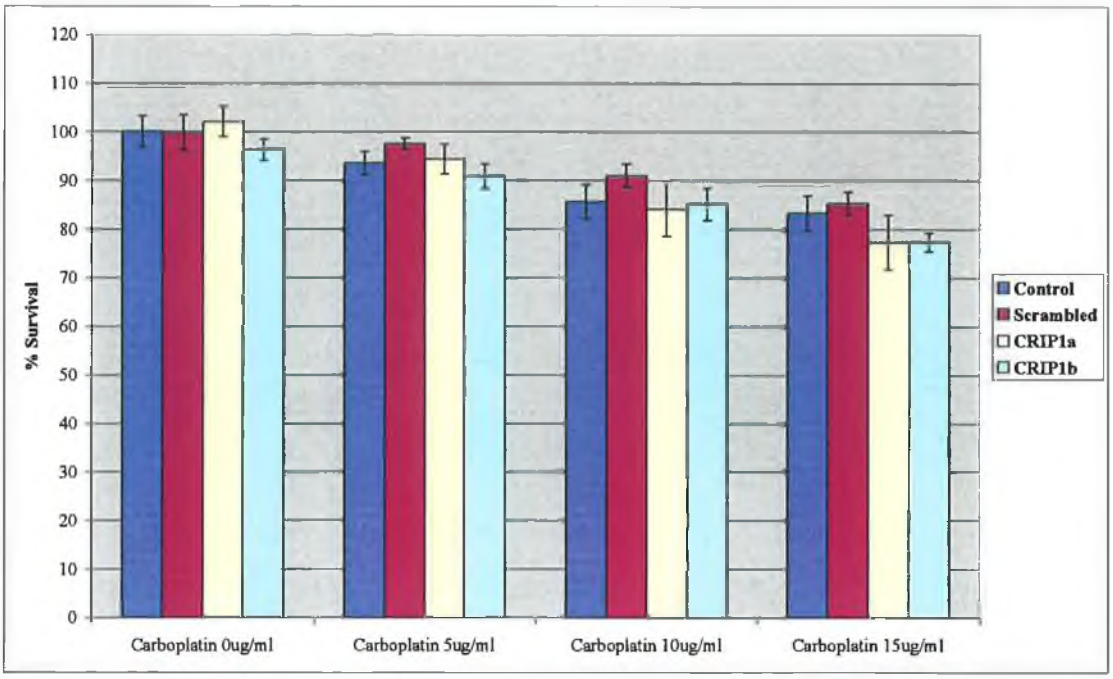

Figure 3.5.49 Effect of transfection of CRIP1 siRNA on carboplatin sensitivity in A549 cells

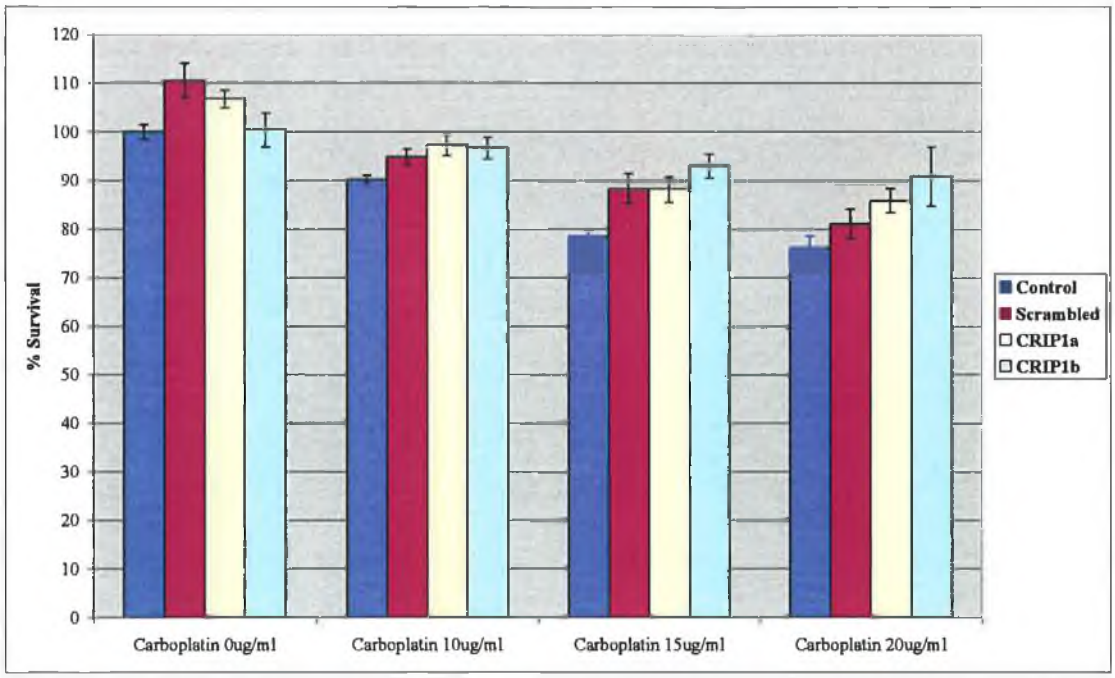

Figure 3.5.50 Effect of transfection of CRIP1 siRNA on carboplatin sensitivity in A549-tax cells

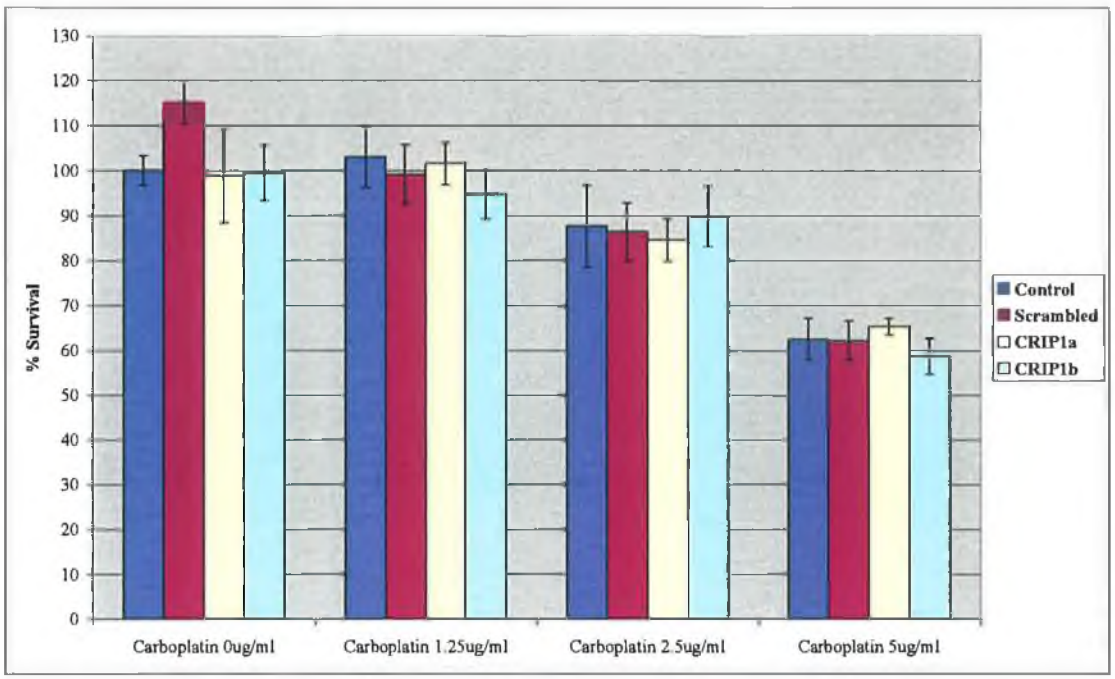

Figure 3.5.51 Effect of transfection of CRIP1 siRNA on carboplatin sensitivity in H460 cells

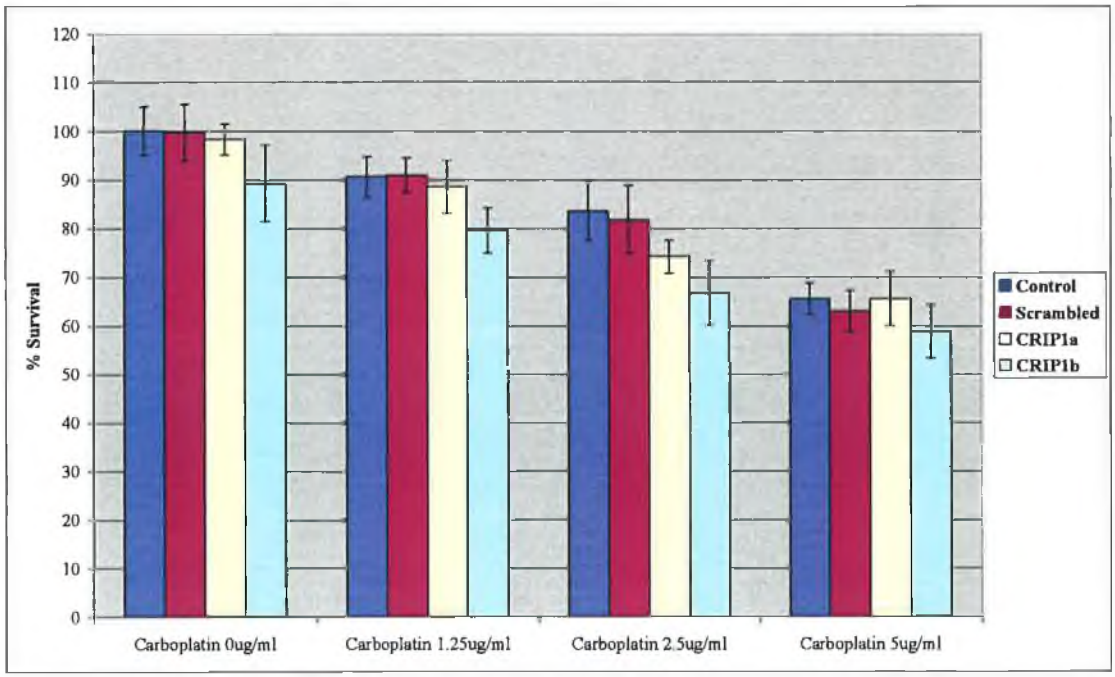

Figure 3.5.52 Effect of transfection of CRIP1 siRNA on carboplatin sensitivity in H460-tax cells

3.5.4 Screening of H1299-tax using siRNA library plates

In order to further identify genes whose expression might play a role in taxol resistance, a number of experiments were carried out in collaboration with Dr. Patrick Gammell on the cell line established in this project, H1299-tax. These experiments used commercially available library plates for high-throughput screening of siRNAs. The library plates used were from Ambion Inc. - *Silencer*® CellReady™ Popular Gene siRNA Library and *Silencer*® CellReady™ Popular Kinase siRNA Library.

Some genes of interest were determined from these assays. The results can be seen in Figures 3.5.53 and 3.5.54. Transfection of caspase 2, CDC2 and Kif11 siRNAa were found to dramatically affect cell growth in H1299-tax. Kif 11 and PLK1 were found to affect cell growth on the kinase library plate. Kif11 was the positive control included in all siRNA proliferation experiments.

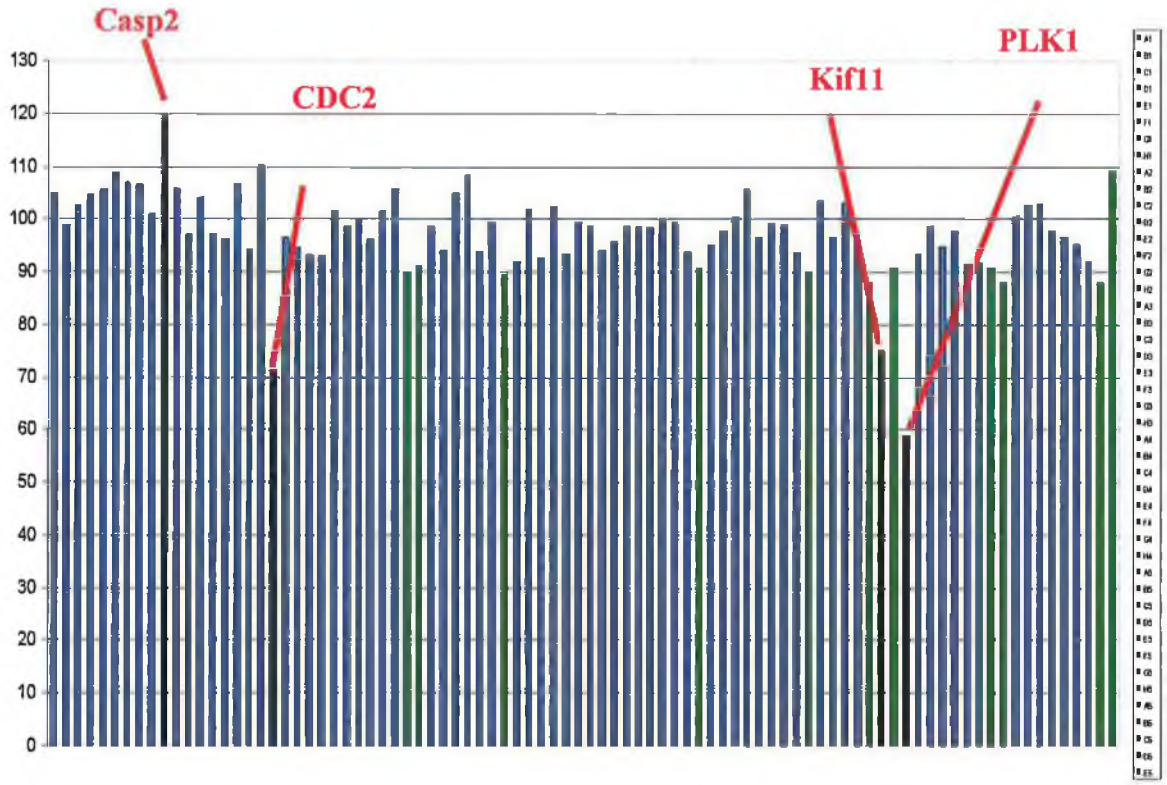

Figure 3.5.53 Transfection of "popular genes" siRNAs in H1299-tax

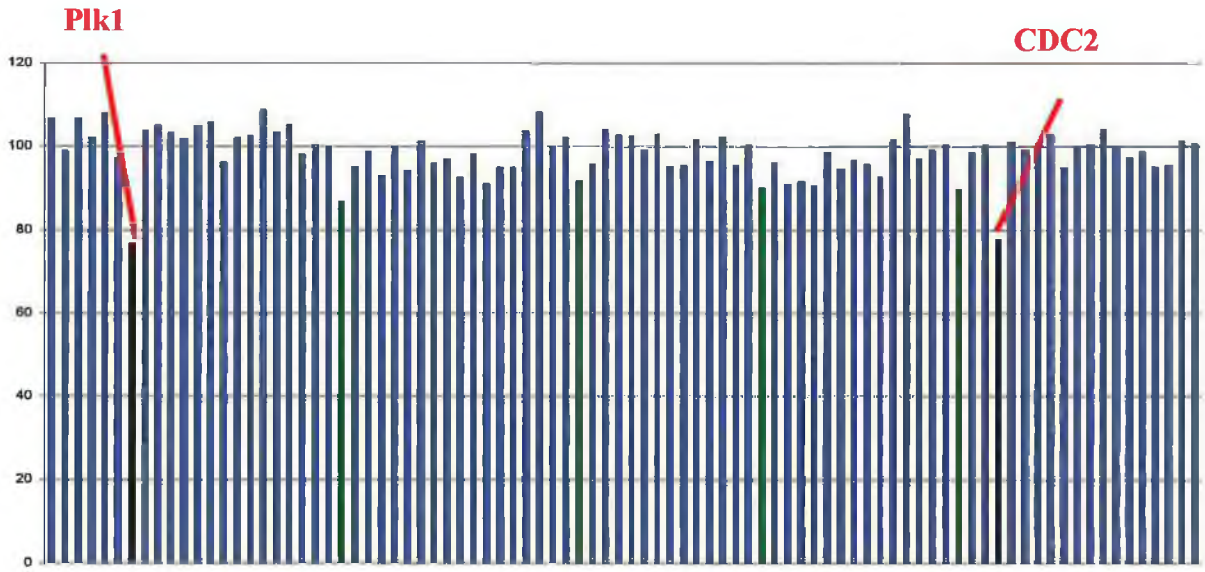

Figure 3.5.54 Transfection of "kinase libraray" siRNAs in H1299-tax

Section 4.0: Discussion

The work described in this thesis aimed to increase our understanding of the mechanisms of chemotherapeutic drug resistance in human lung cancer cell lines using three approaches:

1. Generation and characterising of wild-type p53 transfection of wildtype p53 (A549), mutant p53 (DLKP-SQ) and p53 null (H1299) lung cancer cell lines.
2. Generation and characterisation (especially by expression microarray analysis) of taxol and carboplatin resistant variants of the lung adenocarcinoma cell lines A549 and SKLU1 and the large cell lung carcinoma cell lines H1299 and H460.
3. Using siRNA gene expression knockdown technology to investigate the functional role of chosen genes from the microarray analysis in the taxol-resistant phenotype.

These results are discussed here in the context of previously published reports.

4.1 The role of p53 in drug resistance

The development of acquired drug resistance in tumours is believed to be based on drug-induced mutational changes in the cells. Mutations in tumour suppressor genes have been shown to be important in sensitivity changes to certain chemotherapy drugs.

One well characterised tumour suppressor gene is p53. It has been shown that it is mutated in more than half of all tumours of various types. However, the role of p53 in the development of multidrug resistance in cancer is complex and not yet fully understood. p53 acts as a sensor for DNA damage caused by a drug or any other mutational influence. On one hand, its presence might facilitate chemotherapy by sensing DNA damage and consequently inducing apoptosis of the cell. On the other hand, it might arrest the cell cycle allowing time for the cell to partially repair the damage then allowing mutated cells to continue growing.

Within lung cancer, mutation of the p53 gene is present in about 70% of SCLC and 50% of NSCLC. In NSCLC mutations are more frequently found in squamous cell carcinomas than in adenocarcinomas. (Viktorsson *et al.*, 2005).

Many studies have shown that loss of p53 function confers drug resistance to the cells. Inactivation of p53 has been associated with upregulation of the multidrug resistance gene MDR-1 (Thottassery *et al*, 1997; Sampath *et al.*, 2001). Wild-type p53 has been shown to have transcriptional control of MDR1 (Bahr *et al.*, 2001; Bush & Li, 2002), leading to repression of this gene. Li *et al.* (1997) sought to clarify the relationship between p53 and Mdr1 by introducing a wild-type p53 cDNA into a multidrug-resistant cell line. They found that wild-type p53-transfected cells displayed an increase in Mdr1 mRNA and P-gp protein, however this was associated with a decrease in drug resistance. The p53 family members p63 and p73 have been found to activate rather than repress MDR1 transcription. This may be due to differences in the DNA-binding domains of these proteins (Johnson *et al.*, 2005).

P53 has also been linked, at the transcriptional level, with expression of MRP1. Wang and Beck (1998) demonstrated that the human MRP1 gene is negatively regulated at the transcriptional level by wild-type p53. Another group examined the expression of p53 and MRP1 in colorectal cancers. They found that p53-positive cells expressed MRP1 more frequently than p53-negative cells. The p53 detected is most likely mutant, since aberrant p53 expression leads to accumulation of the protein in the cell. The group concludes that MRP1 expression may be regulated by mutant p53 (Fukushima *et al.*, 1999). Using a temperature-sensitive p53 vector, which when transfected into cells can express mutant p53 at 38°C and wild-type p53 at 32°C, Sullivan *et al.* (2000) showed that MRP1 expression is regulated by the transcriptional ability of p53. When wild-type p53 was expressed they observed repression of MRP1 and when mutant p53 was expressed they observed increased expression of MRP1.

Aside from transcriptional regulations, other factors are in play. Loss of p53 has been associated with poor clinical prognosis in cancer treatment. Wild-type p53 was stably expressed in a p53-null cell line (SaOS-2) in order to examine the relationship between p53 expression and sensitivity to cisplatin (Fan and Bertino, 1999). Both p53-mediated drug resistance and p53-mediated drug sensitivity were observed in the same model under different growth conditions, implying that growth factors may be involved in p53-mediated gene regulation.

Likewise, loss or inactivation of p53 has been correlated with genetic instability. Ceraline *et al.* (1998) took human normal human fibroblasts and inhibited p53 protein expression using antisense oligonucleotides. They found that this led to increased G2/M arrest and also to greater sensitivity to DNA-damaging agents. Hawkins and co-workers (1996) also found that inactivation of p53 can increase the sensitivity of the cells to chemotherapeutic drugs.

In order to investigate the role of p53 status in clinical response to chemotherapy, another group examined the relationship between p53 gene mutations and response to taxol/cisplatin chemotherapy in patients with advanced ovarian cancer. They found that this combination of drugs was effective in tumours with p53 mutations. The overall response rate was significantly higher in patients with mutant p53 tumours than in patients with wild-type p53 tumours. (Lavarino *et al.*, 2000). This suggests that mutant p53 is less effective in causing cell cycle arrest and repair as opposed to apoptosis.

P53 status is usually studied in association with response to DNA-damaging chemotherapeutic agents but may also be associated to non-DNA-damaging agents such as taxol. A study by Rakovitch *et al.* (1999) demonstrated increased sensitivity to taxol in cells with inactivated p53 compared to functional p53. This response was correlated with increased micronucleation and DNA fragmentation. They suggests that p53-independent apoptosis may be the main mechanism of action of taxol in this system, explaining why taxol had a lesser effect in p53 functional cells.

An interesting review of the literature on p53 and anticancer treatment, (Brown and Wouters, 1999) states that short-term assays are inefficient at determining the total cell kill caused by an anticancer agent. This is due to the fact that apoptosis can occur rapidly after exposure and short-term assays tend to underestimate overall killing in cells with mutant p53 or that do not undergo apoptosis, so that some of the studies in this area of research using this methods may not be reliable. This review concluded that genes effecting apoptosis such as p53 might not contribute significantly to the sensitivity of cancer cells to anticancer agents.

4.1.1 Analysis of pulse selections in cell lines with differing p53 status

The first aim of this thesis was to study p53 in a number of lung cancer cell lines in order to determine its role in the development of drug resistance. A panel of lung cell lines were chosen according to their p53 status: A549 and H460 express wild-type p53; H1299 is p53 null; and SKLU1 expresses mutant p53. All cell lines were pulsed with taxol and carboplatin. Interestingly, no correlation was found between the p53 status of the cells and their ability to develop resistance. No previous studies have analysed development of drug resistance in cell lines with differing p53 status. A study by Das *et al.*, (2001) compared the effect of taxol on two lung cancer cell lines: A549 which expresses wild-type p53, and H1299 which does not express p53. Taxol was found to induce apoptosis in both cell lines efficiently at low doses, but the process was more regulated and maximum apoptosis was reached at a lower drug concentration in the presence of p53. G2/M arrest was induced in both cell lines, independent of p53.

4.1.2 Analysis of p53 transfection in lung cancer cell lines

In order to further investigate the role of p53 in drug resistance, three lung cancer cell lines with different p53 status were transfected with wild-type p53. The three cell lines were A549, which expresses wild-type p53, DLKP-SQ which expresses mutant p53 and H1299 which is p53 null.

A549 cells express endogenous wild-type p53 protein. It was expected that introduction of exogenous wild-type p53 may increase the sensitivity of the cells to chemotherapeutic agents. This was based on the findings of many other groups that introduction of wild-type p53 enhances the cytotoxicity of chemotherapeutic agents *in vitro* (Inoue *et al.*, 2000; Miyake *et al.*, 2000). In the present study, A549 cells transfected with p53 were found to over-express functional, wild-type p53 (Section 3.1.5.1). The presence of functional p53 was determined by inducing DNA damage and assaying for stabilisation and accumulation of the protein.

The changes in sensitivity of p53-transfected A549 cells was tested for the three chemotherapeutic agents adriamycin, taxol and carboplatin. Major changes in sensitivity were difficult to detect since transfection alone appeared to have an effect

on the sensitivity of the cells, especially to taxol, where control-transfected cells displayed a 2-fold increase in resistance. Conversely, control-transfected A549 cells were similar to parent cells in their sensitivity to adriamycin. Individual p53-transfected A549 cells displayed up to a 2-fold increase in resistance to adriamycin. In general, these results demonstrate that introduction of wild-type p53 into the cell line A549 does not sensitise the cells to the chemotherapeutic agents tested. In fact, the reverse is true in several cases, where an increase in resistance was observed. The contradictory literature mentioned earlier in this area, Hawkins *et al.*, (1996) found that inactivation of p53 can lead to sensitisation of cells to chemotherapy. It should also be realised that integration of foreign DNA in transfectants is random and in different clones, expression of different genes, some of which could affect drug sensitivity, may be altered.

Analysis of wild-type p53 expression in a mutant-p53 expressing cell line is the most difficult. Mutant p53 is much more stable than wild-type p53 and so is expressed at higher levels in the cell. The most popular method of screening for wild-type p53 involves observing stabilisation and accumulation of the protein after DNA damage. Since the mutant p53 protein is so highly expressed, it is problematic to identify changes in expression of any wild-type protein co-expressed in the cells. Nevertheless, all of the DLKP-SQ transfected clones were tested for changes in sensitivity to adriamycin, taxol and carboplatin. Some of the transfected clones displayed minor changes in sensitivity to the drugs tested, however, similar changes were observed in control transfected cells, suggesting that any changes were more likely to be attributed to transfection, rather than specifically to expression of wild-type p53. Since no significant changes were observed, it is possible that the mutant protein present was sufficient to overpower any exogenous wild-type p53 introduced. A similar study found that, exogenous wild-type p53 was stably expressed in a mutant-p53 cell line after transfection, but at a lower level than the endogenous mutant p53 (Takahashi *et al.*, 1992). Shaw *et al*, (1992) investigated the function of wild-type p53 by studying effects of wild-type p53 re-expression in the human colon tumour cell line EB, which is deficient in endogenous p53. Expression of the p53 gene was induced by induction of the metallothionein promoter. They found that induction of wild-type p53 expression prevented tumour formation in nude mice, wild-type p53 expression eventually resulted in elimination of established tumours in mice.

Many groups have observed the difficulty of expressing wild-type p53 in a cell model that does not express it endogenously. Takahashi *et al*, (1992), examined whether wild-type p53 can suppress growth of lung cancer cells, and whether mutations of single amino acids changes the biological effects of the wild-type p53 gene. They worked with two cell lines, NCI-H358, which is p53 null and NCI-H23, which expresses mutant p53, and transfected each with a wild-type p53 expression vector, and a mutant p53 expression vector. They found that expression of exogenous wild-type p53 was incompatible with cell growth in the p53 null cell line. Other groups have reported expression of truncated or rearranged p53 in p53 null cell lines transfected with wild-type p53 (Cajot *et al.*, 1992; Baker *et al.*, 1990).

The p53 null cell line included in our study was H1299. Similar difficulties were observed in isolating a p53-transfected clone of this cell line that expressed functional protein. P53 was detected in the mixed population of transfected H1299, yet only one clone was determined to express p53. However, the p53 protein expressed in this clone did not appear to be functional. This was determined by inducing DNA damage and observing that no accumulation of the protein occurred. All of the clones isolated from the H1299-p53 transfection were tested for changes in sensitivity to adriamycin, taxol and carboplatin. Although some significant changes were detected in the sensitivity of the clones to the drugs tested, these have to be attributed to the transfection since no p53 protein was detected in most of these clones.

H1299-p53 is the only clone of the H1299-p53 transfectants that expresses the p53 protein. The parent cell line is p53 null. Results show that this p53-expressing clone is less invasive and superinvasive than the parent cell line. Very little is known about the involvement of p53 in invasion and metastasis, however p53 has transcriptional control over a number of genes involved in invasion, such as PAI-1, KAI-1, maspin and Nm23-H1 (Harms *et al.*, 2004). The results also show that some of the other transfected cell lines, including control transfected cells also show changes in invasion potential, so these effects are most likely due to transfection rather than expression of p53.

The p53 protein expressed in H1299-p53 does not seem to function as normal wild-type p53. The assay used to test for functional wild-type p53 involves stressing the cells with a DNA-damaging agent and allowing the protein to stabilise and accumulate in the cell. Wild-type p53 is characterised by low levels of the protein in untreated cells and higher levels of protein after treatment. Mutant p53 will be present at high levels in the cells regardless of DNA damaging treatment. In H1299-p53, p53 is present at quite a low level untreated and does not accumulate after treatment. It is unlikely that the protein is mutant p53 (since wild-type p53 cDNA was transfected), so the probable reason is that the cell has switched to other mechanisms for dealing with DNA damage, since there is no endogenous p53 protein in H1299.

The parent and transfected cells express Mdm2, which is a regulator of p53 and p73, a p53 family member, which acts in a similar manner to p53. A recent study by Yamauchi *et al.*, (2005) found that p53 introduced into H1299 was remarkably stable and had a much longer half-life than in normal cells. They hypothesise that a mediator between ubiquitinated p53 and the proteasome exists and that it is downregulated in H1299. Therefore, there is a possibility that something similar is occurring in the present system, that rather than p53 not accumulating after DNA damage, it is merely more stable before DNA damage.

H1299-p53 clone 8, which was found to express p53 protein after transfection, was compared to control transfected and parent cells by microarray analysis. The negative control for the experiment was H1299 transfected with the empty vector pcDNA3.1Zeo (H1299-EV). To ensure that this control was appropriate to the experiment, clones of H1299-EV were used. The triplicate for this sample was three separate clones isolated from the mixed population of H1299-EV. Section 3.1.11.1 shows the hierarchical cluster for this experiment. The triplicate samples for H1299-EV did not cluster together, and this is probably explained by the fact that three separate clones were used, rather than biological replicates of the same cell line, as for the other samples included.

Taking this into consideration, the experiment was continued, despite the quality control issues. The genes differentially expressed between H1299 parent and H1299-p53, not differentially expressed in H1299-EV were investigated. The microarray analysis results show that the p53-transfected cell line had close to equivalent levels of the p53 transcript compared to the parent, which is in contrast to RT-PCR and western blotting results. This might be explained by an observation from an earlier microarray experiment conducted in our laboratory. In the earlier experiment, a cell line was transfected with a plasmid containing EIF-4E, a translation factor. RT-PCR and western blots confirmed the success of the transfection, but the Affymetrix results showed no appreciable increase in the measured levels of the transcript. This anomaly was investigated and it was discovered that the Affymetrix probe sets had been designed to the 3' UnTranslated Region (UTR) of the gene sequence. In contrast, the plasmid only contained the coding sequence for the gene and as a result, the probe sets were not picking up the increased levels of the transcript that we had observed by RT-PCR.

An outcome of this was that it was realised that sequences transfected by plasmid may not always produce mRNA transcripts that are detectable using the Affymetrix system. Two of the reasons that Affymetrix have designed many of their probes to the 3' UTR is firstly to improve the efficiency of the IVT process and secondly to ensure that full length transcripts are detected (as opposed to 5' fragments).
Since the western blotting and RT-PCR results represent repeated experiments with the inclusion of controls, this result should be a true reflection of the p53 status of the transfected cells

In summary, the results presented in this thesis indicate that p53 status alone does not determine a cell lines response to chemotherapeutic agents. This finding does not agree with the findings in the literature that tumours with inactivated p53 are more likely to be drug resistant since functional p53 is necessary to induce apoptosis (Lowe *et al.*, 1993; Ferreira *et al.*, 2000). Also mutant p53 has been associated with upregulation of Mdr1, (Sampath *et al.*, 2001), so this would be consistent with increased resistance. It has also been shown here that introduction of wild-type p53 into mutant and p53 null cell lines was not sufficient to restore sensitivity to the cell lines. Several groups have successfully shown chemosensitivity upon introaduction of wild-type p53 into cancer cells (Fujiwara *et al.*, 1994; Osaki *et al.*, 2000). As discussed earlier there are several publications indicating that inactivation of p53 is associated with an increase in sensitivity, rather than the other way around (Hawkins *et al.*, 1996; Das *et al.*, 2001). The results presented in this thesis strongly suggest that wild-type p53 alone is not sufficient to significantly alter resistance to chemotherapeutic agents.

4.2 Establishment of drug resistant variants

The most commonly used drugs for the treatment of NSCLC are taxanes and platinum compounds, however, development of resistance to these drugs is frequent and has been described. To study the molecular events giving rise to resistance we repeatedly exposed four lung cell lines to taxol and carboplatin giving rise to eight drug resistant cell lines, which act as models for the *in vitro* investigations. The four parent cell lines derived from two adenocarcinomas (A549, SKLU-1) and two large cell carcinomas (NCI-H1299, NCI-H460) allowing the comparison of two common subclasses of lung cancer.

In the clinical setting patients receive chemotherapy treatment once every 1-3 weeks allowing for recovery in between. To match the clinical setting as close as possible a pulse treatment with drug once per week for four hours was chosen, which also allowed for recovery of the cells in between. The newly established cell lines showed only modest changes in resistance to taxol and carboplatin together with some cross-resistance to other drugs. It is important to note that previous attempts to study drug resistance *in vitro* were based on continuous exposure to clinically non relevant high drug concentrations, which resulted in 100-1000 fold increases in resistance, however, resistant tumour cells *in situ* are usually no more than 5-10 fold resistant (Simon and Schindler, 1994).

The mechanisms involved in the development of low-level resistance may be more relevant for *in vivo* studies and clinical practice than using models with very high resistance levels. Belvedere *et al.* (1996) compared resistance levels and mechanisms of resistance in two cell lines obtained from the ovarian murine reticulosarcoma M5076. One of these cell lines was obtained through continuous selection and the other by pulse selection with the anticancer agent cisplatin. Both cell lines were found to have a stable low-level resistance of 3-fold to cisplatin and showed similar cross-resistance to other alkylating agents. These cell lines were implanted in mice and the tumours were found to be resistant *in vivo* to cisplatin, but not to some other agents to which they were resistant *in vitro*.

4.2.1 Analysis of taxol resistance

Mechanisms of resistance to taxol include increased drug efflux, usually associated with increased P-gp expression, changes in microtubules affecting taxol binding, differential expression of various tubulin isotypes and changes in expression of apoptosis-related proteins e.g. caspases and the bcl-2 family (Wang et al, 2000).

Low concentrations of taxol (10-100nM) lead to suppression of microtubule dynamics by inhibiting the formation of mitotic spindles and resulting in cell cycle arrest at the G2/M phase. This eventually leads to apoptosis. Higher concentrations of taxol lead to massive microtubule damage (Wang et al, 2000). Mechetner *et al.* (1998) studied the expression of P-gp and resistance to taxol and adriamycin in resistant breast cancer cell lines and tumour samples and found that P-gp expression significantly contributed to levels of clinical resistance to MDR drugs and that treatment with chemotherapeutic drugs may induce P-gp expression. This would link taxol resistance to an increase in P-gp expression rather than microtubule damage.

Other groups have demonstrated that resistance to taxol can be due to a P-gp unrelated mechanism. Parekh *et al.* (1997) established a series of taxol-resistant human ovarian carcinoma clones with increasing degrees of resistance. These were used to study the mechanisms by which cancer cells develop resistance to taxol. The cell lines displayed resistance to taxol in the range of 250 to >1500–fold. They found that taxol resistance can develop via P-gp-mediated and non-P-gp-mediated mechanisms. Non-P-gp-mediated resistance to taxol may be due to alterations in the taxol-binding affinity of the microtubules and alterations in tubulins. This was focus of a study by Han *et al.* (2000). The group developed a taxol-resistant NCI-H460 cell line (H460/T800), which is 1000 fold more resistant to taxol than the parent cells and even showed cross-resistance to colchicine, vinblastine and doxorubicin. Beside an increased expression of P-gp the resistant cells had an overexpression of α-and β-tubulin. The down-regulation of the α-tubulin expression by antisense resulted in an increased drug sensitivity of the cell line.

Giannakakou *et al.* (1997) isolated taxol-resistant sublines from a human ovarian carcinoma cell line in the presence of the P-gp antagonist verapamil resulting in

resistant variants, which did not express P-gp. These cell lines were found to be 24-fold resistant to taxol. The study concluded that the taxol resistance was due, at least in part to mutations in β-tubulin.

Martello *et al.* (2003) studied two taxol resistant variants of A549 called A549-T12 and A549-T24. A549-T12 is 9-fold resistant to taxol and does not express P-gp. A549-T24 is 17-fold resistant to taxol and expresses low levels of P-gp. As well as being resistant to taxol these cell lines are dependent on taxol for normal growth. These cell lines display normal taxol-dependent polymerisation of tubulin. However, they have a mutation in the major α-tubulin iso-type Kα1. This report highlights the complexity of taxol resistance in mammalian cells.

The taxol-selected cell lines developed in this project showed resistance in the range from two to over five fold, which was stable even after weeks in culture. The concentrations of taxol used for these pulse-selections ranged from 10-150ng/ml reflecting a pharmacologically achievable concentration.
A recent study by Scripture *et al.* (2005) showed that the achievable levels of taxol in the plasma of a patient ranges from 1.2 - 5.3μg/ml, depending on the dose.

Interestingly A549-tax and NCI-H1299-tax expressed double the fold resistance to taxol compared to taxotere, although the mechanism of action of these two drugs is very similar. Previous studies on another lung cell line, DLKP, in our laboratories have shown similar results; pulse-selection with taxotere resulted in a 420-fold resistance to the pulsing drug and only 210-fold cross-resistance to taxol (Rasha Linehan, PhD thesis, 2003).

A typical MDR phenotype is characterised by a specific cross-resistance pattern, which includes resistance to VP-16, taxanes, anthracyclines and vinca alkaloids and is based on an increased P-gp expression. None of the selected variants represented the classical MDR phenotype and P-gp could not be detected in any of them except in NCI-H1299 and NCI-H1299-tax. microarray analysis of the drug resistant variants revealed a significant upregulation of Mdr1 gene in the taxol-resistant cell lines

compared to the parent. It is possible that a change in mRNA levels of Mdr1 are not translated into an increase in protein levels.

Since P-gp expression was not evident, we tested all cell lines with a combination of GF120918, a P-gp inhibitor, and taxol. GF120918 has been shown to reverse P-gp mediated resistance, but not MRP-mediated resistance (de Bruin *et al.*, 1999). As discussed above, P-gp protein was only detected in two of the cell lines H1299 and H1299-tax and therefore, the most potent effect of the combination was observed in these cell lines. Some effect could be found in A549-tax and SKLU-1 tax suggesting a small level of P-gp protein in these cell lines, which might be enough to contribute to taxol resistance. Studies have shown that even a small increase in P-gp protein can result in an MDR phenotype explaining the cross-resistance pattern of the SKLU-1-tax cell line. Since only small effects can be seen in the taxol selected variants when P-gp is inhibited with GF120918, it is reasonable to assume these cell lines possess alternative mechanisms of taxol resistance.

If P-gp is present in the H460-tax its expression level seem to be even lower and therefore does not show an effect in the combination assays. From microarray intensity values it was evident that Mdr1 is expressed at very low levels compared to the expression levels of other genes studied, which will be discussed in a later chapter.

4.2.2 Analysis of carboplatin resistance

The mechanisms of resistance to carboplatin are not as well characterised as those of taxol. Cisplatin, another platinum-containing anticancer agent has a similar mechanism of action to carboplatin. Resistance to cisplatin and carboplatin has also associated with decreased uptake of the drug into the cells; inactivation of the drug by cellular thiol compounds; enhanced repair of platinum-related DNA damage and absence of mismatch repair. The formation of conjugates between the thiol glutathione (GSH) and platinum drugs results in a complex, which is a substrate for ABC transporter proteins. A study by Ikuta *et al.* (2005) examined the expression of MDR1, MRP1 and LRP in NSCLC cells and compared this with the cells' sensitivity to cisplatin. They found no correlation between expression of these markers and sensitivity to cisplatin in the NSCLC cells.

The range of carboplatin used for pulse-selection of the cell lines used in this thesis was from 10 - 100μg/ml. Achievable plasma concentrations in patients for carboplatin range from 9 - 55μg/ml, depending on the dose (Oguri *et al.*, 1988). The concentrations used for pulse selection were very high and are not as clinically achievable as the taxol pulse selections. Nevertheless, these carboplatin-resistant cell lines are valuable models for the study of carboplatin resistance. The cell lines pulse-selected with carboplatin were found to range in fold resistance to carboplatin from 1.3 to 2.7 fold. This is considerably less than the resistance obtained in the taxol-selected cells. There was no common cross-resistance pattern observed in the carboplatin-resistant cell lines. In general, the cell lines display cross-resistance to cisplatin, which was expected since these drugs share such a common mechanism of action. SKLU1-cpt displays the most cross resistance. This cell line showed upregulation of MRP1 and this is consistent with the cross-resistance to adriamycin and VP-16. The resistance observed in the carboplatin cells were unstable compared to the resistance of the taxol-selected cells. This phenomenon of unstable resistance has been seen in previous studies in our laboratories. The cell RPMI 2650 was pulse-selected with a range of chemotherapeutic agents. This selection led to an initial resistant phenotype, which was quickly reversed with increasing passage number (Rasha Linehan, PhD, 2003).

There is an increase in the expression of MRP1 in some of the carboplatin-selected variants in this study. Sulindac has been shown to circumvent MRP1-mediated resistance *in vitro* (Duffy *et al.*, 1998). In agreement with this, in the present study, the effect of sulindac combined with the chemotherapeutic agent adriamycin appeared more potent in cells expressing MRP1. A549 and H460 parent cell lines express the most MRP1 prior to selection and it is in these cell lines that the greatest synergy can be seen. There is also an increase in MRP1 protein in the carboplatin-selected variants, which leads to greater synergy in the combination of sulindac and adriamycin. These results suggest that carboplatin may lead to an increase in MRP-mediated drug resistance, and that sulindac may be an effective drug for combination in such situations.

4.2.3 The effect of pulse selection on *in vitro* invasion

Pulse-selection with a chemotherapeutic agent has been known to affect other functions of the cell, such as proliferation and invasion. Previous studies in our laboratories have shown that selection with some chemotherapeutic agents can lead to increased *in vitro* invasiveness (Liang *et al.*, 2001). Another study on the invasive breast cancer cell line MDA-MB-435S-F found that selection with the agents taxol and adriamycin led to a more aggressive invasive phenotype termed "superinvasive" (Glynn *et al*, 2004).

The invasive capabilities of the selected cell lines were tested for this reason. In the cell lines A549-tax and H1299-tax, taxol selection was not found to drastically change the invasiveness of the cell lines, with both cell lines displaying a slight increase in invasiveness compared to their respective parent cell line. In the cell lines H460-tax and SKLU1-tax, there was a considerable decrease in the invasiveness compared to the parent cells. It was also found that pulse-selection with taxol did not affect the ability to super-invade to the cells.

Taxol treatment has been linked to decreased invasion. A study by Westerlund *et al.* (1997) examined the effect of taxol on ovarian cancer cell invasion. Taxol was found to suppress invasion, motility and cell attachment of ovarian cell lines. This inhibition of invasion was found to be accompanied by an increase of TIMP-2 protein release. This is in agreement with the results obtained for H460-tax and SKLU1-tax, which were less invasive after pulse-selection with taxol.

Interestingly, all of the carboplatin-selected cell lines were less invasive than the parent cell line. As discussed earlier, some chemotherapeutic agents have been associated with changes in invasion *in vitro*. Previous studied in our laboratories indicated that pulse-selection with cisplatin led to increased *in vitro* invasiveness in the human lung cancer cell line DLKP (Liang *et al.*, 2004). This increased invasiveness was associated with increased expression of the matrix metalloproteases MMP-2 and MMP-13.

In summary, the results presented in this section of the thesis indicate that the pulse-selected variants displayed low-level resistance to the pulsing drug (>10-fold). Since these cell lines were established with the clinical setting in mind, and considering that resistant tumour cells *in situ* are usually no more than 5-10 fold resistant (Simon and Schindler, 1994), these resistant cell lines provide excellent models for the study of taxol and carboplatin resistance. The results indicate that the taxol resistance obtained may be in part associated with upregulation of P-gp, but it is likely that other mechansims are also in play. The carboplatin-resistance observed might be due in part to increased MRP-1 expression, however in some of the variants this was not observed so other mechanisms must be involved. The most interesting result presented for the carboplatin-resistant cell lines was the consistent decrease in invasion observed in these cell lines compared to the parent cells. These cell lines provide a model for the future study of invasion.

4.3 Microarray analysis of taxol-selected variants

The four lung cancer cell lines A549, H1299, H460 and SKLU1, and their taxol-resistant variants were analysed using microarray. The aim of this analysis was to identify genes involved in the development of taxol resistance in lung cancer cell lines. These taxol-resistant cell lines did not display classical MDR, and offered a unique opportunity to study the less-well characterised mechanisms of taxol resistance. Another strong point of this analysis was the straightforward nature of the comparison. The microarray data was used to analyse differences between parental (sensitive) and resistant cell lines, and the only differences were due to taxol treatment. Therefore, any differentially expressed genes identified by the microarray analysis should relate to taxol resistance.

Several groups have used microarrays to identify genes involved in resistance to chemotherapeutic agents. Wittig *et al.* (2002) compared the gene expression patterns of the drug sensitive melanoma cell line MeWo and three sublines with resistance to etoposide, cisplatin and fotemustine in order to identify common genes involved in resistance to these DNA-damaging agents. This study indicates the involvement of two genes in particular, MPP1 and CRYAB, in resistance to DNA-damaging agents. A more general study on genes involved in chemoresistance in gastric cancers was conducted by Suganuma *et al.* (2003). This group compared gene expression and drug resistance patterns in gastric cancer surgical specimen and, although they identified several resistance related candidate genes, they concluded that the mechanisms of resistance to chemotherapeutic agent are very complex.

Similarly to the present study, Lamendola *et al.* (2003) investigated taxol resistance *in vitro* using microarray analysis. This group established taxol-resistant cell lines from the ovarian carcinoma cell line SKOV-3 through continuous selection with increasing concentrations of taxol in order to identify novel candidate gene families involved in taxol resistance. This study used array technology in the area of pattern recognition and similarity clustering to identify many associated changes in gene expression rather than single gene changes. This might provide more insight into the development of a taxol-resistant phenotype. An earlier study by this group discovered a novel gene that was overexpressed in the taxol resistant cell line called taxol resistance associated

gene-3 (TRAG-3). This gene was also found to be overexpressed in other cell lines displaying resistance to taxol. TRAG-3 is not expressed in normal tissue but is expressed in 43% of cancer cell lines (Duan *et al.*, 1999).

4.3.1 Quality control in microarray experiments

The quality control measures used in the microarray experiments in this thesis adds to the strength of the data. Hierarchical clustering of the parent and taxol-resistant lung cancer cell lines was carried out to ensure that the triplicate samples were representative and as a quality control measure. This allows confidence that the differntially expressed genes are indeed involved in taxol resistance. Hierarchical clustering grouped samples together based on similar expression levels of the genes analysed by the microarrays. The first important point about the clustering results is that the biological replicate samples used in the microarray experiment did group together. The taxol-selected variants from each cell line grouped next to the parent samples in each case, showing that these taxol resistant variants remain very similar in overall gene expression to the cell lines from which they were established. This result is verifies that the specific gene changes determined from analysis of the data is solely due to selection for taxol resistance.

Another point that was highlighted by the clustering was that, interestingly, the different lung cancer cell types did not cluster together. A549 and SKLU1 are both lung adenocarcinoma cell lines and H460 and H1299 are both large cell lung carcinomas, however, the clustering shows that A549 and H460 were most similar in gene expression. SKLU1 was then similar to both of these, with H1299 having the least similar gene expression to all the other cell lines.

A study by Bhattacharjee *et al.* (2001) used clustering methods to analyse 186 lung tumour samples, mostly adenocarcinomas. They demonstrated that using different clustering methods, there are distinct subclasses of adenocarcinoma based on specific gene expression. In a sililar study, a 7685-element microarray was employed to create expression profiles for lung tumours and cell lines (Virtanen *et al.*, 2002). Hierarchical clustering resulted in tumour samples and cell lines forming two distinct groups. Within the tumour group, SCLC and NSCLC grouped separately. Most SCLC cell

lines grouped with the SCLC tumour samples. Similarly, most of the squamous cell carcinomas clustered together. None of the adenocarcinoma cell lines tested grouped with adenocarcinoma tumour tissue. This study might explain in part why the different lung cancer cell types in this microarray study did not group together in the hierarchical cluster. Microarray analysis compares the samples at a more detailed level and picks up differences in samples that are not possible to detect at the cellular level. In this way, microarrays have the potential to completely change lung cancer classification and staging to improve diagnosis and hence treatment options for patients.

4.3.2 Differentially expressed genes in taxol-resistant cell lines

Genes that were differentially expressed in the taxol-selected cell lines compared to the parent cell lines were uncovered using parameters of fold change of 1.2, a difference of intensity of 100 and a p value of ≤ 0.05 (see section 2.12.4). Fold change is the most common parameter utilised to generate gene lists from microarray experiments. The shortcoming of this parameter is that there is a bias towards genes that are expressed at very low levels in the parent samples, and "turned on" in the experimental samples. For example, when comparing A549 to A549-tax, for the gene ABCB1 there is a 9-fold increase in A549-tax, and an intensity difference of 109. However, for the gene CRYZ there is a 1.6-fold decrease in A549-tax, but an intensity difference of 1,024. For this reason, a low fold change and also a difference of intensity criteria was used to filter the genelists. These criteria will detect genes that are expressed at low and high levels.

As discussed earlier, the comparison between parent and taxol-resistant cell line is straightforward. However, the limitation is that there are thousands of genes differentially expressed by the taxol-resistant cell lines. It is only feasible to work with a small number of genes at a given time. The stringent filtering criteria used to narrow down genelists to a manageable study inevitably means discarding of potentially interesting genes.

As described in Section 3.3.3, nineteen genes were found to be differentially expressed in all taxol variants compared to the parent cell lines. The nineteen genes were not, however, similarly expressed in all cell lines, for example vascular endothelial growth factor is upregulated in two of the cell lines, but down regulated in the other two cell lines. Two genes were identified as upregulated in all the taxol-resistant cell lines compared to the parent cell lines, Mdr1 and phosphoglucomutase-2. There is no correlation in the literature between these two genes. Mdr1, which codes for the P-gp protein is well characterised as involved with resistance to taxol. However, there have been no reports of phosphoglucomutase-2 (PGM-2) being involved in taxol or resistance to any cytotoxic agent. PGM-2 was not followed up in subsequent experiments, considering the very low fold changes (1.2-fold) and low expression values observed in this gene, it would be difficult to discern any changes in expression and to see effects in functional assays. It is another interesting point that no genes were downregulated in all the taxol selections. PGM-2 is upregulated to the same degree in all of the selections, whereas Mdr1 upregulation ranges from two to nine fold. It was expected that Mdr1 upregulation may correlate with fold taxol resistance, but this was not the case. In fact, the least resistant cell line, A549 displayed the greatest fold increase in Mdr1 (Section 3.3.3).

Ten target genes were chosen for further analysis (Section 3.3.4). Five of these genes were upregulated in taxol resistant cells and five were downregulated. The five upregulated genes were as follows: Mdr1 (ABCB1); inhibitor of DNA-binding 3 (Id3); quinone reductase (CRYZ); engulfment adapter protein (GULP1) and stromal cell protein (SCP). The downregulated target genes were as follows: follistatin-like 1 (FSTL1); epithelial membrane protein 1 (EMP1); connective tissue growth factor (CTGF); cysteine-rich intestinal protein 1 (CRIP1) and insulin-like growth facto receptor binding protein 6 (IGFBP6). Some of the functions of the target genes are not well characterised in the literature. The following paragraphs give a brief description on what is known about these genes.

Mdr1, as discussed earlier is the gene that codes for P-gp. P-gp is drug efflux pump, known to be involved in resistance to a variety of chemotherapeutic agents. Mdr1 was upregulated in all of the taxol variants compared to the parent cell lines.

Inhibitor of DNA binding 3 (ID3) belongs to a subfamily of helix-loop-helix (HLH) proteins, which are a family of transcription factors. The ID proteins for a distinct group within this family, due to their lack of a basic DNA binding domain. They act as dominant-negative regulators of basic HLH proteins through formation of inactive heterodimers with intact basic HLH (bHLH) transcription factors (Sikder *et al.*, 2003). These heterodimers are then unable to bind to DNA. Most bHLH regulate genes involved in cell fate determination and cell differentiation and ID proteins are also known as inhibitors of differentiation (Norton, 2000). ID proteins can also act as positive regulators of cell growth and their function is important for cell cycle progression. These proteins are involved in cellular differentiation and development, but have also been implicated in cell cycle and apoptosis. ID3 has been shown to be phosphorylated in late G1 phase of the cell cycle by cyclin-dependent kinase 2 (cdk2). ID3 has also been found to be a strong inducer of apoptosis in serum-deprived conditions (Norton & Atherton, 1998). The role of ID3 in taxol resistance is discussed later.

CRYZ encodes a crystallin protein which has NADPH-dependent quinone reductase activity. Quinone reductase is a phase II detoxification enzyme. CRYZ lacks alcohol dehydrogenase activity although by similarity it is considered a member of the zinc-containing alcohol dehydrogenase family (Rao *et al.*, 1992). It is expressed at extremely high levels in the lenses of some mammals (Gonzalez *et al.*, 1995). CRYZ was expressed at a relatively high level in A549-tax and H1299-tax, however, the fold changes were quite low (>2-fold).

GULP1 is an evolutionarily conserved adaptor protein required for efficient engulfment of apoptotic cells by phagocytes. Removal of apoptotic cells is an essential part of the apoptotic pathway, since dying cells release toxins that could lead to inflammation (Su *et al.*, 2002). This gene was upregulated in taxol-resistant cells.

SCP stromal cell protein is a poorly annotated gene. Its function is not fully understood. However, this gene was upregulated in taxol-resistant cells. Follistatin-like 1 (FSTL1) encodes a protein with similarity to follistatin.

Follistatin is a monomeric glycoprotein that binds activin A with high affinity. It has been associated with rheumatoid arthritis (Ehara *et al.*, 2004). This gene was down-regulated in taxol-resistant cells.

Epithelial membrane protein 1 (EMP1), also known as tumour membrane protein (TMP) is a member of the PMP22 family of proteins. EMP1 has been found to be downregulated in esophageal cancer (Wang *et al.*, 2003). A recent study by Jain *et al.* (2005) identified EMP-1 as a potential biomarker of gefitinib resistance, both *de novo* and acquired, in NSCLC patient samples. EMP-1 was found to be downregulated in association with taxol resistance to taxol, in agreement with this study.

Connective tissue growth factor (CTGF) is a secreted protein that binds to integrins. It is known that CTGF can modulate the invasive behaviour of cell lines *in vitro*, and this may be moduulated by MMP-2 expression (Fan & Karnovsky, 2002). CTGF gene expression has been shown to be regulated by transforming growth factor-β (TGF-β). As well as its role in invasion, CTGF has been demonstrated to induce apoptosis in certain cell lines (Hishikawa *et al.*, 1999). Connective tissue growth factor was found to be downregulated in taxol-resistant cells. Downregulation gene could possibly explain the decrease in invasiveness observed in H460-tax and SKLU1-tax, although this phenomenon was not observed in A439-tax and H1299-tax.

Cysteine-rich intestinal protein 1 (CRIP1) is a member of the LIM protein family. It is a small protein that is abundant in the intestine and in the immune system (Cousins & Lanningham-Foster, 2000). LIM proteins are characterised by a repeat of a double zinc finger cysteine-rich sequence. There is a shortage of literature on this gene and little is known about its function. CRIP1is believed to be involved in zinc transport, since it has metal-binding abilities (Hempe & Cousins, 1991). Overexpression of CRIP1 in transgenic mice has been found to alter cytokine expression, suggesting a roel for CRIP1 in the immune response (Lanningham-Foster *et al.*, 2002). A recent

microarray study by Mackay *et al.* (2003) identifies a CRIP1 as a differentially expressed gene in ERBB2 expressing breast cancer cells.

Insulin-like growth factor binding proteins act as carrier proteins for IGFs in the bloodstream, modulate the half-lives and cellular bioavailability of the IGFs (Grellier *et al.*, 2002). IGFBP6 is one of these binding proteins and was downregulated in taxol-resistant cells.

4.3.3 Relationships between differentially expressed genes

Pathway analysis was carried out using Pathway Assist in order to determine if a relationship exists between the target genes. A common pathway was built (Section 3.3.5). This pathway contains genes involved in signalling (JAK2, CCL4, TNF and IL6), transcription factors (TCF4) and growth factors (TGFβ). Only two of the target genes shared a direct link, SCP and CRYZ, both of which were upregulated in the taxol resistant cell lines. It was also of interest that GULP1 was found to be related to the major vault protein, also known as lung resistance related protein, though this gene was not found to be differentially expressed in the taxol-resistant cell lines. Pathway analysis is usually carried out on large genelists. Building a pathway based on ten targets is limiting and more could be extracted from this experiment by carrying out pathway analysis on a larger genelist. Nevertheless, the built pathway indicated that transforming growth factor-β is important in this system as it regulates four of the ten genes: CTGF; IGFBP-6; CRYZ and SCP.

4.3.4 Expression of ID3 in pulse-selected variants

ID3 was found to be upregulated in the taxol resistant cell lines A549-tax, H1299-tax and H460-tax. Expression of ID3 protein in the selected cell lines is shown in Section 3.5.2. The protein expression does not parallel with the microarray results, since in A549-tax and H1299-tax there appears to be downregulation of the protein. It is a possibility that post-transcriptional mechanisms may be involved. SKLU1-tax shows an increase in ID3 protein compared to SKLU1, though this was not detected by microarray analysis. ID3 has been implicated in resistance to cisplatin in a recent

study by Koyama *et al.* (2004). Inactivation of a family member of ID3, ID1 was found to lead to increased sensitivity to taxol in prostate cancer cells (Zhang *et al.*, 2005). In addition, this group found that the JNK pathway was activated in ID1-transfected cells and they conclude that inhibition of ID1 is a possible target for increasing taxol-induced apoptosis. It is possible that ID3 is capable of activating similar apoptosis pathways, and this recent study could indicate a possible mechanism for the role of ID3 in taxol resistance. Another study by Cheung *et al.* (2004) found that the expression of ID1 was able to protect nasopharyngeal carcinoma cells from taxol-induced cell death. This study strengthens the possibility that ID family members are involved in taxol resistance. ID1 and ID3 were also recently found to be involved in the activation of angiogenic processes (Sakurai *et al.*, 2004).

4.3.5 Expression of CRIP1 in pulse-selected variants

CRIP1 was found to be downregulated in the taxol resistant cell lines A549-tax, H1299-tax and H460-tax. In fact, in H1299-tax, expression of CRIP1 was virtually "turned off " with an intensity value of less than 20. Section 3.5.3 shows the expression of CRIP1 protein in the cell lines. The protein is downregulated not only in the taxol-selected cells, but also in the carboplatin-selected cells. SKLU1-tax also shows downregulation of the protein, though this was not detected by microarray analysis.

In summary, the microarray analysis revealed ten genes with a possible role in taxol resistance. The roles of some of the genes in taxol resistance, for example Mdr1, are clear and well documented (Section 4.2.1). Many of the genes identified are not well-characterised. These genes are potential markers for taxol resistance in lung cancer. Further study into the function of these genes will provide an insight into their function, and identify possible pathways involved in taxol resistance.

4.4 RNA Interference

RNA interference is a powerful technique to study the functions of genes using siRNAs to specifically silence them (see sections 1.8 and 2.13). The ten target genes mentioned above were silenced using two distinct siRNAs in order to determine their role in taxol resistance. RNA interference is a relatively new technique so the literature on its uses in the investigation of chemotherapy resistance is limited. Celius *et al.* (2003) established a modified colon carcinoma cell line Caco-2 with stable suppression of MDR1 gene expression and associated downregulation of P-gp protein. A more recent study by Stierle *et al.* (2005) downregulated MDR1 and P-gp levels in multidrug-resistant MCF7 cells using an siRNA against MDR1. They found that transfected cells displayed sensitivity to the P-gp substrate daunorubicin and increased cellular accumulation of this agent.

4.4.1 Effects of transfection of target genes siRNA on taxol sensitivity

SiRNAs directed at the ten target genes were transfected into A549, A549-tax, H1299 and H1299-tax and the effect on taxol sensitivity was examined. A summary of the results obtained can be seen in Table 4.1.

Table 4.1 Summary of results from transfection of target genes siRNA

Gene	A549	A549-tax	H1299	H1299-tax
ABCB1	-	+	+	+
ID3	+	-	+	-
CRYZ	-	-	-	+
GULP1	-	-	-	+
SCP	-	-	-	-
CTGF	-	-	-	-
CRIP1	+	+	-	-
IGFBP6	-	-	-	-
EMP1	+	+	-	-
FSTL1	+	+	-	-

+ Indicates that an effect was observed

- Indicates that no effect was observed

The genes ABCB1, ID3, GULP1, SCP and CRYZ were upregulated in the taxol-resistant cell lines. Transfection of the cell lines with siRNAs towards these upregulated genes should lead to increased sensitivity to taxol. Transfection of ABCB1 siRNA into H1299 and especially H1299-tax gave the largest increase in sensitivity observed. Transfection of ID3 siRNA was found to have an effect on proliferation of all the cell lines tested. However, a specific effect of increased sensitivity to taxol was observed in A549, and slightly in H1299. Although H1299-tax had a higher fold change in expression of ID3, the overall protein levels show that ID3 is more highly expressed in A549, which may explain why this effect was only seen in this cell line. Transfection of GULP1 siRNA was found to have no specific effects on A549, A549-tax and H1299-tas, and a slight increase in sensitivity to taxol in H1299-tax. The change in expression of GULP1 was found to be highest in H1299-tax, so this result was expected. Despite increases in its expression in the taxol-resistant cell lines, transfection of SCP siRNA gave no effect on taxol sensitivity in any of the cell lines. Transfection of GULP1 siRNA increased the sensitivity to taxol in H1299, but not in any of the other cell lines. This gene appeared to be expressed quite highly in both A549 and H1299 and the taxol variants, so it is surprising that no effect was observed.

The genes EMP1, CRIP1, FSTL1, CTGF and IGFBP6 were downregulated in the taxol-resistant cell lines. Transfection of the cell lines with siRNAs towards these downregulated genes should lead to increased resistance to taxol. Transfection of EMP1 siRNA had no effect on taxol sensitivity in H1299 or H1299-tax. However, transfection of EMP1 siRNA led to a slight increase in sensitivity to taxol in A549 and A549-tax, which is the opposite effect than expected from the microarray results. This may indicate that EMP1 has involvement in taxol resistance as part of a pathway, rather than on its own.

CRIP1 was almost 3-fold downregulated in A549-tax compared to parent cells in the microarray analyses. In both parent and taxol-selected cells siRNA transfection of CRIP1 led to a dramatic increase in resistance. H1299-tax cells displayed a very large (30-fold) decrease in CRIP1 compared to the parent cells. Unlike A549 cells, siRNA transfection of CRIP1 did not lead to an increase in resistance. This is surprising considering the large fold change compared to the much lower fold change in A549.

Transfection of FSTL1 siRNA into H1299 and H1299-tax had no effect on the sensitivity of these cells to taxol. In A549 and A549-tax, however, there was an unexpected increase in sensitivity to taxol. Transfection of CTGF or IGFBP6 siRNA had no effect on taxol sensitivity in any of the cell lines tested.

In a number of cases, the transfection of siRNA led to the opposite effect on taxol than expected from the microarray results. It is possible that these genes are involved in pathways in taxol resistance and that their function depends on expression of other genes.

4.4.2 Effect of transfection of ABCB1 siRNA on resistance to chemotherapeutic agents

It is evident from the microarray analysis of the taxol-selected cell lines that P-gp plays a role in the development of the resistance observed in these cell lines. In order to determine if the effect of P-gp is taxol-specific, ABCB1 siRNA was transfect cells were tested for sensitivity to taxotere, adriamycin and carboplatin. Taxotere is in the same family of agents as taxol, and these drugs have similar mechanisms of action and resistance. Adriamycin is an anthracycline. It is a substrate for P-gp, but has completely different mechanisms of action from the taxanes, such as DNA intercalation and topoisomerase II inhibition. Carboplatin also has a different mechanism of action, however, it is not a substrate for P-gp.

In a similar manner to taxol, transfection of ABCB1 siRNA led to increases in resistance in A549-tax, H460-tax and especially H1299-tax. H1299 and H1299-tax have been shown to express P-gp. The other taxol-resistant cell lines show an increase in mRNA levels from the microarray experiments, but have no detectable P-gp protein. The increase in sensitivity to taxol and taxotere observed in these variants suggests that P-gp is present in these cell lines. It also indicates that P-gp only needs to be expressed at very low levels to have a substantial effect on the sensitivity of the cells to chemotherapeutic agents. Interestingly, it was only in H1299-tax that an increase in sensitivity to adriamycin was observed after transfection of ABCB1 siRNA. This suggests that the P-gp mechanism active in A549-tax and H460-tax may be taxol specific, which would not be expected from the literature. It is also noteworthy that in

H1299 and H1299-tax a small sensitisation of the cells to carboplatin was observed after transfection of ABCB1 siRNA. This is unusual since carboplatin is not a substrate for P-gp. Overall the results obtained on taxol and taxotere sensitivity from transfection of ABCB1 siRNA are not surprising. P-gp is well characterised as a mechanism of resistance for the taxanes. The lack of an effect in adriamycin sensitivity is surprising. H1299-tax expresses the most P-gp, and was the only cell line to show detectable levels of the protein. However, the taxol and taxotere results, along with results from microarray analysis indicate that there is expression of P-gp in all of the taxol-resistant cell lines. The results from the siRNA experiments with ABCB1 seem to suggest a taxane-specific effect of P-gp, which has not been reported. This may be due to the extremely low levels of protein expressed, and further analysis of the P-gp in the taxol-resistant cell lines would elucidate this mechanism.

4.4.3 Effect of transfection of ID3 siRNA on resistance to chemotherapeutic agents

ID3 showed a slight sensitising effect on taxol in A549, so it was decided to investigate the effect of transfecting ID3 siRNA on the sensitivity of taxotere, adriamycin and carboplatin, as with ABCB1. The effects seen with transfection of ID3 siRNA may not be specific for taxol sensitivity. In A549 transfection with ID3 siRNA led to an increase in sensitivity to taxol. However, the same effect was not observed with taxotere, which is unusual since these drugs share very similar mechanisms of action. No effect was observed on adriamycin sensitivity in any of the cell lines after transfection of ID3 siRNA. Interestingly, a small increase in resistance to carboplatin was observed in both H1299 and H1299 tax after transfection with ID3 siRNA. Conversely, an increase in sensitivity to carboplatin was observed in A549, but not in A549-tax after transfection with ID3 siRNA.

As discussed in Section 4.3.4, a family member of ID3, ID1 has recently been implicated in the response of cancer cells to taxol (Zhang *et al.*, 2005;Cheung *et al.*, 2004). The results demonstrated in this thesis are inconclusive for the role of ID3 in taxol specific resistance, but point to some involvement in drug sensitivity.

4.4.4 Effect of transfection of CRIP1 siRNA on resistance to chemotherapeutic agents

The transfection of CRIP1 siRNA showed a dramatic increase in resistance to taxol in A549 and A549-tax, so the effect on sensitivity to taxotere, adriamycin and carboplatin was examined. These experiments led to some unexpected and interesting results. Transfection of CRIP1 siRNA had the opposite effect on taxotere sensitivity in A549 and A54-tax than taxol, leading to a small increase in sensitivity. This increase in sensitivity was also observed in H1299 and H1299-tax, but not in H460 or H460-tax. Transfection of CRIP1 siRNA also led to an increase in resistance to adriamycin in H1299, H460 and H460-tax. The most interesting results emerged from the carboplatin experiments. Transfection of CRIP1 siRNA led to an increase in resistance to carboplatin in H1299, H1299-tax and A549-tax, but an increase in sensitivity to carboplatin in A549. Despite these interesting effects in A549 and H1299, there was no change in sensitivity to carboplatin in H460 or H460-tax after transfection of CRIP1 siRNA.

Little is known about the functions of CRIP1 in mammalian cells. There is nothing in the literature to suggest the involvement of this gene in the development of chemotherapy resistance. Nonetheless, the results presented here indicate that this gene is involved in determining the sensitivity of lung cancer cells to chemotherapeutic agents. The effects observed on carboplatin sensitivity suggest that this gene is not specifically involved in taxol resistance.

Overall, the results from RNA interference experiments show that the three genes studied in detail have a possible role in taxol resistance, but that it may not be taxol-specific. Although P-gp was well characterised as involved in taxol resistance, two interesting points emerge from the transfection of ABCB1 siRNA. Firstly, the known involvement aided the optimisation of siRNA experiments, since it was expected that silencing of P-gp would lead to increased sensitivity to taxol. In this way, inclusion of ABCB1 in these experiments validates the results obtained in the other siRNA transfections. Secondly, the effects observed after transfection of ABCB1 suggest a taxane-specific effect of P-gp in these cell lines. The results observed after transfection of CRIP1 siRNA demonstrate that this gene has a possible role in resistance not only to taxol, but also to carboplatin. This gene has not been implicated in pathways of resistance before.

Section 5.0: Conclusions & Future work

5.1 Conclusions

1. Wild-type p53 was transfected into three lung cancer cell lines in order to determine the role of p53 in the development of drug resistance. Wild-type p53 transfection into a cell line expressing endogenous wild-type p53 (A549) resulted in populations of this cell line which over-expressed the protein but displyed no considerable changes in sensitivity to adriamycin, taxol or carboplatin. In general, wild-type p53 is associated with decreased resistance to DNA-damaging drugs. However, it is possible that after sensing the DNA damage, p53 is causing the cell cycle to arrest, allowing time for cells, bearing drug-induced mutations, to repair the damage and continue growing. This would result in an observed increase in resistance of the cells. The results presented in this thesis strongly suggest that wild-type p53 alone is not sufficient to significantly alter resistance to chemotherapeutic agents.

2. Of the cell lines transfected, H1299 was chosen to study further since the parental cell line does not express p53. A transfected clone which expresses p53 protein was further analysed H1299-p53 was compared to control transfected clones by microarray analysis. This clone was shown by western blotting to express p53 protein; however, the protein did not seem to be functional since it did not stabilise and accumulate in response to DNA damage. It is probable that the p53 pathway in H1299 has adapted to be controlled by other mechanisms, such as the family member p73, so that introduced p53 no longer interacts with these pathways.

3. Pulse selections were carried out on four lung cancer cell lines, two lung adenocarcinoma cell lines A549 and SKLU1 and two large cell lung carcinoma cell lines H1299 and H460, with either taxol or carboplatin, resulting in eight novel cell lines with relatively low resistance. Selected cell lines show no obvious cross resistance pattern to other drugs except within families of drugs, e.g., taxol and taxotere; carboplatin and cisplatin. The low-level resistance (2-5 fold) observed in these selected cell lines may be more clinically relevant to study than higher levels

of resistance obtained by other methods of selection. Cells pulsed with taxol resulted in more stably resistant cells than those pulsed with carboplatin. It is also worth noting that in the cell line panel pulse selected in the course of this thesis, p53 status did not correlate with development of resistance. A549 and H460 express wild-type p53, H1299 is p53 null and SKLU1 expresses mutant p53.

4. Taxol-resistant cell lines show no consistent alterations in invasion, whereas carboplatin-resistance seems to correlate with a decrease in invasion. In all four cell lines, the carboplatin-selected variants are less invasive than the parent cells. Of the taxol-selected variants, however, two of the variants had decreased invasive potential compared to the parent cell lines and two showed slight increases in ability to invade.

5. Taxol-resistant cell lines were chosen for further analysis using microarrays. Microarray experiments were carried out on four parent cell lines and their taxol-selected variants. Microarray analysis identified nineteen genes which were significantly differentially expressed in all taxol variants compared to parent cell lines. Only two of these genes were up-regulated in all four taxol variants, Mdr1 and phosphoglucomutase 2. Interestingly, no genes downregulated in all four taxol variants.

6. Ten targets were chosen for further analysis based on up-regulation or down-regulation in three out of the four taxol variants compared to parent. These were ATP-binding casette sub-family B member 1 (ABCB1), Quinone reductase (CRYZ), Epithelial membrane protein 1 (EMP1), Inhibitor of DNA binding 3 (ID3), Cysteine-rich intestinal protein (CRIP1), Stromal cell protein (SCP), Insulin-like growth factor binding protein 6 (IGFBP6), Engulfment adaptor PTB domain containing 1 (GULP), Follistatin-like 1 (FSTL1) and Connective tissue growth factor (CTGF). Three of these targets, ABCB1, ID3 and CRIP1 showed an interesting functional effect on taxol sensitivity in the cell lines tested. Based on the results, these genes have definite involvement in the determination of resistance

to taxol in the cell lines studied. Changes in expression of these genes alone is not enough to completely change the sensitivity of the cell lines to taxol and most likely many genes are involved.

7. ABCB1 (P-gp) has a well documented role in modulating resistance to chemotherapeutic agents. The results presented in this thesis indicate a possible taxane specific effect of low levels of P-gp, since transfection of ABCB1 siRNA did not affect sensitivity of adriamycin, a known P-gp substrate, in cells which should express low levels of P-gp.

8. The gene CRIP1 has not been implicated in resistance to chemotherapy resistance before. The results presented in this thesis suggest that, although it is probably not taxol-specific, this gene may have a possible role in the determination of resistance to chemotherapeutic agents.

5.2 Future work

1. The taxol and carboplatin selected cell lines in this thesis represent valuable models for the study of mechanisms of resistance to these drugs. Most of the analysis in this thesis focussed on the taxol-resistant cell lines, however, similar analysis would be interesting in the carboplatin-resistant cell lines. The carboplatin-resistance cell lines could be examined by microarray analysis and candidate genes for development of carboplatin resistance could be identified. Moreover, the genes identified as involved in taxol resistance could be analysed in the carboplatin-resistant cell lines, since most of these genes are probably not taxol-specific.

2. The microarray analyses carried out in this thesis generated vast amounts of data. Only a fraction of this could be analysed further, and consequently, much of the data containing interesting information on the models used still remains to be examined. An alternative method of analysis, other than that used in this thesis involves examining large gene lists generated by dChip in the pathway analysis packages discussed. Pathway analysis of genelists can indicate interesting groups of genes to study based on common pathways they are involved in. Two microarray experiments were included in this thesis, one on taxol resistant lung cancer cell lines and the other on a p53-expressing cell line. Both of these experiments could be further analysed using pathway analysis.

3. Three genes that were candidates for involvement in the development of taxol resistance were identified – ABCB1, ID3 and CRIP1. The involvement of ABCB1 in resistance is well documented, however this is not the case for ID3 and CRIP1. Although the experiments carried out using siRNA transfection suggest a role for these genes in resistance to chemotherapeutic agents, further elucidation of the mechanisms involved is necessary. Firstly, silencing of the genes by siRNA transfection should be verified by western blotting, to show silencing at the protein

levels. The next step would be to include a wider range of chemotherapeutic agents and also more cell lines with varying resistance.

4. During pulse-selection of the cell lines A549, H1299, H460 and SKLU1, cell stocks were established after 2, 4, 6 and 8 pulses before the cells received the full ten pulse of either taxol or carboplatin. These intermediate cell lines have not been charaterised for drug resistance, invasion or expression of any markers. Using these cell lines, it may be possible to track the development of resistance to taxol and carboplatin. In the taxol-resistant variants specifically, it may be possible to identify when the expression of the genes ABCB1, ID3 and CRIP1 began to change, and also if there is a correlation between the level of expression of these genes and the development of taxol resistance.

5. Proteomic analysis of the taxol-resistant lung cancer cell lines, along with the parent cell lines would be an interesting addition to the microarray analysis already carried out. This will involve 2-dimensional gel electrophoretic separation of the proteins in a cell extract in order to determine proteins that are differentially expressed. Differentially expressed proteins will be identified using MALDI.

6. The genes identified in this thesis as potentially involved in taxol resistance should be further analysed. Taxol resistance remains a serious problem in the treatment of cancer, and the genes identified here could help increase our knowledge of the complex mechanisms involved.

Section 6.0: Bibliography

Albini, A. (1998). Tumor and endothelial cell invasion of basement membranes. The matrigel chemoinvasion assay as a tool for dissecting molecular mechanisms. *Pathol Oncol Res.*, **4**, 230-241.

Ambudkar, S.V., Dey, S.,Hrycyna, C.A., Ramachandra, M., Pastan, I., Gottesman, M.M. (1999). Biochemical, cellular, and pharmacological aspects of the multidrug transporter. *Annu. Rev. Pharmacol. Toxicol.*, **39,** 361-398.

Amundson, S.A., Myers, T.G., Scudiero, D., Kitada, S., Reed, J.C., Fornace Jr., A.J. (2000). An informatics approach identifying markers of chemosensitivity in human cancer cell lines. *Cancer Res.*, **60**, 6101-6110.

Bahr, O., Wick, W., Weller, M. (2001). Modulation of MDR/MRP by wild-type and mutant p53. *J. Clin. Invest.*, **107**, 643-646.

Baker, S.J., Markowitz, S., Fearon, E.R., Willson, J.K.V., Vogelstein, B. (1990). Suppression of human colorectal carcinoma cell growth by wild-type p53. *Science*, **249**, 912-915.

Belvedere, G., Imperatori, L., Damia, G., Tagliabue, G., Meijer, C., de Vries, E.G.E., D'Incalci, M. (1996). *In Vitro* and *In Vivo* characterisation of low-resistant mouse reticulosarcoma (M5076) sublines obtained after pulse and continuos exposure to cisplatin. *Eur. J. Cancer*, **32A**, 2011-2018.

Berger, W., Elbling, L., Micksche, M. (2000). Expression of the major vault protein LRP in human non-small cell lung cancer cells: Activation by a short-term exposure to antineoplastic drugs. *Int. J. Cancer*, **88**, 293-300.

Bhalla, K., Huang, Y., Tang, C., Self, S., Ray, S., Mahoney, M.E., Ponnathpur, V., Tourkina, E., Ibrado, A.M., Bullock, G. (1994). Characterisation of a human myeloid leukemia cell line highly resistant to taxol. *Leukemia*, **8**, 465-475.

Bhattacharjee, A., Richards, W.G., Staunton , J., Li, C., Monti, S., Vasa, P., Ladd, C., Beheshti, J., Bueno, R., Gillette, M., Loda, M., Weber, G., Mark, E.J., Lander, E.S., Wong, W., Johnson, B.E., Golub, T.R., Sugarbaker, D.J., Meyerson, M. (2001). Classification of human lung carcinomas by mRNA expression profiling reveals distinct adenocarcinoma subclasses. *Proc. Natl. Acad. Sci.*, **98**, 13790-13795.

Borst, P., Kool, M., Evers, R. (1997). Do cMOAT (MRP2), other MRP homologues, and LRP play a role in MDR? *Semin. Cancer Biol.*, **8**, 205-213.

Brazma, A., Hingamp, P., Quackenbush, J., Sherlock, G., Spellman, P., Stoeckert, C., Aach, J., Ansorge, W., Ball, C.A., Causton, H.C., Gaasterland, T., Glenisson, P., Holstege, F.C.P., Kim, I.F., Markowitz, V., Matese, J.C., Parkinson, H., Robinson, A., Sarkans, U., Schulze-Kremer, S., Stewart, J., Taylor, R., Vilo, J., Vingron, M. (2001). Minimum information about a microarray experiment (MIAME)-toward standards for microarray data. *Nat. Gene.*, **29**, 365-371.

Bridge, A.J., Pebernard, S., Ducraux, A., Nicoulaz, A.L., Iggo, R. (2003). Induction of an interferon response by RNAi vectors in mammalian cells. *Nat. Genet.*, **34**, 263-264.

Brown, J.M., Wouters, B.G. (1999). Apoptosis, p53 and tumour cell sensitivity to anticancer agents. *Cancer Res.*, **59**, 1391-1399.

Bunz, F. (2001). Cell death and cancer therapy. *Curr. Opin. Pharmacol.*, **1**, 337-341.

Bush, J.A., Li, G. (2002). Cancer chemoresistance: The relationship between p53 and multidrug transporters. *Int. J. Cancer*, **98**, 323-330.

Cadwell, C., Zambetti, G.P. (2001). The effects of wild-type p53 tumour suppressor activity and mutant gain-of-function on cell growth. *Gene*, **277**, 15-30.

Cajot, J.F., Anderson, M.J., Lehman, T.A., Shapiro, H., Briggs, A.A., Stanbridge, E.J. (1992). Growth suppression mediated by transfection of p53 in Hut292DM human lung cancer cells expressing endogenous wild-type p53 protein. *Cancer Res.*, **52**, 6956-6960.

Canitrot, Y., Bichat, F., Cole, S.P.C., Deeley, R.G., Gerlach, J.H., Bastian, G., Arvelo, F., Poupon, M.-F. (1998). Multidrug resistance genes (MRP) and MDR1 expression in small cell lung cancer xenografts: relationship with response to chemotherapy. *Cancer Lett.*, **130**, 133-141.

Celius, T., Garberg, P., Lundgen, B. (2004). Stable supression of MDR1 gene expression and function by RNAi in Caco-2 cells. *Biochem. Biophys. Res. Commun.*, **324**, 365-371.

Ceraline, J., Deplanque, G., Duclos, B., Limacher, J.M., Hajri, A., Noel, F., Orvain, C., Frebourg, T., Klein-Soyer, C., Bergerat, J.P. (1998). Inactivation of p53 in normal human cells increases G2/M arrest and sensitivity to DNA-damaging agents. *Int. J. Cancer*, **75**, 432-438.

Chen, J.J.W., Peck, K., Hong, T.-M., Yang, S.-C., Sher, Y.-P., Shih, J.-Y., Wu, R., Cheng, J.-L., Roffler, S.R., Wu, C.-W., Yang, P.-C. (2001). Global analysis of gene expression in invasion by a lung cancer model. *Cancer Res.*, **61**, 5223-5230.

Cheung, H.W., Ling, M.T., Tsao, S.W., Wong, Y.C., Wang, X. (2004). Id-1 induced Raf/MEK pathway activation is essential for its protective role against taxol-induced apoptosis in nasopharyngeal carcinoma cells. *Carcinogenesis*, **25**, 881-887.

Chi, J.T., Chang, H.Y., Wang, N.N., Chang, D.S., Dunphy, N., Brown, P.O. (2003). Genomewide view of gene silencing by small interfering RNAs. *Proc Natl. Acad. Sci USA*, **100**, 6343-6346.

Chrystal, K., Cheong, K., Harper, P. (2004). Chemotherapy of small cell lung cancer: state of the art. *Curr. Opin. Oncol.*, **16**, 136-140.

Colman, M.S., Afshari, C.A., Barrett, J.C. (2000). Regulation of p53 stability and activity in response to genotoxic stress. *Mutation Res.*, **462**, 179-188.

Cousins, R.J., Lanningham-Foster, L. (2000). Regulation of cyteine-rich intestinal protein, a zinc finger protein, by mediators of the immune response. *J. Infect. Dis.*, **182**, S81-S84.

Dan, S., Tsunoda, T., Kitahara, O., Yanagawa, R., Zembutsu, H., Katagiri, T., Yamazaki, K., Nakamura, Y., Yamori, T. (2002). An integrated database of chemosensitivity to 55 anticancer drugs and gene expression profiles of 39 human cancer cell lines. *Cancer Res.*, **62**, 1139-1147.

Das, G.C., Holiday, D., Gallardo, R., Haas, C. (2001). Taxol-induced cell cycle arrest and apoptosis: dose-response relationship in lung cancer cells of different wild-type p53 status and under isogenic condition. *Cancer Letters*, **165**, 147-153.

Debatin, K.-M. (2000). Activation of apoptosis pathways by anticancer treatments. *Toxicol. Lett.*, **112-113**, 41-48.

De Bruin, M., Miyake, K., Litman, T., Robey, R., Bates, S.E. (1999). Reversal of resistance by GF120918 in cell lines expressing the ABC half-transporter, MXR. *Cancer Letters*, **146**, 117-126

Derry, W.B., Wilson, L., Khan, I.A., Luduena, R.F., Jordan, M.A. (1997). Taxol differentially modulates the dynamics of microtubules assembled from unfractionated and purified β-tubulin isotypes. *Biochemisty*, **36**, 3554-3562.

Devroe, E., Silver, P.A. (2004). Therapeutic potential of retroviral RNAi vectors *Expert Opin. Biol. Ther.*, **4**, 319-327.

Dingemans, A.M.C., van Ark-Otte, J., Span, S., Scagliotti, G.V., van der Valk , P., Postmus, P.E., Giaccone, G. (2001). Topoisomerase II and other drug resistance markers in advanced non-small cell lung cancer. *Lung Cancer*, **32**, 117-128.

Duan, Z., Brakora, K.A., Seiden, M.V. (2004). MM-TRAG (MGC4175), a novel intracellular mitochondrial protein, is associated with the taxol- and doxorubicin-resistant phenotype in human cancer cell lines. *Gene*, **340**, 53-59.

Duan, Z., Feller, A.J., Toh, H.C., Makastorsis, T., Seiden, M.V. (1999). TRAG-3, a novel gene isolated from a taxol-resistant ovarian carcinoma cell line. *Gene*, **229**, 75-81.

Duffy, C.P., Elliott, C.J., O'Connor, R.A., Heenan, M.M., Coyle, S., Cleary, I.M., Kavanagh, K., Verhaegen, S., O'Loughlin, C.M., NicAmhlaoibh, R., Clynes, M. (1998). Enhancement of chemotherapeutic drug toxicity to human tumour cells *in vitro* by a subset of non-steroidal anti-inflammatory drugs (NSAIDs). *Eur. J. Cancer*, **34**, 1250-1259.

Dumontet, C., Duran, G.E., Steger, K.A., Beketic-Oreskovic, L., Sikic, B.I. (1996). Resistance mechanismd in human sarcoma mutants derived by single-step exposure to paclitaxel (taxol). *Cancer Res.*, **56**, 1091-1097.

Ehara, Y., Sakurai, D., Tsuchiya, N., Nakano, K., Tanaka, Y., Yamaguchi, A., Tokunaga, K. (2004). *Clin. Exp. Rheumatol.*, **22**, 707-712.

Eisen, M.B, Spellman, P.T., Brown, P.O., Botstein, D. (1998). Cluster analysis and display of genome-wide expression patterns. *Proc. Natl. Acad. Sci. USA*, **95**, 14863-14868.

Fan, J., Bertino, J.R. (1999). Modulation of cisplatinum cytotoxicity by p53: Effect of p53-mediated apoptosis and DNA repair. *Mol. Pharmocol.*, **56**, 966-972.

Fan, S., El-Deiry, W.S., Bae, I., Freeman, J., Jondle, D., Bhatia, K., Fornace, A.J., Magrath, I., Kohn, K.W., O'Connor, P.M. (1994). P53 gene mutations are associated with decreased sensitivity of human lymphoma cells to DNA damaging agents. *Cancer Res.*, **54**, 5824-5830.

Fan, W.H., Karnovsky, M.J. (2002). Increased MMP-2 expression in connective tissue growth factor over-expression vascular smooth muscle cells. *J. Biol. Chem.*, **277**, 9800-9805.

Ferreira, C.G., Tolis, C., Span, S.W., Peters, G.J., van Lopik, T., Kummer, A.J., Pinedo, H.M., Giaconne, G. (2000). Drug-induced apoptosis in lung cancer cells is not mediated by the Fas/FasL (CD95/APO1) signaling pathway. *Clin. CancerRes.*, **6**, 203-212.

Ferreira, C.G., Tolis, C., Giaconne, G. (1999). P53 and chemosensitivity. *Ann.Oncol.*, **10**, 1011-1021.

Ferreira, P., Oliveira, M.J., Beraldi, E., Mateus, A.R., Nakajima, T., Gleave, M., Yokota, J., Carneiro, F., Huntsman, D., Seruca, R., Suriano, G. (2005). Loss of functional E-cadherin renders cells more resistant to the apoptotic agent taxol *in vitro*. *Exp. Cell Res.*, **310**, 99-104.

Francis, P.A., Kris, M.G., Rigas, J.R., Grant, S.C., Miller, V.A. (1995). Paclitaxel (Taxol) and docetaxel (Taxotere): active chemotherapeutic agents in lung cancer. *Lung Cancer*, **12**, S163-S172.

Fujiwara, T., Grimm, E.A., Mukhopadhyay, T., Zhang, W.-W., Owen-Schaub, L.B., Roth, J.A. (1994). Induction of chemosensitivity in human lung cancer cells *in vivo* by adenovirus-mediated transfer of the wild-type p53 gene. *Cancer Res.*, **54**, 2287-2291.

Fukushima, Y., Oshika, Y., Tokaunaga, T., Hatanaka, H., Tomisawa, M., Kawai, K., Ozeki, Y., Tsuchida, T., Kijima, H., Yamazaki, H., Ueyama, Y., Tamaoki, N., Miura, S., Nakamura, M. (1999). Multidrug resistance-associated protein (MRP) expression is correlated with expression of aberrant p53 protein in colorectal cancer. *Eur. J. Cancer*, **35**, 935-938.

Gallagher, W.H., Brown, R. (1999). P53-oriented therapies: current progress. *Ann. Oncol.*, **10**, 139-150.

Galmarini, C.M., Falette, N., Tabone, E., Levrat, C., Britten, R., Voorzanger-Rousselot, N., Roesch-Gateau, O., Vanier-Viornery, A., Puisieux, A., Dumontet, C. (2001). Inactivation of wild-type p53 by a dominant negative mutant renders MCF-7 cells resistant to tubulin-binding agent cytotoxicity. *Br. J. Cancer*, **85**, 902-908.

Germann, U.A., Pastan, I., Gottesman, M.M. (1993). P-glycoproteins: mediators of multidrug resistance. *Semin. Cell Biol.*, **4**, 63-76.

Giannakakou, P., Sackett, D.L., Kang, Y.K., Zhan, Z., Buters, J.T.M., Fojo, T., Poruchynsky, M.S. (1997). Paclitaxel-resistant human ovarian cancer cells have mutant β-tubulins that exhibit impaired paclitaxel-driven polymerization. *J. Biol. Chem.*, **272**, 17118-17125.

Gidding, C.E., Kellie, S.J., Kamps, W.A., de Graaf, S.S. (1999). Vincristine revisited. *Crit. Rev. Oncol. Hematol.*, **29**, 267-287.

Glynn, S.A., Gammell, P., Heenan, M., O'Connor, R., Liang, Y., Keenan, J., Clynes, M. (2004). A new superinvasive in vitro phenotype induced by selection of human breast carcinoma cells with the chemotherapeutic drugs paclitaxel and doxorubicin. *Br. J. Cancer*, **91**, 1800-1807.

Go, R.S., Adjei, A.A. (1999). Review of the comparative pharmacology and clinical activity of cisplatin and carboplatin. *J. Clin. Oncol.*, **17**, 409-422.

Goncalves, A., Braguer, D., Kamath, K., Martello, L., Briand, C., Horwitz, S., Wilson, L, Jordan, M.A. (2001). Resistance to taxol in lung cancer cells associated with increased microtubule dynamics. *Proc. Natl. Acad. Sci. USA*, **98**, 11737-11741.

Gonzalez, P., Rao, P.V., Nunez, S.B., Zigler, J.S. (1995). Evidence for independent recruitment of ξ-crystallin/quinone reductase (CRYZ) as a crystallin in camelids and hystricomorph rodents. *Mol. Biol. Evol.*, **12**, 773-781.

Grellier, P., Berrebi, D., Peuchmaur, M., Babajko, S. (2002). The IGF system in neuroblastome xenografts: focus on IGF-binding protein-6. *J. Endocrinol.*, **172**, 467-476.

Han, E.K.H., Gehrke, L., Tahir, S.K., Credo, R.B., Cherian, S.P., Sham, H., Rosenberg, S.H., Ng, S. (2000). Modulation of drug resistance by alpha-tubulin in paclitaxel-resistant human lung cancer cell lines. *Eur. J. Cancer*, **36**, 1565-1571

Hande, K.R. (1998). Etoposide: four decades of development of a topoisomerase II inhibitor. *Eur. J. Cancer*, **34**, 1514-1521.

Hansen, L.T., Lundin, C., Helleday, T., Skovgard Poulsen, H., Storgaard Sorensen, C., Norgard Petersen, L., Spang-Thomsen, M. (2003). DNA repair rate and etoposide (VP-16) resistance of tumor cell subpopulations derived from a single human small cell lung cancer. *Lung Cancer*, **40**, 157-164.

Harms, K., Nozell, S., Chen, X. (2004). The common and distinct target genes of the p53 family transcription factors. *Cell. Mol. Life Sci.*, **61**, 822-842.

Hawkins, D.S., Demers, G.W., Galloway, D.A. (1996). Inactivation of p53 enhances sensitivity to multiple chemotherapeutic agents. *Cancer Res.*, **56**, 892-898.

Hecht, S.S. (2002). Cigarette smoking and lung cancer: chemical mechanisms and approaches to prevention. *Lancet Oncol.*, **3**, 461-469.

Hempe, J.M., Cousins, R.J. (1991). Cysteine-rich intestinal proteinbinds zinc during trasnmucosal zinc transport. *Proc. Natl. Acad. Sci. USA*, **88**, 9671-9674.

Hirsch, F.R., Fischer, J.R., Niklinsky, J., Zochbauer-Muller, S. (2002). Future developments in the treatment of lung cancer. *Lung Cancer*, **38**, S81-S85.

Hoffman, P.C., Mauer, A.M., Vokes, E.E. (2000). Lung cancer. *The Lancet*, **355**, 479-485.

Hillgenberg, M. Schlerhofer, J.R., Knebel Doeberitz M. and Klein-Bauernschmitt, P. (1999) Enhanced sensitivity of small cell lung cancer cell lines to cisplatin and etoposide after infection with adeno-associated virus type 2. *European Journal of Cancer* **35,**106-110.

Hishikawa, K., Oemar, B.S., Tanner, F.C., Nakaki, T., Luscher, T.F., Fujii, T. (1999). Connective tissue growth factor induces apoptosis in human breast cancer cell line MCF-7. *J. Biol. Chem.*, **274**, 37461-37466.

Huang, T.G., Ip, S.-M., Yeung, W.S.B., Ngan, H.Y.S. (2000). Changes in $p21^{WAF1}$, pRb, Mdm-2, Bax, Bcl-2 expression in cervical cancer cell lines transfected with a p53 expressing adenovirus. *Eur. J. Cancer*, **36**, 249-256.

Huang, Y., Ibrado, A.M., Reed, J.C., Bullock, G., Tang, C., Bhalla, K. (1997). Co-expression of several molecular mechanisms of multidrug resistance and their significance for paclitaxel cytotoxicity in human AML HL-60 cells. *Leukemia*, **11**, 253-257.

Huang, Y., Ray, S., Reed, J.C., Ibrado, A.M., Tang, C., Nawabi, A., Bhalla, K. (1997). Estrogen increased intracellular p26Bcl2 to p21Bax ratios and inhibits taxol-induced apoptosis of human breast cancer MCF-7 cells. *Breast Cancer Res. Treat.*, **42**, 73-81.

Hutvagner, G., Zamore, P.D. (2002). RNAi: Nature abhors a double strand. *Curr. Op. Gen. Dev.*, **12**, 225-232.

Ikuta, K., Takemura, K., Sasaki, K., Kihara, M., Nishimura, M., Ueda, N., Naito, S., Lee, E., Shimizu, E., Yamauchi, A. (2005). Expression of multidrug resistance proteins and accumulation of cisplatin in human non-small cell lung cancer cells. *Biol. Pharm. Bull.*, **28**, 707-712.

Inoue, A., Narumi, K., Matsubara, N., Sugawara, S., Saijo, Y., Satoh, K., Nukiwa, T. (2000). Administration of wild-type p53 adenoviral vector synergistically enhances the cytotoxicity of anticancer drugs in human lung cancer cells irrespective of the status of p53 gene. *Cancer Letters*, **157**, 105-112.

Jackson, A.L., Bartz, S.R., Schelter, J., Kobayashi, S.V., Burchard, J., Mao, M., Li, B., Cavet, G., Linsley, P.S. (2003). Expression profiling reveals off-target gene regulation by RNAi. *Nat. Biotechnol.*, **21**, 635-637.

Jain, A., Tindell, C.A., Laux, I., Hunter, J.B., Curran, J., Galkin, A., Afar, D.E., Aronson, N., Shak, S., Natale, R.B., Agus, D.B. (2005). Epithelial membrane protein-1 is a biomarker of gefitinib resistance. *Proc. Natl. Acad. Sci. USA*, **102**, 11858-11863.

Jassem, E., Niklinski, J., Rosell, R., Niklinska, W., Jakobkiewicz, J., Monzo, M., Chyczewski, L., Kobierska, G., Skokowski, J., Zylicz, M., Jassem, J. (2001). Types and localisation of p53 mutations. A report on 332 non-small cell lung cancer patients. *Lung Cancer*, **34**, S47-S51.

Johnson, R.A., Shepard, E.M., Scotto, K.W. (2005). Differential regulation of MDR1 transcription by the p53 family members: Role of the DNA binding domain. *J. Biol. Chem.*, **280**, 13213-13219.

Jordan, M.A. (2002). Mechanism of action of antitumor drugs that interact with microtubules and tubulin. *Curr. Med. Chem.*, **2**, 1-17.

Kang, H.-C., Kim, I.-J., Park, J.-H., Shin, Y., Ku, J.-L., Jung, M.S., Yoo, B.C., Kim, H.K., Park, J.-G. (2004). Identification of genes with differential expression in acquired drug-resistant gastric cancer cells using high-density oligonucleotide microarrays. *Clin.Cancer Res.*, **10**, 272-284.

Kavallaris, M., Kuo, D.Y.S., Burkhart, C.A., Regl, D.L., Norris, M.D., Haber, M., Horwitz, S.B. (1997). Taxol-resistant epithelial ovarian tumors are associated with altered expression of specific β-tubulin isotypes. *J. Clin. Invest.*, **100**, 1282-1293.

Kawai, H., Kiura, K., Tabata, M., Yoshino, T., Takata, I., Hiraki, A., Chikamori, K., Ueoka, H., Tanimoto, M., Harada, M. (2002). Characterization of non-small cell lung cancer cell lines established beofre and after chemotherapy. *Lung Cancer*, **35**, 305-314.

Ke, X.S., Liu, C.M., Liu, D.P., Liang, C.C. (2003) MicroRNAs: key participants in gene regulatory networks. *Curr. Opin. Chem. Biol.*, 7, 516-523.

Kim, V.N. (2003). RNA interference in functional genomics and medicine. *J. Koream Med. Sci.*, **18**, 309-318.

Klein, I., Sarkadi, B., Varadi, A. (1999). An inventory of the human ABC proteins. *Biochim. Biophys. Acta.*, **1461**, 237-262.

Koyama, T., Suzuki, H., Imakiire, A., Yanase, N., Hata, K., Mizuguchi, J. (2004). Id3-mediated enhancement of cisplatin-induced apoptosis in a sarcoma cell line MG-63. *Anticancer Res.*, **24**, 1519-1524.

Krishna, R., Mayer, L.D. (2000). Multidrug resistance (MDR) in cancer. Mechanisms, reversal using modulators of MDR and the role of MDR modulators in influencing the pharmacokinetics of anticancer drugs. *Eur. J. Pharmaceut. Sci.*, 11, 265-283.

Kudoh, K., Ramanna, M., Ravatn, R., Elkahloun, A.G., Bittner, M.L., Meltzer, P.S., Trent, J.M., Dalton, W.S., Chin, K.-V. (2000). Monitoring the expression profiles of doxorubicin-induced and doxorubicin-resistant cancer cells by cDNA microarray. *Cancer Res.*, **60**, 4161-4166.

Kurschat, P., Mauch, C. (2000). Mechanisms of metastasis. *Clin. Exp. Dermatol.*, **25**, 482-489.

Lamendola, D.E., Duan, Z., Yusuf, R.Z., Seiden, M.V. (2003). Molecular description of evolving paclitaxel resistance in the SKOV-3 human ovarian carcinoma cell line. *Cancer Res.*, **63**, 2200–2205.

Lane, D.P., Lain, S. (2002). Therapeutic exploitation of the p53 pathway. *Trends Mol. Med.*, **8**, S38-S42

Lanningham-Foster, L., Green , C.L., Langkammp-Henken, B., Davis, B.A., Nguyen, K.T., Bender, B.S., Cousins, R.J. (2002). Overexpression of CRIP in transgenic mice alters cytokine patterns and the immune response. *Am. J. Physiol. Endocrinol. Metab.*, **282**, E1197-E1203.

Lavarino, C., Pilotti, S., Oggionni, M., Gatti, L., Perego, P., Bresciani, G., Pierotti, M.A., Scambia, G., Ferrandina, G., Fagotti, A., Mangioni, C., Lucchini, V., Vecchione, F., Bolis, G., Scarfone, G., Zunino, F. (2000). P53 gene status and response to platinum/paclitaxel-based chemotherapy in advanced ovarian carcinoma. *J. Clin. Oncol.*, **18**, 3936-3945.

Levine, A.J. (1997). p53, the cellular gatekeeper for growth and division. *Cell,* **88**, 323-331.

Li, Z.H., Zhu, Y.J., Lit, X.T. (1997). Wild-type p53 gene increases MDR1 gene expression but decreases drug resistance in an MDR cell line KB_{V200}. *Cancer Lett.*, **119**, 177-184.

Liang, Y., O'Driscoll, L., McDonnell, S., Doolan, P., Oglesby, I., Duffy, K., O'Connor, R., Clynes, M. (2004). Enhanced *in vitro* invasiveness and drug resistance with altered gene exppression patterns in a human lung carcinoma cell line after pulse selection with anticancer drugs. *Int. J. Cancer*, **111**, 484-493.

Liang, Y., McDonnell, S., Clynes, M. (2002). Examining the relationship between cancer invasion/metastasis and drug resistance. *Curr. Cancer Drug Targets*, **2**, 257-277.

Liang, Y., Meleady, P., Cleary, I., McDonnell, S., Connolly, L., Clynes, M. (2001) Selection with melphalan or paclitaxel (Taxol) yields variants with different patterns of multidrug resistance, integrin expression and *in vitro* invasiveness. *Eur. J. Cancer*, **37**, 1041-1052.

Lin-Lee, Y.-C., Tatebe, S., Savary, N., Ishikawa, T., Kuo, M.T. (2001). Differential sensitivities of the MRP gene family and γ-glutamylcysteine synthetase to prooxidants in human colorectal carcinoma cell lines with different p53 status. *Biochem. Pharmacol.*, 61, 555-563.

Lin, M., Wei, L.J., Sellers, W.R., Lieberfarb, M., Wong, W.H., Li, C. (2004). dChipSNP: Significance Curve and Clustering of SNP-Array-Based Loss-of-Heterozygosity Data. *Bioinformatics*, **20**, 1233-1240.

Ling, X., Bernacki, R.J., Brattain, M.G., Li, F. (2004). Induction of survivin expression by taxol (paclitaxel) is an early event, which is independent of taxol-mediated G2/M arrest. *J. Biol. Chem.*, **279**, 15196-15203.

Liu, J.R., Fletcher, B., Page, C., Hu, C., Nunez, G., Baker, V. (1998). Bcl-X_L is expressed in ovarian carcinoma and modulated chemotherapy-induced apoptosis. *Gynecol. Oncol.*, **70**, 398-403.

Liu, T.-J., El-Naggar, A.K., McDonnell, T.J., Steck, K.D., Wang, M., Taylor, D.L., Clayman, G.L. (1995). Apoptosis induction mediated by wild-type p53 adenoviral gene transfer in squamous cell carcinoma of the head and neck. *Cancer Res.*, **55**, 3117-3122.

Liu, X.D., Ma, S.M., Liu, Y., Liu, S.Z., Sehon, A. (2004). Short hairpin RNA and retroviral vector-mediated silencing of p53 in mammalian cells. *Biochem. Biophys. Res. Commun.*, **324**, 1173-1178.

Longley, D.B., Johnston, P.G. (2005). Molecular mechanisms of drug resistance. *J. Pathology*, **205**, 275-292.

Lowe, S.W., Ruley, H.E., Jacks, T., Housman, D.E. (1993). P53-dependent apoptosis modulates the cytotoxicity of anticancer agents. *Cell*, 74, 957-967.

Lyon, R., Cohen, J.S., Faustino, P.J., Megnin, F., and Myers, C.E. (1988). Glucose metabolism in drug-sensitive and drug-resistant human breast cancer cells monitored by magnetic resonance spectroscopy. *Cancer Res.*, **48**, 870-877.

Mackay,A., Jones, C., Dexter, T., Silva, R.L., Bulmer, K., Jones, A., Simpson, P., Harris, R.A., Jat, P.S., Neville, A.M., Reis, L.F., Lakhani, S.R., O'Hare, M.J. (2003). CDNA microarray analysis of genes associated with ERBB2 (HER2/neu) overexpression in human mammary luminal epithelial cells. *Oncogene*, **22**, 2680-2688.

Manegold, C. (2002). Chemotherapy for advanced non-small cell lung cancer (NSCLC). *Lung Cancer*, **38**, S47-S50.

Marcus, A.L., Peters, U., Thomas, S.L., Garrett, S., Zelnak, A., Kapoor, T.M., Giannakakou, P. (2005). Mitotic kinesin inhibitors induce mitotic arrest and cell death in taxol-resistant and sensitive cancer cells. *J. Biol. Chem.*, **280**, 11569-11577.

Martello, L.A., Verdier-Pinard, P., Shen, H.J., He, L., Torres, K., Orr, G.A., Horwitz, S.B. (2003). Elevated levels of microtubule destabilizing factors in a taxol-resistant/dependent A549 cell line with an α-tubulin mutation. *Cancer Res.*, **63**, 1207-1213.

Martinez, L.A., Naguibneva, I., Lehrmann, H., Vervisch, A., Tchenio, T., Lozano, G., Harel-Bellan, A. (2002). Synthetic small inhibiting RNAs: efficient tools to inactivate oncogenic mutations and restore p53 pathways. *Proc. Natl. Acad. Sci. USA*, 99 14849-14854.

Matsumoto, H., Takahashi, A., Wang, X., Ohnishi, K., Ohnishi, T. (1997). Transfection of p53 knockout mice fibroblasts with wild-type p53 increases the thermosensitivity and stimulates apoptosis induced by heat stress. *Int. J. Radiation Oncology Biol. Phys.*, **39**, 197-203.

McManus, M.T., Sharp, P.A. (2002). Gene silencing in mammals by small interfering RNAs. *Nat. Rev. Genetics*, **3**, 737-747.

Mechetner, E., Kyshtoobayeva, A., Zonis, S., Kim, H., Stroup, R., Garcia, R., Parker, R.J., Fruehauf, J.P. (1998). Levels of multidrug resistance (MDR1) P-glycoprotein expression by human breast cancer correlate with *in vitro* resistance to taxol and doxorubicin. *Clin. Cancer Res.*, **4**, 389-398.

Meschini, S., Marra, M., Calcabrini, A., Monti, E., Gariboldi, M., Dolfini, E., Arancia, G., (2002). Role of lung resistance-related protein (LRP) in the drug sensitivity of cultured tumor cells. *Toxicology In Vitro*, **16**, 389-398.

Miller, M.L., Ojima, I. (2001). Chemistry and chemical biology of taxane anticancer agents. *Chem. Rec.*, **1,** 195-211.

Miyake, H., Hara, I., Hara, S., Arakawa, S., Kamidona, S. (2000). Synergistic chemosensitization and inhibition of tumour growth and metastasis by adenovirus-mediated p53 gene transfer in human bladder cancer model. *Urology*, **56**, 332-336.

Monzo, M., Rosell, R., Sanchez, J.J., Lee, J.S., O'Brate, A., Gonzalez-Larriba, J.L., Alberola, V., Lorenzo, J.C., Nunez, L., Ro, J.Y., Martin, C. (1999). Paclitaxel resistance in non-small cell lung cancer associated with beta-tubulin gene mutations. *J. Clin. Oncol.*, **17**, 1786-1793.

Nielsen, L.L., Lipari, P., Dell, J., Gurnani, M., Hajian, G. (1998). Adenovirus-mediated p53 gene therapy and paclitaxel have synergistic efficacy in models of human head and neck, ovarian, prostate and breast cancer. *Clin. Cancer Res.*, **4**, 835-846.

Norton, J.D. (2000). ID helix-loop-helix proteins in cell growth, differentiation and tumorigenesis. *J. Cell Sci.*, **113**, 3897-3905.

Norton, J.D., Atherton, G.T. (1998). Coupling of cell growth control and apoptosis functions of ID proteins. *Mol. Cell. Biol.*, **18**, 2371-2381.

O'Connor, R., Heenan, M., Connolly, L., Larkin, A., Clynes, M. (2004). Increased anti-tumour efficacy of doxorubicin when combined with sulindac in a xenograft model of an MRP-1-positive human lung cancer. *Anticancer Res.*, **24**, 457-464.

Oguri, S., Sakakibara, T., Mase, H., Shimizu, T., Ishikawa, K., Kimura, K., Smyth, R.D. (1988). Clinical pharmacokinetics of carboplatin. *J. Clin. Pharmacol.*, **28**, 208-215.

Orr, G.A., Verdier-Pinard, P., McDaid, H., Horwitz, S.B. (2003). Mechanisms of taxol resistance related to microtubules. *Oncogene*, **22**, 7280-7295.

Osaki, S., Nakanishi, Y., Takayama, K., Pei, X.-H., Ueno, H., Hara, N. (2000). Alteration of drug chemosensitivity caused by the adenovirus-mediated transfer of the wild-type p53 gene in human lung cancer cells. *Cancer Gene Ther.*, 7, 300-307.

Ota, I., Ohnishi, K., Takahishi, A., Yane, K., Kanata, H., Miyahara, H., Ohnishi, T., Hosoi, H. (2000). Transfection with mutant p53 gene inhibits heat-induced apoptosis in a head and neck cell line of human squamous cell carcinoma. *Int. J. Radiation Oncology Biol. Phys.*, **47**, 495-501.

Padar, S., van Breemen, C., Thomas, D.W., Uchizono, J.A., Livesey, J.C., Rahimian, R. (2004). Differential regulation of calcium homeostasis in adenocarcinoma cellline A549 ands its taxol-resistant subclone. *Br. J. Pharmacol.*, **142**, 305-316.

Parekh, H.K., Deng, H.B., Choudhary, K., Houser, S.R., Simpkins. H. (2002). Overexpression of sorcin, a calcium-binding protein, induces a low level of paclitaxel resistance in human ovarian and breast cancer cells. *Biochem. Pharmacol.*, **63**, 1149-1158.

Parekh, H., Wiesen, K., Simpkins, H. (1997). Acquisition of taxol resistance via p-glycoprotein and non-p-glycoprotein-mediated mechanisms in human ovarian carcinoma cells. *Biochem. Pharmacol.*, **53**, 461-470.

Pedersen, N., Mortensen, S., Sorensen, S.B., Pedersen, M.W., Rieneck, K., Bovin, L.F., Skovgaard Poulsen, H. (2003). Transcriptional gene expression profiling of small cell lung cancer cells. *Cancer Res.*, **63**, 1943-1953.

Pfeifer, G.P., Holmquist, G.P. (1997). Mutagenesis in the p53 gene. *Biochim. Biophys. Acta*, 1333, M1-M8.

Pluquet, O., Hainaut, P. (2001). Genotoxic and non-genotoxic pathways of p53 induction. *Cancer Letters*, 174, 1-15.

Qin, L.F., Ng, I.O.L. (2002). Induction of apoptosis by cisplatin and its effect on cell cycle-related proteins and cell cycle changes in hepatoma cells. *Cancer Letters*, **175**, 27-38.

Rakovitch, E., Mellado, W., Hall, E.J., Pandita, T.J., Sawant, S., Geard, C.R. (1999). Paclitaxel sensitivity correlates with p53 status and DNA fragmentation, but not G2/M accumulation. *Int. J. Radiation Oncology Biol. Phys.*, **44**, 1119-1124.

Rao, P.V., Krishna, C.M.,Zigler, J.S. (1992). Identification and characterization of the enzymatic activity of zeta- crystallin from guinea pig lens. A novel NADPH:quinone oxidoreductase. *J. Biol. Chem.*,**267**, 96-102.

Reinecke, P., Kalinski, T., Mahotka, C., Schmitz, M., Dejosez, M., Gabbert, H.E., Gerharz, C.D. (2005). Paclitaxel/Taxol sensitivity in human renal cell carcinoma is not determined by the p53 status. *Cancer Lett.*, **222**, 165-171.

Roussel, E., Belanger, M.M., Couet, J. (2004). G2/M blockade by paclitaxel induces caveolin-1 expression in A549 lung cancer cells: caveolin-1 as a marker of cytotoxicity. *Anticancer Drugs*, **15**, 961-967.

Ryan, K.M., Phillips, A.C., Vousden, K.H.(2001). Regulation and function of the p53 tumor suppressor protein. *Curr. Opin. Cell Biol.*, **13**, 332-337.

Sakurai, D., Tsuchiya, N., Yamaguchi, A., Okaji, Y., Tsuno, N.H., Kobata, T., Takahashi, K., Tokunaga, K. (2004). Crucial role of inhibitor of DNA binding/differentiation in the vascular endothelial growth factor-induced activation and angiogenic processes of human endothelial cells. *J. Immunol.*, **173**, 5801-5809.

Sampath, J., Sun, D., Kidd, V.J., Grenet, J., Gandhi, A., Shapiro, L.H., Wang, Q., Zambetti, G.P., Schuetz, J.D. (2001). Mutant p53 cooperates with ETS and selectively upregulates human MDR-1 and not MRP1. *J. Biol. Chem.*, **276**, 39359-39367.

Saxena, S., Jonsson, Z.O., Dutta, A. (2003). Small RNAs with imperfect match to endogenous mRNA repress translation. Implications for off-target activity of small inhibitory RNA in mammalian cells. *J. Biol. Chem.*, **278**, 44312-44319.

Schinkel, A.H. (1997). The physiological function of drug-transporting P-glycoproteins. *Semin. Cancer Biol.*, **8**, 161-170.

Schinkel, A.H., Jonker, J.W. (2003). Mammalian drug efflux transporters of the ATP binding cassette (ABC) family: an overview. *Adv. Drug Deliv. Rev.*, **55**, 3-29.

Scripture, C.D., Szebeni, J., Loos, W.J., Figg, W.D., Sparreboom, A. (2005). Comparative in vitro properties and clinical pharmacokinetics of placlitaxel following the administration of taxol and paxene. *Cancer Biol. Ther.*, **4**, 555-560.

Semizarov, D., Frost, L., Sarthy, A., Kroeger, P., Halbert, D.N., Fesik, S.W. (2003). Specificity of short interfering RNA determined through gene expression signatures. *Proc. Natl. Acad. Sci. USA*, **100**, 6347-6352.

Shaw, P., Bovey, R., Tardy, S., Sahli, R., Sordat, B., Costa, J. (1992). Induction of apoptosis by wild-type p53 in a human colon tumor-derived cell line. *Proc. Natl. Acad. Sci.*, **89**, 4495-4499.

Shen, C., Buck, A.K., Liu, X., Winkler, M., Reske, S.N. (2003). Gene silencing by adenovirus-delivered siRNA. *FEBS Lett.*, **539**, 111-114.

Sikder, H.A., Devlin, M.K., Dunlap, S., Ryu, B., Alani, R.M. (2003). Id proteins in cell growth and tumorigenesis. *Cancer Cell*, **3**, 525-530.

Simon, S.M., Schindler, M. (1994). Cell biological mechanisms of multidrug resistance in tumours. *Proc. Natl. Acad. Sci. USA*, **91**, 3497-3504.

Sioud, M. (2004). Therapeutic siRNAs. *Trends Pharmacol. Sci.*, **25**, 22-28.

Siva, A.C., Raval-Fernandes, S., Stephen, A.G., La Femina, M.J., Scheper, R.J., Kickhoefer, V.A., Rome, L.H. (2001). Up-regulation of vaults may be necessary but not sufficient for multidrug resistance. *Int. J. Cancer*, **92**, 195-202.

Sledz, C.A., Holko, M., de Veer, M.J., Silverman, R.H., Williams, B.R. (2003). Activation of the interferon system by short-interfering RNAs. *Nat. Cell Biol.*, **5**, 834-839.

Sorrentino, B. (2002). Gene therapy to protect haematopoietic cells from cytotoxic cancer drugs. *Nat. Rev. Cancer*, **2**, 431-441.

Stewart, S.A., Dykxhoorn, D.M., Palliser, D., Mizuno, H., Yu, E.Y., An, D.S., Sabatini, D.M., Chen, I.S., Hahn, W.C., Sharp, P.A., Weinberg, R.A., Novina, C.D. (2003). Lentivirus-delivered stable gene silencing by RNAi in primary cells. *RNA*, **9**, 493-501.

Stierle, V., Laigle, A., Jolles, B. (2005). Modulation of MDR1 gene expression in multidrug resistant MCF7 cells by low concetrations of small interfering RNAs. *Biochem. Pharmacol.*, **70**, 1424-1430.

Su, H.P., Nakada-Tsukui, K., Tosello-Trampont, A.C., Li, Y., Bu, G., Henson, P.M., Ravichandran, K.S. (2002). Interaction of CED-6/GULP, an adapter protein involved in engulfment of apoptotic cells with CED-1 and CD91/low density lipoprotein receptor-related protein (LRP). *J. Biol. Chem.*, **277**, 11772-11779.

Suganuma, K., Kubota, T., Saikawa, Y., Abe, S., Otani, Y., Furukawa, T., Kumai, K., Hasegawa, H., Watanabe, M., Kitajima, M., Nakayama, H., Okabe, H. (2003). Possible chemoresistance-related genes for gastric cancer detected by cDNA microarray. *Cancer Sci.*, **94**, 355-359.

Sugita, M., Geraci, M., Gao, B., Powell, R.L., Hirsch, F.R., Johnson, G., Lapadat, R., Gabrielson, E., Bremnes, R., Bunn, P.A., Franklin, W.A. (2002). Combined use of oligonucleotide and tissue microarrays identifies cancer/testis antigens as biomarkers in lung carcinoma. *Cancer Res.*, **62**, 3971-3979.

Sui, G., Soohoo, C., Affar, B., Gay, F., Shi, Y., Forrester, W.C., Shi, Y. (2002). A DNA vector-based RNAi technology to suppress gene expression in mammalian cells. *Proc. Natl. Acad. Sci. USA,* **99**, 5515-5520.

Sullivan, G.F., Yang, J.-M., Vassil, A., Yang, J., Bash-Babula, J., Hait, W.N. (2000). Regulation of expression of the multidrug resistance protein MRP1 by p53 in human prostate cancer cells. *J. Clin. Invest.*, **105**, 1261-1267.

Tang, C., Willingham, M.C., Reed, J.C., Miyashita, T., Ray, S., Ponnathpur, V., Huang, Y., Mahoney, M.E., Bullock, G., Bhalla, K. (1994). High levels of p26BCL-2 oncoprotein retard taxol-induced apoptosis in human pre-B leukemia cells. *Leukemia*, **8**, 1960-1969.

Takahashi, T., Carbone, D., Takahashi, T., Nau, M.N., Hida, T., Linnoila, I., Ueda, R., Minna, J.D. (1992). Wild-type but not mutant p53 suppresses the growth of human lung cancer cells bearing multiple genetic lesions. *Cancer Res.*, **52**, 2340-2343.

Thottassery, J.V., Zambetti, G.P., Arimori, K., Schuetz, E.G., Schuetz, J.D. (1997). p53-dependent regulation of *MDR1* gene expression causes selective resistance to chemotherapeutic agents. *Proc. Natl. Acad. Sci.*, **94**, 11037-11042.

Tiscornia, G., Singer, O., Ikawa, M., Verma, I.M. (2003). A general method for gene knockdown in mice by using lentiviral vectors expressing small interfering RNA. *Proc. Natl. Acad. Sci. USA*, **100**, 1844-1848.

Towbin, H., Staehelin, T. and Gordon, J. (1979). Electrophoretic transfer of proteins from polyacrylamide gels to nitrocellulose sheets: procedures and some applications. *Proc. Natl. Acad. Sci. USA*, **76**, 4350-4354.

Van Ark-Otte, J., Samelis, G., Rubio, G., Lopez Saez, J.B., Pinedo, H.M., Giaccone, G. (1998). Effects of tubulin-inhibiting agents in human lung and brease cancer cell lines with different multidrug resistance phenotypes. *Oncol. Rep.*, **5**, 259-255.

Viktorsson, K., De Petris, L., Lewwnsohn, R. (2005). The role of p53 in treatment responses of lung cancer. *Biochem. Biophys. Res. Commun.*, **331**, 868-880.

Virtanen, C., Ishikawa, Y., Honjoh, D., Kimura, M., Shimane, M., Miyoshi, T., Nomura, H., Jones, M.H. (2002). Integrated classification of lung tumours and cell lines by expression profiling. *Proc. Natl. Acad. Sci. USA*, **99**, 12357-12362.

Vogelstein, B., Lane, D., Levine, A.J. (2000). Surfing the p53 network. *Nature*, **408,** 307-310.

Wall NR, Shi Y. (2003). Small RNA: can RNA interference be exploited for therapy? *Lancet*, **362**, 1401-1403.

Wang, Q., Beck, W.T. (1998). Transcriptional supression of multidrug resistance-associated protein (MRP) gene expression by wild-type p53. *Cancer Res.*, **58**, 5762-5769.

Wang, T.H., Wang, H.S., Soong, Y.K. (2000). Paxlitaxel-induced cell death where the cell cycle and apoptosis come together. *Cancer*, **88**, 2619-2628.

Wang, X., Ling, M.T., Guan, X.Y., Tsao, S.W., Cheung, H.W., Lee, D.T., Wong, Y.C. (2004). Identification of a novel function of TWIST, a bHLH protein, in the development of acquired taxol resistance inhuman cancer cells. *Oncogene*, **23**, 474-482.

Weinberg, R.A. (1996). How cancer arises. *Sci Am.*, **275**, 62-70.

Westerlund, A., Hujanen, E., Hoyhtya, M., Puistola, U., Turpeenniemi-Hujanen, T. (1997). Ovarian cancer cell invasion is inhibited by paclitaxel. *Clin. Exp. Metastasis*, **15**, 318-328.

Whiteside, M.A., Chen, D.-T., Desmond, R.A., Abdulkadir, S.A., Johanning, G.L. (2004). A novel time-course cDNA microarray analysis method identifies genes associated with the development of cisplatin resistance. *Oncogene*, **23**, 744-752.

Wittig, R., Nessling, M., Will, R.D., Mollenhauer, J., Salowsky, R., Munstermann, E., Schick, M., Helmbach, H., Gschwendt, B., Korn, B., Kioschis, P., Lichter, P., Schadendorf, D., Poustka, A. (2002). Candidate genes for cross-resistance against DNA-damaging drugs. *Cancer Res.*, **62**, 6698-6705.

Woodhouse, E.C., Chuaqui, R.F., Liotta, L.A. (1997). General mechanisms of metastasis. *Cancer*, **80**, 1529-1537.

Wu, H., Hait, W.N., Yang, J.M. (2003). Small interfering RNA-induced suppression of MDR1 (P-glycoprotein) restores sensitivity to multidrug-resistant cancer cells. *Cancer Res.*, **63**, 1515-1519.

Yamauchi, M., Suzuki, K., Kodama, S., Watanabe, M. (2005). Abnormal stability of wild-type p53 protein in a human lung carcinoma cell line. *Biochem. Biophys. Res. Commun.*, **330**, 483-488.

Yang, C.P.H., Galbiati, F., Volonte, D., Horwitz, S.B., Lisanti, M.P. (1998). Upregulation of caveloin-1 and caveolae organelles in taxol-resistant A549 cells. *FEBS Lett.*, **439**, 368-372.

Young, L.C., Campling, B.G., Voskoglou-Nomikos, T., Cole, S.P.C., Deeley, R.G., Gerlach, J.H. (1999). Expression of multidrug resistance protein-related genes in lung cancer: correlation with drug response. *Clin. Cancer Res.*, **5**, 673-680.

Zaffaroni, N. Pennati, M., Collella, G., Perego, P., Supino, R. Gatti, L., Pilotti, S., Zunino, F., Daidone, M.G. (2002). Expression of the anti-apoptotic gene survivin correlates with taxol resistance in human ovarian cancer. *Cell. Mol. Life Sci.*, **59**, 1406-1412.

Zeimet, A.G., Riha, K., Berger, J., Widschwendter, M., Hermann, M., Daxenbichler, G., Marth, C. (2000). New insights into p53 regulation and gene therapy for cancer. *Biochem. Pharmacol.*, **60**, 1153-1163.

Zeng, Y., Yi, R., Cullen, B.R. (2003). MicroRNAs and small interfering RNAs can inhibit mRNA expression by similar mechanisms. *Proc. Natl. Acad. Sci. USA.*, **100**, 9779-9784.

Zhang, X., Ling, M.T., Wang, X., Wong, Y.C. (2005). Inactivation of Id-1 in prostate cancer cells: A potential therapeutic target in inducing chemosensitization to taxol through activation of JNK pathway. *Int. J. Cancer* [Epub ahead of print].

Zhu, G.H., Wong, B.C.Y., Ching, C.K., Lai, K.C., Lam, S.K. (1999). Differential apoptosis by indomethacin in gastric epithelial cells through the constitutive expression of wild-type p53 and/or up-regulation of c-myc. *Biochem. Pharmacol.*, **58**, 193-200.

Zunino, F., Perago, P., Pilotti, S., Pratesi, G., Supino, R., Arcamone, F. (1997). Role of apoptotic response in cellular resistance to cytotoxic agents. *Pharmacol. Ther.*, **76**, 177-185.